

Preface

The research contained herein was completed by the candidate while based in the Discipline of Mechanical Engineering of the College of Agriculture, Engineering and Science at the University of KwaZulu-Natal, Howard Campus, South Africa. The research was financially supported by The Armaments Corporation of South Africa (ARMSCOR).

The contents of this work have not been submitted in any form to another university and, except where the work of others is acknowledged in the text, the results reported are due to investigations by the candidate.

As the candidate's Supervisor I agree to the submission of this thesis.

Signed: _____ Date: _____

Mr. Jean-François Pitot de la Beaujardiere

As the candidate's Co-Supervisor I agree to the submission of this thesis.

Signed: _____ Date: _____

Dr. Clinton Bemont

Declaration 1: Plagiarism

I, Saién Rugdeo, declare that

- (i) The research reported in this dissertation, except where otherwise indicated, is my original work.
- (ii) This dissertation has not been submitted for any degree or examination at any other university.
- (iii) This dissertation does not contain other persons' data, pictures, graphs or other information, unless specifically acknowledged as being sourced from other persons.
- (iv) This dissertation does not contain other persons' writing, unless specifically acknowledged as being sourced from other researchers. Where other written sources have been quoted, then:
 - a) Their words have been re-written but the general information attributed to them has been referenced;
 - b) Where their exact words have been used, their writing has been placed inside quotation marks, and referenced.
- (v) This dissertation does not contain text, graphics or tables copied and pasted from the Internet, unless specifically acknowledged, and the source being detailed in the dissertation and in the References sections.

Signed : _____ Date: _____

Mr Saién Rugdeo

Declaration 2: Publications

Publications that form part and/or include research presented in this dissertation.

Rugdeo, S. Bemont, C. Pitot de la Beaujardiere, J, 2017. Independent Assessment and Benchmarking of No-cost/Low-cost Finite Element Analysis Software.

In Preparation

Acknowledgments

I would like to express my sincere gratitude to my supervisor Mr. Jean-François Pitot de la Beaujardiere and my co-supervisor Dr. Clinton Bemont for their guidance and support and throughout my work.

I would like to thank my friends and colleagues from my office for their motivation and support throughout my postgraduate studies. I would like to give special thanks to Ms Kirsty Veale for her guidance and assistance.

I would like to acknowledge Dr Michael Brooks for his assistance with obtaining the funding for this research.

I would like to acknowledge Mr Victor Kemp for supplying a free licence for Mecway for use in this research, as well as for his advice and guidance pertaining to the use of the software.

Finally I would like to thank my family, particularly my mother, Marlini, and my father Inder Rugdeo for their love, support and motivation.

Abstract

The aim of this research was to determine if the development of low-cost (less than 500 USD) or no-cost analysis software, specifically in the area of computational structural mechanics through finite element analysis (FEA), has advanced to the point where it can be used in place of trusted commercial FEA software packages for linear and non-linear static structural analyses using isotropic materials. This was done by conducting an initial market research study and identifying a range of available no-cost/low-cost FEA packages. Eighteen suitable packages were identified and a preliminary analysis was done to identify analysis capabilities, presence of internal modules, extent of available user documentation, and end user support. The packages underwent a process of systematic elimination from the preceding phases of the research if they were unable to meet the minimum imposed criteria. Six packages were deemed suitable and were further investigated. From these, three packages were chosen to be subjected to performance benchmarking, namely: Code_Aster/Salome Meca; Mecway and Z88 Aurora.

SimScale, a browser-based analysis package was included as well because it met all the baseline criteria and has the potential to offer a completely cloud-based approach to computer aided engineering, potentially reshaping the way an engineering business views its operational capabilities.

Performance benchmarking assessed the ability of a package to generate a model and obtain accurate solutions relative to industry accepted benchmark publications, trusted analytical solutions found in reputable engineering text, as well as experimental results obtained in this work. The benchmarking process was also done on commercial FEA packages so that a comparison can be made between the no-cost/low-cost packages and those considered to be the premium FEA software packages available.

It was found that the no-cost/low-cost options were able to perform adequately for most of the test cases. SimScale and Z88 Aurora had difficulties with generating suitable meshes which meant that compromises in model generation approaches needed to be made. Overall, the results yielded by the low-cost/no-cost options showed good correlation with test case target values as well as exhibiting many capabilities and tools found in the high-cost, trusted commercial packages investigated. It is therefore concluded that there are no-cost/low-cost FEA packages that can be used in place of high-cost commercial packages for linear and non-linear static structural analyses of isotropic materials.

Table of Contents

Preface.....	i
Declaration: Plagiarism.....	ii
Proposed Titles for Future Publications.....	iii
Acknowledgments.....	iv
Abstract.....	v
List of Tables.....	ix
List of Figures.....	x
Nomenclature.....	xiii
CHAPTER 1 : Introduction.....	1
1.1 Research Problem.....	3
1.2 Research Question.....	3
1.3 Research Objectives.....	4
1.4 Delineations and limitations.....	4
1.5 Dissertation overview.....	5
CHAPTER 2 : Literature Review.....	6
2.1 The Impact of FEA in the Engineering Industry.....	6
2.2 The Finite Element Method.....	8
2.3 The Process of Finite Element Analysis.....	16
2.4 Errors and Uncertainty Present During the FEA Process.....	22
2.5 Significance of Verification and Validation.....	23
2.6 Different Licensing Approaches for FEA Packages.....	25
2.6.1 Commercial Proprietary Software Licences.....	25
2.6.2 Open Source Software Licences.....	26
2.6.3 Freeware.....	26
2.7 Independent Studies Conducted on the Performance of No-Cost/Low-Cost FEA Software Packages.....	26
2.8 No-Cost/Low-Cost FEA Package Investigation.....	28
2.8.1 Selected software Packages.....	28
2.8.2 Capabilities.....	29
2.8.3 Operating System.....	29
2.8.4 Internal Modules Present in Selected Packages.....	29
2.8.5 Compatible File Types.....	31
2.8.6 User Support and Documentation.....	31

2.8.7	Software Pricing.....	32
2.9	Premium Commercial FEA Package Investigation.....	33
2.9.1	Selected Software Packages.....	33
2.9.2	Capabilities.....	34
2.9.3	Operating Systems	34
2.9.4	Internal Modules	35
2.9.5	Compatible File Types	36
2.9.6	User Support and Documentation	36
2.10	Browser-Based FEA simulation platforms	37
2.10.1	SimScale Browser-based FEA simulation platform.....	37
2.11	Benchmarks and Standards for Performance of FEA Packages.....	38
2.12	Chapter Discussion.....	39
2.13	Chapter Conclusion.....	41
CHAPTER 3 : Methodology		42
3.1	Research Methodology.....	42
3.1.1	Identify and Investigate No/Low Cost FEA Packages Available.	42
3.1.2	Identification of Independent Benchmarking Studies relating to No-Cost/Low-Cost FEA Packages	42
3.1.3	Subjection of No-Cost/Low-cost Packages to Selection Criteria.....	42
3.1.4	Selection of One or More Available Premium Commercial Package.....	44
3.1.5	Review and Selection of Benchmarking Test Cases	44
3.1.6	Solution of Test Cases Using FEA Software Packages	44
3.1.7	Processing and Interpretation of Results.....	45
3.2	Limitations	47
3.3	Conclusion	47
CHAPTER 4 : Chosen Benchmark Test Cases		48
4.1	Linear Static Structural Analysis Test Cases	48
4.1.1	Grid Point Load on an Articulated Truss	48
4.1.2	Thin Shell Wall in Pure Bending	50
4.1.3	Axisymmetric Pressure Vessel.....	51
4.1.4	Internal Pressure on Thick-Walled Spherical Container.....	53
4.1.5	Flat Bar with Stress Concentration.....	55
4.2	Non-Linear Static Structural Analysis test cases	58
4.2.1	Large deflection of a Z-Shaped Cantilever Beam under End Load	58

4.2.2	Plastic Deformation of Tensile Test Specimen	59
CHAPTER 5 :	Model Generation Procedure and Presentation of Results	64
5.1	Model Generation	64
5.1.1	Mecway	64
5.1.2	Z88 Aurora	67
5.1.3	SimScale	69
5.1.4	Code_Aster/Salome Meca	71
5.1.5	ANSYS	73
5.1.6	Siemens NX	76
5.2	Presentation of Simulation Results	78
5.2.1	Test Case 1: Grid Point Load on an Articulated Truss	78
5.2.2	Test Case 2: Thin Shell Wall in Pure Bending	81
5.2.3	Test Case 3: Axisymmetric Pressure Vessel	82
5.2.4	Test Case 4: Internal Pressure on Thick-Walled Spherical Container	82
5.2.5	Test Case 5: Flat Bar with Stress Concentration	86
5.2.6	Test Case 6: Large deflection of a Z-Shaped Cantilever Beam	87
5.2.7	Test Case 7: Plastic Deformation of Tensile Test Specimen	88
CHAPTER 6 :	Discussion of Results	92
6.1	Mecway	92
6.2	Z88 Aurora	94
6.3	SimScale	96
6.4	Code_Aster/Salome Meca	97
6.5	ANSYS	99
6.6	Siemens NX	101
6.7	Overall Discussion of Results	103
CHAPTER 7 :	Conclusion	106
7.1	Findings	106
7.2	Recommendations for Further Research	109
REFERENCES	110
APPENDIX A	114
APPENDIX B	115
APPENDIX C	116
APPENDIX D	126
APPENDIX E	156

List of Tables

Table 2-1. Overview of typical structural finite elements.....	18
Table 2-2. Typical boundary constraints encountered in Structural FEA.....	19
Table 2-3. Typical Loads encountered in Structural FEA	20
Table 2-4. Capabilities of selected no-cost/low-cost FEA packages	29
Table 2-5. Supported operating systems for selected open source FEA packages	29
Table 2-6. Internal modules present in selected no-cost/low-cost FEA packages	30
Table 2-7. File types compatible with selected FEA packages.....	31
Table 2-8. User support and documentation available for selected FEA packages	32
Table 2-9. Price per licence per year for chosen packages	32
Table 2-10. Analysis capabilities of available commercial FEA packages	34
Table 2-11. Supported operating systems for available commercial FEA packages	34
Table 2-12. Internal modules present in available commercial FEA packages	35
Table 2-13. File types compatible with available commercial FEA packages	36
Table 2-14. User support and documentation available.....	36
Table 4-1. Given information for truss analysis.....	49
Table 4-2. Given target solutions for truss problem.....	49
Table 4-3. Given information for wall in pure bending analysis problem.	50
Table 4-4. Given target solutions for wall in bending problem.	51
Table 4-5. Information given for axisymmetric pressure vessel test case.....	52
Table 4-6. Given target solutions for axisymmetric pressure vessel analysis problem.....	52
Table 4-7. Given information for spherical pressure vessel analysis problem	54
Table 4-8. Given target solutions for spherical pressure vessel analysis problem.....	54
Table 4-9. Properties to be used for the flat bar with stress concentration analysis problem.	56
Table 4-10. Calculated results for the flat bar with stress concentrations analysis problem..	57
Table 4-11. Given properties for Z-Shaped cantilever problem.	58
Table 4-12. Given result for Z-Shaped cantilever problem.	59
Table 4-13. Model properties for Tensile test specimen analyses	63
Table 5-1. Final solution deviation for cantilever beam deflection	87
Table 5-2. Average deviation of simulation results measured against experimental result ...	91

List of Figures

Figure 2-1. Ladder represented as a discretized element-node model	9
Figure 2-2. Complex geometry discretized using a finite element model	9
Figure 2-3. General 3-D body	13
Figure 2-4. Basic overview of the FEA process.....	16
Figure 2-5. General procedure for the interpretation of post-processing structural FEA results	21
Figure 3-1. Package selection procedure	43
Figure 3-2. Computational simulation process	46
Figure 4-1. Truss system geometry.....	48
Figure 4-2. Wall geometry represented as a 2-D shell.....	50
Figure 4-3. Axisymmetric representation of pressure vessel	52
Figure 4-4. Quarter sphere geometry	53
Figure 4-5. Geometry of flat bar with stress concentrations	55
Figure 4-6. Stress concentration factors for flat bars under tensile loading (Beer et al., 2012).	56
Figure 4-7. Cantilever geometry	58
Figure 4-8. Specimen geometry created following SABS standards for metallic material tensile testing.....	60
Figure 4-9. Custom tensile test specimen geometry	60
Figure 4-10. Seven result sets of stress (MPa) vs strain (%) for standard specimen geometry	61
Figure 4-11. Median material curve showing 0.2% offset line.	62
Figure 4-12. Six result sets of stress vs strain for custom specimen geometry	63
Figure 5-1. Error dialog box displayed when attempting to create a 2-D mesh.....	67
Figure 5-2. Graph of target output “X-directional displacement at node C” for each package.	79
Figure 5-3. Graph of target output “Y-directional displacement at node C” for each package.	79
Figure 5-4. Graph of target output “X-directional displacement at node D” for each package.	80
Figure 5-5. Graph of target output “Y-directional displacement at node D” for each package.	80
Figure 5-6. Graph of target output “Maximum Z-Direction deflection” for each package. ..	81
Figure 5-7. Graph of target output “Z-Directional Stress” for each package.....	81
Figure 5-8. Graph of target output “Maximum Y-Directional Stress” for each package.....	82
Figure 5-9. Graph of target output “Maximum σ (rr) on internal surface” for each package.	83
Figure 5-10. Graph of target output “Maximum σ (rr) on external surface” for each package.	83
Figure 5-11. Graph of target output “Maximum σ (θ) on internal surface” for each package.	84

Figure 5-12. Graph of target output “Maximum σ (θ) on external surface” for each package.	84
Figure 5-13. Graph of target output “Maximum displacement on internal surface” for each package.....	85
Figure 5-14. Graph of target output “Maximum displacement on external surface” for each package.....	85
Figure 5-15. Graph of target output “Maximum Stress at Hole” for each package.	86
Figure 5-16. Graph of target output “Maximum Stress at Fillet” for each package.	86
Figure 5-17. Graph of incremental target outputs “Z-directional tip deflection”.....	87
Figure 5-18. ANSYS result for test case 7.....	88
Figure 5-19. NX result for test case 7.	89
Figure 5-20. Code_Aster result for test case 7.....	89
Figure 5-21. SimScale result for test case 7.....	90
Figure 5-22. Mecway result for test case 7.	90
Figure D.1. Displacement in X-direction.....	127
Figure D.2. Displacement in Y-direction.....	127
Figure D. 3. Displacement in X-direction.....	128
Figure D. 4. Displacement in Y-direction.....	128
Figure D. 5. Displacement in X-direction.....	129
Figure D. 6. Displacement in Y-direction.....	129
Figure D. 7. Displacement in X-direction.....	130
Figure D. 8. Displacement in Y-direction.....	130
Figure D. 9. Displacement in X-direction.....	131
Figure D. 10. Displacement in Y-direction.....	131
Figure D. 11. Displacement in Z-direction.	132
Figure D. 12. Stress in Z-direction.....	132
Figure D. 13. Displacement in Z-Direction (SI units).....	133
Figure D. 14. Stress in Z-direction (SI units).....	133
Figure D. 15. Displacement in Z-direction.	134
Figure D. 16. Stress in Z-direction.....	134
Figure D. 17. Displacement in Z-direction.	135
Figure D. 18. Stress in Z-direction.....	135
Figure D. 19. Stress (YY).	136
Figure D. 20. Stress (YY).	136
Figure D. 21. Stress (YY).	137
Figure D. 22. Stress (YY).	137
Figure D. 23. Stress (YY)..	138
Figure D. 24. Stress (YY).	138
Figure D. 25. Stress σ (rr).	139
Figure D. 26. Stress σ (Θ).	139
Figure D. 27. Displacement magnitude.....	140
Figure D. 28. Displacement magnitude.....	140
Figure D. 29. Stress σ (rr).	141
Figure D. 30 Stress σ (Θ).	141

Figure D. 31. Displacement magnitude.....	142
Figure D. 32. Stress σ (rr).....	142
Figure D. 33. Stress σ (Θ).....	143
Figure D. 34. Displacement magnitude.....	143
Figure D. 35. Stress σ (rr).....	144
Figure D. 36. Stress σ (Θ).....	144
Figure D. 37. Displacement magnitude.....	145
Figure D. 38. Stress σ (rr).....	145
Figure D. 39. Stress σ (Θ).....	146
Figure D. 40. Displacement magnitude.....	146
Figure D. 41. Stress along X-axis.....	147
Figure D. 42. Stress along X-axis.....	147
Figure D. 43. Stress along X-axis.....	148
Figure D. 44. Stress along X-axis.....	148
Figure D. 45. Stress along X-axis.....	149
Figure D. 46. Stress along X-axis.....	149
Figure D. 47. Displacement in Z-direction.....	150
Figure D. 48. Displacement in Z-direction.....	150
Figure D. 49. Displacement in Z-direction.....	151
Figure D. 50. Displacement in Z-direction.....	151
Figure D. 51. Displacement in Z-direction.....	152
Figure D. 52. Displacement in Z-direction.....	152
Figure D. 53. Stress observed after extension causes plastic deformation.....	153
Figure D. 54. Stress observed after extension causes plastic deformation.....	153
Figure D. 55. Stress observed after extension causes plastic deformation.....	154
Figure D. 56. Stress observed after extension causes plastic deformation.....	154
Figure D. 57. Stress observed after extension causes plastic deformation.....	155

Nomenclature

Abbreviations

1-D	One Dimensional
2-D	Two Dimensional
3-D	Three Dimensional
APDL	ANSYS Parametric Design Language
ANSYS	Analysis Systems
ASM	American Society for Metals
ASME	American Society for Mechanical Engineers
CAD	Computer Aided Design
CAE	Computer Aided Engineering
CFD	Computational Fluid Dynamics
CSC	Computer Sciences Corporation
CSM	Computational Structural Mechanics
DOF	Degrees of Freedom
FEA	Finite Element Analysis
FEM	Finite Element Method
GUI	Graphical User Interface
MPC	Multipoint Constraint
MSC	Macneal-Schwendler Corporation
NAFEMS	National Agency for Finite Element Methods and Standards
NASA	National Aeronautics and Space Administration
NASTRAN	NASA Structure Analysis.
NRMSD	Normalised Root Mean Square Deviation
OS	Operating System
PDE	Partial Differential equation
PLM	Product Lifecycle Management

RMSD	Root Mean Square Deviation
SABS	South African Bureau of Standards
UKZN	University of KwaZulu-Natal
USD	United States Dollar
UTS	Ultimate Tensile Stress

Symbols

A	Area
C	Stress-Strain Material Matrix
E	Young's Modulus of Elasticity
E_{model}	Model Form Error
E_{num}	Numerical Error
f^B	Externally Applied Body Force
f^{S_f}	Prescribed Surface Force on S_f
F	Force
K	Stress Concentration Factor
K	Stiffness Matrix
M	Moment
R	Body Force Vector
R_c^i	Concentrated Point Load
S_f	Point on the Surface of a General Body
S_u	Constrained Area on a General Body
u	Displacement
U	Displacement of a General Body
$U_{S_u}^S$	Prescribed Displacement on S_u
X_{pred}	Predicted System Response
X_{true}	True System Response

\bar{U}	Virtual Displacement
\bar{u}	Displacement Vector
σ_{max}	Maximum Stress
$\bar{\epsilon}$	Virtual Strain
ϵ	Strain
ν	Poisson's Ratio
σ	Stress
σ_{rr}	Radial Stress
σ_{θ}	Circumferential Stress
τ	Stresses Corresponding to ϵ
ϵ	Strain Corresponding to U

CHAPTER 1 : Introduction

Engineering problems for real-world physical systems can often be represented by mathematical models. These mathematical models are often in the form of differential equations which are derived from applying fundamental laws to a system over a finite region (Moaveni, 1999). It is often possible to obtain exact solutions to these equations. These exact analytical solutions comprise of two parts, namely, the *homogenous* and the *particular* part. The *homogenous* part refers to the natural behaviour of the undisturbed system i.e. density, viscosity, and so on. The *particular* part refers to external disturbances to the system i.e. forces, applied temperatures, pressure differences across fluid flow etc (Moaveni, 1999).

There are practical engineering problems which cannot be solved by analytical methods to gain exact solutions. The inability to obtain exact solutions to real-world problems can be attributed to difficulties in capturing complex physical phenomena, physical properties and initial boundary conditions. To address this shortcoming, analysts have resorted to numerical methods, such as the finite element method, to solve complex problems. In contrast to analytical solutions which depict the exact behaviour at any point within the system, numerical solutions can only yield approximate solutions at discrete points within the system (Moaveni, 1999).

The origin of the modern finite element method can be traced back to the early 1900s (Moaveni, 1999), however it was Richard L. Courant, who has been credited as the first person to develop the finite element method. In 1942, he submitted a paper to the American Mathematical Society containing a two page appendix which is seen as the first official appearance of the finite element method (Pelosi, 2007). The next major step forward in the development of the finite element method (FEM) was made by the Boeing company in the 1950s (Clough, 1990). During this period, aircraft designers implemented the same structural theory used by civil engineers in the analysis of buildings. In both disciplines, a structure was defined as an assemblage of discrete structural elements (Clough, 1990).

An important advancement made in the field of structural analysis, initiated by work in the field of aeronautical engineering, was the introduction of matrix notation in the formulation of the analysis. By 1952, aircraft structural analysis had advanced to the point where a complex structure, represented by an assemblage of simple beams and plane elements, could

be analysed by a series of matrix operations using a digital computer (Clough, 1990). In 1952, an engineering professor by the name of Ray W. Clough joined Boeing. In 1957, Clough began developing a matrix algebra program which would carry out any sequence of matrix operations. This made it possible for him to study practical plane stress problems using triangular plate elements. Clough is credited with creating the term “finite elements”.

During the 1960s, researchers began to see the potential of the FEM and began applying it to different physical phenomenon such as heat transfer and fluid flow. In 1965, NASA issued a request for the development of a structural analysis tool. The resulting software tool would come to be known as NASTRAN (NASA Structural Analysis). Interest began to surface over the FEM during the years to come, as evidenced in the book by O. C. Zienkiewicz and Y. K. Cheung in 1967. Their work titled “*The finite element method in structural and continuum mechanics*” is credited as the first book to be entirely devoted to FEM (Moaveni, 1999).

In 1968, the Computer Sciences Corporation (CSC) officially released NASTRAN to NASA. In 1969, NASTRAN was commercialized by MacNeal-Schwindler Corporation (MSC) as MSC/NASTRAN. Finite element procedures were fast becoming taught in universities in both the mathematical and engineering disciplines. Finite element solvers were being developed and commercialized. Packages such as ANSYS, first released in 1971, were fast becoming valuable tools for researchers and analysts alike (Moaveni, 1999).

In the year 1991, the first textbook, written by Szabó and Babušk, was the first book published that focused purely on the practical approach to finite element analysis. In 2006, the American Society of Mechanical Engineers (ASME) released the first guide to verification and validation in computational structural mechanics. (American Society for Mechanical Engineers, 2006). It was ground-breaking, as it gave users a set of guidelines for mitigating and controlling simulation errors. In 2011, Szabó and Babušk published a follow up to their first text which was pitched towards teaching students the process of FEA from fundamentals to application. Currently FEA is a welcomed tool in industry. Practical FEA is commonly taught at university level so as to familiarise students with the concepts of computational analyses.

1.1 Research Problem

The rapid increase of computational power over the past few decades has been a catalyst for change in the engineering field. Software developers are able to take advantage of increasing computational power and can create numerical modelling packages capable of dealing with a range of physical problems encountered (Mac Donald, 2011). Consequently, increasing confidence is being placed in the results of computational simulations (Jackson, 2013).

The increasing acceptance of computational analysis results has created a problem. Software developers have been pushed to improve their packages capabilities, which subsequently increases costs. The cost of trusted proprietary numerical modelling packages is generally quite high and in some cases, exorbitant. These packages are typically used by large companies or research institutions with the resources to acquire them. The inability to readily acquire these numerical modelling software packages puts small to medium sized engineering businesses at a disadvantage, as it limits their operational capabilities. Fortunately, there have been a growing number of small proprietary software developers as well as an active open source development community, creating and improving relevant software packages in fields such as CFD and FEA, which can potentially be used in place of the expensive commercial proprietary packages.

1.2 Research Question

Has the development of low-cost/no-cost software packages, specifically in the field of FEA in computational structural mechanics (CSM), advanced to the point where a capable analyst can use one of these packages in the place of a globally trusted proprietary FEA software package?

1.3 Research Objectives

The primary objective of this research is to determine if low-cost/no-cost finite element analysis software packages have advanced to the point such that they can be used in place of a high-cost, trusted, proprietary software by a user that is capable in the field of FEA. The decision will be made based primarily on the accuracy of the solutions generated by the investigated package, in relation to proven analytical results and accepted benchmarking standards for FEA packages.

The secondary objective will be to qualitatively assess the appropriate packages and comment on the general user experience.

1.4 Delineations and limitations

This research focuses on determining if there are no-cost/low-cost FEA packages that are capable of accurately modelling static structural problems for isotropic materials of varied geometry, subjected to a variety of boundary conditions. The research will not include analysis of non-isotropic materials such as composites. There may be some mention of a package's ability to perform analysis on non-isotropic material models, but the modelling accuracy of the package will not be investigated in this regard.

This research will not focus on a packages' ability to perform other FEA such as thermal analysis, dynamic structural analysis or vibrational analysis etc. due to time constraints. The research will not focus on a packages ability to conduct any other type of numerical simulation method such as computational fluid dynamics (CFD).

The research will not aim to investigate or verify the fundamental accuracy of the code within these FEA packages nor will it endeavour to create a code for an FEA package capable of the aforementioned requirements. This research will not serve as an in-depth study into the mathematics and formulation of the numerical methods used in a finite element analysis.

1.5 Dissertation overview

This research will potentially yield results that can directly affect the operational capabilities of small to medium sized engineering companies in the manufacturing, design or consulting fields.

Chapter 2 contains a literature review which discusses the impact that FEA has on the engineering industry. A brief section of the mathematics behind the finite element method is presented. A selection of the more capable no-cost/low-cost packages are further investigated and the findings are presented within this chapter. A summarised generic process for conducting an FEA is presented. The associated errors incurred and importance of result verification is discussed.

Chapter 3 presents the research methodology employed when conducting this research. The factors that limit the scope and detail of the research are also discussed here.

Chapter 4 presents the linear and non-linear test cases that were chosen for the performance benchmarking phase of this research.

Chapter 5 contains the model generation procedures for each test case done on each of the chosen FEA packages. This chapter also presents the results for each test case yielded by the chosen packages.

Chapter 6 contains a discussion of the results from each package used in the benchmarking phase of this research. An overall discussion comparing all the results is contained in the chapter as well.

Chapter 7 presents the conclusion of this work and recommendations for further research.

CHAPTER 2 : Literature Review

2.1 The Impact of FEA in the Engineering Industry

Finite element analysis was primarily used for structural problems in the past but is now a widely accepted tool used in many industries and fields of research. FEA experiences widespread popularity as it allows for designs to be virtually tested, even before a single prototype is manufactured. It also allows for systems which cannot be experimentally tested easily, to be investigated (Mahendran, 2007). In the discipline of structural design, laboratory testing was done to develop appropriate design rules as well as new products and systems. Reliance on these time consuming methods of testing often hindered progress in the field. Consequently, product manufacturers decided on overly conservative designs so that they could avoid the need for this expensive and time consuming testing phase (Mahendran, 2007).

The advancement in computing power and the rapidly increasing capabilities of simulation software over the past two decades have significantly changed the way in which manufacturers and designers view product conceptualization and design. Computational simulation is no longer being viewed as a supplement to analytical methods but as a critical part of the design process. This acceptance of results from simulation software packages has made its way through many areas of engineering and non-engineering fields. Looking specifically at the advancement in FEA software packages, it has allowed for significant innovation and the development of accurate design methods (Mahendran, 2007).

Within the automotive industry for example, FEA has become an invaluable tool in the design process. With the demanded timeframe for a design going from concept to prototype being as little as 18 months, increasing numbers of manufacturers have moved to implement FEA simulations into the early design phase. Several areas of vehicle design are guided by the results of finite element analyses. FEA models are generated and tested for various phenomena relevant to vehicle design, such as: the deformation of the vehicles body during a collision, the responses of various suspension components during operation, thermal analysis of the brake discs during operation, to name a few (Abbey, 2014).

With the increase in capability and assumed reliability of the available packages, FEA has added to a new market trend in industry. The term, “simulation-driven product development”, is commonly used in the simulation industry to describe the integration of simulation software packages into the early design process and basing decisions on simulation results. This can be seen as a sign that a new industrial revolution is happening, as computers and simulation software are increasingly influential in changing product development and manufacturing processes (Banthia, 2014).

Evidence to validate the above statement can be found in a relevant report published in 2013 by the principle industry analyst of a research and advisory firm, in conjunction with several recognised associations in the simulation field (Jackson, 2013). The report is titled “The 2013 State of Simulation Design”. The aim of the report was to answer the following question: “Are today’s engineers making decisions based on simulations?” The findings of the report were based on survey responses from 826 respondents who are from a wide range of industries across the world. The majority of the respondents were from the automotive, industrial equipment manufacture, aerospace and defence industries. (Jackson, 2013). The survey targeted various countries, with the majority being from North America and Europe. Furthermore, respondents of the survey held a number of roles including: general staff, high ranking executives as well as CEO’s, all of which were employed by companies with annual revenues ranging from less than USD 100 million to in excess of 1.25 billion USD (Jackson, 2013). The survey focused mainly on how respondents used simulation to drive decisions during the concept design phase, as well as the employment of simulation in the more detailed design phase.

There are many adverse effects on a company caused by failed prototypes and concept designs. Many of these waste time and resources and could potentially cause the termination of a design project (Jackson, 2013). Key business value findings showed that best-in-class manufacturers will need to hit roughly 86% of their cost and release targets while releasing 1.6 fewer prototypes than competitors on average (Aberdeen Group, 2006). A large majority of respondents stated that simulation is used to avoid development delays and its incurred costs. In excess of 70% of respondents stated that simulation results are used to select or improve conceptual designs (Jackson, 2013).

When looking at the more detailed design phase, more than 75% of the respondents stated that simulation is used to refine or select ideas. In excess of 60% of respondents stated that using simulation reduces testing and prototyping and hence avoids downstream development delays and the costs associated. Through simulation based design refinements, companies

were able to better determine correct sizing and appropriate material selection, which in turn drives production costs down (Jackson, 2013). The results of the survey indicated that less than 10% of the respondents within major engineering fields did not make use of any simulation during their design process. It would therefore appear that simulation techniques such as FEA and CFD have become an industry standard.

2.2 The Finite Element Method

There are several problem areas of interest in engineering that are solvable through the use of an analytical mathematical solution. An analytical mathematical solution is one that is given by a mathematical expression which yields an exact value for the quantity of interest, at an infinite number of locations in a continuous domain. These analytical mathematical expressions generally require the solution of an ordinary or partial differential equation which may not be possible for problems involving complicated geometries, loading conditions or material properties. Hence there is a need to rely on alternate methods for the solution of complex engineering and mathematical physics problems. Subsequently, numerical methods have become a popular instrument in giving acceptable approximate solutions for these problems (Logan, 2012).

The finite element method (FEM) is the most commonly used class of numerical method (Logan, 2012). It is one of several approximate numerical techniques that can be used for the solution of engineering boundary value problems (Logan, 2012). The finite element formulation of a problem results in a system of simultaneous algebraic equations, as opposed to complex partial differential equations, which can be solved effectively by a modern computer (Logan, 2012). Numerical methods can only yield approximate solutions to unknown values at discrete points within a system. This means that applying the FEM to a continuous domain requires that the domain be represented as a collection of discrete points. The process of dividing a body into a finite collection of equivalent, interconnected, non-overlapping units, called elements, is known as discretization (Logan, 2012). The FEM formulates equations for each of the finite elements and then assembles the individual solution for the response of each element to create an overall solution for the response of the entire body of interest. In structural analysis, discretization of the model may involve either of the two discretization model types; the element-node model and the finite element model.

For simple beam and truss elements it is far more efficient to employ the element-node model of discretization. Here, structural elements are represented as individual beam/truss elements connected by nodes. Each node has 6 degrees of freedom (DOF) which can either be free or constrained. The geometric and material properties of the structure are characterized by the line elements which are able to simulate the structure's physical behaviour by following mathematical relationships. Figure 2-1 below shows a simple ladder structure represented as a discretized element –node model.

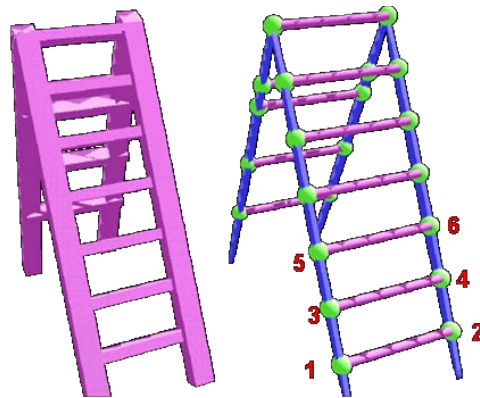


Figure 2-1. Ladder represented as a discretized element-node model (BSB Technocrats, 2016)

Models that contain more complex geometry cannot easily be discretised by the element-node model. The finite element model approach uses a meshing procedure to create a network of elements connected at nodes. Figure 2-2 below shows the discretization of a complex geometry using a finite element model.

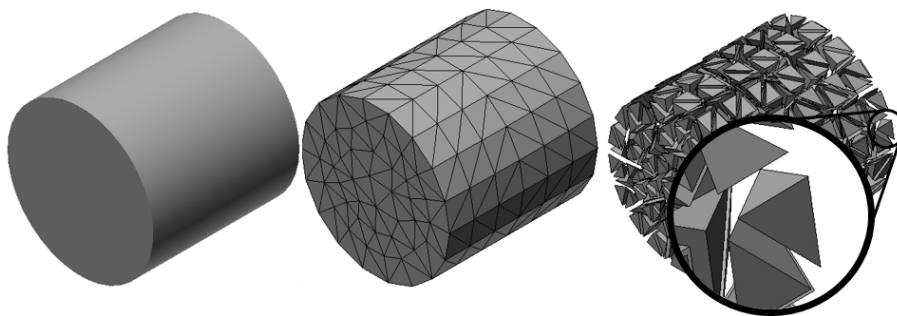


Figure 2-2. Complex geometry discretized using a finite element model (AU Workshop, 2014)

Note that other methods of general FEM with respect to computational solid mechanics such as vibrational analysis or modal analysis have not been discussed here as this research focuses only on static structural analysis.

There are two common direct approaches associated with the FEM when applied to structural analysis problems only (Logan, 2012). The first direct approach is called the *force* or *flexibility* method. This method sets the internal forces as the unknown quantities in the problem. The second direct approach is called the *displacement* or *stiffness* method. This method assumes that the displacements are the unknowns in the system of equations (Logan, 2012).

The direct *force* method has the ability to operate directly on the stress parameters and thus can potentially provide more accurate results as compared to the direct stiffness method. In the pre-computer era, when hand calculations were solely used, the direct force method was favoured because it results in a much smaller set of simultaneous equations. With the appearance of computers, a greater set of simultaneous equations did not prove to be a problem and thus the direct stiffness method became favoured due to the ease of automation and lower computational cost (Logan, 2012).

With respect to the direct stiffness method, the finite element provides a linear relation between nodal forces and nodal displacements. It seeks the solution first in terms of the displacements in the system. The displacements at the nodal points in the discrete model of the system contain the primary solution or the degrees-of-freedom in the system. The nodal points accept external forces to the system as well as transmit internal forces through the system (Logan, 2012). The finite element method creates a global system of equations in the form:

$$\mathbf{K}\bar{\mathbf{u}} = \mathbf{R} \quad (2.1)$$

Where: **K** - Stiffness matrix,
 $\bar{\mathbf{u}}$ - Displacement vector
 R - Body force vector

An element in the finite-element mesh can be understood to be analogous to a spring, except that the FEM mesh involves many degrees-of-freedom instead of just the one that a spring possesses (Kress, 2014). The governing equations for the system are obtained by firstly applying the equilibrium equations. For a finite size element or joint, a substructure, or a complete structural system, the following six equilibrium equations must be satisfied:

$$\begin{aligned} \sum F_x = 0 ; \sum F_y = 0 ; \sum F_z = 0 \\ \sum M_x = 0 ; \sum M_y = 0 ; \sum M_z = 0 \end{aligned} \quad (2.2)$$

Where F_i - Resultant force in the in the i direction

M_i - Moment about the i axis

Equilibrium equations in general are not sufficient to solve a structural analysis problem. They are indeterminate and thus determinacy must be achieved by adding compatibility conditions to the continuum. For solid mechanics problems, the compatibility conditions were first formulated in terms of strains for deformable bodies by St Venant in 1864 (Logan, 2012). A solution is compatible if the displacement at all points are not a function of a path. The compatibility conditions for a structural system of discrete elements require that elements connected at a common node, along a common edge or on a common surface prior to loading, must have the same absolute displacement (Logan, 2012).

For completeness, the general steps of the finite element method will be presented here with short descriptions, as well as important points to consider during these steps. Firstly, the system must be discretized into an equivalent system of finite elements, which is commonly referred to as a *mesh*. The element size as well as areas of mesh density refinement are a matter of engineering judgement which is developed through experience. It is important that the mesh uses element types that will be most capable of modelling physical reality. Table 2-1 shows the finite element types available and their appropriate uses (Logan, 2012).

The next step is the definition of the displacement function that will be used for the finite element formulation. The strain-displacement and stress-strain relationships need to also be defined. These are necessary for defining the equations for small displacements. The strain is related to displacement by:

$$\varepsilon_i = \frac{du}{di} \quad (2.3)$$

Where ε_i - Strain for element i

u_i - Displacement of element i

Furthermore the stresses need to be related to the strains through a stress-strain law generally known as the Constitutive Law. The simplest stress-strain law used is Hooke's Law, which describes the elastic response of a body:

$$\sigma = E \varepsilon \quad (2.4)$$

Where σ - Stress

E - Young's Modulus of Elasticity

So to summarize the above. The basic process is that the complete structure is idealized as an assemblage of individual structural elements. Element stiffness matrices corresponding to the global DOF for the structure are calculated, and the total stiffness matrix is formed by the addition of each element stiffness matrix. The solution of the global system of equations yields the element displacements, which are used to calculate element stress (Bathe, 1996).

Considering the analysis of beam or truss assemblages, there is a difference in these solutions when compared to a general analysis of a 2-D or 3-D problem. With 1-D truss or beam problems, the exact element stiffness matrices can be calculated. The stiffness properties of a beam element are physically the element forces that correspond to the end displacements. These forces can be evaluated by solving the equations of the element when subjected to the appropriate boundary conditions. All three requirements of an exact solution, with respect to beam theory, namely stress equilibrium, the compatibility requirements and the constitutive requirements throughout each element are fulfilled. Hence the exact element internal displacements and stiffness matrices are calculated. In an alternative approach, the element forces could also be evaluated by performing a variational solution based on the Ritz method or the Galerkin Method (Bathe, 1996).

When considering more general 2-D or 3-D finite element analyses, variational approaches are used with functions that approximate the actual displacements because the exact displacement functions are not known, unlike in the case of truss or beam problems. The result is that the equations are not satisfied in general, but the error is reduced as the finite element idealization of the structure is refined.

Usually, the principle of virtual displacements is used in the general formulation of the FEM, however the use of the Galerkin method or the Ritz method yields equivalent results. These methods, however will not be presented here. The principle of virtual displacement is discussed. Consider a general 3-D body with an 8-node 3-D element mesh. Note that the notation used is that which is presented by Bathe (Bathe, 1996).

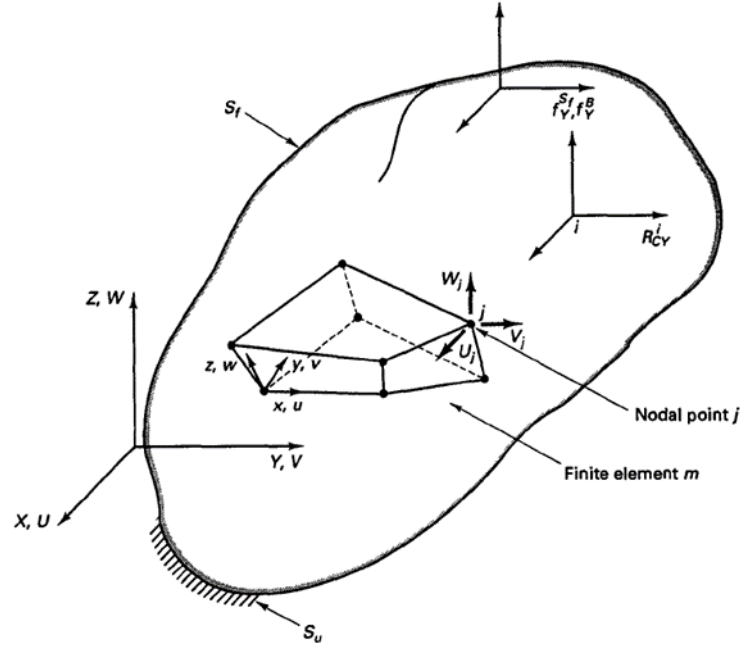


Figure 2-3. General 3-D body (Bathe, 1996)

Consider the body shown in Figure 2-3, fixed within the coordinate system. The body is constrained on the area S_u with prescribed displacement U^S_u and being subjected to surface force f^{Sf} on surface S_f . The body is also subjected to externally applied body forces f^B , and concentrated point load R_c^i , imposed at point i . These external forces would have three components corresponding to the X, Y, Z coordinate axes:

$$f^B = \begin{bmatrix} f_x^B \\ f_y^B \\ f_z^B \end{bmatrix} \quad f^{Sf} = \begin{bmatrix} f_x^{Sf} \\ f_y^{Sf} \\ f_z^{Sf} \end{bmatrix} \quad R_c^i = \begin{bmatrix} R_{cx}^i \\ R_{cy}^i \\ R_{cz}^i \end{bmatrix} \quad (2.5)$$

The displacements of the body in the unloaded configuration are measured in the coordinate system X, Y, Z and are denoted by U , where:

$$U(X, Y, Z) = \begin{bmatrix} U \\ V \\ W \end{bmatrix} \quad (2.6)$$

$\mathbf{U} = \mathbf{U}^{\text{su}}$ on the surface S_u . The strains corresponding to \mathbf{U} are the normal strains ϵ and the engineering shear strains γ :

$$\boldsymbol{\epsilon}^T = [\epsilon_{xx} \ \epsilon_{yy} \ \epsilon_{zz} \ \gamma_{xy} \ \gamma_{yz} \ \gamma_{xz}] \quad (2.7)$$

Where:

$$\begin{aligned} \epsilon_{xx} &= \frac{\partial \mathbf{U}}{\partial x}; & \epsilon_{yy} &= \frac{\partial \mathbf{U}}{\partial y}; & \epsilon_{zz} &= \frac{\partial \mathbf{U}}{\partial z}; \\ \gamma_{xy} &= \frac{\partial \mathbf{U}}{\partial y} + \frac{\partial \mathbf{V}}{\partial x}; & \gamma_{yz} &= \frac{\partial \mathbf{V}}{\partial z} + \frac{\partial \mathbf{W}}{\partial y}; & \gamma_{xz} &= \frac{\partial \mathbf{U}}{\partial z} + \frac{\partial \mathbf{W}}{\partial x} \end{aligned} \quad (2.8)$$

The stresses corresponding to ϵ are:

$$\boldsymbol{\tau}^T = [\tau_{xx} \ \tau_{yy} \ \tau_{zz} \ \tau_{xy} \ \tau_{yz} \ \tau_{xz}] \quad (2.9)$$

Where:

$$\boldsymbol{\tau} = \mathbf{C} \boldsymbol{\epsilon} + \boldsymbol{\tau}' \quad (2.10)$$

\mathbf{C} in equation 2.10 is the stress-strain material matrix and the vector $\boldsymbol{\tau}'$ is the given initial stresses.

Assume linear analysis conditions, which require that:

- The displacements be small
- The equilibrium of the body can be established with respect to its unloaded configuration
- The stress-strain matrix can vary as a function of X, Y, Z but is constant otherwise, i.e. C does not depend on current state of stress.

The basis of the finite element solution is the principle of virtual displacement, also referred to as the principle of virtual work. The principle states that the equilibrium of the body requires that for any compatible small virtual displacements imposed on the body in its state of equilibrium, the total internal virtual work is equal to the total external virtual work:

Internal virtual work = External virtual work

$$\int \bar{\boldsymbol{\epsilon}}^T \boldsymbol{\tau} dV = \int \bar{\mathbf{U}}^T \mathbf{f}^B dV + \int \bar{\mathbf{U}}_{S_f}^T \mathbf{f}_f^S dS + \sum_i \bar{U}^{iT} R_C^i \quad (2.11)$$

Where $\bar{\mathbf{U}}$ denotes the virtual displacements and $\bar{\boldsymbol{\epsilon}}$ denotes the corresponding virtual strains. The “virtual” term used denotes that the virtual displacements are not real displacements which the body actually experiences as a result of the applied loading on the body. Instead, the virtual displacements are totally independent from the actual displacements and are used only to establish the integral equilibrium equation seen in (2.11).

In equation (2.11)

- The stresses $\boldsymbol{\tau}$ are unique stresses that exactly balance the applied external loads.
- The virtual strains $\bar{\boldsymbol{\epsilon}}$ are calculated by the differentiations given in 2.8 from the assumed virtual displacements.
- The virtual displacements $\bar{\mathbf{U}}$ must represent a continuous virtual displacement field, to be able to evaluate $\bar{\boldsymbol{\epsilon}}$, with $\bar{\mathbf{U}}$ equal to zero on S_u . $\bar{\mathbf{U}}_{S_f}$ are the virtual displacements evaluated on the surface S_f .
- All integrations are performed over the original volume and surface area of the body, unaffected by the imposed virtual displacements.

When the principle of virtual displacements is satisfied with the stresses $\boldsymbol{\tau}$ properly obtained from a continuous displacement field, \mathbf{U} , that satisfies the displacement boundary conditions on S_u , all three fundamental requirements of mechanics are satisfied:

1. Equilibrium hold, as this principle is an expression of equilibrium.
2. Compatibility holds because the displacement field, \mathbf{U} is continuous and satisfies the displacement boundary conditions.
3. The stress-strain law holds because the stresses have been determined using the constitutive relationships from the strains.

Thus far it has been assumed that there is sufficient support conditions on the body for a unique displacement solution. The principle of virtual displacement also holds when all displacement supports are removed and the correct reaction forces are applied instead, assuming these are already known.

2.3 The Process of Finite Element Analysis

FEA programs can perform complex analyses in relatively small amounts of time. Their user interfaces have become more aesthetically pleasing, convenient and, for a user with the necessary theoretical background, self-explanatory (Mac Donald, 2011). This section will examine the computational finite element analysis process and focus more on the practical procedure of going from a physical problem to generating a corresponding finite element solution. It was decided to conduct a further study into the practical procedures of conducting a computational FEA so that reliable models may be generated in this research.

Figure 2-4 represents the basic overview of the FEA process, adapted from (Mac Donald, 2011).

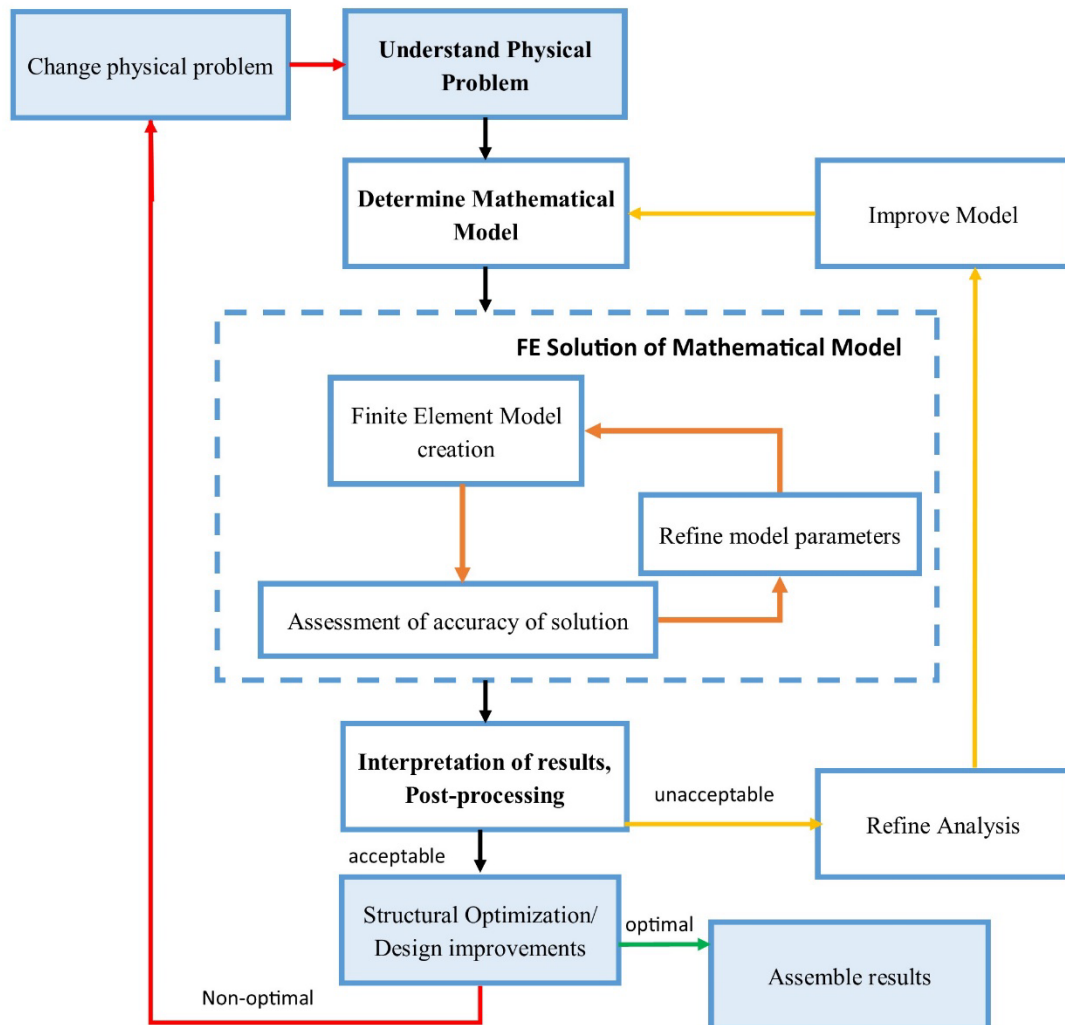


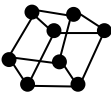
Figure 2-4. Basic overview of the computational FEA process

1. Understand the Physical Problem: The accuracy of the entire process is based purely on the expertise of the analyst displayed at this step of the analysis. The design objective must be outlined. The purpose of the study as well as the quantities of interest must be known. This step should see the analyst identifying all the distinctive features of the domain. The material properties and loading conditions must also be identified (Mac Donald, 2011).

2. Determine the Mathematical Model: Once the essential features of the physical model have been identified, it is necessary to translate these into a mathematical representation of the problem. This stage involves two tasks. Firstly, it is required that the problem domain be defined i.e. the physical shape of the problem. This step usually entails the creation of appropriated CAD geometry or an assemblage of nodes and elements. Secondly, a mathematical formulation best representing the physical problem must be selected. A practical example would be the requirement of plane strain on an axisymmetric component. This can be achieved using a two-dimensional element model which can be used due to the presence of symmetry. The identification of what element type to use at this point before discretization is crucial as it greatly influences solution time and computational cost of the model (Mac Donald, 2011).

3. Finite Element Solution of the Model: This step encompasses various aspects of the creation of the finite element model process as seen in Figure 2-4. The first step in this process is the finite element model creation. This starts off with model discretization. Once the element type and mathematical formulation is selected, the next step is to actually divide the model into the specified elements. Most commercial FEA software can automatically discretize the model using automatic mesh generators. Auto-meshing cannot necessarily predict occurrences such as areas of localized stress and will in such cases not be able to rationalize the need for mesh refinement. Thus the analyst will need to specify refinement based on the understanding of the physical problem as well as engineering experience (Mac Donald, 2011). Table 2-1 shows an overview of typical structural finite elements.

Table 2-1. Overview of typical structural finite elements

Basic Shape	Representative Geometry	Application
Point		Mass Elements
Line		Truss/ Spar Element Spring Element Beam Elements Pipe Elements Axisymmetric Shell Elements 2-D Contact Elements 2-D surface Effect Elements
Area	  Triangular Quadrilateral	2-D Surface Element - Plane Stress - Plane Strain - Axisymmetric - Plate Element
Volume	  Tetrahedral Hexahedral	3-D Solid Element

Following discretization, boundary conditions are applied to the model. The locations and types of boundary conditions are based on the understating of the physical problem. Table 2-2 shows typical constraints that are encountered and Table 2-3 shows several loading conditions that can be applied in structural FEA problems. The contents of these tables were both adapted from (Mac Donald, 2011).

Once the model is created, the computational strategy must be selected. For each particular problem, the user must select a particular solution method, and if applicable, the time step or load step size. At this point, the solver is generally set to solve the problem. A common problem experienced with non-linear or transient problems is solution convergence within the given time steps. Generally there would not be any indication of how to fix the error and hence fixing the error would rely on the experience of the analyst (Mac Donald, 2011). Once results are obtained, an experienced analyst would be able to assess the quality of results and make a judgement as to the acceptability of the results. If it is seen that there is a potential that key areas were not adequately captured by the mesh or that the solution results deviate from what was expected then the model parameters should be refined in order to better analyse the problem (Mac Donald, 2011).

Table 2-2. Typical boundary constraints encountered in Structural FEA

Boundary Constraint	Description
Fixed Support	This is the most basic type of boundary condition. It constrains a specified region of the model in all degrees of freedom (DOF)
Frictionless Support	This constraint allows for only one degree of freedom to be constrained. It is useful when modelling effects of adjoining structures to prevent the model moving across boundaries.
Symmetry Constraint	These are frictionless constraints imposed on symmetry cut planes.
Multipoint Constraint (MPC) / Coupled DOF	Applying a constraint to a single node will result in stress concentrations (singularities) around the node. An MPC avoids singularities by creating a master node, to which a constraint is applied, and multiple slave nodes. The slave nodes follow the behaviour of the master, thus coupling the nodes.
Forced Displacement	A location in space where a selected group of nodes will be at the end of the analysis is specified, rather than a force or pressure. This forces nodes to move to a location and hold this position.
Constraints with Coordinate Systems	These are constraints that are assigned to a defined coordinate system. These constraints are useful when applying supports that are inclined at an angle to the global coordinate system.
Time-Varying Constraints	This implies that the constraint changes in some manner during the course of the simulation. An example of this is contact problems. A model will be unconstrained until it comes into contact with other bodies.

Table 2-3. Typical Loads encountered in Structural FEA

Load Type	Description
Force	This is the most basic type of load. Forces can be applied as single values for static analyses with small deflections or time varying when large deflections are expected.
Moment	Moments/Torque can be directly applied to nodes provided they have free rotational degrees of freedom.
Pressure	These loads can be applied to edges of 2-D and faces of 3-D geometry. Pressure loads generally act perpendicularly to the edge or surface selected.
Velocity	Linear velocities can be applied to groups of nodes. These are usually only used for non-linear analyses such as impact analysis or material forming analysis.
Acceleration	Acceleration loads are also used in dynamic analyses and impact analyses. The most common acceleration load used is gravity
Non-Linear Loads	<p>There are 3 types of non-linear effect loads.</p> <p>Large deformation loads, which cause the structure to greatly deform and hence need to be applied incrementally.</p> <p>Contact loads, which occur when two bodies intersect and deform against each other.</p> <p>Follower forces, which are locally defined in relation to a node. This force will adjust its orientation as the structure deforms to maintain a specific application angle relative to the chosen node.</p>
Multiple Loads and Load Steps	The structure has multiple loads specified. These can all be applied in one load step simultaneously or over multiple load steps, separately. The loads can be anything from forces to pressure loads etc.

4. Interpretation of Results, Post-Processing: In this step, the results must be interpreted before any information can be used to make design decisions. One must determine if the model accurately represents the physical problem. In the results of a structural FEA, each node in the finite element mesh will have a corresponding displacement. Post processing converts these displacements into more useful results such as contour plots of stress or strain throughout the domain.

It is important to check results and determine if the results obtained are realistic. An analyst should ask certain questions about the result such as:

- Has the yield or ultimate tensile stress been exceeded?
- Are displacement magnitudes excessive?
- Are stresses/strains excessively large?
- Do stresses /strains transition smoothly throughout the domain?
- Are expected errors acceptable?

Figure 2-5 shows a general procedure for the interpretation of structural FEA results adapted from (Mac Donald, 2011)

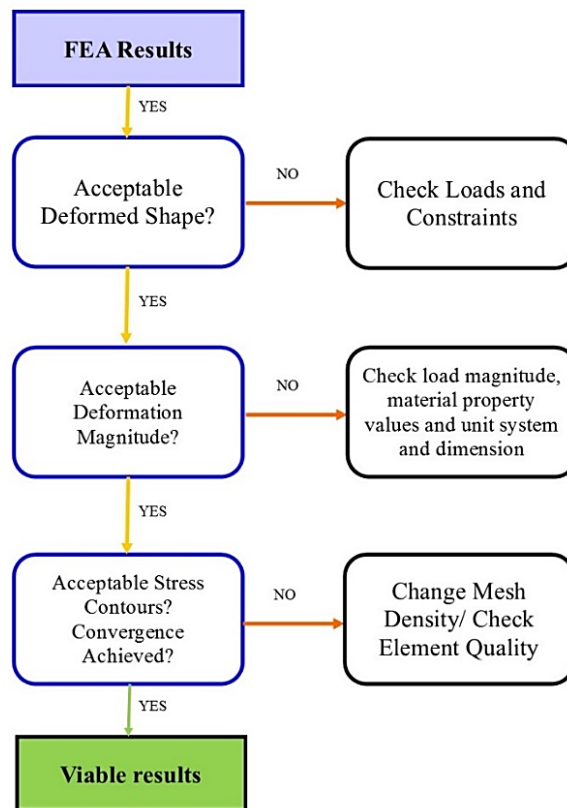


Figure 2-5. General procedure for the interpretation of post-processing structural FEA results

If the model is checked and found to be viable based on the obtained results, then the next stage is to validate the solution results against experimental results or analytical solutions. If the error observed is too significant then assumptions made at the beginning of the modelling process must be re-evaluated and further analysis cycles would be required.

2.4 Errors and Uncertainty Present During the FEA Process

Finite element analyses are approximations of physical systems and are subject to several types of error that can compromise the accuracy of the solution. Various sources of error must be identified and addressed to ensure a reliable model can be created. According to (Liang and Mahadevan, 2011), the error present in computational analyses comprises of two parts, namely: the model form error, E_{model} , and the numerical error E_{num} . There are mathematical models and extensive theory concerning quantifying numerical and model form error, however these require access to the original partial differential equations of the system (Oden et al., 2005). It would be impossible to employ these methods on most FEA packages and they function as a ‘black box’. A simplified approach to error quantification for the computational code is presented by (Rebba et al., 2006). Assuming the true response of the system is denoted as X_{true} and the predicted model value is X_{pred} , it follows that:

$$X_{true} = X_{pred} + E_{model} + E_{num} \quad (2.12)$$

The model form error depends on the ability of the selected numerical model to properly analyse the real phenomena of the physical system. Examples of this would be the choice of linear-elastic versus elasto-plastic material models or small deformation versus large deformation. The model form choice affects the outcome of numerical error and hence the two error types are not independent (Liang and Mahadevan, 2011).

The three typical numerical error components are: user input error, surrogate model error and discretization error (Liang and Mahadevan, 2011). Input error can take the form of a simple typographical error for material properties or boundary conditions. User errors can also arise from improper use of the FEA package. Ideally, a computational model will have the same properties as that of the physical system. In practice, the reported values of the system are subject to factors such as measurement error, instrumentation error and experimental condition variability. Using these measured values subjects the computational model to this input error, as the actual system varies from the reported values. User error can be mitigated by developing a comprehensive checklist that reviews and verifies all inputs of the model match the exact system values (Shah, 2002). Improper use of a package can be prevented by obtaining a better understanding of FEA theory and appropriate training in the software being used (Shah, 2002).

Often, it is too computationally expensive or complex to create a completely accurate system, hence many assumptions and simplifications are made. A surrogate model, which is computationally much cheaper, can be used (Liang and Mahadevan, 2011). Geometrical simplifications may be made to reduce run times and keep model sizes manageable. Loading and boundary constraints may be approximated, for these may not be accurately known or be impractical/impossible to apply (Shah, 2002). If the assumptions and the significance of simplifications made becomes excessive, the accuracy of results may be compromised. The only way to mitigate this error is to increase the complexity of the model. The success of this error alleviation method is based on the expertise and ability of the analyst.

The error due to unsuitable discretization of the domain is denoted as the discretization error component of E_{num} (Liang and Mahadevan, 2011). Using an inappropriate element type will introduce further error into the system. Furthermore, if a mesh is too coarse, it may not capture the true response of the component properly. If the mesh is too coarse in areas of high stress, the gradients in the response values will not be accurately predicted (Shah, 2002). There are several methods for error estimation in boundary value problems associated with computational solid mechanics including: explicit error estimation methods, element residual methods, extrapolation methods, to name a few (Liang and Mahadevan, 2011). These methods provide a means of identifying relative error (used in the implementation of adaptive mesh refinement algorithms) but do not help quantifying the actual error. Mesh discretization errors can be mitigated by evaluating the quality of a mesh and developing an ability to evaluate the adequacy of the mesh through experience (Shah, 2002).

2.5 Significance of Verification and Validation

The discussion above has shown that FEA has become an increasingly valuable tool in design and the analysis of engineering problems. Several critical industries make imperative decisions based on the results of computational models (Jackson, 2013). The credibility of these results are seldom questioned by the decision makers. Complete trust is placed in the analyst and the software code used. Simple problems in structural mechanics can be solved and verified analytically. Peer review for these types of problems have generally been considered sufficient. With the increasing complexity of solid mechanics problems and increased reliance on computational methods for solving these problems, there is a need for verification and validation of the approach used for solving these problems (American Society for Mechanical Engineers, 2006). Analysts need to ensure that the approximate

solution of the physical problem being modelled is appropriate for answering specific questions about the system. Primarily, an analyst should endeavour to establish that the accuracy of a computational model is adequate for its intended use, as the accuracy requirements vary from one problem to the next. The verification and validation process is one in which evidence is generated, therefore credibility is established that the computational model has sufficient accuracy for the intended use (Szabó and Babušk, 2011).

The concept of systematic verification and validation is not a new one, with several groups in physics and engineering adopting application-specific verification and validation practices (American Society for Mechanical Engineers, 2006). Members in the Computational Solid Mechanics (CSM) field formed a committee which undertook the task of creating a guide on verification and validation of CSM models (American Society for Mechanical Engineers, 2006). This document, titled “Guide for Verification and Validation in Solid Mechanics”, and published by the American Society of Mechanical Engineers, aims to explain the principles of the verification and validation process so that analysts can better understand how decisions made can impact the credibility of the models generated.

It is stated that *verification* must always precede *validation*. To disambiguate these two terms, verification is concerned with the numerical accuracy of the computational model. *Code verification* addresses the errors in the software used to perform the analysis. (American Society for Mechanical Engineers, 2006). The individuals responsible for the proper function of the code are the code developers themselves (Szabó and Babušk, 2011). *Calculation verification* is concerned with the numerical errors created due to the inherent nature of a discrete representation of a system being only an approximation of the real continuous system (American Society for Mechanical Engineers, 2006). Note that for verification, the term “accuracy” is understood to be with respect to the exact solution of the mathematical model, not with respect to physical reality (Szabó and Babušk, 2011)

Validation assesses the degree to which the computational model represents the physical system being analysed. Validation is based on comparisons between the simulation and relevant experimental data. Through validation, the analyst must assess the predictive capability of the computational model and address the uncertainties that exist, the experimental and the computational procedures. (American Society for Mechanical Engineers, 2006). For a validation experiment, one or more metrics and the corresponding target results are defined. If the predictions meet the expected criteria within a specified accuracy, then the model is said to have passed the validation test, otherwise the model is rejected and model refinement is required (Szabó and Babušk, 2011).

The verification and validation process should be done concurrently with the generation of the model. *Code verification* should be done prior to the generation of the finite element model and *calculation verification* should be done to ensure that the correct numerical method is used to obtain results (American Society for Mechanical Engineers, 2006).

The final step entails documenting of the entire process. The essence of conducting verification and validation is to gather evidence and justifications for the decisions made during the creation of the computational model.

2.6 Different Licensing Approaches for FEA Packages

The licensing approach of a software package determines the restrictions and rights given to users of the software. Commercially available software packages generally have a private proprietary licence with their own custom terms and conditions of use. No-cost packages are often associated with the terms “open source” or “freeware”. For small businesses or academic research institutions desiring to make use of an FEA package, it is important that they are aware of the licensing approach of that particular package. This section aims to explain the terms used to describe the licensing approaches available.

2.6.1 Commercial Proprietary Software Licences

Proprietary software is owned by an individual or company who retains the rights to dictate the use of their software. Users are restricted with regards to aspects such as terms of use, distribution as well as access to the software’s source code. The source code of software is the form of the program that was originally written by the software developer before being converted to machine code, which is a form readable by a computer’s processor. Access to the source code is necessary if one wishes to modify or improve a program (The Linux Information Project, 2005). For example, a user would not be able to view the code used by ANSYS to conduct composite analysis calculations so that it they may copy it and add it to their own proprietary software. Trusted commercial FEA packages such as MSC/NASTRAN are examples of packages under custom proprietary licences, each having their own terms of use.

There are some that believe the prominence of proprietary software will decrease in the future due to the rising competition of suitable free software. This shift towards free software may not be as noticed in certain niche markets where the demand from industries and

businesses are relatively small and users are willing to pay relatively high prices to ensure a quality product is obtained (The Linux Information Project, 2005).

2.6.2 Open Source Software Licences

The term “open source” is often misunderstood to mean a software that is simply free of cost. The fundamental concept is that it is publicly accessible and free to be modified and shared (opensource.com, 2015). This freedom may not have any impact on an analyst who wants a package that is reliable and provides relatively accurate simulations to help drive their designs. However, the ability to modify the source code of a software may be useful to researchers who wish to modify existing code to suit their custom needs. Open source software packages are generally licensed under a version of the GNU General Public License (GNU Operating System, 2007).

2.6.3 Freeware

As the name would suggest, freeware is software that is free to use. Freeware does not require initial payment or licensing fees. Users are able to legally download and operate freeware software packages, however there are generally some restrictions. While being free to use, it still is copyrighted, and unlike open source software, users do not have access to modify the source code (opensource.com, 2015). There are FEA packages such as Mecway (Mecway, 2014) that release freeware versions with simulation restrictions, in an attempt to display the capabilities of the package and entice users to purchase the full version.

2.7 Independent Studies Conducted on the Performance of No-Cost/Low-Cost FEA Software Packages

A literature review has revealed that there is a noticeable lack of literature concerning the performance and solution accuracy of no-cost/low-cost FEA packages. This section assesses independent studies in the area of no-cost/low-cost FEA package performance conducted by other researchers. It was noted that there are several discussion forums on reputable engineering and research internet websites that are focused on discussing available open source and low cost packages. There is an active discussion thread on the academic research collaboration website, ResearchGate titled “What is the best open source finite element software for mechanical problems?” which was started by a user in January 2014 and is still actively contributed to (researchgate.net, 2014). There is another forum hosted on Quora

(quora.com, 2014) where a user posed the same basic question: “What is the best open source FEA package?”. The responses given were based on the user’s experience with using the software, the usability and the GUI. More often than not, it was observed that no mention was made of the solver or meshing capabilities within the package. There was almost no mention of any benchmarking or standards that were used to validate the software.

During the literature review, a very insightful series of books written by (Thakore, 2014) were found. One of these books, “*Finite Element Analysis using Open source Software*” discusses the process that Thakore goes through to conduct full finite element analyses on structures using an open source FEA Package. Thakore goes into great detail about the user interface and functionality of the popular open source FEA package, Code_Aster bundled with Salome Meca. This text is comprehensive and practical but no emphasis was placed on benchmarking or validation efforts.

The contents of several online forums for open source FEA package were also examined. It was evident that there is an active community of researchers and analysts making use of open source FEA packages. One particular article was rather insightful. The author of the article, who has a background in the electronics industry, made use of two open source FEA packages, Salome Meca and Elmer, to model the thermal spreading between two dissimilar materials. It was interesting to note the method used by the analyst. An analytical solution was used as the benchmark to test the accuracy of the two packages. The geometry and loading conditions were kept constant on both the packages and the deviation was described as a percentage error from the calculated analytical solution. A qualitative analysis was also offered based on the authors overall impression of the packages (Ellison, 2013).

One piece of work found that is relevant to this research was a paper written by (Galeano et al., 2007). This paper is titled “General Public License Tools for Finite Element Modelling”. This paper was a mostly qualitative comparison of several open source FEA packages. The major portion of the research focused on the presence of internal modules and the reported capabilities of the packages. Also included were the author’s personal ratings of usability, user interface quality, access to documentation as well as end user support. There was some investigation into the performance of the packages through an attempt to benchmark the packages solvers against the results generated by ANSYS for a few thermal and structural problems. It was noted that there was no mention or reference to any accepted benchmarking standards or analytical results whatsoever.

2.8 No-Cost/Low-Cost FEA Package Investigation

Details of the initial research that investigated eighteen no-cost/low-cost FEA packages and three proprietary FEA packages can be found in Table A.1 of Appendix A. This section only presents the no-cost/low-cost FEA software packages that were considered to be more suitable for this research as compared to the other investigated packages.

2.8.1 Selected software Packages

CalculiX: CalculiX is an open source explicit and implicit finite element analysis suite with its own pre and post-processor available for download as well. The solver is based on a subset of the program Abaqus (Dhondt and Wittig, 2015). It was originally coded to be run on Linux OS but has since been ported to Windows (Dhondt and Wittig, 2015); (Convergent Mechanical, 2013).

Code_Aster/Salome Meca: Code_Aster is a freely available open source solver package commonly used in civil and structural engineering. It is most commonly used through Salome Meca, which acts as the GUI for pre and post-processing. It was developed by the French company, EDF and the software and documentation was previously only maintained in French (EDF-R&D, n.d).

Elmer: Elmer is a finite element software package that can be used for the solution of PDEs. Elmer can deal with many different types of equations, making Elmer a versatile tool for multiphysics problem simulation (Råback and Malinen, 2014).

LISA: LISA is a Windows based package that allows users to solve different problems in the engineering field using the finite element method. It is released as a freeware version of the full software which has all of the same capabilities as the full software but has a 1300 node limit for the model (LISAfea, 2013).

Mecway: Mecway is an inexpensive FEA package that is based on the original code of LISA. Mecway has a few more capabilities that LISA does not have. (Mecway, 2014)

Z88 Aurora: Z88 is a free, open source, cross platform package that can be used for the solution of various engineering problems through numerical simulation by the finite element method. There are 2 versions currently available. Z88 V14, an open source version lacking a pre-processor, and Z88 Aurora, a freeware version with built-in pre-processor (Rieg, 2014a).

2.8.2 Capabilities

Table 2-4 shows FEA capabilities of the chosen software packages. The scope of this research only concerns itself with linear and non-linear static structural FEA, however Table 2-4 also includes multi-body contact models, dynamic structural and composite material analysis. Fields denoted with * will not be investigated in this research study but are presented for informative purposes.

Table 2-4. Capabilities of selected no-cost/low-cost FEA packages

Package	Linear Static Structural analysis	Non-Linear Static structural analysis	*Multi-body Contact models	*Dynamic structural analysis	*Composite structural analysis
<i>CalculiX</i>	✓	✓	✓	✓	x
<i>Code_Aster/ Salome-meca</i>	✓	✓	✓	✓	✓
<i>Elmer</i>	✓	✓	x	x	x
<i>LISA</i>	✓	✓	x	✓	x
<i>Mecway</i>	✓	✓	✓	✓	✓
<i>Z88 Aurora</i>	✓	✓	x	x	x

2.8.3 Operating System

Many open source software packages began on the Linux operating system, however it is desirable for versions of software be compatible with different operating systems. The supported operating systems for the chosen packages can be seen in Table 2-5.

Table 2-5. Supported operating systems for selected open source FEA packages

Package	Linux	MS Windows	MAC OSX
<i>CalculiX</i>	✓	✓	x
<i>Code_Aster/ Salome-meca</i>	✓	✓	x
<i>Elmer</i>	✓	✓	x
<i>LISA</i>	x	✓	x
<i>Mecway</i>	x	✓	x
<i>Z88 Aurora</i>	✓	✓	✓

2.8.4 Internal Modules Present in Selected Packages

Information regarding the presence and capabilities of the pre-processor, solver and post-processor are found within Table 2-6.

Table 2-6. Internal modules present in selected no-cost/low-cost FEA packages

Package	Pre-Processor	Solver/Processor	Post-Processor
<i>CalculiX</i>	Allows for generation of geometrical entities, mesh generation, and specification of material types and boundary conditions. (Dhondt and Wittig, 2015).	The solver, CCX contains several linear and non-linear options as well as math libraries which give the program increased solution speed (Dhondt and Wittig, 2015).	The post-processor allows for viewing results in the form of scalar plots. It allows for output of results in graphical formats (Dhondt and Wittig, 2015).
<i>Code_Aster/ Salome-meca</i>	Salome-Meca is the pre-processor tool bundled with Code_Aster. It allows for importing CAD geometry, mesh creation and the generation of the command file needed for the solver (EDF, 2008).	Code_Aster contains both linear and non-linear direct and iterative solvers. (EDF-R&D, n.d).	Salome-Meca is the postprocessor tool used by Code_Aster. It can generate and export MED files which can be read by other external post-processing software, It can generate scalar plots for various phenomenon of interest (EDF, 2008).
<i>Elmer</i>	Elmer has built in pre-processor modules called ElmerGrid and ElmerGui which can convert an external mesh file into an appropriate file for use. These also generate the model by allowing physical properties and loading conditions to be input into the simulation (Lyly, 2014).	Elmer has a built in solver called ElmerSolver which is responsible for performing necessary finite element calculations. Solver type is not explicitly stated.	ElmerPost is the built-in post processor. The different modules of the package can be used independently and as such, the results from the solver can be used in third party graphical post processing tools as well (Råback and Malinen, 2014).
<i>LISA</i>	Built in pre-processor which allows for import of CAD geometry as well as geometry definition. Mesh files can be imported or mesh can be generated within LISA. LISA has an included materials library and allows for the application of various types of loads and constraints. (LISAFE, 2013).	Type of built-in solver used is not explicitly stated.	Built in postprocessor used for the graphical representation of solution results. Able to do contour plots as well as animated deformation plots. Result can be written to files and exported to external graphical post-processing .software. (LISAFE, 2013).
<i>Mecway</i>	Built in pre-processor which allows for CAD geometry import as well as geometry allows for geometry construction. Contains an auto-mesher and allows for user to create a manual mesh. Contains a wide variety of element types, loading conditions, constraints and material types. Allows user to input custom material properties.(Mecway, 2014).	Type of built-in solver used is not explicitly stated.	Built in postprocessor used for the graphical representation of solution results. Able to do contour plots as well as animated deformation plots. Result files can be written to files and exported to external graphical post-processing software. (Mecway, 2014).
<i>Z88 Aurora</i>	Allows users to import CAD geometry and provides a variety of meshing options Pre-processor contains and editable and expandable materials library and allows for various boundary condition to be applied (Rieg, 2014b).	Z88 contains 4 direct numerical solvers, an iterative solver for large displacement problems, and a solver for frequency analysis. (Rieg, 2014b)	Contains a built-in postprocessor which allows for the visualization of the results in the form of scalar plots. Results can also be exported in text format (Rieg, 2014b)

2.8.5 Compatible File Types

Geometry created in external CAD modelling software may not be in a format native to the FEA package. It is advantageous for a package to allow for a range of file type imports. It would also be beneficial for a package to allow for a range of file type exports. The available file type import/exports for the chosen software packages are indicated in Table 2-7 .

Table 2-7. File types compatible with selected FEA packages

Package	Import	Export
<i>CalculiX</i>	Internal CAD translation tools to allow for the import of CAD geometry and mesh files.	Allows for several different file types to be exported including postscript and .xwd. Can also generate main files for Code_Aster.
<i>Code_Aster/ Salome-meca</i>	Generated mesh files and CAD files of various formats.	Code_Aster generates a MED file which can be exported to Salome Meca or any other compatible post-processing software in order to view results of solution.
<i>Elmer</i>	Generated mesh files.	Output file type not explicitly stated in reviewed resources.
<i>LISA</i>	CAD geometry import: .iges, .step. Generated mesh files e.g. Gmsh, NetGen.	Users are able to export a model results as an image file, stereolithography (binary or ASCII), and VRML format.
<i>Mecway</i>	CAD geometry import: .iges, .step. Generated mesh files e.g. Gmsh, NetGen.	Can export result files in VRML format to graphical processing tools to generate contour plots.
<i>Z88 Aurora</i>	CAD geometry import capabilities Generated mesh files.	Allows for FE structure data such as ANSYS, NASTRAN and ABAQUS files to be exported.

2.8.6 User Support and Documentation

It is important for analysts to have easily accessible and coherent reference documentation available to them when using a package. It is also beneficial to have an active user community discussion forum to accelerate the flow of knowledge between users. Table 2-8 contains findings regarding user support and documentation for the selected packages.

Table 2-8. User support and documentation available for selected FEA packages

Package	Findings
<i>CalculiX</i>	Helpful online documentation found on the organisations webpage. Active discussion forum linked to the webpage. No indication as to latest stable release date from CalculiX website. An independent company has ported the CalculiX software to windows and has released a free stable version
<i>Code_Aster / Salome-meca</i>	Documentation is presented in French. Machine translations of these documents exist but are difficult to follow. Active development and community.
<i>Elmer</i>	Documentation is freely and easily available from the package website. The last stable release of the package was in February 2013 however development is still continuing. There is an organisational webpage that exists purely as a host for an active community driven discussion forum.
<i>LISA</i>	Very helpful beginner user guides available from organisations webpage. Last stable version released in 2013. No dedicated community discussion forum found
<i>Mecway</i>	Mecway has a community discussion forum linked to the organisations webpage. The webpage contains links to manuals and tutorial guides as well as background theory which is freely available to users. Mecway offers free technical support to its users through links on the webpage.
<i>Z88 Aurora</i>	Theory guide and user manual available from organisation webpage. Links to several video tutorials. Links to community discussion forums on the webpage.

2.8.7 Software Pricing

Table 2-9 shows associated upfront purchase price per year for the investigated FEA packages.

Table 2-9. Costs associated with chosen packages

Package	Purchase price	Training material costs	Support resources
<i>CalculiX</i>	Free	No evidence of training courses available	Freely available
<i>Code_Aster / Salome-Meca</i>	Free	Freely available online training courses supplied by developer.	Freely available
<i>Elmer</i>	Free	No evidence of training courses available	Freely available
<i>LISA</i>	USD 99.99 per year per licence.	No evidence of training courses available	Freely available
<i>Mecway</i>	USD 99.99 per year per licence.	No evidence of training courses available	Freely available
<i>Z88 Aurora</i>	Free	No evidence of training courses available	Freely available

2.9 Premium Commercial FEA Package Investigation

This section lists three commercial FEA packages available at UKZN. The inclusion of one or more proprietary FEA packages in the research was done so that a comparative analysis can be done on the variance of solution accuracy between no-cost/low-cost FEA packages and trusted commercial packages. These packages were investigated and presented so that a direct comparison can be made between what is offered by the low-cost/no-cost packages and the premium packages.

2.9.1 Selected Software Packages

ANSYS Mechanical: ANSYS Mechanical is a module within *the ANSYS Workbench* package. It is able to offer comprehensive solution to structural linear and non-linear analysis. The product is capable of providing a variety of element types, loading conditions, material models and solvers. (ANSYS inc, 2013)

Siemens NX: Nastran has been a trusted FEA Solver for over 40 years. It is used in industries such as aerospace, automotive, electronics as well as structural design industries. Siemens PLM offers the Nastran solver as a standalone solver, NX NASTRAN or bundled with their NX CAE package, which serves as a CAD Modeller, a pre-processor and a postprocessor (Siemens PLM Software, n.d).

Solidworks Simulation: Solidworks Simulation is an additional module within the Solidworks CAD software. Introduced in 2014, this module gives users access to FEA capabilities within Solidworks (Dassault Systèmes SolidWorks Corp, 2015).

2.9.2 Capabilities

Table 2-10 denotes the capabilities of each proprietary software investigated.

Table 2-10. Analysis capabilities of available commercial FEA packages

Package	Linear Static Structural analysis	Non-Linear structural analysis	*Multibody Contact models	*Dynamic structural analysis	*Composite structural analysis
<i>Ansys Mechanical</i>	✓	✓	✓	✓	✓
<i>Siemens NX</i>	✓	✓	✓	✓	✓
<i>Solidworks Simulation</i>	✓	✓	✓	✓	✓

Note: Fields denoted with * will not be investigated in this research study but are presented for informative purposes in the event that this research is expanded to include those capabilities in the future.

2.9.3 Operating Systems

The different available operating system versions for the chosen software packages are shown in Table 2-11.

Table 2-11. Supported operating systems for available commercial FEA packages

Package	Linux	MS Windows	MAC OSX
<i>ANSYS Mechanical</i>	✓	✓	x
<i>Siemens NX</i>	✓	✓	x
<i>Solidworks Simulation</i>	x	✓	x

2.9.4 Internal Modules

Table 2-12 denotes the internal modules contained within the chosen software packages.

Table 2-12. Internal modules present in available commercial FEA packages

Package	Pre-Processor	Solver/Processor	Post-Processor
<i>ANSYS Mechanical</i>	ANSYS Mechanical contains a comprehensive pre-processor that allows for various CAD file types to be imported. It allows for simple geometry creating. It can deal with shell and solid elements and has extended capabilities to deal with composite layup analysis. It has an automatic mesh generator and adaptive mesh refinement tools. The pre-processor in ANSYS Mechanical also allows for several loads and boundary conditions. (ANSYS inc, 2015).	ANSYS contains a library with both direct and iterative solvers. The user can select the solver that they wish to use or allow ANSYS to control which solver is used (Poole, 2002).	ANSYS Mechanical has built-in post-processing capabilities to generate reports. It allows for the generation of contour plots, vector displays, iso-surface displays. It can generate files that can be exported to text editing software as well as other graphical processing software (ANSYS inc, 2013).
<i>Siemens NX</i>	The NX CAE environment supports various loading and boundary conditions. It allows for adaptive meshing which provides better solution convergence. Geometry can be created by the CAD modeller within this environment.	NX Nastran is the FE solver capable of linear and non-linear analysis as well as dynamic response (Siemens PLM Software, 2012).	NX CEA environment allows results to be graphically viewed in the form of contour plots and animated plots.
<i>Solidworks Simulation</i>	Built in pre-processor which allows for the creation of appropriate mesh and the addition of material properties. Loading conditions as well as boundary constraints can be specified. Solidworks Simulation has the advantage of being bundled into the Solidworks CAD modeller which means that geometry creation and import into the Simulation module is seamless.	Solidworks Simulation makes use of two direct solvers and one iterative solver. The software package can be set to auto select solvers and will do so based on problem type, analysis options, contact types etc. (Dassault Systèmes SolidWorks Corp, 2015)	Module has a built in postprocessor. The postprocessor has the ability to create contour plots, animated deformation plots as well as vector plots. Results can be viewed in the post-process or can be viewed in an automatically generated report which gets exported as a Word file.

2.9.5 Compatible File Types

The allowable file type import/export for the software packages are indicated in Table 2-13

Table 2-13. File types compatible with available commercial FEA packages

Package	Import	Export
<i>ANSYS Mechanical</i>	Allows for various CAD file formats to be imported e.g. .stp, .stl. .iges. Mesh data files prepared in external packages can be imported.	Results can be written to text files and exported to text editor packages. Results can be written directly to an excel file.
<i>Siemens NX</i>	Various CAD format files can be imported. Model files from other FEA packages can be used to generate a model in NX	Results can be used to generate full reports on the simulation. Result files can be written to a text file.
<i>Solidworks Simulation</i>	Allows for a variety of CAD formats to be imported	Allows for a variety of CAD formats to be exported. Results can be exported in image formats. Reports of results can be automatically generated and saved to a word document

2.9.6 User Support and Documentation

Table 2-14 below presents the findings concerning user support and documentation available for the chosen packages.

Table 2-14. User support and documentation available

Package	Findings
<i>ANSYS Mechanical</i>	Extensive documentation and support available. ANSYS is one of the most used simulation packages and as such is being continually developed and updated. Several discussion forms and testimonials exist which indicate the wide acceptance of the software in the engineering community
<i>Siemens NX</i>	Available documentation and product brochures giving information on the various aspects of the packages. User guides and manuals are available. Customer support is available via organisations webpage. Software package has a large client base and receives continual updates.
<i>Solidworks Simulation</i>	Extensive documentation available to users. Solidworks is a well-known and widely used CAD Modeller which has gained a large following of those who also make use of the Simulation Module. The software package goes through annual version releases and continual updates.

2.10 Browser-Based FEA simulation platforms

This section introduces a relatively new approach to FEA simulations. Simulation platforms are maintained by hosts with large computing facilities. Users are allowed access to computational resources. The analyst connects to the host's website and selects the type of simulation required. The user is able to use the available GUI to create the required model. The model is then solved on the host's computational facilities. One such platform, SimScale, is presented in this section.

2.10.1 SimScale Browser-based FEA simulation platform

SimScale is a web-based simulation platform for the solution of certain physics problem types through numerical methods. All SimScale users can access the full capabilities of this software for free. However, users wanting personalized assistance from the SimScale team as well as certain premium facilities can join under a "Professional Account" and are charged a monthly fee of 170 Euros per month. SimScale performs as the front-end web-based interface for other open source numerical solvers. It allows users to upload geometry to a workspace, generate a mesh and apply material properties, loading conditions and constraints. Once the model is generated, it is sent to the computational facilities maintained by SimScale. It is queued and then solved when the computational resources become available (SimScale GmbH, 2015).

SimScale Analysis capabilities

SimScale has the analysis capabilities to provide solutions to only 3-D problems in structural analysis, thermodynamics and heat transfer, CFD, particle analysis, acoustics as well as coupled multiphysics problems. Lower dimension problems are not currently solvable (SimScale GmbH, 2015).

SimScale Internal Modules

Pre-processor: The pre-processing capabilities of the *SimScale* platform match what one would expect from a commercially available FEA package. It allows for uploading of various CAD file formats. It permits several mesh element types and allows for custom material types to be created (SimScale GmbH, 2015).

Processor/Solver: Wide selection of direct and iterative solvers available to the user. The solution is run on the facilities hosted by SimScale and not on the user's workstation. Once the solution is obtained, the user is emailed if they are not logged in to the SimScale interface and are prompted to view the results (SimScale GmbH, 2015).

Post-processing: The post-processing interface of SimScale is used once the results are generated. It is very basic and it is suggested that external post-processing software could be used for better representation of the solution if required (SimScale GmbH, 2015).

Operating System

The operating system used is irrelevant, provided that a web-browser can be used.

SimScale User Support and Documentation

There is evidence of continual software development. Extensive documentation and user-friendly video and text tutorials are available. There is an active community discussion forum with well separated discussion topic threads.

2.11 Benchmarks and Standards for Performance of FEA Packages

The inherent nature of finite element analysis means that it is only an approximation of a real system. This exposes FEA to scrutiny regarding its reliability and accuracy. Generally, commercial FEA packages do not allow users to access the source codes. This would leave one with the sense that there is no way to determine if the methods used by the package, or the results obtained from solutions are in fact reliable. This research resulted in the examination of verification and validation manuals for the commercial FEA software packages investigated. In these manuals, codes are compared to well-known analytical models that can be easily verified from results found in many engineering and strengths of materials texts. (ANSYS inc, 2013), (UGS Corp. , 2007), (Dassault Systèmes, 2012).

Looking specifically at the verification manual for Siemens' NX, the solver is validated against a range of linear static problems which were taken from accepted engineering texts. These tests begin with simple problems such as point loads and distributed loads on 2-D cantilevered beams and increase in complexity of geometry and loading conditions. These all still appear to be simple enough for any adept analyst with some prior knowledge of FEA to properly replicate (UGS Corp. , 2007).

The review of verification and validation manuals also revealed that software codes are validated against test cases contained in trusted publications such as The National Agency for Finite Element Methods and Standards (NAFEMS) Benchmark standards (ANSYS inc, 2013), (UGS Corp. , 2007), (Dassault Systèmes, 2012). NAFEMS funded several studies that published benchmarks deemed suitable to assess the basic accuracy of FEA packages.

(NAFEMS, 1990). The benchmark tests are designed such that any competent system should produce satisfactory results. The solution targets are generally single point values for quantities such as maximum stress, displacement, temperature etc. For those tests with no analytical solution, target results were derived from numerical solutions which were checked on more than one system. (NAFEMS, 1990). These benchmark tests stipulate model geometry, material properties, boundary conditions and the expected solution. These can all be used by an analyst to generate a model with an appropriate mesh, in order to determine the accuracy of the FEA package. Another benchmark publication was found titled “Guide de validation des logiciels de calcul des structures” published by Société Française des Mécaniciens (Société Française des Mécaniciens, 1990). This benchmark publication is presented in almost the exact format as seen in NAFEMS benchmark standards.

The benchmark publications are widely viewed as the industry standard for validating an FEA package. Most of the major FEA software developers are members of NAFEMS and it would appear that they all subscribe to validating their packages through NAFEMS Standard Benchmarks or some other industry accepted benchmark publication.

2.12 Chapter Discussion

Finite element analysis has its roots in structural analysis, but has since branched off into various fields of research (Moaveni, 1999). Use of FEA software has steadily increased as greater confidence is placed in the accuracy of computational results. Evidence of this can be seen in (Jackson, 2013). This survey revealed the extent to which industries were incorporating FEA into their design process. It is notable that only 10% of respondents made no use of numerical simulation packages in their design processes (Jackson, 2013).

It is evident that industries are making imperative decisions based on the results of finite element analyses. With the reliability of the results seldom being questioned, the need for verification and validation is that much more significant. This is especially true for a no-cost FEA package that may not yet have the credibility of renowned commercial FEA packages. Looking at the no-cost packages, there was little to no evidence found of performance benchmarking having been done. An insightful paper by (Galeano et al., 2007) was reviewed. This paper assessed the various aspects of the packages, such as internal modules, user interface and documentation available. This is a good qualitative study and some of the methods used in that study will be carried over into this research. This paper however, along

with most work found relating to assessing no-cost FEA software, paid very little to no attention on the accuracy of the results produced

The verification manuals of the available commercial software packages have assisted in gaining insight into how to set up a verification study on FEA software packages. Applicable analytical problems from engineering text along with benchmark test cases would be sufficient in testing the static structural capabilities of any FEA software package.

The research investigated several open source and low cost FEA packages that showed potential to be used by an independent consultant, small engineering companies wishing to free themselves of the need to justify the cost of infrequently used software or by research institutions who cannot afford the proprietary options.

The no-cost/low-cost packages that will be investigated further in the performance benchmarking phase of the research are: Code_Aster/Salome Meca, Mecway and Z88 Aurora. Code_Aster was chosen over CalculiX as it appeared the more capable Linux based package. Mecway is a more comprehensive version of LISA and also appeared more capable than Elmer, so was therefore chosen as the Windows based package. Z88 was chosen as it appeared capable enough for the extents of this research and was the only package that works on Linux, Windows and Mac OSX. The package investigation also covered the concept of browser-based FEA. This approach to conducting finite element analysis could potentially change the way a small engineering business would view computational simulations, as it removes the need to invest in costly computational infrastructure and software. For this reason, it was decided to include SimScale in the benchmarking phase.

UKZN holds licences for Siemens NX, ANSYS as well as Solidworks Simulation available for use. Solidworks Simulation is still relatively new and the reputation of the software is not yet at the level of ANSYS or Siemens NX. It was decided to omit it from the next phase of the research. It was decided to subject both ANSYS and Siemens NX to the benchmarking phase to better understand the capabilities available in what are considered premium packages and to determine how closely the results yielded by the packages are to each other.

2.13 Chapter Conclusion

The research conducted has revealed that FEA has had a tangible impact on product design. The majority of industries are making use of analysis software, even during early design phase. FEA software development is quite a niche market and as such, software developers tend to charge a premium rate for the use of their packages. Price is not often an issue for large companies that make use of these packages frequently. This may not be the case for a small business that wishes to make use of FEA as part of their operation. Several open source packages were investigated and a preliminary selection was done on the basis of certain aspects which made some packages more suitable for this research than others. The no-cost/low-cost packages; *Code_Aster*, *Mecway* and *Z88 Aurora*, were chosen to be included in the benchmarking phase of this research. The browser-based simulation platform, SimScale, will be subjected to the benchmarking phase. ANSYS as well as Siemens NX will also be used in the benchmarking phase as well, to offer a measure of accuracy of the open source packages against what is considered a premium commercial FEA package.

CHAPTER 3 : Methodology

This chapter presents the method used to investigate the research problem stated in Chapter 1. This chapter also addresses the limitations which are present in the research.

3.1 Research Methodology

3.1.1 Identify and Investigate No/Low Cost FEA Packages Available.

This was done in order to gain some familiarity with the available packages. A literature review, and suggestions made by individuals with experience in the field, allowed for the identification of several low-cost/no-cost FEA packages.

3.1.2 Identification of Independent Benchmarking Studies relating to No-Cost/Low-Cost FEA Packages

This step investigated literature which focused on independent research into the performance of no-cost FEA packages. The investigation was conducted through accessible academic databases, journal articles, as well as renowned web-based academic discussion forums. This was done to produce a better understanding of what has already been done, in order to identify aspects in the field have yet to be investigated.

3.1.3 Subjection of No-Cost/Low-cost Packages to Selection Criteria

It was impractical to subject all chosen packages to the benchmarking tests. Choosing a limited number of no-cost/low-cost packages that pass certain baseline criteria before proceeding to the performance benchmarking phase of the research aided in streamlining the entire process. The selection procedure used is illustrated in Figure 3-1. It is seen in that the inability to perform the required type of analysis immediately excluded a package from further investigation.

Once the analysis capability criteria was met, the price of the package and licencing approach was verified. If the package was considered ‘expensive’ (greater than 500 USD per year) or licenced such that it prohibits the use of the package in this research, it was excluded. If a package passed the aforementioned criteria, the presence of the internal modules were checked. The lack of either a pre-processor or a post-processor did not immediately exclude the package. This resulted in the package going into a consideration process. A judgement was made based on the ability of the solver to accept various imported file formats as well as export post-processing file formats

If the package was deemed to be capable with respect to file type compatibility, the documentation and user support was investigated. If it appeared that no user support was readily available then the package would return to the consideration process. If it was deemed that the package was not user friendly as well as lacking a pre or post-processor, it would be excluded from the benchmarking phase of the research.

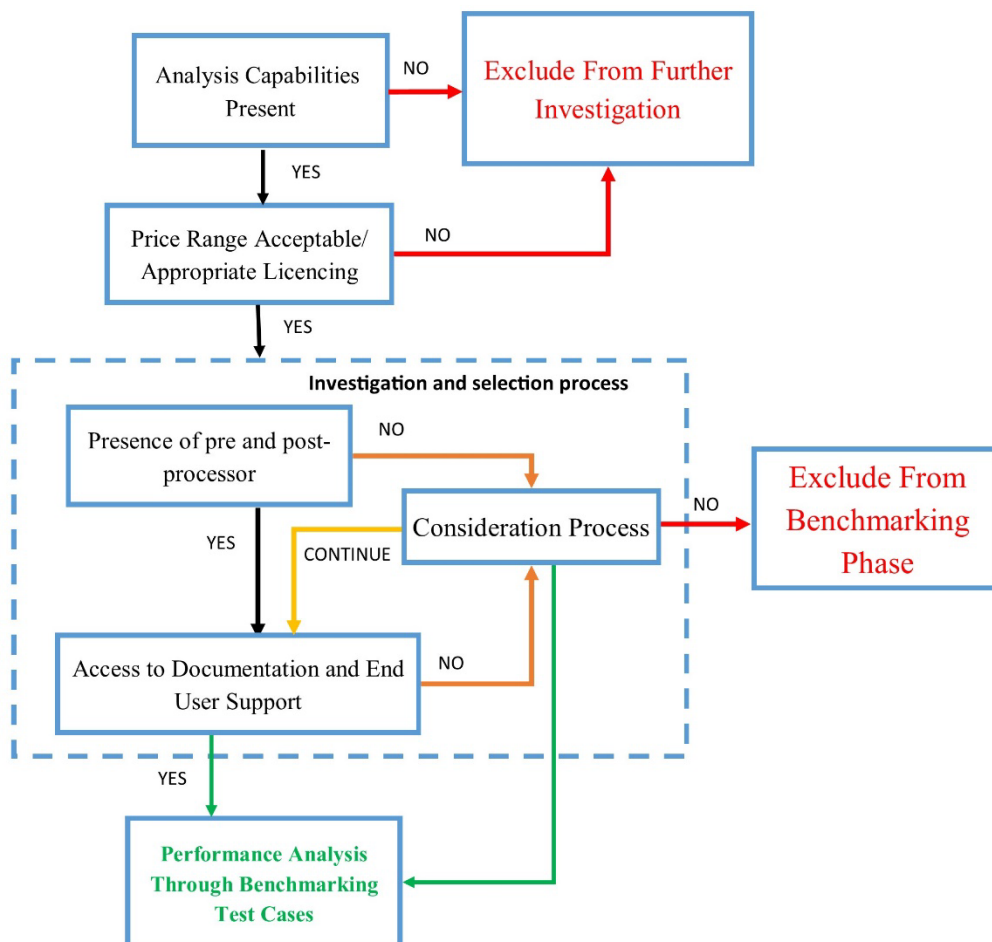


Figure 3-1. Package selection procedure

3.1.4 Selection of One or More Available Premium Commercial Package

This was done for quantitative comparison between what is considered a premium package and the chosen no-cost/low-cost packages. The selection of commercial FEA software was based on software availability at the University of KwaZulu-Natal.

3.1.5 Review and Selection of Benchmarking Test Cases

Appropriate benchmark tests cases were selected to be simulated on the chosen packages. This process began by investigating the verification manuals of renowned, commercially available FEA software packages. By doing this, insight was gained into the method and approach used by industry leaders in the verification of their product. It revealed that the leading software developers verify their codes through a benchmarking process that utilizes well-known analytical solutions as well as examples from NAFEMS and other benchmark publications.

With this knowledge, a variety of test cases were selected that fell within the scope of this research. Test cases were separated into analytical problems with known solutions and benchmark standards. It was also decided that laboratory testing would be conducted in order to and generate experimental data that will serve as a test case.

Selection of the test cases was based on:

- The test case falling within the static structural analysis field.
- The problem geometry and loading conditions being easily replicatable.
- The possibility of the problem being readily tested and validated experimentally.

3.1.6 Solution of Test Cases Using FEA Software Packages

The chosen packages were subjected to the selected test cases. The computational simulation process for the test cases can be seen in Figure 3-2. The process began with the creation of the appropriate geometry. FreeCAD, a freely available parametric CAD modelling software package, was used to create the geometries that were imported into the packages investigated. The package's internal pre-processor was used for the creation of the finite element model. Once the model was created, the simulation was run to produce a result for the test case concerned. The result was then analysed and classified within one of three result categories.

The first category, “Realistic results, acceptable accuracy”, would see the solution exhibiting the expected response to the loading and constraints, with the value of the solution strongly correlating to expected values stipulated by the test case.

The second category, “realistic results, unacceptable accuracy”, pertains to situations when the solution exhibited the expected response but yielded a solution with an unacceptable accuracy. This occurrence indicates that the boundary conditions were most probably correct. To address the inaccuracy in the solution, the mesh parameters or mathematical model used to solve the model should be re-evaluated. This loop can be run until satisfactory results are obtained. Research was conducted to determine what the industry accepted measure of ‘accuracy’ is. There is no agreed upon value as it appears that ‘accuracy’ is very application-specific. Trusted discussion forums show claims from industry analyst that inaccuracies up to 10% for linear static examples are acceptable for certain applications. Others report that for some complex examples such as material non-linearities or contact problems, errors may be as high as 20% (ResearchGate, 2014). For the purpose of this research, accurate solutions must fall within 5% of the target solution. This value is lower than what industry analysts suggest as it was felt that the types of analyses selected for this research are relatively simple and that a capable FEA package should be able to generate accurate solutions quite easily.

The third category, “unrealistic results”, pertains to situations where results generated do not exhibit expected response to the loading conditions or yield grossly inaccurate numerical values. This phenomenon could be attributed to various factors. In such cases it would be advisable to revisit the various aspects of the model creation, as shown in Figure 3-2 and verify that these aspects represent the physical system being modelled as closely as possible. This loop can be run until satisfactory results are obtained.

3.1.7 Processing and Interpretation of Results

This validation phase assessed the performance of the selected packages. Results for each test case were gathered and processed. The results were compared against expected theoretical solutions so that a measure of accuracy could be obtained.

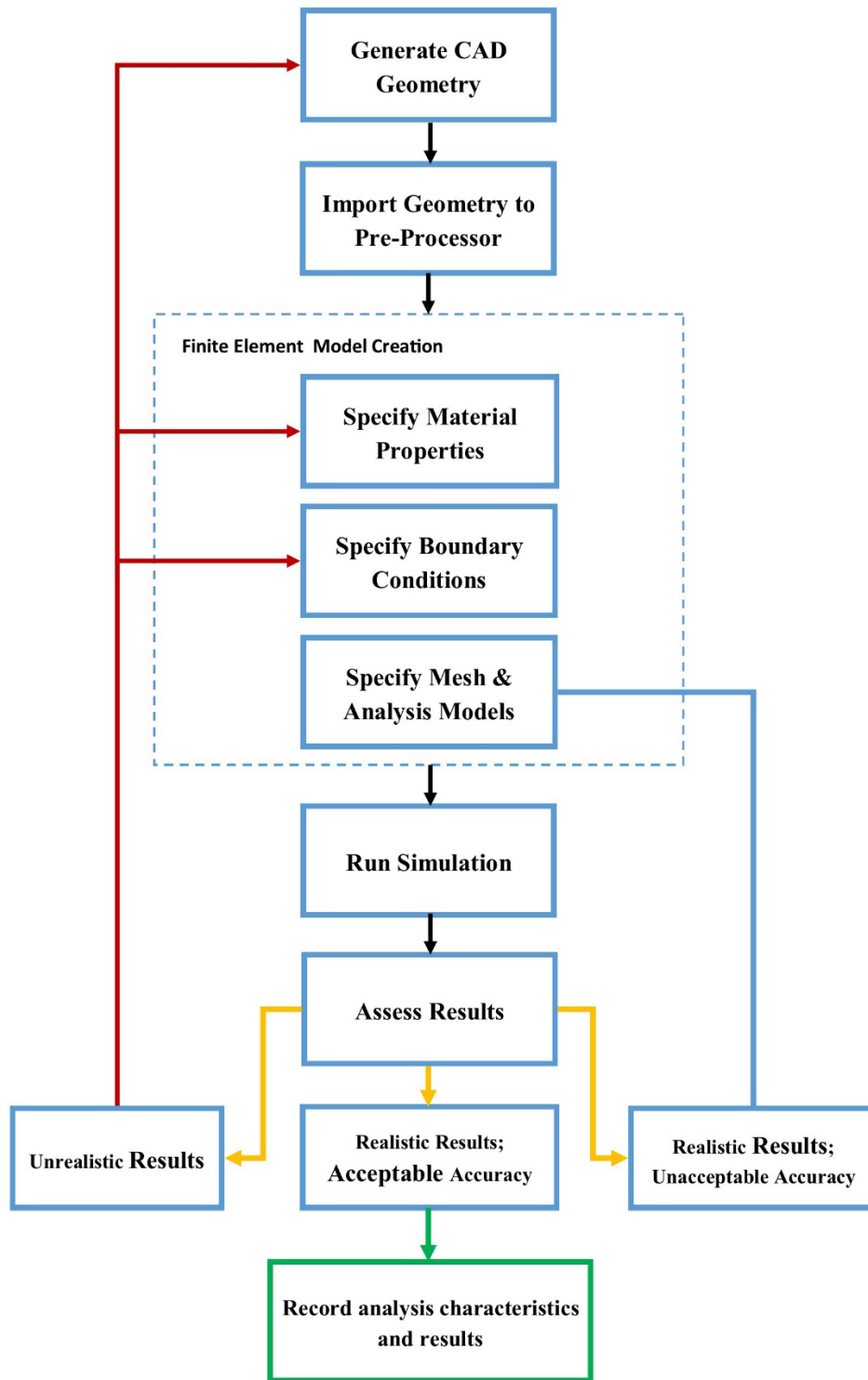


Figure 3-2. Computational simulation process

3.2 Limitations

This research was subject to certain restrictions which limited the scope and detail that could be explored. The time available for this research restricted how many packages could practically be investigated. The limited computing resources and time available restricted the number of simulated test cases that could be considered. The exclusion of composite material analysis was due to the lack of expertise in the part of the researcher and the limited time available for acquiring a better understanding of this analysis procedure.

3.3 Conclusion

The research had certain limitations which restricted the scope and detail to an extent. The research methodology presented was developed with the intent of streamlining the process of identifying the no-cost/low-cost FEA software packages that are appropriate for use in place of established proprietary FEA software packages for linear and non-linear static structural analyses.

CHAPTER 4 : Chosen Benchmark Test Cases

4.1 Linear Static Structural Analysis Test Cases

This section introduces the test cases that were used to measure the performance of the FEA packages with respect to linear static structural analyses. These cases were taken from accepted standards within the FEA industry, trusted engineering text, or were derived from empirical models. Several sources were initially considered and many potential cases were identified. The following cases were chosen from amongst the available possibilities as these would test a range of analysis capabilities with respect to linear static structural analyses, with minimal repetition of model types.

4.1.1 Grid Point Load on an Articulated Truss

This test case was taken from an industry accepted standards publication titled, “Guide de validation des progiciels de calcul des structures” published by Société Française des Mécaniciens. (Société Française des Mécaniciens, 1990). This test, labelled SSSL11/89 in the standards publication, is a 2-D linear static analysis of 1D truss system (Société Française des Mécaniciens, 1990). Figure 4-1 below presents the 1D line geometry for this test case. Note that dimensions are in millimetres.

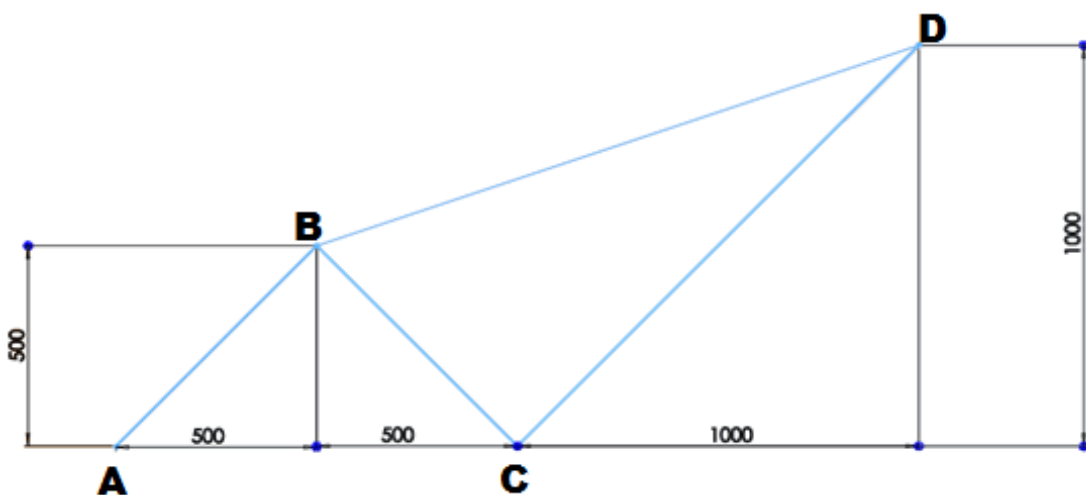


Figure 4-1. Truss system geometry (Société Française des Mécaniciens, 1990)

Table 4-1 below shows the information associated with this test case.

Table 4-1. Given information for truss analysis.

Material Properties	E = 1.962 E+11 Pa	
Geometrical properties	Element	Area (m²)
	AB	2 E-4
	BC	2 E-4
	BD	1 E-4
	CD	1 E-4
Boundary Conditions	Node	Constraint/Load
	A	Zero X and Y displacement
	B	Zero X and Y displacement
	D	Force = 9810 N in -Y direction

Table 4-2 presents the target solutions for this test case as given in test case publication.

Table 4-2. Given target solutions for truss problem.

Node point	Target	Benchmark Value (m)
C	X - displacement	0.26520 E-3
C	Y - displacement	0.08839 E-3
D	X - displacement	3.47900 E-3
D	Y - displacement	-5.60100 E-3

This test case was chosen due to the following: The problem originates from a trusted publication on FEA standards, therefore the results for this test case have been reviewed. The geometry is simple to replicate. The two cross-sectional areas of the truss members would give a good measure of the 1-D element creation capabilities of the pre-processor. The assumption when selecting this test case was that it would be similar to types of problems often encountered in industry. It was assumed that this test case provides a sufficiently complex 1-D truss problem, adequately revealing a package's ability to create 1-D elements as well as to specify commonly used boundary conditions.

To successfully model this test case, a suggested approach would be to import/create the geometry to the pre-processor and assign the two required truss element types where applicable. The prescribed boundary conditions must also be applied to the relevant nodes. Lastly, the post-processing module of the package must be able to represent the target solutions on an appropriate plot.

4.1.2 Thin Shell Wall in Pure Bending

This test case was taken from the engineering text, “Mechanical Engineering Design” (Shingley and Mitchel, 1983). This test case is a 3-D linear static analysis which investigates the maximum deflection and stress in an edge loaded wall, which is represented as a 2-D shell for analysis. Figure 4-2 shows the geometry of the 2-D shell representation of the wall that will be used for this test case.

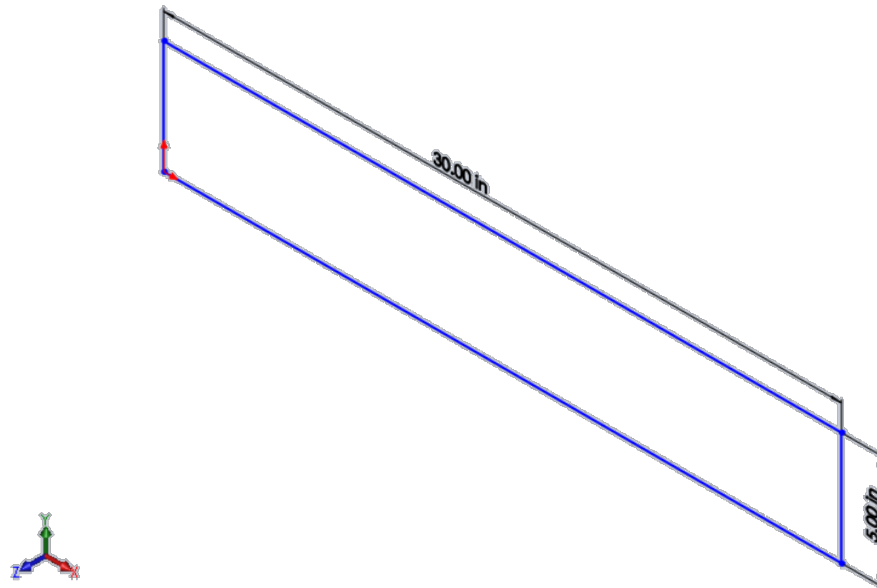


Figure 4-2. Wall geometry represented as a 2-D shell (Shingley and Mitchel, 1983)

Table 4-3 presents the given information associated with this standard test case (Shingley and Mitchel, 1983)

Table 4-3. Given information for wall in pure bending analysis problem.

Material Properties	E = 30 E-6 psi
	$\nu = 0.03$
Geometric Properties	Length = 30 in
	Width = 5 in
	Thickness = 0.1 in
Boundary Conditions	Zero displacement for upright edge situated at the origin
	Edge load = 6 lbf on remaining upright edge

Table 4-4 presents the target solutions for this test case

Table 4-4. Given target solutions for wall in bending problem.

Target	Benchmark Value
Maximum Z Deflection	4.320 in
Maximum Z Stress	2.160 E+4 psi

The decision to include this test case in the research was made due to the following: The test case originated from the fourth edition of a trusted engineering text, implying that the validity of the results has been established. The geometry is simple to replicate. This 2-D representation of the geometry, albeit lacking complexity, can sufficiently reveal the packages analysis capabilities with respect to shell elements. It is important that a package has this capability as 2-D shell analysis is commonplace in structural FEA.

To successfully model this test case, a suggested approach would be to import a 2-D shell geometry into the pre-processor of the package. An appropriate 2-D element must be used to mesh the geometry and the stipulated material properties must be assigned. The pre-processor must be used to stipulate the required boundary conditions. The post-processing module of the package should be used to represent the target solutions on appropriate plots.

4.1.3 Axisymmetric Pressure Vessel

This test case was taken from an industry accepted publication “The NAFEMS Standard Benchmarks” (NAFEMS, 1990). This test case, labelled LE7 in the publication, is a linear static analysis of a cylindrical pressure vessel with spherical end caps. Due to the geometrical symmetry of the model, it can be modelled as a 2-D axisymmetric surface.

Figure 4-3 below shows a 2-D axisymmetric representation of the pressure vessel presented in millimetres

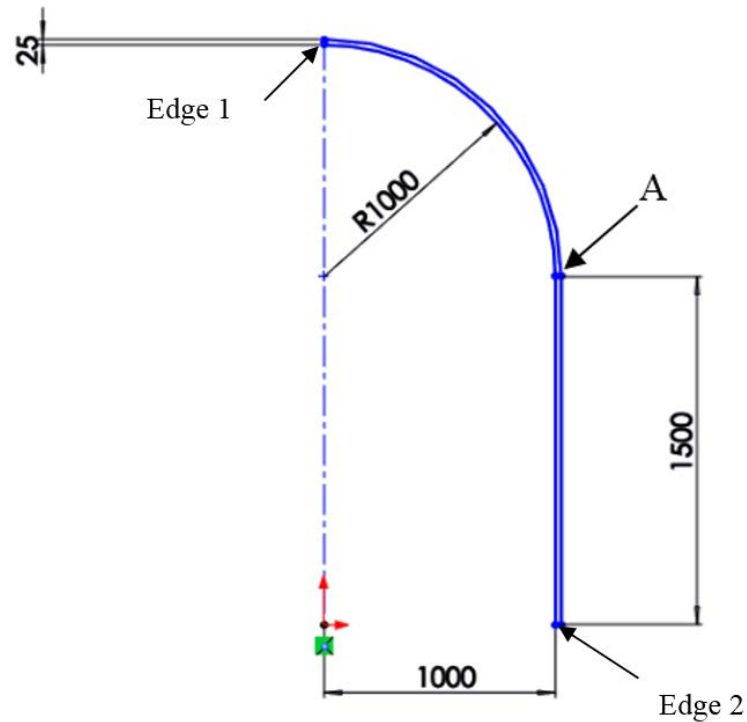


Figure 4-3. Axisymmetric representation of pressure vessel (NAFEMS, 1990)

Table 4-5 below presents the given information associated with this standard test case.

Table 4-5. Information given for axisymmetric pressure vessel test case.

Material Properties	E = 2100 MPa
	$\nu = 0.3$
Geometric Properties	Axisymmetric 2-D Shell with given dimensions
Boundary Conditions	Edge 1 – Zero X-Displacement
	Edge 2 – Zero Y-Displacement
	Uniform internal pressure = 1 MPa

Table 4-6 presents the target solutions for this test case.

Table 4-6. Given target solutions for axisymmetric pressure vessel analysis problem

Target	Benchmark Value
Axial Stress σ_{yy} on outer surface at specified point	25.86 MPa

It is assumed that this type of analysis would commonly be encountered by an analyst in industry, therefore the ability to correctly analyse these problems is necessary. The decision to include this test case in the research was made due to the following: The test case originates from an industry-accepted standards publication therefore, the results have been reviewed and validated. The geometry is simple to replicate. The test case would reveal the capabilities of a software to handle axisymmetric geometry and loading conditions.

To successfully analyse this test case, a suggested approach would be to import the 2-D geometry into the pre-processor. It would be ideal if the package had a dedicated 2-D axisymmetric analysis option available. The pre-processor should be used to specify 2-D elements with the required material properties assigned. The boundary conditions should be applied in a manner that correctly represents the axisymmetry present. The target solution requires a specific directional stress and hence the solver should be able to compute this stress value. Lastly, the post-processing module of the package must be used to represent the target solution on an appropriate plot.

4.1.4 Internal Pressure on Thick-Walled Spherical Container

This test case was taken from an industry-accepted standards publication titled, “*Guide de validation des progiciels de calcul des structures*” published by Société Française des Mécaniciens (Société Française des Mécaniciens, 1990). This test labelled SSLV 03/89 is a 3-D linear static analysis of a thick-walled spherical vessel experiencing an internal pressure loading. Due to the geometrical symmetry, the vessel can be modelled as a quarter sphere as seen in Figure 4-4. Dimensions are presented in millimetres

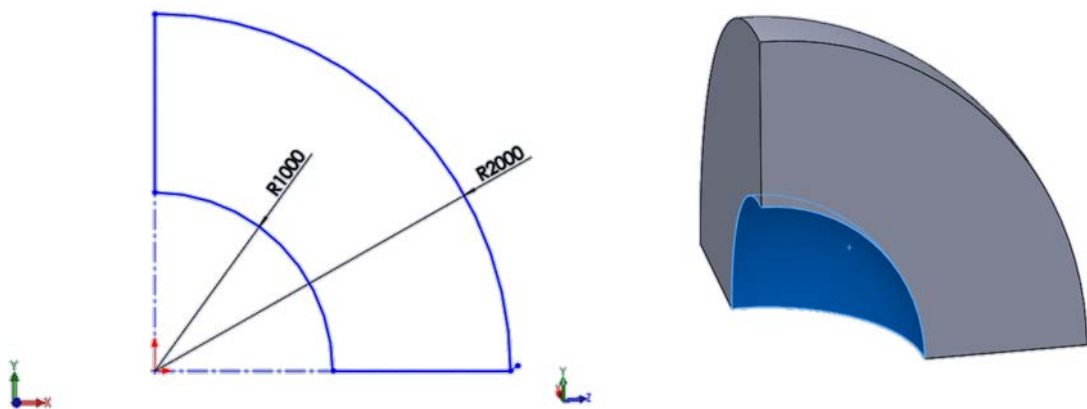


Figure 4-4. Quarter sphere geometry (Société Française des Mécaniciens, 1990)

Table 4-7 below presents the given information associated with this standard test case

Table 4-7. Given information for spherical pressure vessel analysis problem

Material Properties	E = 200 MPa
	$\nu = 0.30$
Geometric Properties	Quarter spherical geometry with specified dimensions
Boundary Conditions	Symmetry conditions apply at orthogonal flat faces
	Uniform internal pressure = 100 MPa

Table 4-8 presents the target solutions for this test case given in the standards publication.

Table 4-8. Given target solutions for spherical pressure vessel analysis problem.

Results : Internal Surface	
Target	Benchmark Value
σ_{rr}	-100 MPa
σ_{θ}	71.43 MPa
u	0.4 E-3 m
Results : External Surface	
Target	Benchmark Value
σ_{rr}	0 MPa
σ_{θ}	21.43 MPa
u	0.15 E-3 m

It is assumed that 3-D linear static FEA would be most frequently encountered by analysts. The decision to include this test case was based on the following: The test case originates from an industry accepted standards publication and hence, the results have been reviewed and validated. The geometry is easily replicatable. The target solutions are displacement values as well as two principle stress values. It is assumed that solving for more than one type of target would give a better insight into the accuracy of the solved model.

To successfully analyse this test case, a suggested approach would be to import the 3-D quarter sphere geometry into the pre-processing module of the package. The pre-processor must be used to assign appropriate mesh elements for the model. The symmetry conditions must be properly represented using appropriate constraints. The pressure loading must be applied on the appropriate curved face. Noting that the target solution requires two directional stresses as well as a displacement, the solver should be able to solve for these results. Lastly, the post-processing module of the package must be used to represent the target solution on an appropriate plot.

4.1.5 Flat Bar with Stress Concentration

This test case was developed based on empirical models found in Mechanics of Materials by (Beer et al., 2012). This test case is a 3-D linear static analysis of a flat bar with stress concentrations under a tensile load. Figure 4-5 below shows the chosen geometry for this test case presented in millimetres.

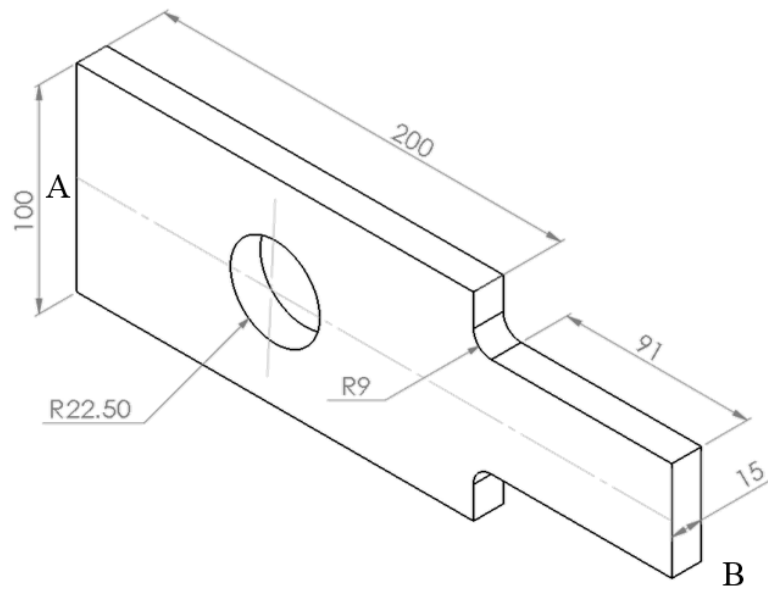


Figure 4-5. Geometry of flat bar with stress concentrations

Table 4-9 presents the model properties and boundary conditions that were chosen to be applied to the geometry for this analysis problem.

Table 4-9. Properties to be used for the flat bar with stress concentration analysis problem.

Material Properties chosen	E= 210 GPa
	$\nu = 0.3$
Geometric properties chosen	Dimensions as specified in mm
	Thickness = 15 mm
Boundary conditions chosen	Zero translation at face A
	Normal force = 1000 N at face B

Results calculated:

$$\sigma_{max} = K \left(\frac{F}{A} \right) \tag{4.1}$$

Where:

- σ_{max} - Maximum stress
- K - Stress concentration factor
- F - Applied Force
- A - Cross Sectional Area

Using Stress concentration factors for flat bars under tensile loading from (Beer et al., 2012) in Figure 4-6 , K_{hole} and K_{fillet} were obtained.

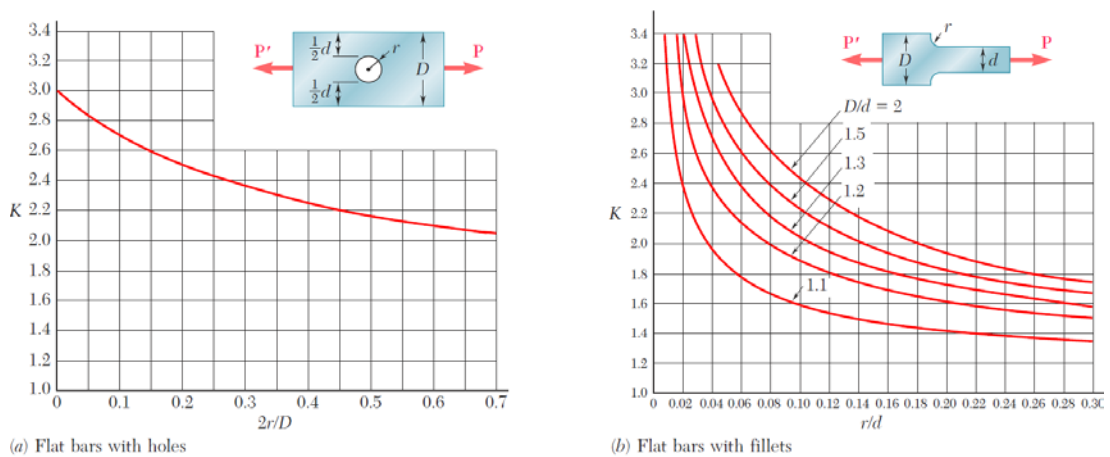


Figure 4-6. Stress concentration factors for flat bars under tensile loading (Beer et al., 2012).

From Figure 4-6 (a) it was determined that $K_{hole} = 2.2$.

Using $F = 100N$, $A = 825 \text{ mm}^2$ and $K_{hole} = 2.2$:

$$\sigma_{hole} = 2.2 \left(\frac{1000 \text{ N}}{825 \text{ mm}^2} \right)$$
$$\sigma_{hole} = 2.667 \text{ MPa}$$

From Figure 4-6 (b) it was determined that $K_{fillet} = 2.0$.

Using $F = 100N$, $A = 750 \text{ mm}^2$ and $K_{fillet} = 2.0$:

$$\sigma_{fillet} = 2.0 \left(\frac{1000 \text{ N}}{750 \text{ mm}^2} \right)$$
$$\sigma_{fillet} = 2.667 \text{ MPa}$$

Table 4-10 below shows the calculated results that will serve as target solutions

Table 4-10. Calculated results for the flat bar with stress concentrations analysis problem.

Point	Target	Benchmark Value
Fillet	Maximum Stress	2.66 MPa
Hole	Maximum Stress	2.66 MPa

It was assumed that since 3-D linear static finite element analyses would be the most frequently encountered problem and as such, one showing areas of high stress concentrations should be included in the research. The decision to generate a problem of this type is that the results could be easily verified by reference to empirical models for holes and fillet stress concentrations in an accepted engineering text. The geometry can be easily replicated and the loading and boundary conditions are easily applied to the model. The target solution is an axial stress value that should be easily solved for and output by any competent FEA package.

To successfully model this test case, the 3-D geometry would need to be imported into the pre-processor of the FEA package. The appropriate material properties and a suitable mesh should be applied. The loading and boundary conditions must be applied to the relevant faces of the model. The post-processor of the FEA package must be used to output the target solution on an appropriate plot.

4.2 Non-Linear Static Structural Analysis test cases

This section presents the non-linear static structural test cases chosen. The first test case was taken from a NAFEMS standards publication. The second case is derived from results of experimental testing done as part of this work using facilities available to the Discipline of Mechanical Engineering at the University of KwaZulu-Natal. These test cases were chosen as they examine the analysis capabilities of the packages with respect to geometric non-linearity and material non-linearity, respectively.

4.2.1 Large deflection of a Z-Shaped Cantilever Beam under End Load

This test case was taken from an industry-accepted FEA standards publication known as “Benchmark Problems for Geometric Non-Linear Behaviour of 3-D Beams and Shells”. This test case, labelled 3DNLG1 in the publication, is a geometrically non-linear static analysis of a z-shaped cantilevered beam (Prinja and Clegg, 1993). Figure 4-7 shows the 2-D geometry of the cantilever with the specified thickness. Dimensions presented are in millimetres

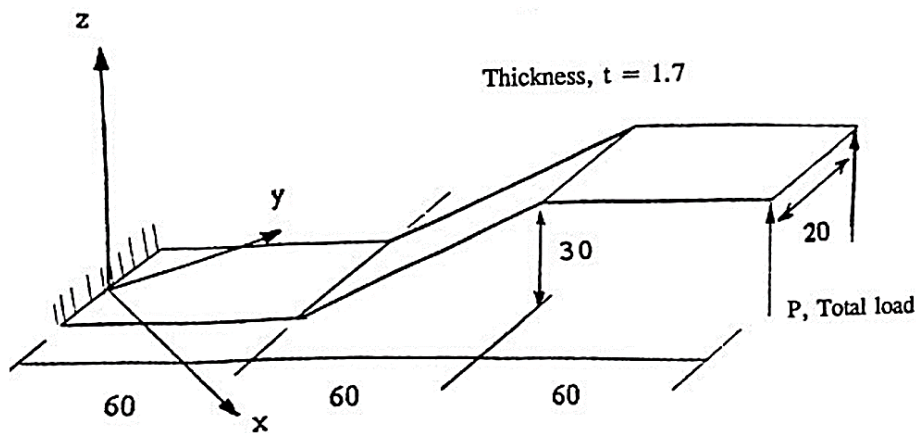


Figure 4-7. Cantilever geometry (Prinja and Clegg, 1993)

Table 4-11 presents the model properties and loading conditions that were chosen to be applied to the geometry for this analysis problem.

Table 4-11. Given properties for Z-Shaped cantilever problem.

Material Properties	$E = 2 \text{ E}+11 \text{ Pa}$ $\nu = 0.30$
Geometric Properties	Given in figure above (mm).
Boundary Conditions	Fully fixed edge at origin Tip Load $P = 4000 \text{ N}$

Table 4-12 below shows the target solution as specified in the benchmark problem.

Table 4-12. Given result for Z-Shaped cantilever problem.

Point	Target	Benchmark Value
Free end	Z-directional displacement	143.4 mm

It is assumed that geometrically non-linear analyses are likely to be encountered by an analyst in the engineering field, hence the ability to analyse these types of problems correctly is necessary. The decision to include this test case in the research was made due to the following: The test case originates from an industry accepted standards publication and hence, the results have been reviewed and validated. The geometry and boundary conditions are simple to replicate.

To successfully analyse this test case, the 2-D shell geometry representation of the cantilever must be imported into the pre-processor. The pre-processor should be able to assign shell elements that have the stipulated material properties assigned to it. The required loading and boundary conditions should be able to be applied. The test case data gives a tabulated set of incremental load values and corresponding tip deflection outputs. It would be convenient if the tabulated load data could be entered into the package. Lastly, the post-processing module of the package must be able to represent the target solution on an appropriate plot. It would be advantageous if incremental results could be recorded for each load step.

4.2.2 Plastic Deformation of Tensile Test Specimen

This test case was created from results obtained through experimental testing done as part of this work using facilities available at the University of KwaZulu-Natal. Initially, the material used for this experiment was sent to an external material testing laboratory in order to obtain the mechanical material properties for the batch used during testing. This was done so that a trusted external source could be referenced for the actual material data used in the computational analysis. However the results provided by the laboratory deviated considerably within the test batch and it was financially impractical to commission more tests to be done. It was therefore considered acceptable that testing for the material data as well as the generation of a target solution for the computational testing be done internally.

A standard tensile test piece geometry, shown in Figure 4-8, was created following guidelines specified in the document, “Standards for metallic materials tensile testing” published by the SABS standards division (South African Bureau of Standards, 2010). This specimen was used to obtain the mechanical properties of the material being used. Dimensions are presented in millimetres.

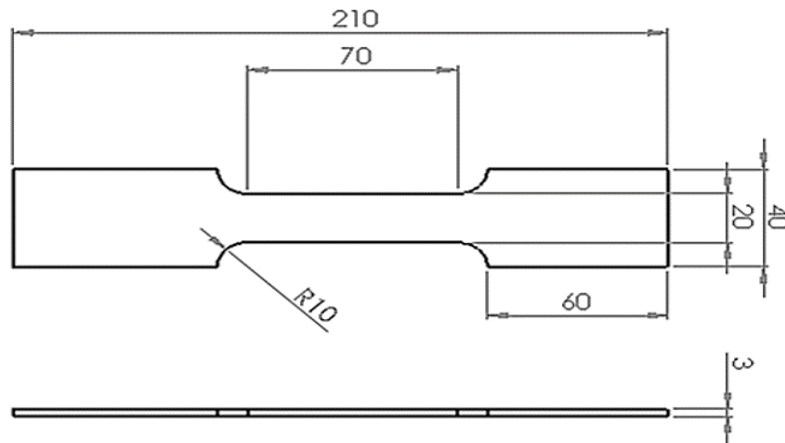


Figure 4-8. Specimen geometry created following SABS standards for metallic material tensile testing.

Another geometry following the same guidelines was created, as seen in Figure 4-9. This specimen contained a custom-shaped cut-out along the gauge length. This was done to add complexity to the model. The cut-out also ensured that the fracture will occur within the narrowed portion along the gauge length. This portion is shorter than the minimum reach of the extensometer (a device used to measure strain). This was important as it ensured that the extensometer would be able to read the strain during the entire tensile test.

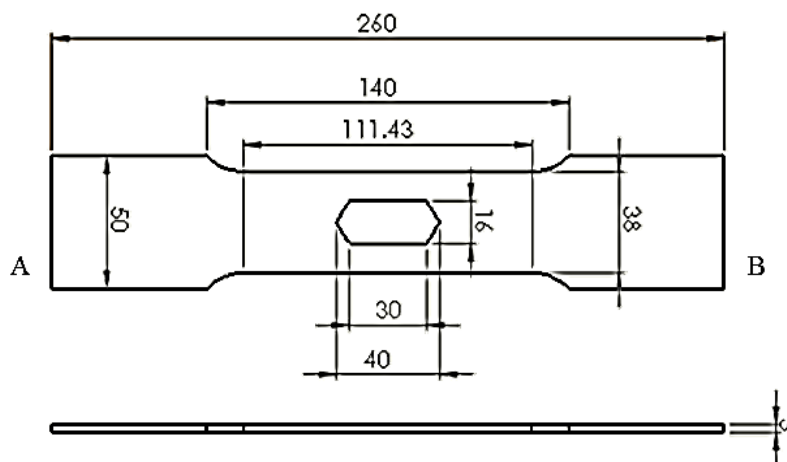


Figure 4-9. Custom tensile test specimen geometry

The specimens were water-jet cut from 3 mm thick 1050 H14 aluminium sheet. Water-jet cutting was employed to eliminate the formation of heat-affected zones, associated with laser cutting metals. Testing was conducted on an Instron 5500R material testing machine. The extension was conducted at a constant strain rate of 2 mm/min. An extensometer with a 50 mm gauge length and a 10 mm extension was used. A 100 KN load cell was used to record the tensile force experienced by the specimens.

A lecturer from the Discipline of Statistics of the University of KwaZulu-Natal was consulted with regards to the handling of the data extracted from the Instron machine. It was advised that the way in which these curves were generated prevented the data from easily being averaged to find a best-fit curve. For small sample sizes such as this, the lecturer suggested that it was good practice to choose a median curve and ensure that the majority of result sets fell within one standard deviation of this curve. (Roberts, 2016)

Figure 4-10 shows the stress vs strain curves from the standard specimen geometry. The results were used to determine the flow curve and elastic modulus that was applied in the FEA packages when modelling this test case. A total of ten tests were done using the standard specimen geometry. Three data sets were omitted as they deviated excessively and were considered to be influenced by inconsistencies in geometry or experimental conditions. The median curve can be seen with error bars indicated. It can be seen that the majority of the result sets fall within one standard deviation of the median. Curves 2, 5 and 8 appear to drop off suddenly, as the fracture occurred outside the bounds of the extensometer.

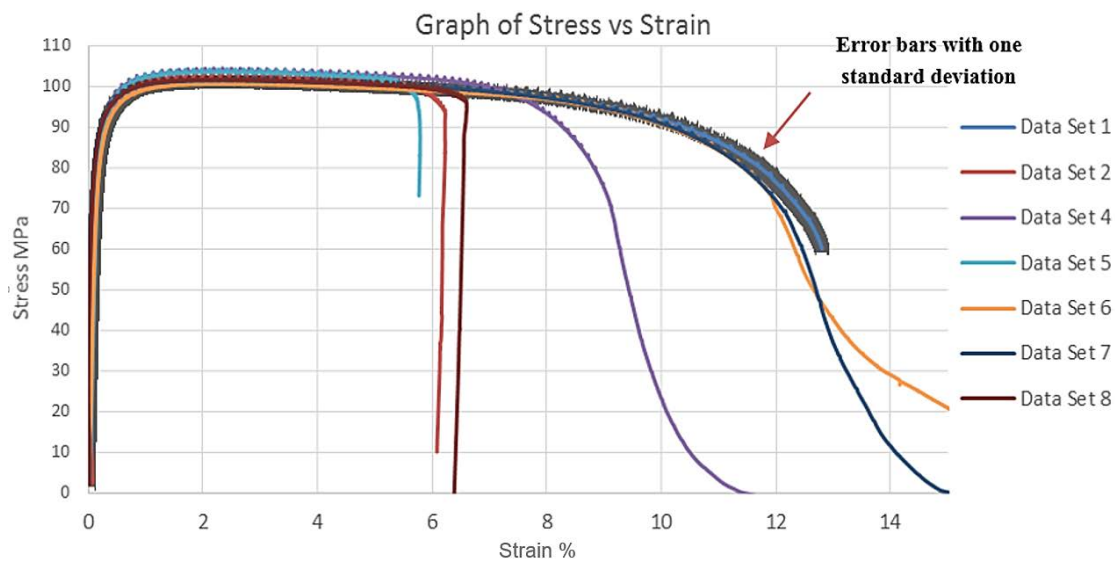


Figure 4-10. Seven result sets of stress (MPa) vs strain (%) for standard specimen geometry.

Intuitively, the elastic limit of a material is the point at which plastic deformation first occurs i.e. the stress-strain curve begins to deviate from linearity. This is not a very useful definition as the ability to determine this point depends on how accurately the stress and strain can be measured. To avoid this problem, the onset of the plasticity is usually described by an offset yield strength (ASM International, 2004). It can be found by constructing a straight line parallel to the initial linear portion of the stress-strain curve, but offset by $\epsilon = 0.002$ or 0.2 % (ASM International, 2004). The 0.2% offset line can be seen in Figure 4-11.

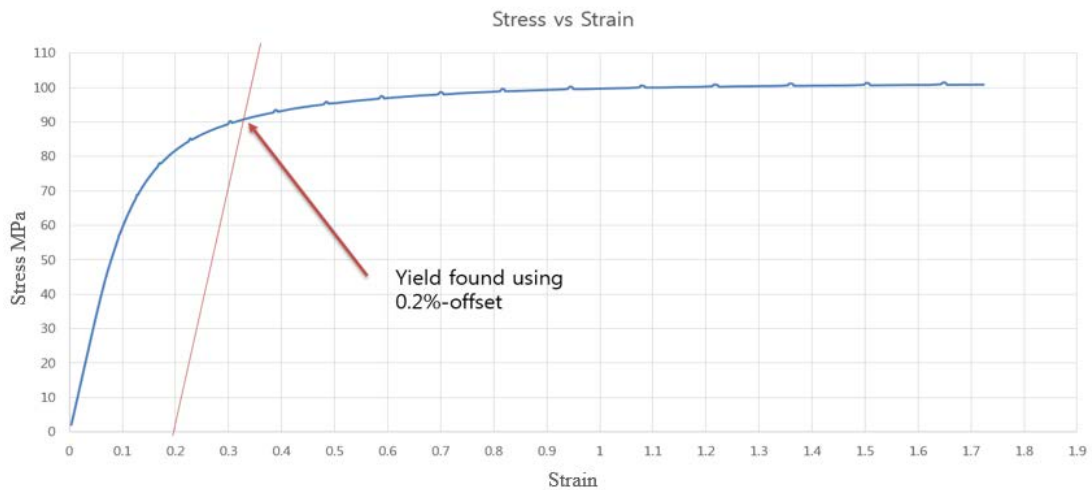


Figure 4-11. Median material curve showing 0.2% offset line.

Finite element analysis packages accept stress-strain data in the form of true stress and true strain. The following formulae found in (ASM International, 2004), were used to convert engineering stress and strain to true stress and strain.

$$\sigma_{true} = \sigma(1 + \epsilon) \quad (4.2)$$

$$\epsilon_{true} = \ln(1 + \epsilon) \quad (4.3)$$

At lower strains, the differences between true and engineering stresses and strains are very small. It must be noted that these equations are only valid for uniform deformation. They are no longer valid once necking begins, thus only valid up to the ultimate tensile stress (UTS) (ASM International, 2004).

Table 4-13 shows the mechanical material properties that are used for this test case.

Table 4-13. Model properties for Tensile test specimen analyses

Material Properties chosen	E= 63 GPa (Measured from chosen curve)
	$\nu = 0.3$ (From material specification sheet)
	Yield Stress= 91.44 MPa
Geometric properties chosen	As seen in Figure 4-9
Boundary conditions chosen	Fully fixed end on face A
	Displacement face B

Figure 4-12 shows six of the twelve result sets obtained. These fell within one deviation of the chosen median curve for most of the extension. The median curve was used as the target solution for this test case.

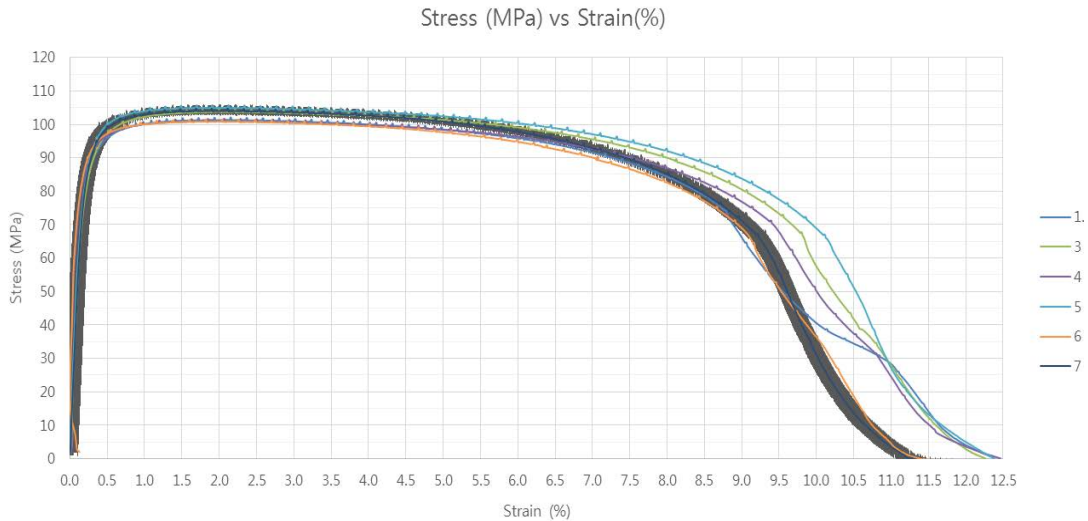


Figure 4-12. Six result sets of stress vs strain for custom specimen geometry

Material non-linearities are less frequently analysed, however it was decided that it was important that a package have the capabilities to perform this type of analysis nonetheless. It was also decided that this case be carried out experimentally so that results could be verified. To successfully analyse this test case, the 3-D solid geometry representation of the specimen must be imported into the pre-processor. The pre-processor must be able to apply an appropriate material plasticity model to the finite element model and allow for the material properties to be entered. The required boundary conditions should be applied. It would be necessary for the incremental results could be recorded for each load step. Lastly, the post-processing module of the package must be able to represent the target solution on an appropriate plot.

CHAPTER 5 : Model Generation Procedure and Presentation of Results

The first section of this chapter describes the package-specific model generation procedure for the test cases described in Chapter 4. The next section of this chapter presents the simulation results yielded by each package for the various test cases.

5.1 Model Generation

The associated figures for this chapter can be found in Appendix B.

5.1.1 Mecway

The model generation procedure for the chosen test cases simulated within Mecway is presented here. A full licence of Mecway v 5.0 was freely provided by the developers for the purpose of this research.

Test Case 1: Grid Point Load on an Articulated Truss

This test case was generated in the suggested approach stated in Section 4.1.1. The elements and nodes for the geometry were created within the 2-D structural analysis environment. Images depicting geometry creation can be seen in Figure B.1 and Figure B.2. Application of the appropriate geometrical and material properties, and boundary conditions specified can be seen in Figure B.3 through to Figure B.5. The relevant solutions were obtained through graphical plots by the internal post-processor.

Test Case 2: Thin Shell Wall in Pure Bending

This test case was generated in the suggested approach stated in Section 4.1.2. Appropriate 2-D geometry was imported into the 2-D structural analysis environment. The input of material and geometric properties, meshing parameters and appropriate boundary conditions can be seen in Figure B.7 through to B.10. Imposing the required boundary conditions took some effort as Mecway required that the edge of every element lying on the edge of interest be individually selected. Solutions were obtained through graphical plots by the internal post-processor. The mesh size was refined until results began to correlate more closely with

target solutions. Second order elements were used as they were found to provide more accurate results.

Four mesh sizes were recorded in order to give an indication of solutions tending towards a converging value. These were tetrahedral element meshes of sizes: 1 inch, 0.5 inch, 0.3 inch, and 0.15 inch.

Test Case 3: Axisymmetric Pressure Vessel

This test case was generated in the suggested approach stated in Section 4.1.3. Appropriate 2-D geometry was imported into an axisymmetric structural analysis environment, seen in Figure B.11. Appropriate material properties and 2-D meshing parameters were used. The input of displacement fixtures and loads can be seen in Figure B.12 through to Figure B.14. The cumbersome method of selecting an edge per element to apply a load was once again experienced in this test case. Solutions were obtained through graphical plots by the internal post-processor. The mesh size was refined until the simulation results began to correlate more closely with the target solution. The mesh sizes used were: 25 mm, 12.5 mm and a 5mm second-order triangular surface mesh.

Test Case 4: Internal Pressure on Thick-Walled Spherical Container

This test case was generated in the suggested approach stated in Section 4.1.4. A 3-D geometry was imported into the structural analysis environment. Appropriate material properties and meshing parameters were used. Application of frictionless supports and the pressure loading can be seen in Figure B.15 and Figure B.16 respectively. Solutions were obtained through graphical plots by the internal post-processor. The mesh size was refined until simulation results began to correlate more with the target solution. Quadratic tetrahedral elements were used as they were found to result in a more accurate solution compared to linear elements. Three result sets were recorded. The element sizes of the tetrahedral meshes used were: 200mm, 100mm, and 50mm.

Test Case 5: Flat Bar with Stress Concentration

This test case was generated in the suggested approach stated in Section 4.1.5. Appropriate geometry was imported into a 3-D structural analysis environment. Appropriate material properties and 3-D meshing parameters were applied. Images depicting the application of the fixture and load can be found in Figure B.16 and B.17 respectively. Relevant solutions were obtained through graphical plots in the internal post-processor. The mesh size was refined until the simulation results began to correlate more with the target solution. The element sizes of the tetrahedral meshes used were: 10mm, 5mm, 3mm and 1.5mm.

Test Case 6: Large deflection of a Z-Shaped Cantilever Beam Under End Load

This test case was not generated in the suggested approach in Section 4.2.1. 2-D shell elements are not accepted in the non-linear structural analysis environment, as seen in Figure B.18. Hence 3-D geometry was used. The non-linear analysis settings used can be seen in Figure B.19. Appropriate material properties and meshing parameters were used. A fully fixed constraint was applied to one end of the geometry and an incremental load following values given in the test case data were used. Application of the incremental load can be seen in Figure B.20. The relevant solutions were obtained through graphical plots by the post-processor. One result set was recorded. It used a 0.85 mm second-order tetrahedral mesh. This solution showed good accuracy. Attempts to refine the mesh any further resulted in excessive solve times and would cause the package to close unexpectedly.

Test Case 7: Plastic Deformation of Tensile Test Specimen

This test case was generated in the suggested approach stated in Section 4.2.2. Appropriate 3-D geometry was imported into the non-linear structural analysis environment. The Mecway solver cannot account for elasto-plastic materials however, Mecway allows users to download and add-on the CalculiX solver to the package. Selecting the CalculiX solver adds in a CalculiX tab (CCX) in the model tree, as seen in Figure B.20, extending the capabilities of the Mecway package to include elasto-plastic material analysis. Under the CCX tab, the custom material properties and stress-strain point data were entered, as seen in figure B.21. The model definition code can be seen in Figure B.22 and Figure B.23.

A fully fixed displacement constraint was imposed on one end of the specimen and a 4 mm prescribed displacement was defined on the other, as seen in Figure B.24. A 1.5mm second order tetrahedral mesh was used to obtain the solution. Attempts were made to refine the mesh and it was noted that this did not affect the result substantially and did not warrant the greatly increased solution times.

Mecway does not output tabulated results but rather generates a graph of stress versus time. This graph was imported into a freeware package called Webplot Digitizer, which generates data points from an image of a graph. Knowing that the displacement loading is linearly ramped to the final value, a stress versus extension graph was generated. The relevant data points were then obtained and recorded so that comparisons could be made to the target solution.

5.1.2 Z88 Aurora

The model generation procedure for the test cases simulated in Z88 Aurora is presented here.

Test Case 1: Grid Point Load on an Articulated Truss

This test case was generated in the suggested approach. The elements and nodes were created within the structural analysis environment of Z88 Aurora. The process of geometry creation can be seen in Figure B.25 through to Figure B.27. A new material was created in the material database and applied to the model. Nodal fixtures and force were applied to the relevant nodes in the ‘Loads and Constraints’ window shown in Figure B.28 and Figure B.29 respectively. Relevant solutions were obtained through graphical plots by the internal post-processor.

Test Case 2: Thin Shell Wall in Pure Bending

This test case is best modelled as a 2-D surface. Despite numerous attempts, a working 2-D mesh could not be generated. Figure 5-1 shows the error message received when trying to create a 2-D mesh within Z88 Aurora.

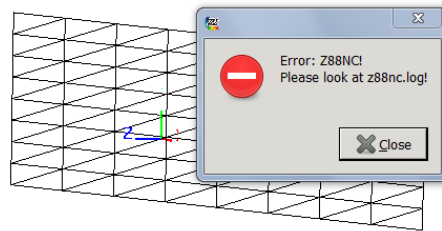


Figure 5-1. Error dialog box displayed when attempting to create a 2-D mesh.

Attempts were made to use 3-D geometry, however the thickness of the geometry required that a very fine mesh be used. This proved difficult for the software to mesh and a suitable 3-D mesh was not obtained, as the software would close unexpectedly.

Test Case 3: Axisymmetric Pressure Vessel

This test case was not generated in the suggested approach. A suitable 2-D mesh was not generated, therefore a 3-D quarter-geometry was used. The meshing parameters can be seen in Figure B.30. A 25mm first-order tetrahedral mesh was used. The material properties were added to the ‘Material Database’, seen in Figure B.31. The application of the displacement constraints and pressure load can be seen in Figure B.32 and Figure B.33 respectively. The solutions obtained showed expected response but it was evident that mesh refinement was necessary, however any attempt to do so would result in the package closing unexpectedly.

Test Case 4: Internal Pressure on Thick-Walled Spherical Container

This test case was generated in the suggested approach. A 3-D geometry was imported into the structural analysis environment. Appropriate material properties and 3-D meshing parameters were used. Application of a displacement constraint and the pressure load can be seen in Figure B.34 and Figure B.35 respectively. Solutions were obtained through graphical plots by the internal post-processor. The model was rerun using the mesh sizes from the previous benchmarking process for Mecway. This was done so that there is a control variable when comparing the results of the packages. Z88 was able to generate second-order tetrahedral meshes of 200mm and 100mm element size but not with 50mm element size and hence only 2 result sets were obtained.

Test Case 5: Flat Bar with Stress Concentration

This test case was generated in the suggested approach. A 3-D geometry was imported into the structural analysis environment. Appropriate material properties and 3-D meshing parameters were applied. The fixture and the force were applied to the appropriate faces. Solutions were obtained through graphical plots in the internal post-processor. The mesh size was refined until the simulation results began to correlate more with the target solution. The simulation was rerun using the tetrahedral mesh sizes used in the previous benchmarking process for Mecway i.e. 10 mm, 5mm, 3mm and 1.5mm.

Test Case 6: Large deflection of a Z-Shaped Cantilever Beam under End Load

This test case was not generated in the suggested approach. A 2-D mesh was not produced, therefore 3-D geometry was used. The material properties was added to the material database as seen in Figure B.37. A 1.7mm second-order tetrahedral elements were selected to mesh this model, as the meshing module was unable compute a second-order tetrahedral element with a smaller base size. The second-order element showed better accuracy than first-order element mesh of a smaller size. The fixture and incremental load was applied to the relevant faces. The load value was linearly ramped up to the total value over the given time steps. The non-linear solver settings can be seen in Figure B.38. The incremental solution results were obtained from graphical plots in the post-processor and recorded manually.

Test Case 7: Plastic Deformation of Tensile Test Specimen

This test case was not completed in the suggested approach. Suitable 3-D geometry was imported into the non-linear mechanical analysis environment. The material properties and flow curve were added to the material database, as seen in Figure B.39. Z88 is unable to impose a displacement constraint while conducting a non-linear analysis. This fact was confirmed through email correspondence from the Z88 support staff (Z88-Support, 2016).

An attempt was made to use an incremental force loading that corresponded to the maximum observed force during experimental testing and compare the results yielded for the stress and displacement solutions to the target values. This simulation did not yield meaningful results with respect to analysing plastic deformation.

5.1.3 SimScale

This section discusses the model generation procedure of the test cases simulated on the SimScale platform. As SimScale is completely web-based, no software installation was needed. In keeping with the concept of web-based engineering, a web-based parametric CAD modelling package called OnShape was used to create the geometries for use by SimScale only. All other packages used geometry generated in FreeCAD. The quality of the geometry created in both packages were inspected when they were imported into a commercial CAD modeller and verified to be suitable.

Test Case 1: Grid Point Load on an Articulated Truss

SimScale is unable to perform 1D analyses at this stage of its development.

Test Case 2: Thin Shell Wall in Pure Bending

SimScale is unable to perform 2-D analyses at this stage of development. Attempts were made to use 3-D geometry, however a suitable mesh was not generated.

Test Case 3: Axisymmetric Pressure Vessel

This test case was not generated in the suggested approach. SimScale is unable to perform 2-D analyses therefore a 3-D quarter-geometry was used. The required material properties and meshing parameters were applied to the model as shown in Figure B.40 and Figure B.41 respectively. The application of the displacement constraint and the pressure load can be seen in Figure B.42 and Figure B.43 respectively. The ‘Spooles’ direct solver was selected as this is recommended to be used for most 3-D problems, as seen in Figure B.44. Results were obtained from graphical plots through the internal post-processor. The result sets recorded used a 25mm second-order tetrahedral mesh and 12.5mm first-order tetrahedral mesh. Mesh creation failed when attempting to generate mesh using second-order elements or reducing the mesh size to 5mm.

Test Case 4: Internal Pressure on Thick-Walled Spherical Container

This test case was generated in the suggested approach. 3-D geometry was imported into the structural analysis environment. Appropriate material properties and mesh parameters were applied to the model, seen in Figure B.45. The application of the symmetry constraints and internal pressure load can be seen in Figure B.46 and Figure B.47. Relevant solutions were obtained through graphical plots in the web based post-processor. The model was rerun with mesh sizes used in the previous benchmarking processes.

Test Case 5: Flat Bar with Stress Concentration

This test case was generated in the suggested approach. A 3-D geometry was imported into the structural analysis environment. The appropriate material properties and meshing parameters were applied to the model. The application of the fixture and load can be seen in Figure B.48 and Figure B.49. The relevant solutions were obtained through graphical plots by the internal post-processor. The simulation was rerun using the mesh sizes used in previous benchmarking.

Test Case 6: Large deflection of a Z-Shaped Cantilever Beam under End Load

This test case was not generated in the suggested approach in Section 4.2.1 as SimScale is unable to analyse 2-D elements, a 3-D geometry was used. The analysis type was set to “Advanced Static Structural”, seen in Figure B.50, as this allows for non-linearities to be considered. Appropriate meshing parameters and material properties were applied to the model. The required fixed constraint was applied through the ‘Boundary Constraints’ window. The incremental force values given in the test case data were input to the model via a .csv file which stipulates the force value at a given time step. This can be seen in Figure B.51. The PETSC iterative solver was chosen for this analysis, as seen in Figure B.52. The simulation settings and time step definition used can be seen in Figure B.53. The incremental results appeared to cause difficulty for the internal post-processor. SimScale suggests using ParaView, an open source post-processing package (SimScale GmbH, 2015). The incremental results were viewed and recorded from ParaView manually.

Test Case 7: Plastic Deformation of Tensile Test Specimen

This test case was generated in the suggested approach in Section 4.2.2. The analysis type was set to “Advanced Static Structural” to model the elasto-plastic material behaviour. The mesh parameters and material properties, including flow curve data, were specified.

The initial point on the flow curve corresponded to the end point along the purely elastic range of the flow curve. It was recommended by the user documentation that this point be used, as there have been convergence issues if the point does not correspond to the value of the Young's modulus (SimScale GmbH, 2015). The flow curve data was imported into SimScale as a .csv file. The flow curve can be seen in Figure B.54. A fully fixed displacement constraint was used on one end of the specimen and a 4 mm imposed displacement was defined on the other end. SimScale recommends the direct multifrontal-type solver called MUMPS for this type of analysis. Manual time-stepping was enabled and set to calculate 100 load steps and save the incremental results.

Once the solutions were generated, the result set was exported to ParaView for post-processing. The incremental solutions were manually recorded. The results were tabulated and a graph was generated for comparison with the target response curve.

5.1.4 Code_Aster/Salome Meca

This section presents the model generation procedure of the chosen test cases simulated in Code_Aster/Salome Meca. These programs operate on the Linux OS. A version of Linux known as CAELinux was installed, which contains several open-source CAE software packages such as OpenFoam, Elmer FEA and FreeCAD, to name a few. CAELinux contained the 2013 version of Salome Meca. Though not the most recent version of the software, the capabilities have not changed significantly.

Test Case 1: Grid Point Load on an Articulated Truss

This test case was generated in the suggested approach. The elements and nodes for the geometry were created within the geometry module of Salome Meca. Images depicting geometry creation can be seen in Figure B.56 through to and Figure B.58. This process involved creating nodal points, then lines bodies. From these nodes and lines, an analysable body known as a compound in Salome Meca was created. The 1-D meshing rule can be seen in Figure B.59. The mesh is saved as a .med file that can be read by the Aster module. The Aster module is responsible for solving the finite element model. It does this through commands generated in a .comm file.

These .comm files were coded manually in the past and as such, introduced the potential for syntax errors. The Salome Meca platform comes bundled with an application called Efficas. Efficas allows users to select the various 'components' that are required for the given FEA and it creates the .comm file with the correct syntax from these inputs. Note that the Efficas

application is presented in French and requires effort on the part of the non-French speaking user to understand the operations and commands. The generated Eficas input file can be seen in Figure B.60. The generated .comm file (with comments explaining components used) can be seen in Appendix C.1. Once the .comm file was generated, the mesh and .comm file were saved to an Aster job file to be run, as seen in Figure B.61. The post-processing module was activated and the results were observed and recorded.

Test Case 2: Thin Shell Wall in Pure Bending

This test case was generated in the suggested approach. Appropriate 2-D geometry was imported and prepared for analysis, shown in Figure B.62. A second-order triangular surface mesh was created in the meshing module, seen in Figure B.63. Eficas was used to generate the .comm file for this analysis. The Eficas inputs can be seen in Figure B.64. The generated .comm file with comments can be seen in Appendix C.2. Once the solution was run, the post-processing module was activated and the results were observed and recorded. The simulation was rerun, varying the mesh sizes as per previous packages.

Test Case 3: Axisymmetric Pressure Vessel

This test case was generated in the suggested approach. The 2-D geometry was imported and prepared for analysis within the geometry module, as seen in Figure B.65. A second-order triangular mesh was created within the meshing module, shown in Figure B.66. Salome Meca has a ‘wizard’ that allows for a .comm file to be generated (provided that only a pressure load is used as well as free/fixed displacement constraints). The wizard allows for an axisymmetric analysis environment to be specified. Figure B.67 through to Figure B.70 show the options selected in the wizard dialog boxes. The generated .comm file can be seen in Appendix C.3. Once the solution was generated, the post-processing module was activated and the results were observed through graphical plots. The simulation was rerun, varying the mesh sizes as per previous packages.

Test Case 4: Internal Pressure on Thick-Walled Spherical Container

This test case was generated in the suggested approach. The 3-D geometry was imported and prepared in the geometry module, as seen in Figure B.71. A second order tetrahedral mesh was created using the meshing module, as shown in Figure B.72. The .comm file could be generated through the ‘wizard’. Figure B.73 through to Figure B.77 show the wizard inputs. The .comm file for this test case can be seen in Appendix C.4. Once the solution was generated, the post-processing module was activated and the results were observed. The simulation was rerun, varying the mesh sizes according to element sizes used in previous benchmarking processes. The result sets required were then recorded.

Test Case 5: Flat Bar with Stress Concentration

This test case was generated in the suggested approach. Appropriated 3-D geometry used. A second-order tetrahedral mesh was generated. The Efficas input file is shown in Figure B.78 and the generated .comm file can be found in Appendix C.4. Once the solution was generated, the post-processing module was activated and the results were observed. The simulation was rerun, varying the mesh sizes as per previous packages.

Test Case 6: Large deflection of a Z-Shaped Cantilever Beam under End Load

This test case was not generated in the suggested approach. The non-linear solver does not permit 2-D elements, therefore a 3-D geometry was used. A second-order tetrahedral mesh was used for this model. Efficas was used to generate the .comm file for this analysis. The Efficas inputs can be seen in Figure B.79 and the generated .comm file can be found in Appendix C.5. The process for conducting non-linear analysis differed slightly from the linear problems. The functions of the non-linear operators were initially quite difficult to understand. The syntax used in the available software relative to the current documentation often varied, causing unexpected errors, which proved difficult to identify within the error log. Once the solution was generated, the post-processing module was activated and the results were observed. Code_Aster solves and stores the incremental results. These results were manually recorded.

Test Case 7: Plastic Deformation of Tensile Test Specimen

This test case was generated in the suggested approach. The 3-D geometry was imported into the geometry module of Salome Meca. A second-order tetrahedral mesh based on sizes used in previous benchmarking tests was generated. Efficas was used to generate the .comm file for this analysis. See Figure B.80 for the Efficas input file as well as Appendix C.6 for the generated command file (with comments explaining components used). The non-linear solver was set to record incremental results. The stress results were recorded and tabulated, and a graph was generated for comparison between the output and target results.

5.1.5 ANSYS

The model generation procedure for the test cases simulated within the ANSYS platform is presented here. The version used, ANSYS 16.1, is licensed to the University of KwaZulu-Natal. The two ANSYS environments used in this research are the ANSYS Static Structural Mechanical environment and the ANSYS Mechanical APDL (ANSYS Parametric Design Language) environment.

Test Case 1: Grid Point Load on an Articulated Truss

This test case was generated in the suggested approach. Through prior experience with ANSYS Static Structural Mechanical environment it was noted that this environment was restrictive in the creation of 1D truss structures. It was decided to use the Mechanical APDL environment to generate this model. The Mechanical APDL environment differs from the ANSYS Mechanical environment in that the APDL environment requires more text based input as opposed to the 'point and click' method seen amongst contemporary FEA packages. The process of creating the model geometry can be seen in Figure B.82 through to Figure B.84. The required material properties were applied to the structure as seen in Figure B.85. The application of the required nodal fixture and force can be seen in Figure B.86 and Figure B.87 respectively. After the model was generated, the simulation was run and the relevant solutions were obtained in a post processing window within the same environment.

Test Case 2: Thin Shell Wall in Pure Bending

This test case was generated in the suggested approach. Suitable 2-D geometry was imported into ANSYS Static Structural Mechanical. The geometrical properties were applied to the surface geometry as shown in Figure B.88. The given material properties were added to the material library. The ANSYS meshing parameters were mostly set to its automatic programme controlled option, an example of which can be seen in Figure B.89. It was assumed that by doing this, a near-optimal mesh would be created. The edge fixture and load were applied as shown in Figure B.90 and B.91 respectively. The relevant solutions were obtained through graphical plots generated by the internal post-processor. The model was rerun varying the mesh sizes accordingly. The recorded result sets consisted of second-order quadrilateral meshes with a maximum element size of 1.0 in, 0.5 in, 0.3 in and 0.15 in.

Test Case 3: Axisymmetric Pressure Vessel

This test case was generated in the suggested approach. The 2-D geometry was imported into ANSYS Static Structural Mechanical within an axisymmetric analysis environment, as shown in Figure B.92. The required material properties were entered into the material library. The meshing parameters, an example of which can be seen in Figure B.93, were mostly set to the programme-controlled settings. This resulted in a second order quadrilateral mesh. The application of the frictionless supports and internal pressure load can be seen in Figure B.94 and Figure B.95. The relevant solutions were obtained through graphical plots generated by the internal post-processor. The model was rerun using the mesh sizes as per previous packages.

Test Case 4: Internal Pressure on Thick-Walled Spherical Container

This test case was generated in the suggested approach. Appropriate 3-D geometry was used. The required material data was entered into the material library. The meshing parameters were set to the automatic programme controlled settings. The application of the frictionless supports and pressure load can be seen in Figure B.96 and Figure B.97. The simulation was run and the relevant solutions were obtained through graphical plots generated by the internal post-processor. The model was rerun using the mesh sizes used in the previous benchmarking processes.

Test Case 5: Flat Bar with Stress Concentration

This test case was generated in the suggested approach. The 3-D geometry for this test case was imported into ANSYS. The material data was added into the material library. Meshing parameters were set mostly to programme-controlled options, resulting in a second order hexahedral mesh. The fixture and force were applied to the relevant faces, seen in Figure B.98 and Figure B.99. The relevant solutions were obtained through graphical plots generated by the internal post-processor. The model was rerun using the mesh sizes from previous benchmarking processes.

Test Case 6: Large deflection of a Z-Shaped Cantilever Beam under End Load

This test case was generated using the suggested approach. The 2-D geometry was imported into ANSYS. The 'Geometry Definition' tab was used to specify the thickness of the surface. The given material data was added into the material library. The mesh settings were set to programme-controlled. The required fixture was created using a fixed boundary constraint on the relevant edge. The incremental force values given in the test case data were specified through tabulated data. The time step and load information entered can be seen in Figure B.100. Most of the analysis settings were left as programme-controlled. The number of simulation time steps were set to match the load steps from the test case data. The solution was set to allow large deflection. The model was run using an iterative solver. The relevant solutions were obtained through graphical plots by the post-processor. Incremental solutions were also output in tabular form.

Test Case 7: Plastic Deformation of Tensile Test Specimen

This test case was generated using the suggested approach. The 3-D geometry was imported into ANSY. The material for this test case was created in the material library. In order to model the elasto-plastic behaviour effects, it was required that a plasticity model be used. The multilinear isotropic hardening model was used as it offers greater accuracy as compared to the bilinear isotropic hardening model also available. This plasticity model

allowed for the input of the flow curve in terms of true stress and plastic strain. The meshing parameters were mostly set to programme-controlled. The sizing was based on previous benchmarking tests. The fixed edge was imposed using a fully-fixed constraint. The displacement load was applied linearly over 100 increments. The analysis settings were left to programme-controlled. The solver was set to allow for large deformations, which is required when modelling material non-linearity. The model was run and the incremental solutions were output by ANSYS in tabular form.

5.1.6 Siemens NX

The model generation procedure for the various test cases simulated within the Siemens NX package is presented here. The version of NX 10.0 is licensed to the School of Engineering at the University of KwaZulu-Natal and was available for use in this research. Conducting finite element analyses in NX is particularly simple as it is a comprehensive package which seamlessly links the modelling environment with the analysis environment. All the geometry used for simulation within NX was created in the NX modelling environment.

Test Case 1: Grid Point Load on an Articulated Truss

This test case was generated in the suggested approach. The analysis type was set to 'Structural' with the 2-D analysis option enabled, as seen in Figure B.101. NX applies meshing parameters to a body through creation of a mesh collector which stores the relevant mesh information. Two mesh collectors were required to be created to model the two different cross-sections present in the model. One of the mesh collectors created can be seen in Figure B.102. The creation of the required geometric and material properties can be seen in Figure B.103 and Figure B.104 respectively. The application of the nodal fixtures and force can be seen in Figure B.105 and Figure B.106 respectively. The relevant solutions were obtained through graphical plots generated by the internal post-processor.

Test Case 2: Thin Shell Wall in Pure Bending

This test case was generated in the suggested approach. A 2-D mesh collector was created to contain the meshing and material properties, as seen in Figure B.107. A second-order triangular element was used. The shell thickness was defined through the creation of a shell element in the mesh collector, seen in Figure B.108. The application required edge fixture and load can be seen in Figure B.109 and Figure B.110. The relevant solutions were obtained through graphical plots by the internal post-processor. The model was rerun using the mesh sizes from previous benchmarking processes.

Test Case 3: Axisymmetric Pressure Vessel

This test case was generated in the suggested approach. The FEM environment allows for an axisymmetric structural analysis to be performed, as shown in Figure B.111. A 2-D mesh collector was created to contain the meshing and material properties for the model. A second-order triangular element was used to mesh the shell. The application of a user-defined displacement constraint and edge load can be seen in Figure B.112 and B.113. The relevant solutions were obtained through graphical plots by the internal post-processor. The model was rerun using mesh sizes from previous benchmarking processes.

Test Case 4: Internal Pressure on Thick-Walled Spherical Container

This test case was generated in the suggested approach. A 3-D mesh collector was created to store the meshing parameters and required material properties for this model. A second-order tetrahedral element was used to mesh the geometry. Tetrahedral elements are only available for 3-D structural analysis. The required displacement constraint and pressure load can be seen in Figure B.114 and Figure B.115. The simulation was run and the relevant solutions were obtained through graphical plots generated by the internal post-processor. The model was rerun using the mesh sizes used in the previous benchmarking processes.

Test Case 5: Flat Bar with Stress Concentration

This test case was generated in the suggested approach. A 3-D mesh collector was created to store the meshing parameters and required material properties for. A second-order tetrahedral element was used to mesh the geometry. The application of the fully fixed constraint and the force can be seen in Figure B.116 and Figure B.117. The relevant solutions were then obtained through graphical plots by the internal post-processor. The model was rerun using the mesh sizes from previous benchmarking processes.

Test Case 6: Large deflection of a Z-Shaped Cantilever Beam under End Load

This test case was generated in the suggested approach. The solver was set to the 'NX NASTRAN' solver and the analysis type was set to 'structural'. The solution type was set to SOL106 which allows for non-linear static analyses to be done. A 2-D mesh collector was created to contain the meshing and material and geometric properties. A second-order triangular element was used to mesh the surface. The required fixed edge was constrained by creating a user-defined displacement constraint. The linearly ramped force was applied to the relevant edge and the non-linear parameters were set to create 36 time steps so the incremental load could be applied. The solution parameters can be seen in figure B.118. The 'Large Deflection' setting was enabled so that the geometrical non-linearities could be

properly modelled. The non-linear solution was run and the relevant outputs were observed through graphical plots in the post-processor. Incremental results were recorded manually.

Test Case 7: Plastic Deformation of Tensile Test Specimen

This test case was generated in the suggested approach. The solver was set to ‘NX NASTRAN’ and the analysis type was set to ‘structural’. The solution type was set to SOL106 which allows for non-linear material effects to be analysed. A 3-D mesh collector was created to contain the meshing and material properties. The stress-strain data was also entered within the collector, as seen in Figure B.119. A second-order tetrahedral element was used to mesh the solid. The required fixed constraint and imposed displacement were applied to the relevant faces. The non-linear parameters were set to create 100 time steps so that the incremental extension could be applied. The ‘Large Deflection’ setting was enabled so that the material non-linearities can be properly modelled.

The non-linear solution was run and the relevant outputs were observed through graphical plots in the post-processor. The incremental solutions were recorded manually and tabulated in order to generate a response curve for comparison with the target solution.

5.2 Presentation of Simulation Results

This section will present the simulation results for the chosen benchmark test cases of each of the FEA software packages. Images of resulting plots generated by packages’ post-processors can be seen in Appendix D. In each section, the test case results are tabulated, followed by a graphical representation of the results. Though they may appear to show solution convergence graphically, they should not be viewed as convergence studies. The graphs are presented so that solutions from each package can be easily compared visually. Note that the dotted line shown in the graphs presented here represent the expected test case solution value.

5.2.1 Test Case 1: Grid Point Load on an Articulated Truss

The specific result outputs from each package is presented graphically in Figure 5-2 through to Figure 5-5. Note that SimScale was unable to perform 1-D element analyses. The tabulated results corresponding to these graphs can be found in Appendix E within Table E. 1 through to Table E. 5.

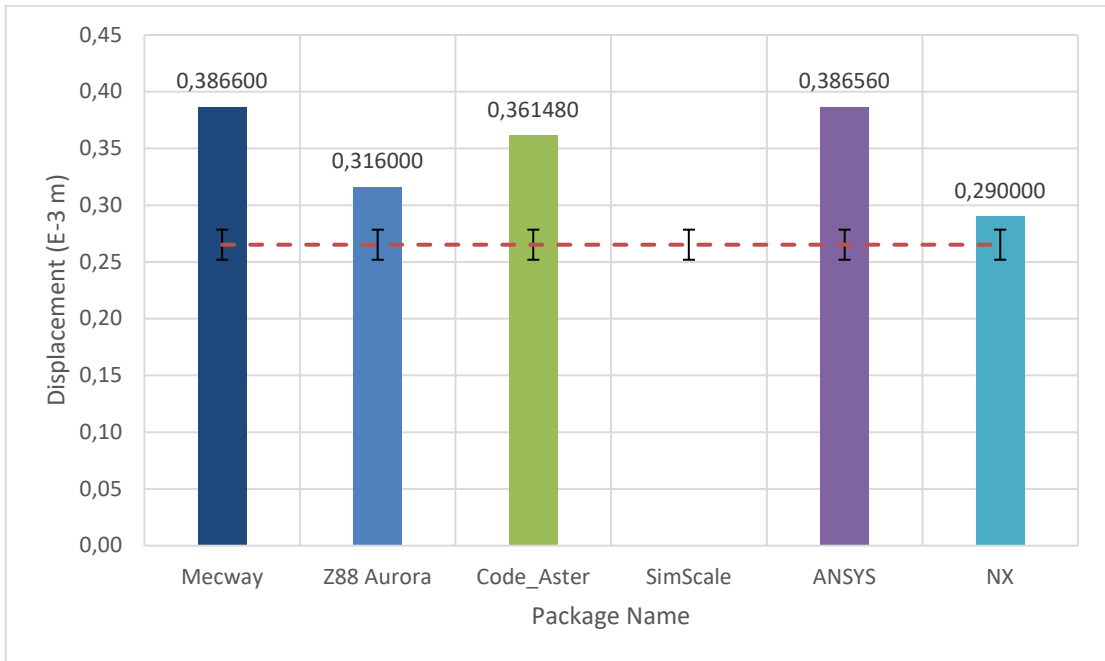


Figure 5-2. Graph of target output “X-directional displacement at node C” for each package.

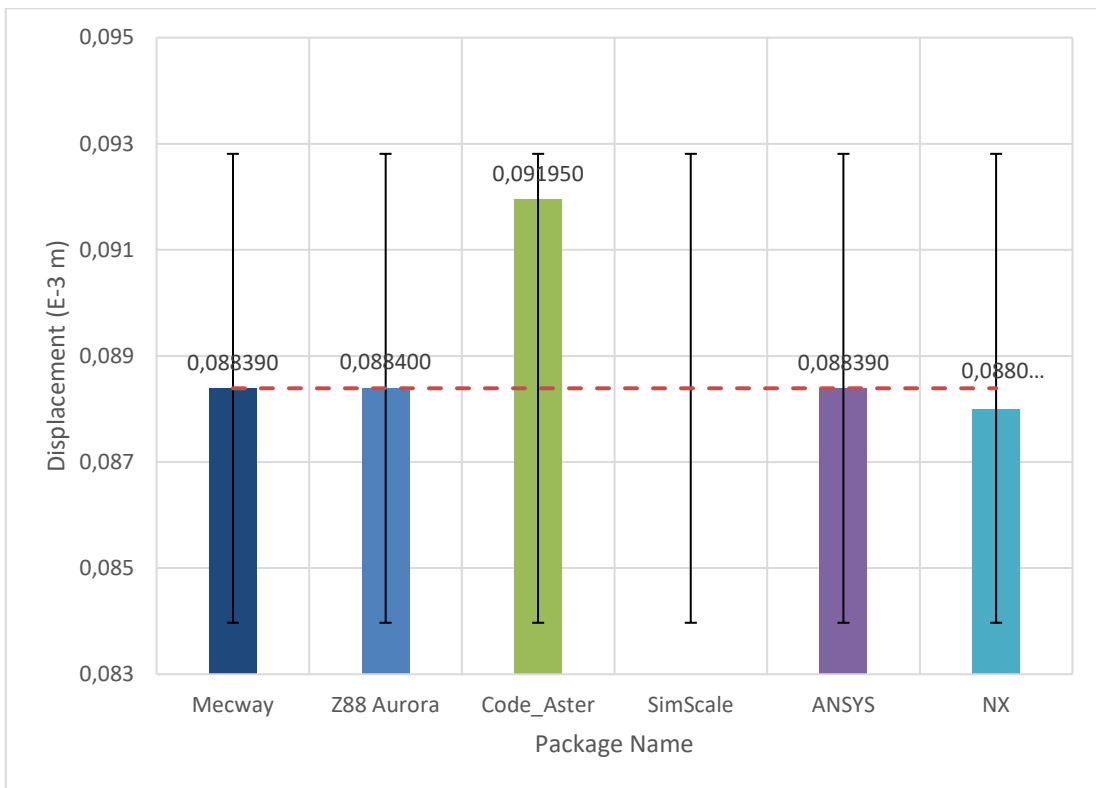


Figure 5-3. Graph of target output “Y-directional displacement at node C” for each package.

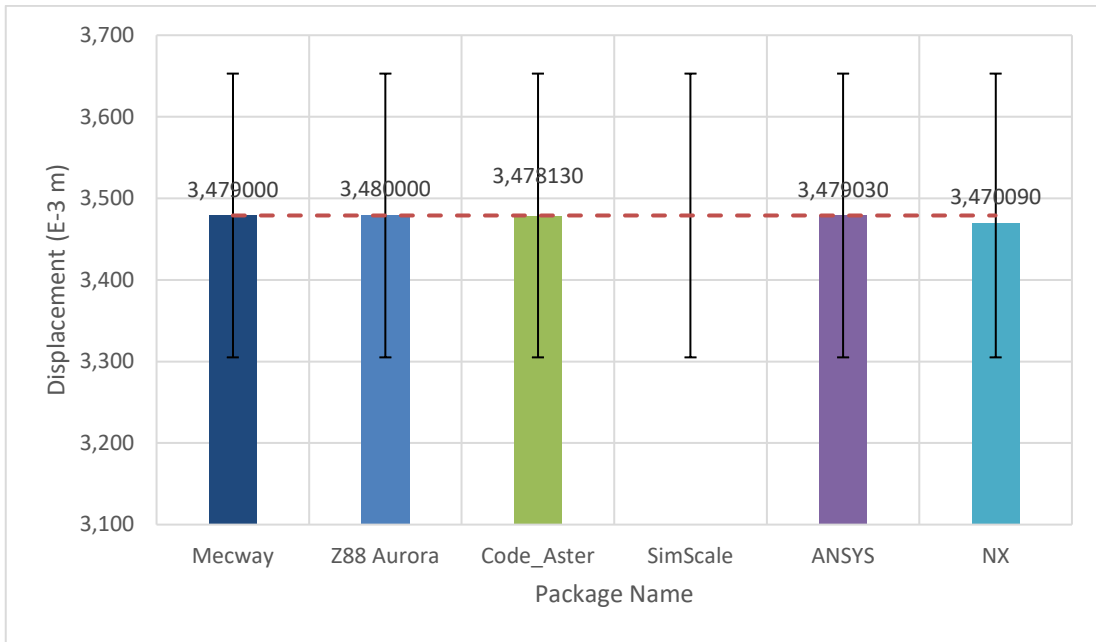


Figure 5-4. Graph of target output “X-directional displacement at node D” for each package.

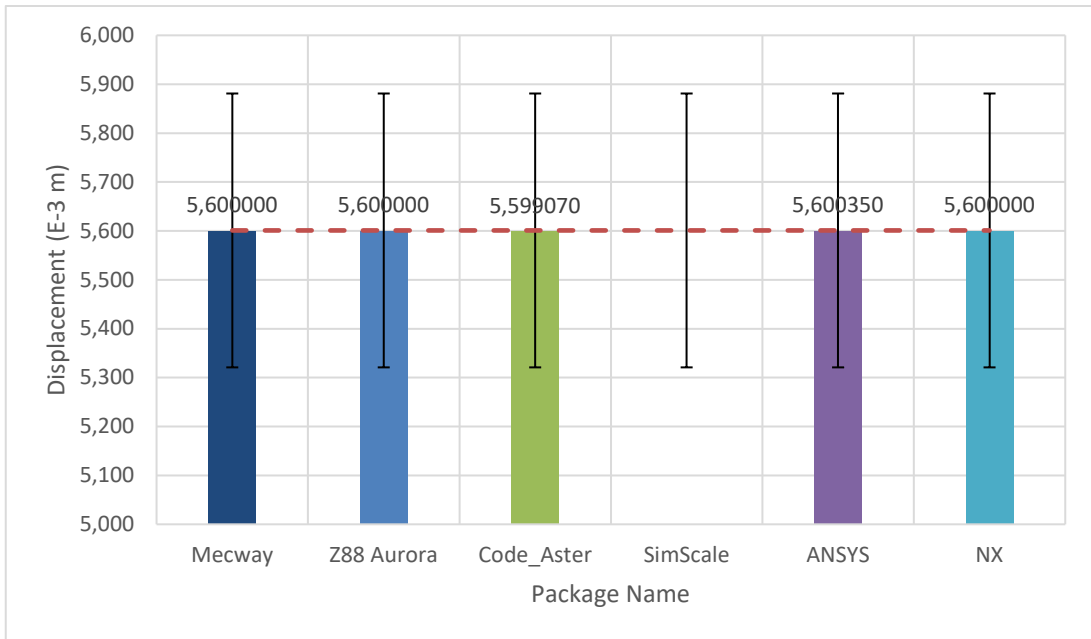


Figure 5-5. Graph of target output “Y-directional displacement at node D” for each package.

5.2.2 Test Case 2: Thin Shell Wall in Pure Bending

This section presents the results for Test Case 2: Thin Shell Wall in Pure Bending. Result sets 1, 2, 3, and 4 correspond to mesh sizes 1.0 in, 0.5 in, 0.3 in and 0.15 in, respectively. The specific result outputs from each package is presented graphically below in Figure 5-6 and Figure 5-7. The tabulated results corresponding to these graphs can be found in Appendix E within Table E. 6 through to Table E. 9.

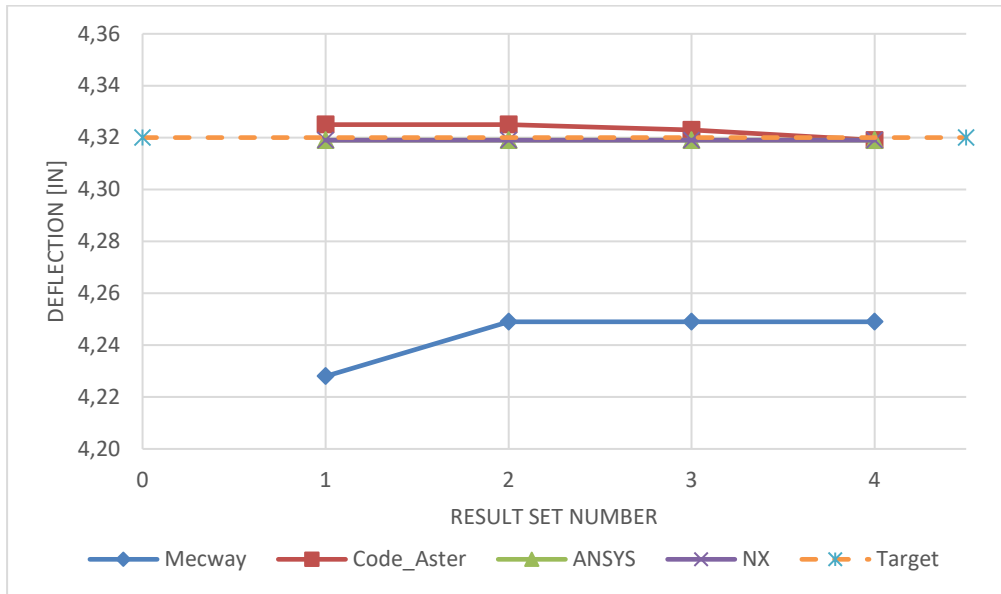


Figure 5-6. Graph of target output “Maximum Z-Direction deflection” for each package.

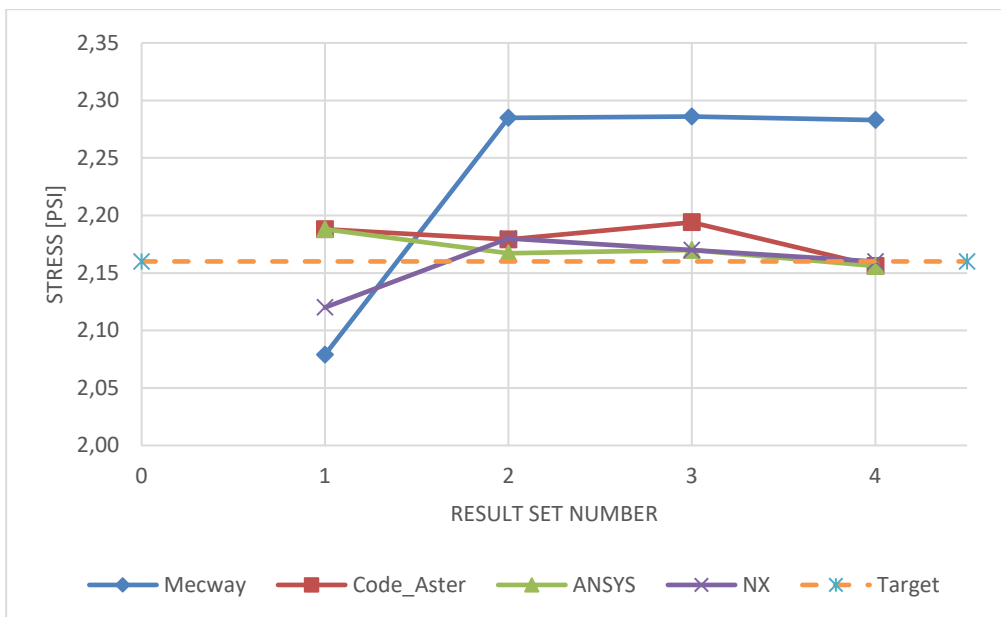


Figure 5-7. Graph of target output “Z-Directional Stress” for each package.

5.2.3 Test Case 3: Axisymmetric Pressure Vessel

This section presents the results for Test Case 3: Axisymmetric Pressure Vessel. Result sets 1, 2, and 3 correspond to mesh sizes 25 mm, 12.5mm and 5mm respectively. The specific result outputs from each package is presented graphically here in Figure 5-8. The tabulated results corresponding to these graphs can be found in Appendix E within Table E. 10 through to Table E. 15.

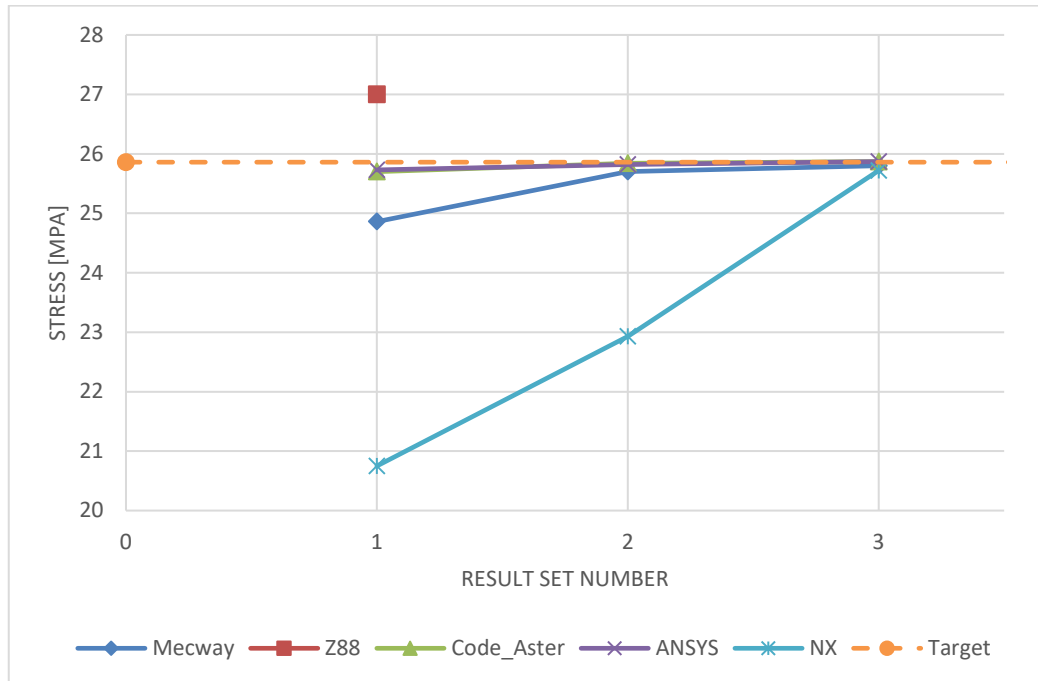


Figure 5-8. Graph of target output “Maximum Y-Directional Stress” for each package

5.2.4 Test Case 4: Internal Pressure on Thick-Walled Spherical Container

This section presents the results for Test Case 4: Internal Pressure on Thick-Walled Spherical Container. Result set 1, 2, and 3 correspond to mesh size 200mm, 100 mm and 50 mm respectively. The tabulated results corresponding to these graphs can be found in Appendix E within Table E. 16 through to Table E. 21. The specific result outputs from each package is presented graphically here in Figure 5-9 through to Figure 5-14

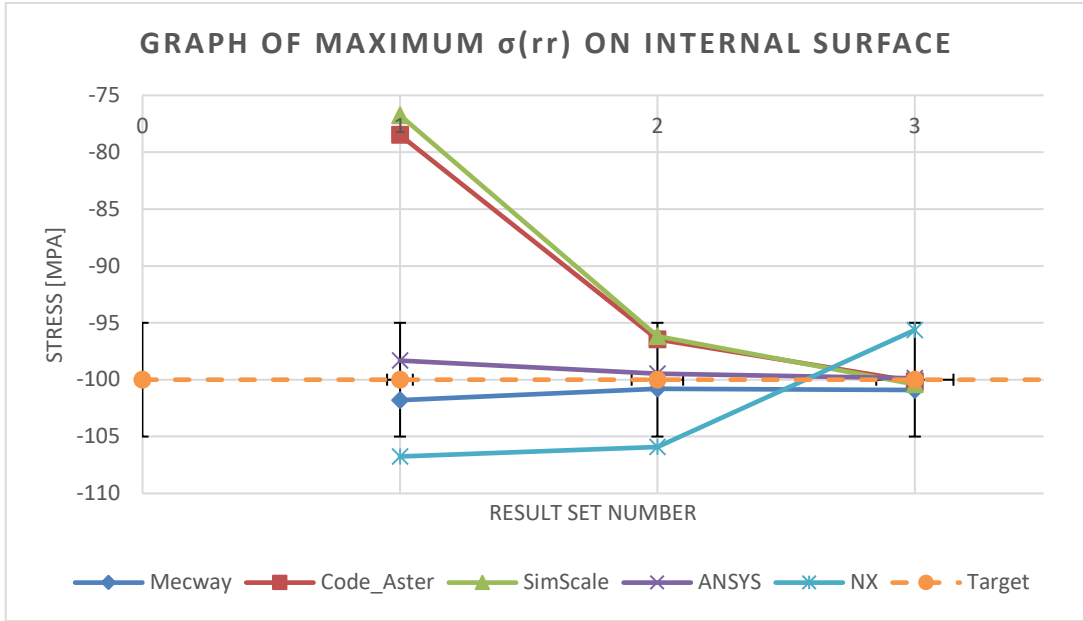


Figure 5-9. Graph of target output “Maximum $\sigma(rr)$ on internal surface” for each package.

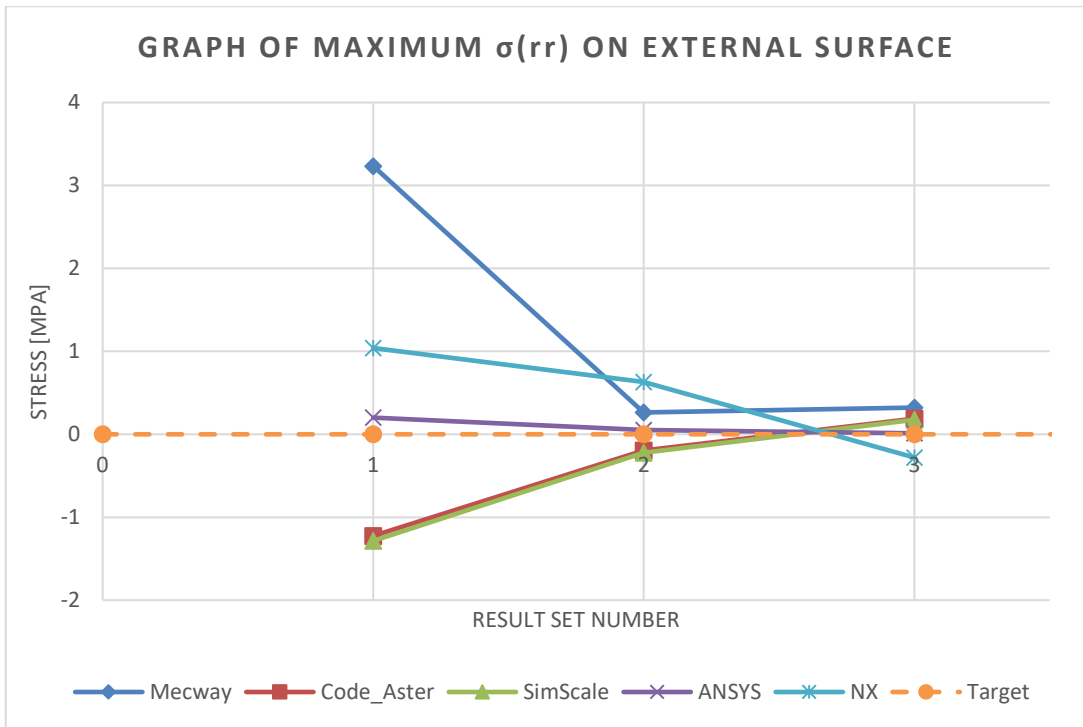


Figure 5-10. Graph of target output “Maximum $\sigma(rr)$ on external surface” for each package.

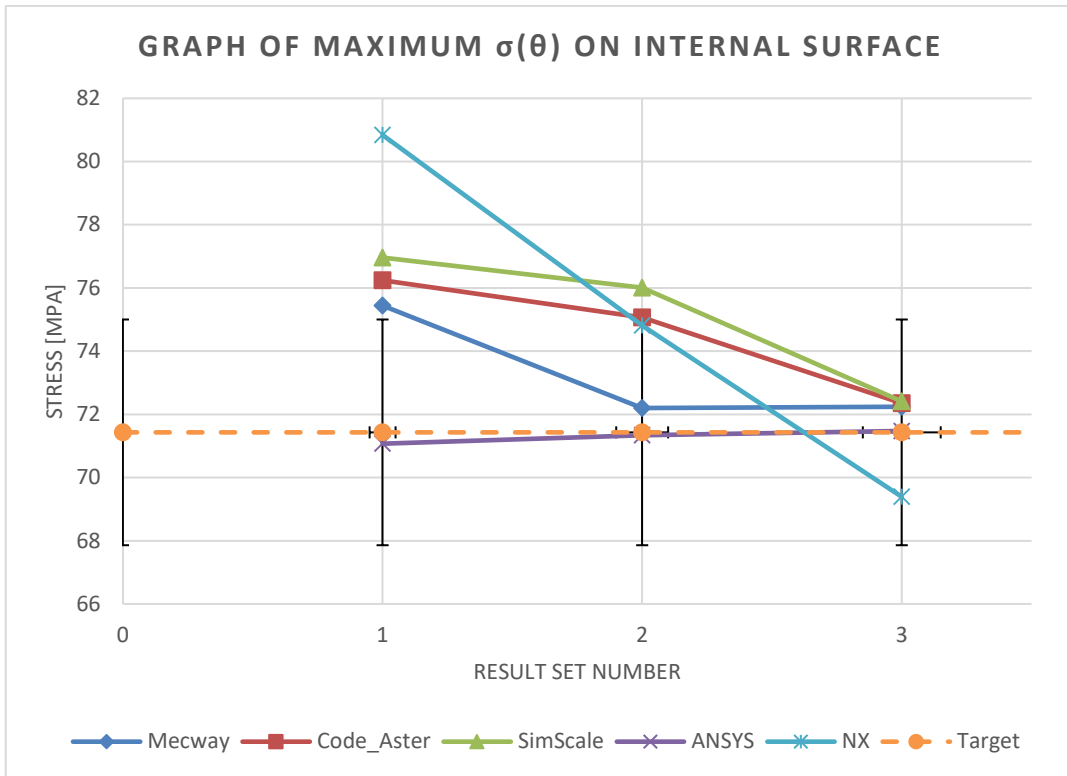


Figure 5-11. Graph of target output “Maximum $\sigma(\theta)$ on internal surface” for each package.

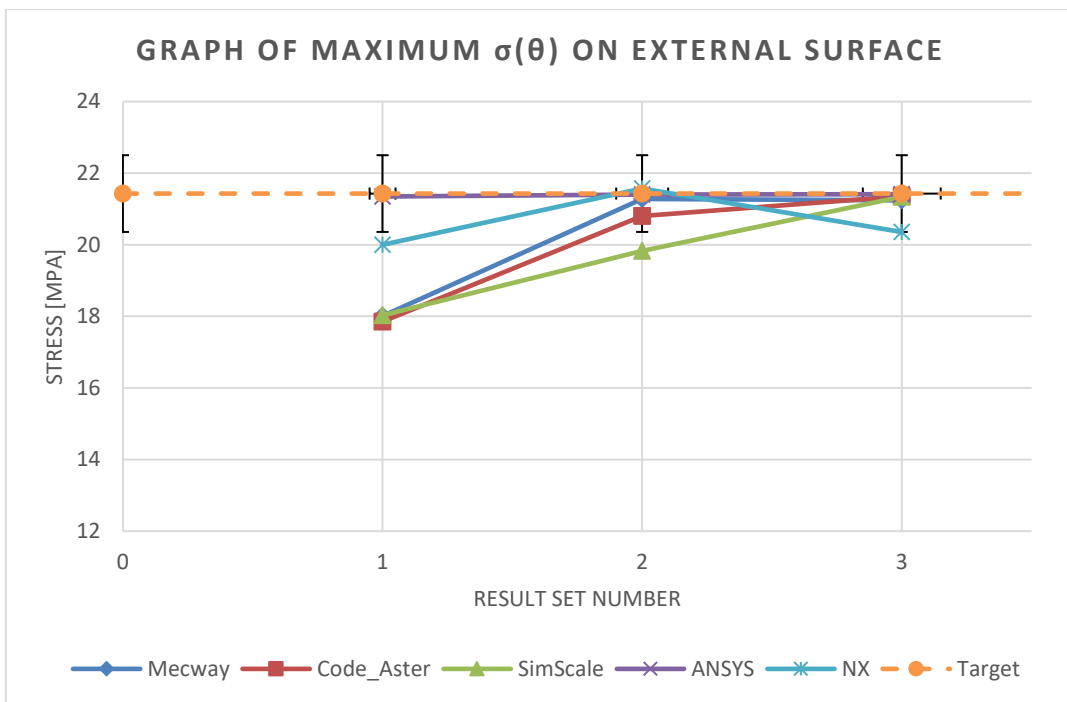


Figure 5-12. Graph of target output “Maximum $\sigma(\theta)$ on external surface” for each package.

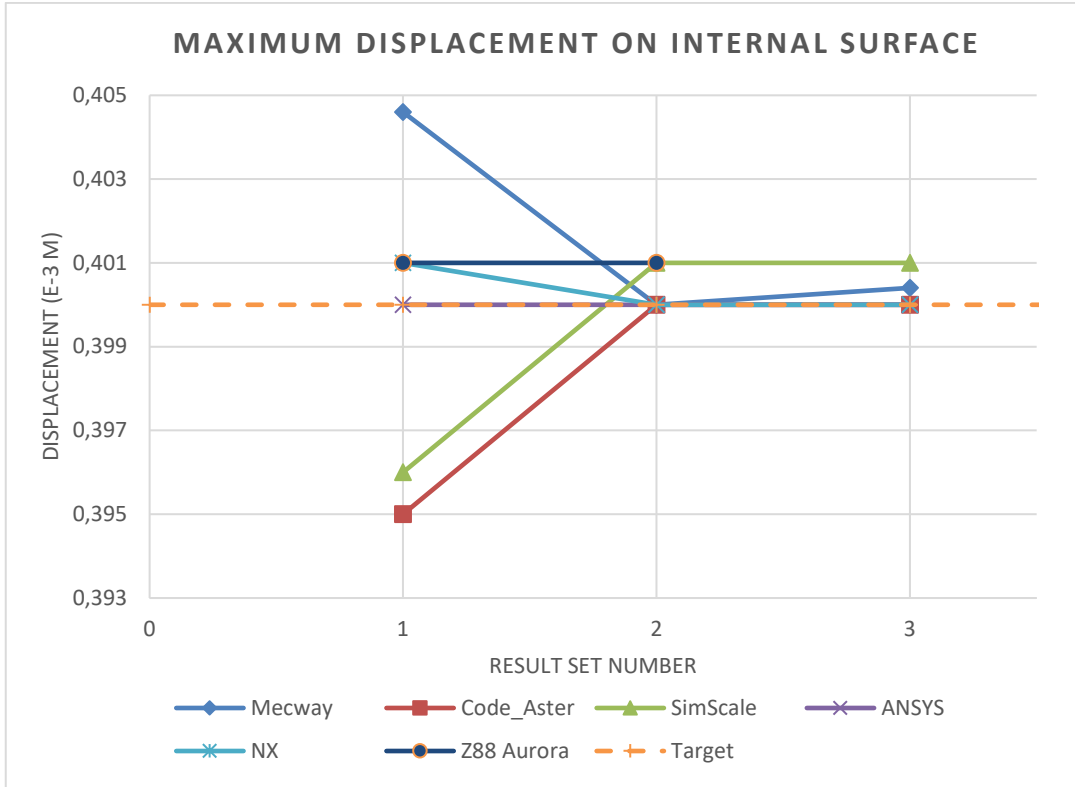


Figure 5-13. Graph of target output “Maximum displacement on internal surface” for each package.

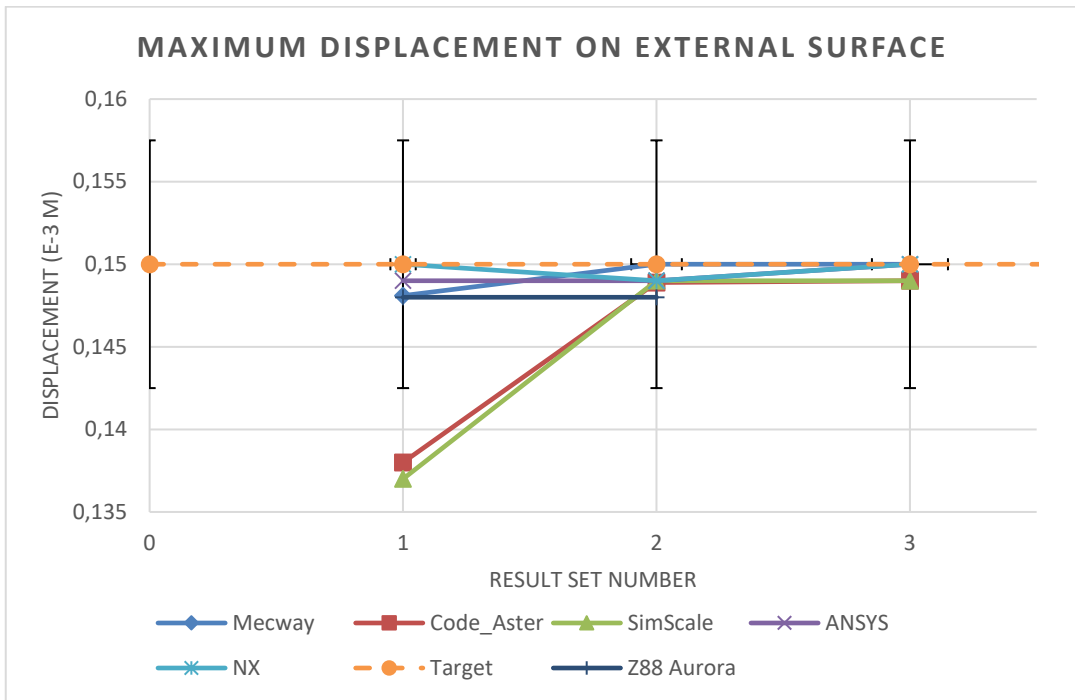


Figure 5-14. Graph of target output “Maximum displacement on external surface” for each package.

5.2.5 Test Case 5: Flat Bar with Stress Concentration

This section presents the results for Test Case 5: Flat Bar with Stress Concentration. Result sets 1, 2, 3, and 4 correspond to mesh sizes 10 mm, 5mm, 3mm and 1.5mm respectively. The specific result outputs from each package is presented graphically here in Figure 5-15 and Figure 5-16. The tabulated results corresponding to these graphs can be found in Appendix E within Table E. 22 through to Table E. 27.

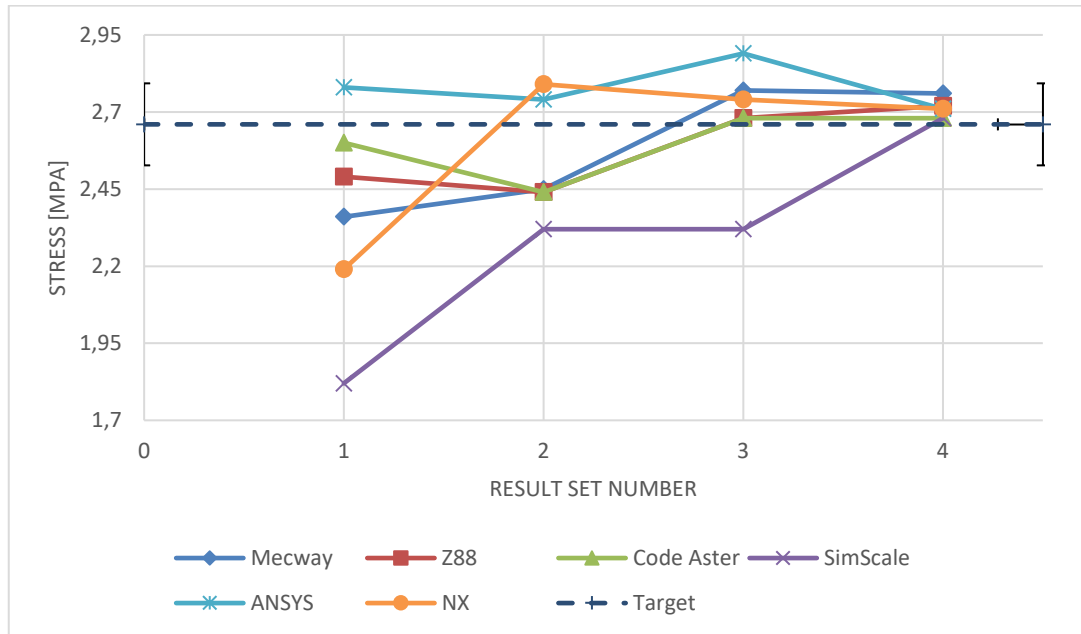


Figure 5-15. Graph of target output “Maximum Stress at Hole” for each package.

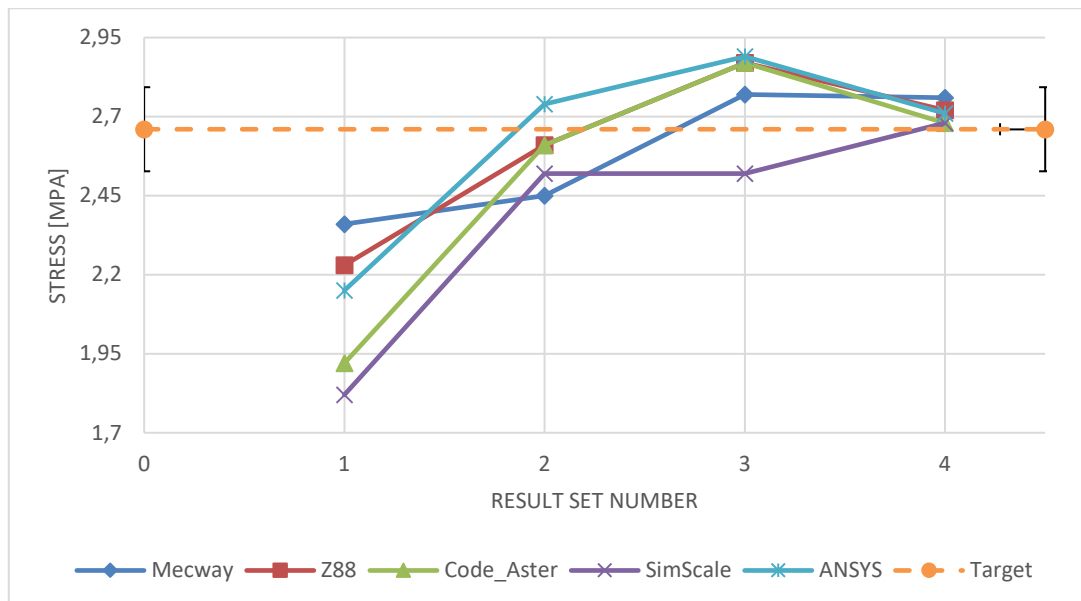


Figure 5-16. Graph of target output “Maximum Stress at Fillet” for each package.

5.2.6 Test Case 6: Large deflection of a Z-Shaped Cantilever Beam under End Load

This section presents the results from each FEA package for Test Case 6: Large deflection of a Z-Shaped Cantilever Beam under End Load. The packages that were unable to perform the loading given in the test case data i.e. applied a ramped load instead of the given iterative load, are denoted with a * in Table 5-1. Note how the manner in which the load was applied changed the rate of deflection.

The deviation with respect to the final solution is presented in Table 5-1 below

Table 5-1. Final solution deviation for cantilever beam deflection

	ANSYS	SimScale	Mecway	Z88*	NX 10.0*	Code_Aster*
Deviation	0.30 %	0.21 %	0.21 %	0.42 %	0.45%	0.21%

Figure 5-17 below shows the graphical results from the FEA packages used.

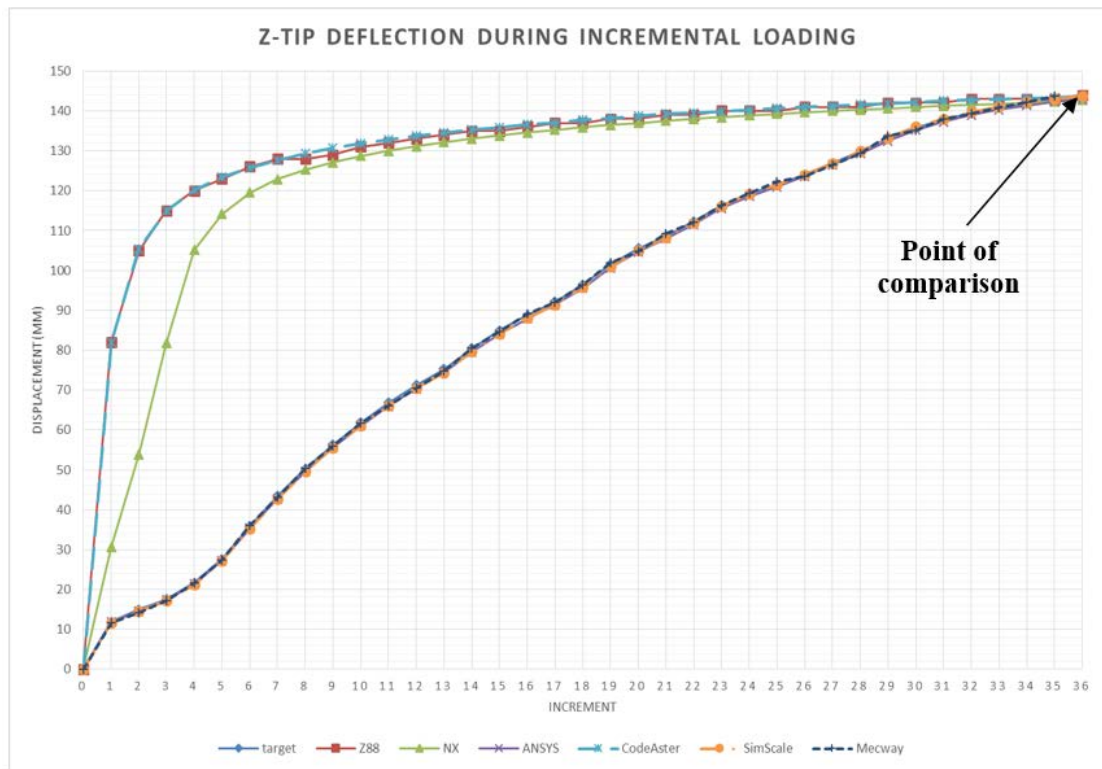


Figure 5-17. Graph of incremental target outputs “Z-directional tip deflection”.

5.2.7 Test Case 7: Plastic Deformation of Tensile Test Specimen

This section presents the results for Test Case 7: Plastic Deformation of Tensile Test Specimen. Graphical results for ANSYS, Siemens NX, Code_Aster, SimScale and Mecway are presented in Figure 5-18 to Figure 5-22. These graphs show the results obtained from the package against the target response obtained experimentally.

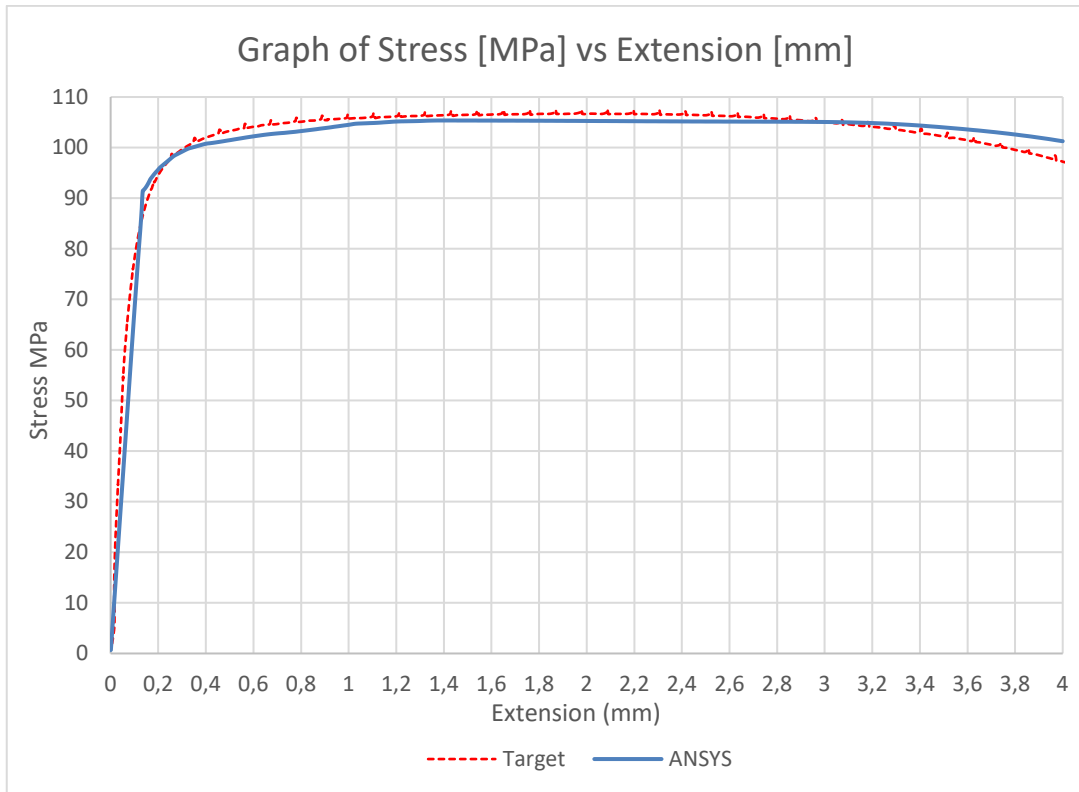


Figure 5-18. ANSYS result for test case 7.

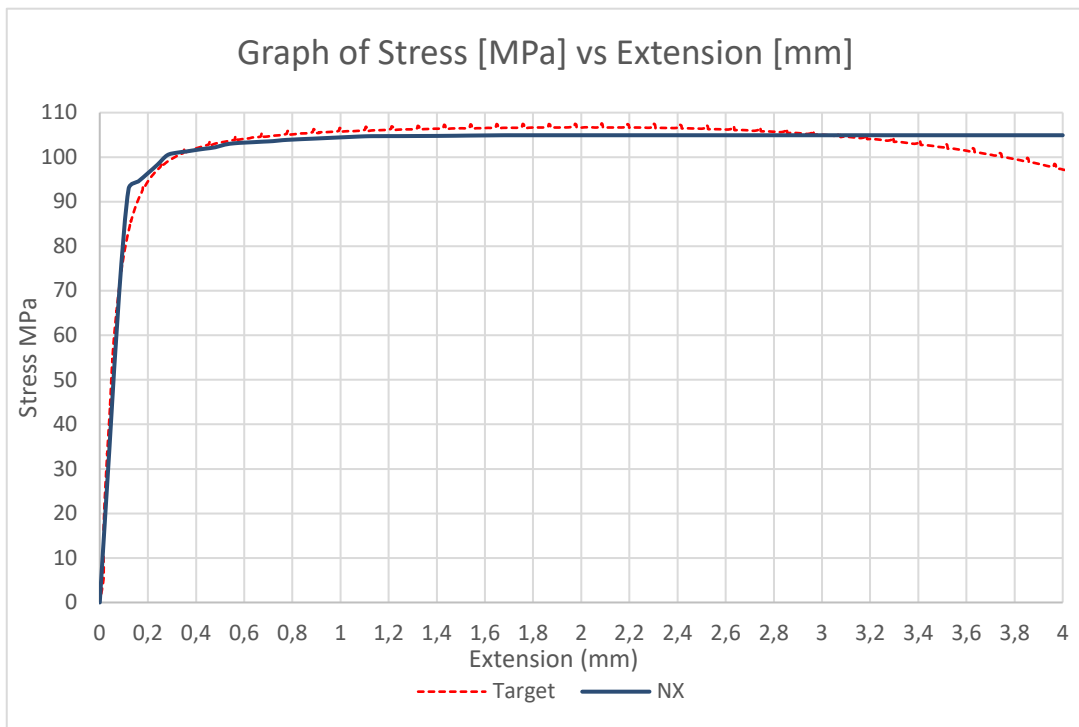


Figure 5-19. NX result for test case 7.

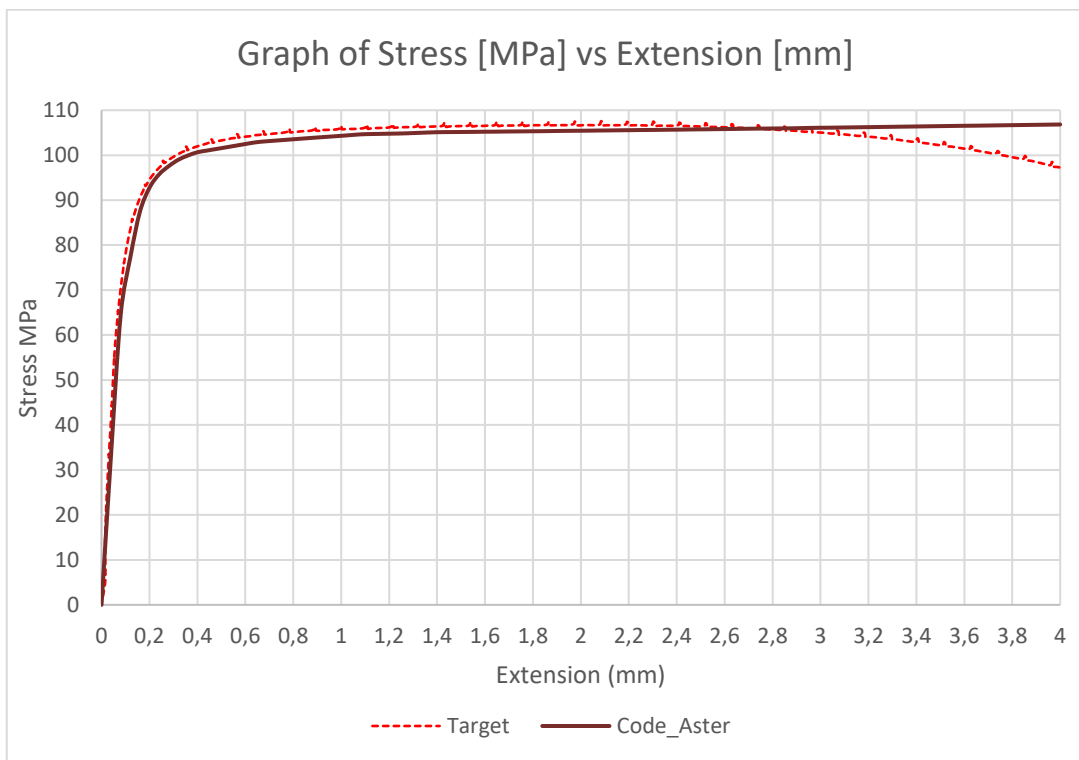


Figure 5-20. Code_Aster result for test case 7.

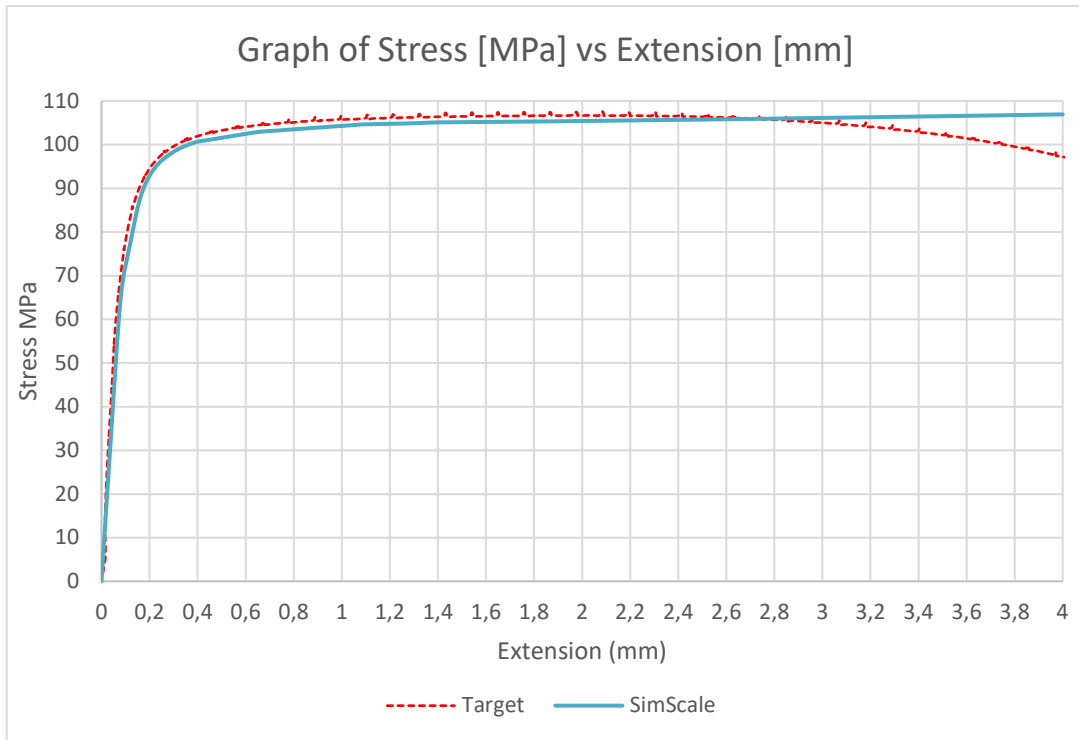


Figure 5-21. SimScale result for test case 7.

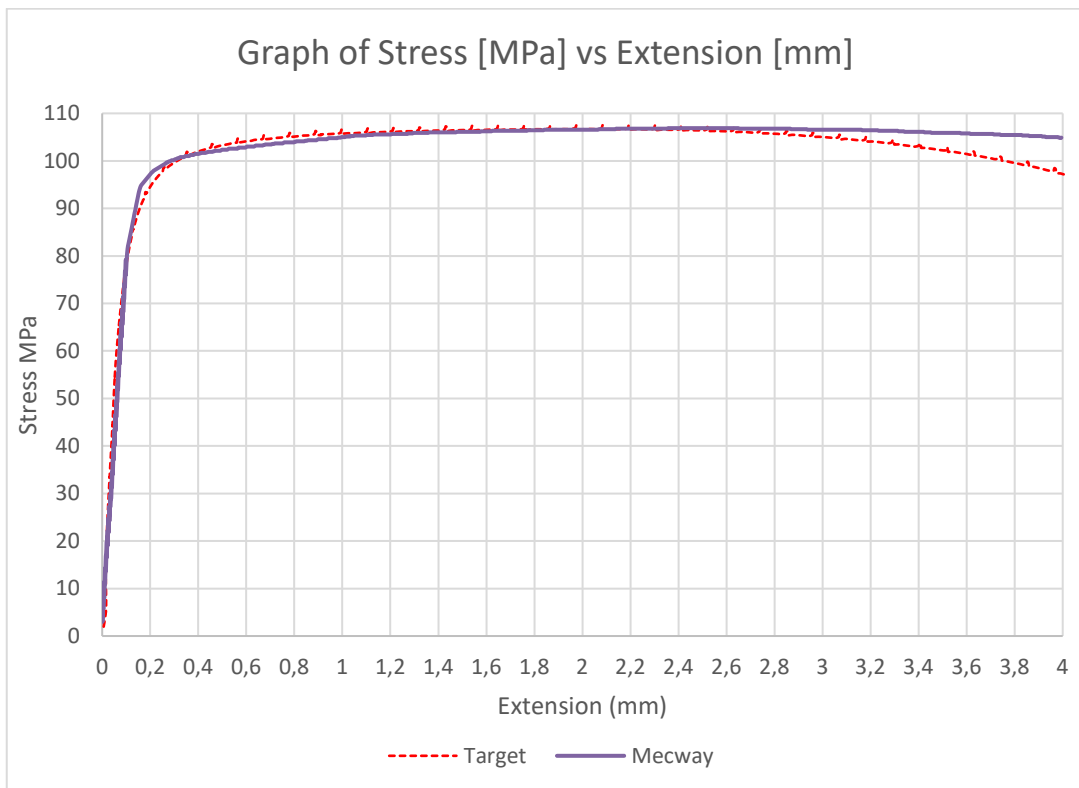


Figure 5-22. Mecway result for test case 7.

The table below presents the Root Mean Square Deviation (RMSD) and Normalized Root Mean Square Deviation (NRMSD) for the simulation results relative to the experimental target solution.

$$RMSD = \sqrt{\frac{\sum_{i=1}^n (X1_i - X2_i)^2}{n}} \quad (5.1)$$

Where:

n - Number of instances in a series
X - Series of data containing n instances

$$NRMSD = \frac{RMSD}{y_{max} - y_{min}} \quad (5.2)$$

Where:

y_{max} - Maximum value in a data series of interest
 y_{min} - Minimum value in a data series of interest

These measures were used as they offer a good measure of the magnitude of deviation between samples of a population. Using a maximum value for stress of 107.316 MPa from the experimental results, the RMSD was normalized into a percentage deviation.

Table 5-2. Average deviation of simulation results measured against experimental result

Package	ANSYS	NX	Code_Aster	SimScale	Mecway
RMSD	2.81 MPa	2.51 MPa	3.00 MPa	3.00 MPa	2.41 MPa
NRMSD	2.6228 %	2.3428 %	2.8000 %	2.7919 %	2.2442 %

CHAPTER 6 : Discussion of Results

This chapter presents a discussion of the results of this research. The chapter will be broken into subsections of each package and will contain a discussion of the results for each test case. The last subsection will be an overall result discussion which will assess the benchmarking phase results in their entirety.

It is important to note that the results presented in the benchmark publications' test cases are computational solution results that were computationally verified on several workstations by different analysts. Therefore the non-analytical results presented are approximations themselves. The experimental results obtained are subject to errors introduced by several factors including measurement error, instrumentation error and experimental condition variability. The selection of the target solution was done by a selection of a median curve of a small sample size, which may not represent the response of the material under perfect analysis conditions. Overall, the test case results are the best possible approximation of true solutions and hence the term 'deviation' was used when comparing the computational solution to the benchmark solution.

6.1 Mecway

Mecway was able to generate results for each test case, but not all were generated using the suggested approaches presented in Chapter 4.

The model associated with Test case 1: Grid Point load on an Articulated Truss was generated using the suggested approach. The solver was able to yield the required nodal displacement results. On one node of interest it can be seen that there is a deviation 50.10 % in the X-direction and 0.00 % in the Y-direction. These results would appear to be of unacceptable accuracy collectively. On the remaining node of interest we see a deviation of 0.00 % in the X-direction and 0.001 % in the Y-direction. These nodal displacement results are of acceptable accuracy.

The model associated with Test Case 2: Thin Shell Wall in Pure Bending was generated in the suggested approach. The solver was able to yield the required stress and displacement outputs. The displacement results went from a deviation of 4.32 % to 1.64 % as the mesh

was refined. These results fall within acceptable accuracy. The stress result goes from a deviation of 3.75 % at the largest mesh size and fluctuates between 5.83 % and 5.69 % as mesh size is reduced. These stress results appear to tend towards unacceptable accuracy.

The model associated with Test Case 3: Axisymmetric Pressure Vessel was generated in the suggested approach. Mecway was able to solve for the desired stress output. The stress result deviated from 3.87 % to 0.23% as the mesh size was reduced. These stress results continued showing acceptable accuracy throughout the mesh refinement process.

The model associated with Test Case 4: Internal Pressure on Thick-Walled Spherical Container was generated in the suggested approach. Mecway was able to solve for the required stress and displacement outputs. For the circumferential stress, the deviation of results went from 5.60 to 1.10 % on the internal surface and from 16.07 % to 1.02 % on the external surface. For the radial stress output, the deviation of results went from 1.80 % to 0.90 % on the internal surface and from 3.23 MPa to 0.322 MPa on the external surface. The results tend towards acceptable accuracy as the mesh was refined. For the displacement magnitude, the deviation goes from 1.15 % to 0.1 % on the internal surface and from 1.27 % to 0.00 % on the external surface. The displacement results show acceptable accuracy throughout the mesh refinement process.

The model associated with Test Case 5: Flat Bar with Stress Concentration was generated in the suggested approach. Mecway was able to solve for the required stress output. A deviation of 11.27 % was observed at both points of interest using the largest mesh size and this reduced to a deviation of 3.75 % at both observed points using the smallest mesh size. The results tended towards acceptable accuracy as the mesh size was reduced.

The model associated with Test Case 6: Large Deflection of a Z-Shaped Cantilever Beam under End Load was not generated in the suggested approach. The non-linear solver does not permit the use of 2-D elements, consequently, 3-D tetrahedral elements were used. The solver was able to compute the required directional displacement output. A deviation of 0.21% was observed for the final load step. The result showed acceptable accuracy.

The model associated with Test Case 7: Plastic Deformation of Tensile Test Specimen was generated in the suggested approach. As previously stated, Mecway made use of the CalculiX solver to perform the elasto-plastic material analysis. The CalculiX Solver was used to compute the solution for the desired stress output. The normalized root mean square deviation of the response curve of the stress value was 2.24 %. The result shows acceptable accuracy.

It appears that Mecway is a capable package that offers many of the tools for conducting structural FEA that would be expected from a premium FEA package. Dealing with linear test cases was simple and routine; the one possible downfall being the cumbersome manner in which the application of boundary conditions to 2-D geometries is handled. The method of workflow ensures that no steps for creating the model are omitted. The results obtained showed generally high correlation to the target values. Looking at non-linear analysis, it appears that the inability to analyse 2-D elements was a downfall of the package, however the accuracy of the model generated showed high correlation to the target response. The analysis of elasto-plastic materials should be an intrinsic capability to Mecway in future versions of the software as the incorporation of CalculiX into the package may give the appearance of an incapable native solver. The need to manually code the CalculiX deck may also lead to the possibility of erroneous results, which is again a reason to extend the capabilities of the native Mecway solver.

6.2 Z88 Aurora

Z88 has some restrictive aspects that made it difficult, and at times impossible to obtain meaningful results for some of test cases.

The model associated with Test case 1: Grid Point Load on an Articulated Truss was generated in the suggested approach. Z88 was able to yield the required nodal displacement results. A deviation 19.10 % is seen on one node in the X-direction and 0.011 % in the Y-direction. These results would appear to be of unacceptable accuracy collectively. On the remaining node, a deviation of 0.028 % in the X-direction and 0.018 % in the Y-direction is seen. These nodal displacement results appear to be of acceptable accuracy

The model associated with Test Case 2: Thin Shell Wall in Pure Bending was not completed by Z88 Aurora as it was not possible to generate a 2-D mesh. Attempts to generate a suitable 3-D mesh caused the package to close unexpectedly.

The model associated with Test Case 3: Axisymmetric Pressure Vessel was not generated in the suggested approach. A suitable 2-D mesh could not be generated hence a 3-D geometry was used. A coarse tetrahedral mesh was used and the solver was able to compute the required stress output. A deviation of 4.41 % was observed. The result was deemed acceptable in terms of accuracy however further mesh refinement was not achieved as a suitable mesh could not be created.

The model associated with Test Case 4: Internal Pressure on Thick-Walled Spherical Container was generated in the suggested approach. Z88 did not output values for circumferential stress and radial stress. The deviation in displacement magnitude fluctuated from 0.5 % to 0.1 % on the internal surface and from 1.27% to 0.00 % on the external surface. These results showed acceptable accuracy.

The model associated with Test Case 5: Flat Bar with Stress Concentration was generated in the suggested approach. Z88 was able to solve for the required stress outputs. A deviation of 6.39 % was observed at the hole using the maximum mesh size, and this decreased to 2.25 % as the mesh size was reduced to the minimum value. A deviation of 16.16 % was observed at the fillet for the maximum mesh size and fluctuated down to 2.25% as the mesh size was reduced. It can be seen that the results tended towards a more acceptable accuracy as the mesh size was decreased.

The model associated with Test Case 6: Large deflection of a Z-Shaped Cantilever Beam under End Load was generated in the suggested approach. An appropriate mesh was used, though not at the level of refinement that was possible in other packages, as Z88 would close unexpectedly when further mesh refinement was attempted. The incremental results for the directional displacement were obtained. A deviation of 0.42 % for the final load increment was observed. The accuracy of the result was deemed acceptable.

The model associated with Test Case 7: Plastic Deformation of Tensile Test Specimen was not completed as the required displacement loading condition could not be applied. Attempts were made to apply a force loading up to the maximum load measure by the load cell during experimental testing, however this effort yielded no meaningful results.

Z88 performed well when dealing with 1-D element creation and analysis. The results generated from Test Case 1 showed strong correlation to the target values. The main downfall of Z88 is its restrictive meshing module. That being said, it performed adequately when using 3-D elements, and when solutions were obtained, they correlated strongly with the target outputs. The non-linear analysis environment is only capable of applying a force or pressure as the loading condition. This may be sufficient in many instances but could pose a problem in certain cases, as is evident from this research.

6.3 SimScale

SimScale is a completely web-based FEA package that can be accessed on any computer with an internet connection. However, it has some limitations to its analysis capabilities which made it impossible to solve some of the test cases.

The model associated with Test case 1: Grid point load on an articulated truss was not analysed by SimScale as it currently lacks the capability to perform analyses on 1-D geometry.

The model associated with Test Case 2: Thin Shell Wall in Pure Bending was not completed. SimScale does not allow for the creation of a 2-D mesh and a suitable 3-D mesh could not be produced.

The model associated with Test Case 3: Axisymmetric Pressure Vessel was not modelled using the suggested approach. A 3-D geometry was used for this test case. SimScale was able to compute the required directional stress output. The deviation for the directional stress went from 13.22 % to 2.39 % as the mesh size was refined. The results appear to tend towards an acceptable solution as the mesh size is decreased.

The model associated with Test Case 4: Internal Pressure on Thick-Walled Spherical Container was generated using the suggested approach. SimScale was able to solve for the required stress and displacement outputs. For the circumferential stress, the deviation of results go from 7.74 % to 1.37 % on the internal surface and 15.86 % to 0.42 % on the external surface. These results tend towards acceptable accuracy with mesh refinement. For the radial stress output, results deviated from 23.25 % to 0.14 % on the internal surface, and from 1.285 MPa to 0.175 MPa on the external surface. For the displacement magnitude, the results deviated from 1.00 % to 0.25 % on the internal surface, and from 8.00 % to 0.66 % on the external surface. The results tend towards acceptable accuracy with mesh refinement.

The model associated with Test Case 5: Flat Bar with Stress Concentration was generated in the suggested approach. SimScale was able to solve for the required stress output. A deviation of 31.57 % was observed at both points of interest using the largest mesh size and this reduced to a deviation of 0.75 % at both observed points using the smallest mesh size. The results tended towards acceptable accuracy as the mesh size was reduced.

The model associated with Test Case 6: Large deflection of a Z-Shaped Cantilever Beam under End Load was not generated using the suggested approach. SimScale does not permit the use of 2-D elements therefore, 3-D tetrahedral elements were used. SimScale was able to compute the required directional displacement output. A deviation of 0.21% was observed for the final load step. The result shows acceptable accuracy.

The model associated with Test Case 7: Plastic Deformation of Tensile Test Specimen was generated in the suggested approach. The solver was able to compute the solution for the desired stress output. The normalized root mean square deviation of the response curve of the stress value was 2.79 %. This result shows acceptable accuracy.

The SimScale platform offered a range of tools to create a 3-D finite element model. It is very capable and offered analysis capabilities and tools that are to be expected from premium commercial FEA packages. The inability to perform 1-D and 2-D analyses at the current stage of development was the downfall of SimScale. There is evidence on SimScale forums that lower dimension analysis capabilities are being developed. It is seen that there was generally strong correlation between target solutions and the results yielded by SimScale. Conducting a linear elastic analysis on isotropic materials was simple and routine. Conducting non-linear analyses were straightforward and systematic, with additional information being visible on-screen during every step of model generation. Overall, the SimScale package offered a good user experience and yielded accurate results in terms of the test case target solutions.

6.4 Code_Aster/Salome Meca

Code_Aster was able to produce all the results required, however not all of the models could be generated using the suggested approach put forth in Chapter 4.

The model associated with Test case 1: Grid Point Load on an Articulated Truss was generated using the suggested approach. Code_Aster was able to compute the required nodal displacements. On one node of interest a deviation 36.30 % in the X-direction and 4.03 % in the Y-direction is seen. These results would appear to be of unacceptable accuracy collectively. On the remaining node we see a deviation of 0.025 % in the X-direction and 0.034 % in the Y-direction. These nodal displacement results were of acceptable accuracy.

The model associated with Test Case 2: Thin Shell Wall in Pure Bending was generated using the suggested approach. Code_Aster solver was able to yield the required stress and displacement result outputs. The displacement results deviated from 0.11 % to 0.02% as the mesh was refined. The stress result deviated from 1.29 % at the largest mesh size and fluctuates between 1.57% and 0.18 % with mesh refinement. These results appeared to remain within an acceptable accuracy at all points during the mesh refinement process.

The model associated with Test Case 3: Axisymmetric Pressure Vessel was generated in the suggested approach. Code_Aster was able to solve for the directional stress output. The stress result deviated by 0.5 % for the largest mesh size to 0.04% with mesh refinement. These stress results were of acceptable accuracy.

The model associated with Test Case 4: Internal Pressure on Thick-Walled Spherical Container was generated in the suggested approach. Code_Aster was able to solve for the required stress outputs and displacement magnitudes. For the circumferential stress, the results deviated from 6.74 % to 1.29 % on the internal surface and 16.69 % to 0.35 % on the external surface. For the radial stress output, the results deviated from 21.51 % to 0.157% on the internal surface and from 1.225 MPa to 0.188 MPa on the external surface. For the displacement magnitude, the deviation goes from 1.25 % to 0.00 % on the internal surface and from 8.00 % to 0.66 % on the external surface. These results tended towards acceptable accuracy with mesh refinement.

The model associated with Test Case 5: Flat Bar with Stress Concentration was generated in the suggested approach. Code_Aster was able to solve for the required stress output. A deviation of 2.25 % was observed at the hole when analysed with the maximum mesh size, and this decreased to 0.75 % as the mesh size was reduced. A deviation of 27.82 % was observed at the fillet for the maximum mesh size and fluctuated down to 0.75 % as the mesh size was reduced. It can be seen that the results tended towards acceptable accuracy with mesh refinement.

The model associated with Test Case 6: Large deflection of a Z-Shaped Cantilever Beam under End Load was not generated using the suggested approach. Code_Aster does not permit the use of 2-D elements for the solution of non-linear structural problems so therefore, 3-D tetrahedral elements were used. Code_Aster was able to compute the required directional displacement outputs and save individual incremental results. A deviation of 0.21% was observed for the final load step. The result shows acceptable accuracy.

The model associated with Test Case 7: Plastic Deformation of Tensile Test Specimen was generated using the suggested approach. Code_Aster was used to compute the solution for the desired stress output. The normalized root mean square deviation of the response curve of the stress output was 2.80 %. The result shows acceptable accuracy.

Overall, Code_Aster, used with Salome Meca provides a comprehensive library of element types, material models and boundary conditions. The sheer number of options to choose from may be daunting to a user that is unfamiliar with the exact formulation/application of each of these components. That being said, with a proper understanding of the package it is rather powerful and flexible, able to generate custom models that may even be difficult to generate using some commercial packages. The 1-D element test case analysis produced generally acceptable results. Conducting 2-D and 3-D linear static test cases took some effort to understand the proper procedure and learn the correct coding for the command files, but provided results that tended towards acceptable accuracy with a bit of mesh refinement. The non-linear examples took a lot of effort to acquire an understanding of proper procedure and coding to correctly model these problems. The main reason was that the information regarding these analyses were hidden amongst archives of poorly machine-translated English versions of user manuals. However, once the models were set up correctly, the solver was able to yield results of acceptable accuracy.

6.5 ANSYS

ANSYS 16.1 is a premium commercial analysis package available at UKZN. ANSYS Static Structural Mechanical, the module capable of computational structural mechanics through FEA, was used to solve the selected test cases. ANSYS 16.1 was capable of providing the necessary tools to solve all the test cases in the suggested approach.

The model associated with Test case 1: Grid point load on an articulated truss was generated using the suggested approach. ANSYS Mechanical APDL was able to compute the required nodal displacements. On one node, a deviation 49.15 % in the X-direction and 0.00 % in the Y-direction is seen. These results would appear to be of unacceptable accuracy collectively. On the remaining node a deviation of 0.00 % in the X-direction and 0.011 % in the Y-direction is seen. These displacement results appear to be of acceptable accuracy.

The model associated with Test Case 2: Thin Shell Wall in Pure Bending was generated using the suggested approach. ANSYS Mechanical was able to yield the required stress and displacement result outputs. The displacement results remained at a deviation of 0.02 % with mesh refinement. The stress result deviated from 1.29 % at the largest mesh size and decreased to 0.18 % as the mesh size was reduced. These results showed acceptable accuracy throughout the mesh refinement process.

The model associated with Test Case 3: Axisymmetric Pressure Vessel was generated using the suggested approach. ANSYS Mechanical was able to solve for the directional stress output. The stress result deviated by 0.5 % for the largest mesh size to 0.03% with mesh refinement. These stress results are of acceptable accuracy.

The model associated with Test Case 4: Internal Pressure on Thick-Walled Spherical Container was generated using the suggested approach. ANSYS Mechanical was able to compute the required stress outputs as well as the displacement magnitudes. For the circumferential stress, the deviation of results goes from 0.5 % to 0.05 % on the internal surface, and from 0.38 % to 0.08 % on the external surface. For the radial stress output, the deviation of results go from 1.68 % to 0.13 % on the internal surface and from 0.20 MPa to 0.012 MPa on the external surface. For the displacement magnitude, the value stays constant at the exact solution as the mesh size is reduced on the internal surface and goes from a deviation of 0.66 % to 0.00 % on the external surface. These results appear to remain acceptable throughout the mesh refinement process.

The model associated with Test Case 5: Flat Bar with Stress Concentration was generated using the suggested approach. ANSYS Mechanical was able to solve for the required stress output. A deviation of 4.51 % was observed at the hole when analysed with the maximum mesh size, and this decreased to 1.88 % as the mesh was refined. A deviation of 19.17 % was observed at the fillet for the maximum mesh size and fluctuated down to 1.88 % as the mesh size was reduced. It can be seen that the results tended towards a more acceptable accuracy as the mesh size was decreased.

The model associated with Test Case 6: Large deflection of a Z-Shaped Cantilever Beam under End Load was generated using the suggested approach. The solver was able to compute the required directional displacement outputs and present tabulated incremental results. A deviation of 0.3 % was observed for the final load step. The result showed acceptable accuracy.

The model associated with Test Case 7: Plastic Deformation of Tensile Test Specimen was generated using the suggested approach. The solver was able to compute the solution for the desired stress output. The normalized root mean square deviation of the response curve for the stress value was 2.62 %. The result showed acceptable accuracy.

ANSYS Mechanical and Mechanical APDL were able to provide the necessary tools to create the required finite element models. It is clear why ANSYS is considered premium software. The software is pleasant to use and is very systematic. The results obtained appear to be of acceptable accuracy for most test case target outputs. Furthermore, the results often had acceptable accuracy at the largest mesh size and showed little change with mesh refinement. Overall, ANSYS provided a good standard to which other packages may be compared.

6.6 Siemens NX

Siemens NX 10 provided a comprehensive design modeller and capable analysis environment. It allows for seamless transition between modules. It provided solutions for each test case.

The model associated with Test case 1: Grid point load on an articulated truss was generated using the suggested approach. The solver was able to compute the required nodal displacements. On one node, a deviation of 9.35 % in the X-direction and 0.44 % in the Y-direction is seen. These results would appear to be of unacceptable accuracy collectively. On the remaining node we see a deviation of 0.00 % in the X-direction and 0.018 % in the Y-direction. These nodal displacement results were of acceptable accuracy.

The model associated with Test Case 2: Thin Shell Wall in Pure Bending was generated using the suggested approach. NX NASTRAN was able to yield the required stress and displacement result outputs. The displacement results remained at a deviation of 0.02 % with each mesh refinement. The stress result went from a deviation of 1.85 % to 0.00 % as the mesh size was reduced. These results showed acceptable accuracy throughout the mesh refinement process.

The model associated with Test Case 3: Axisymmetric Pressure Vessel was generated using the suggested approach. NX NASTRAN was able to compute the directional stress output. The stress result deviated from 19.76 % to 0.54% with mesh refinement. The results tended towards acceptable accuracy throughout mesh refinement.

The model associated with Test Case 4: Internal Pressure on Thick-Walled Spherical Container was generated using the suggested approach. The solver was able to compute the required stress and displacement outputs. For the circumferential stress, the result deviation went from 13.17 % to 2.86 % on the internal surface and 6.67 % to 0.65 % on the external surface as mesh size was reduced. For the radial stress output, the deviation of results went from 6.75 % to 4.37 % on the internal surface and from 1.04 MPa to 0.028 MPa on the external surface as mesh size was decreased. For the displacement magnitude, the deviation went from 0.25 % to 0.00 % on the internal surface and fluctuated from 0.00 % to 0.67 % back to the exact solution on the external surface. These results generally tended towards acceptable accuracy as the mesh size was reduced.

The model associated with Test Case 5: Flat Bar with Stress Concentration was generated using the suggested approach. The NX NASTRAN solver was able to compute the required stress output. A deviation of 17.70 % was observed at both points of interest using the largest mesh size and this reduced to a deviation of 1.88 % at both observed points using the smallest mesh size. These results tended towards acceptable accuracy with mesh refinement.

The model associated with Test Case 6: Large deflection of a Z-Shaped Cantilever Beam under End Load was generated using the suggested approach. The solver was able to compute the required directional displacement outputs and present tabulated incremental results. A deviation of 0.21 % was observed for the final load step. The result showed acceptable accuracy.

The model associated with Test Case 7: Plastic Deformation of Tensile Test Specimen was generated using the suggested approach. The solver was able to compute the solution for the desired stress output. The normalized root mean square deviation of the response curve for the stress value was 2.34 %. The result showed acceptable accuracy.

NX provided an extensive range of tools which enabled the creation of the relevant finite element models. It is evident why NX NASTRAN is considered one of the more renowned premium FEA packages. The user interface is quite straightforward however it appeared more tedious to generate the model at times, relative to ANSYS. The generated results showed very good accuracy when implementing appropriate mesh refinement. Overall, NX NASTRAN provided a good standard for which the low-cost/ no-cost packages could be compared.

6.7 Overall Discussion of Results

As expected, the premium commercial packages readily solved all test cases. ANSYS and NX were able to generate results showing acceptable accuracy for every test case. For the most part, the no-cost/low cost FEA packages also dealt well with the generation and solution of the test cases.

For Test Case 1: Grid Point Load on an Articulated Truss, all packages besides SimScale were able to generate results. Looking at the X-direction displacement of what is labelled as Node C, none of the packages seemed to be able to generate accurate solutions. We see the largest deviation of 50.1 % from Mecway, a deviation of 49.15% from ANSYS and the smallest deviation of 9.35 % from Siemens NX. Bearing in mind that the target solutions are based on results verified computationally, it could be argued that this particular target solution may be inaccurate. The results for the remaining nodes from all the packages fell within an acceptable accuracy range.

Looking at Test Case 2: Thin Shell Wall in Pure Bending, it caused problems for Z88 and SimScale as 2-D meshes could not be created and suitable 3-D meshes could not be produced. The premium packages both produced essentially exact solutions which showed very little deviation as the mesh size was reduced. Looking at the target results in the test case data, it could be argued that round-off error is present as the test case data is presented with only two decimal points, whereas the packages tended to yield results with more than two decimal points. Code_Aster and Mecway produced displacement results with acceptable accuracy that showed little variation as the mesh size was reduced. We see the stress results from both packages remain within an acceptable accuracy throughout the mesh refinement process. However, the stress results do appear to fluctuate. An explanation for this is offered by (Kurowski, 2001). When a coarse mesh is used, larger elements in an FEM model tends to overlook the localized areas of high stresses. Using smaller elements reveals the higher stress concentrations at these areas. As element size is reduced, there may be no sign of convergence.

In Test Case 3: Axisymmetric Pressure Vessel the inability for SimScale and Z88 to create a 2-D mesh was the reason for a 3-D model being used. The 3-D representation of the model could potentially affect the simulation results. Both packages were able to generate solutions of acceptable accuracy eventually. The remaining packages were able to analyse this test case in axisymmetric environments and generate acceptable solutions with some mesh refinement. It can be seen that all of the packages were able to generate solutions within a 0.5% deviation of the target solution within three mesh refinements.

For Test Case 4: Internal Pressure on Thick-Walled Spherical Container, all the packages besides Z88 were able to analyse the test case and yield the required stress and displacement outputs. The overall displacement results across all packages fell within acceptable accuracy and showed little deviation. For the circumferential and radial stress results, it appeared that the accuracy of the solutions was improved through mesh refinement and all packages were able to yield acceptable results with the smallest mesh size used. Noting that the stress value does not give a good indication of convergence, and taking into account that the displacement results showed apparent convergence for the mesh sizes used, it was deemed unnecessary to refine the mesh further.

All packages were able to analyse Test Case 5: Flat Bar with Stress Concentration and yield solutions. It is seen that the stress result generated by each package was heavily influenced by the mesh size. Noting that the purpose of this test was to assess a package's capability when dealing with stress concentrations, we see that the results tended towards a more accurate solution as the mesh size was reduced. There was no evidence of a converged solution and no sign that one could be obtained considering once again that stress is not necessarily a good measure of solution convergence. It was decided that given all of the solutions yielded an acceptable accuracy solution, there was no need to further refine the mesh in pursuit of a more accurate solution.

All of the packages were able to analyse Test Case 6: Large deflection of a Z-Shaped Cantilever Beam under End Load. NX 10, Code_Aster and Z88 did not use the prescribed incremental loading values but rather applied a linearly ramped load up to the full value over the increments. All this affected was the rate that the geometry deflected. Looking at the final deflection value from each package we see that the packages have generated solutions with high accuracy as the deviations range from 0.45 % to 0.21 %.

For Test Case 7: Plastic Deformation of Tensile Test Specimen, all packages besides Z88 were able to generate desired solutions. The material data and stress-strain curve used was chosen as the median of a small sized data set. This could have affected the accuracy of the solution as it may not be the curve that best represents the actual material. The engineering stress and strain were converted to true stress and true strain using formulae that are only valid up to the UTS of a material. The target solution curve was chosen as it was the median of a small sized data set. The results yielded by the packages showed high correlation with the target response curve. The normalized root mean square deviation ranged from 2.24 % to 2.8% across the packages. It can be seen that in NX, Code_Aster and SimScale, the package solves for the stress output up to the UTS specified in the flow curve and then assumes a perfectly plastic material beyond that point. It would appear that ANSYS and Mecway (using the CalculiX solver) take into account geometrical effects and thus a dip in the stress value starts to appear beyond the point of the UTS.

CHAPTER 7 : Conclusion

7.1 Findings

In chapter 2, it was demonstrated that finite element analysis has become an invaluable tool in various industries. It was shown that FEA is being incorporated into the early design phase and that pertinent decisions are often made based on FEA results. Bearing this in mind, it is quite evident that this research can have a tangible financial impact on businesses or individuals wishing to integrate affordable FEA into their operational capabilities.

This work endeavoured to determine if no-cost or low-cost FEA packages have advanced to the point where they can be used in place of a trusted commercial FEA package for linear and non-linear static structural analyses of varied geometries and for isotropic materials. In pursuit of this answer, a market review was done to determine the open source or low cost (500 USD or less) FEA packages available. The market review, as well as suggestions made by individuals with experience in the field of FEA, allowed for the identification of eighteen no-cost/low-cost commercial FEA packages. These packages were investigated and key aspects of each package were identified. The packages were subjected to baseline selection criteria and packages that did not meet these criteria were immediately excluded from further investigation. Six no-cost/low-cost FEA packages were found to meet with the baseline criteria and were subjected to further consideration. Of these, three packages were selected to be subjected to the performance benchmarking phase, these were: Code_Aster/Salome Meca; Mecway and Z88 Aurora.

The browser-based simulation platform, SimScale, was chosen as well, as it offered a different approach for individuals or businesses to incorporating FEA into their operational capabilities. Utilizing SimScale does not only remove the need to invest in costly commercial FEA packages, but coupled with the web-based parametric CAD modeller, OnShape, it can largely remove the need to invest in costly computational infrastructure.

ANSYS and Siemens NX were chosen as the premium FEA packages to be included in the benchmarking phase of the research so as to set a standard in performance, based on what are considered to be best-in-class software packages. The reason for including both ANSYS and NX was out of interest, to determine how their capabilities and performance compared to each other.

Following the selection of the packages, a review concerning the nature of benchmarking done on premium packages was conducted. Through investigating the validation manuals of premium commercial packages, it was found that performance benchmarking is typically done through the simulation of test cases, often with particular target values of displacement, strain or stress etc. These test cases generally originate from analytical or empirical models or from industry-accepted benchmark publications such as the NAFEMS standards. In addition to these sources, it was decided to include a benchmark test case showing material non-linearities that was validated experimentally. The chosen test cases aimed at assessing various capabilities of the packages with minimal repetition.

The six packages were all subjected to the benchmarking test cases and the modelling procedure was directed by a suggested approach. This procedure was adhered to unless impossible to accomplish within a specific package. With the modelling procedure kept constant, the control variable was the mesh element size. Mesh refinement was done during the test with the intent of obtaining mesh independence. With many of the target outputs being stress values, it was difficult to obtain converged solutions for these cases, however it noted that mesh refinement did result in more accurate results being obtained for both stress and displacement solutions.

Looking at the overall performance of Mecway, it can be said that this package offers excellent value for money. It possesses a user-friendly interface and the layout ensures a systematic approach to model generation that mitigates the chance of omitting any steps. It was adequately capable when dealing with the test cases. Linear elastic cases were routine and the results showed good accuracy relative to the test case target solutions as well as the premium packages used. Mecway also has the ability to conduct several other analysis types such as vibrational analysis, electrostatic and thermal analysis to name a few. Its inherent elastic non-linear capabilities are sufficient to conduct analyses on basic geometries. At the current stage of development, it is unable to conduct material non-linearity analyses and hence utilizes the CalculiX solver for this purpose. From the experience of using Mecway and the standard of results produced, it can be safely said that Mecway can be used in place of trusted commercial software for linear and non-linear isotropic structural analysis. Mecway can integrate seamlessly into the operational capabilities of an established company looking to replace their high-cost commercial package for linear and non-linear static structural analyses using isotropic materials. It would be useful in academic institutions for the purpose of supporting the education of students in the process of FEA.

Z88 Aurora was limited by its pre-processor capabilities. The interface is acceptable but the manner in which a model is created feels laborious at times. Possibly the biggest shortcoming is the inability for Z88 Aurora's pre-processor to generate a suitable 2-D mesh. It is possible to import mesh files, but that goes against the convenience of being an all-inclusive FEA package option. That being said, it was adequately capable when dealing with 3-D geometry, apart from being unable to solve for directional stresses. Results that were generated showed good accuracy relative to the test case target solutions as well as the premium packages. Z88 Aurora was adequately capable of dealing with geometrical non-linearities, and was even able to output incremental solutions. It was unable to perform the necessary displacement loading for test case 7, however, the capabilities for non-linear material analyses are present. All things considered, it would be difficult, at this stage of development, for Z88 to be used in place of a trusted commercial package for linear and non-linear static structural FEA. In its current state of development, Z88 Aurora would be a good tool to implement at academic institutions for teaching purposes.

Using Code_Aster/Salome Meca was a daunting task at first, as it proved to be unlike conventional contemporary FEA packages. Salome Meca requires users to be quite well versed with a package-specific model generation procedure. Pre-processing procedure is very modular. Each stage requires a specific module and its environment to be loaded, which does give a very systematic and structured model generation procedure. The fact that there is such a significant library of functions available may appear intimidating at first, but with some training and understanding, the model customization potential associated with Code_Aster is immense. With some effort, Code_Aster would be able to serve a user far better than many entry to mid-level commercial FEA packages. The model generation capabilities and result accuracy relative to the target solutions and premium packages, have led to the conclusion that Code_Aster/Salome Meca can be used in place of a trusted commercial package for linear and non-linear static structural FEA.

SimScale was found to be quite a capable package, besides its inability to deal with 1-D and 2-D elements. The web-based interface looks appealing. It has tools and capabilities that would be expected from commercial FEA packages. With a free account, a user is entitled to all of the analysis capabilities that a paid user has, apart from a direct line of contact with the developers. Using SimScale with OnShape allows for a completely cloud-based approach to computer aided engineering, removing the need for costly computational infrastructure. The results yielded by SimScale showed good accuracy relative to the target solutions as well as the premium software packages. With the promise of lower-dimensional analysis capabilities

being under development, it makes SimScale a viable candidate for use in place of trusted commercial packages for linear and non-linear static structural FEA. It must be noted however, that basing one's operational capabilities on web-based CAE packages has an obvious drawback. The user is vulnerable to the possibility that the service may be interrupted or even terminated in the future. Incorporating SimScale into commercial operations should therefore be approached with careful consideration. It would be advisable to possess another no-cost/low-cost option as a contingency if ever SimScale's services are interrupted.

Overall, it has been shown that there are in fact no-cost/low-cost options for users wishing to avoid the high cost of premium commercial FEA packages for the analysis of linear and non-linear static structural problems with isotropic materials. It must be stated that this research has not sought to determine if any of the investigated packages are better or worse overall than a given premium commercial package. If the resources are available to acquire a premium package, it would be advised to do so, as these packages have been refined to a point where model generation is highly streamlined and they possess extended tools and capabilities that are often invaluable. The high cost is justifiable if a comprehensive multi-physics analysis package is required.

7.2 Recommendations for Further Research

This research has determined that there are indeed low-cost/no-cost options that can perform adequately with respect to linear and non-linear static structural analysis in the context of isotropic materials. This particular scope of research arose from limitations expressed earlier in the dissertation. It would therefore be recommended to extend this research to consider non-isotropic materials such as composites, as the increasing application of composite materials in industry warrants the effort of investigating this capability. It is also recommended that other analysis types such as steady and transient thermal analyses be investigated. Future work could also endeavour to compare how the different codes can handle problems with a large number of DOFs from both a speed and memory perspective. Lastly, one could go further to investigate no-cost/low-cost CFD packages, although no-cost/low-cost software options in this area do currently appear to be more limited than that of FEA.

REFERENCES

ABBEY, T. 2014. Structural FEA in the Automotive Industry. Available: <http://www.deskeng.com/de/structural-fea-in-the-automotive-industry/> [Accessed 10 May 2015].

ABERDEEN GROUP. 2006. Simulation Driven Design Benchmark Report.

AMERICAN SOCIETY FOR MECHANICAL ENGINEERS 2006. Guide for Verification and Validation in Computational Solid Mechanics. American Society for Mechanical Engineers,.

ANSYS INC 2013. ANSYS Mechanical APDL Verification Manual, ANSYS inc.

ASM INTERNATIONAL 2004. *Tensile Testing*, Ohio , USA, ASM International.

AU WORKSHOP 2014. Fundamentals of Simulation CFD Meshing. *In: AEC-CFD_MESHING2_FUNDAMENTALS_R2_FINAL_IMAGE1.JPG* (ed.). Autodesk.

BANTHIA, P. 2014. The Future of Simulation-Driven Product Development. Available: <http://www.deskeng.com/de/category/simulate/> [Accessed 17 May 2015].

BATHE, K. J. 1996. *Finite Element Procedures*, New Jersey, Prentice-Hall Inc. .

BEER, F. P., JOHNSTON, E. R., DEWOLF, J. T. & MAZUREK, D. F. 2012. *Mecahnics of Materials*, New York, Mcgraw-Hill.

BSB TECHNOCRATS 2016. FINITE ELEMENT METHOD- SIMULATION. *In: 2.GIF* (ed.). BSB Technocrats.

CLOUGH, R. W. 1990. Original formulation of the finite element method. *Finite Elements in Analysis and Design*, 7, 89.

CONVERGENT MECHANICAL. 2013. *bConverged Products* [Online]. Available: <http://bconverged.com/products.php> [Accessed 2 February 2015].

DASSAULT SYSTÈMES 2012. Abaqus 6.12 Benchmarks Manual. *Verification Manual*. Rhode Island, United States of America: Dassault Systèmes,

DASSAULT SYSTÈMES SOLIDWORKS CORP. 2015. *SOLIDWORKS Simulation Packages* [Online]. Available: <https://www.solidworks.com/sw/products/simulation/packages.htm> [Accessed 5 April 2015].

DHONDT, G. & WITTIG, K. 2015. *CALCULIX : A Free Software Three-Dimensional Structural Finite Element Program* [Online]. Available: <http://www.calculix.de/> [Accessed 3 March 2015].

- EDF-R&D. n.d. *Code_Aster- Analysis of Structures and Thermodynamics for Surveys and Research* [Online]. EDF-R&D. Available: http://www.code-aster.org/V2/UPLOAD/DOC/Presentation/plaquette_aster_en.pdf [Accessed 6 April 2015].
- ELLISON, G. 2013. Thermal Spreading and More Using Open-Source FEA Software. [Accessed 13 June 2016].
- GALEANO, C., MANTILLA, J., DUQUE, C. & MEJIA, M. 2007. General Public Licence tools for Finite Element Modelling. *Dyna*, 74, 313-325.
- GNU OPERATING SYSTEM. 2007. GNU General Public Licence. Available: <http://www.gnu.org/licenses/gpl-3.0.en.html> [Accessed 30 April 2015].
- JACKSON, C. 2013. The 2013 State of Simulation Driven Design Report Lifecycle Insights.
- KRESS, G. 2014. *Structural Analysis with FEM*, Zurich, Switzerland, Swiss Federal Institute of Technology.
- KUROWSKI, P. 2001. Easily made errors mar FEA results. *Machine Design*, 1-6.
- LIANG, B. & MAHADEVAN, S. 2011. Error and Uncertainty Quantification and Sensitivity Analysis in Mechanics Computational Models. *International Journal for Uncertainty Quantification*, 1, 15.
- LOGAN, D. L. 2012. *A First Course in the Finite Element Method*, Stamford, USA, Cengage Learning.
- MAC DONALD, B. J. 2011. *Practical Stress Analysis with Finite Elements*, Glasnevin, Ireland, Glasnevin Publishing.
- MAHENDRAN, M. Applications of Finite Element Analysis in Structural Engineering. International Conference on Computer Aided Engineering, 2007 Chennai, India. Faculty of Built Environment and Engineering, Queensland University of Technology, Australia, 38-46.
- MECWAY 2014. Manual- Mecway Finite Element Analysis.
- MOAVENI, S. 1999. *Finite Element Analysis : Theory and Application with ANSYS*, New Jersey, Prentice-Hall Inc.
- NAFEMS 1990. *The Standard NAFEMS Benchmarks*.
- ODEN, J. T., BABUSKA, I., NOBILE, F., FENG, Y. & TEMPONE, R. 2005. Theory and methodology for estimation and control of errors due to modeling, approximation, and uncertainty. *Computer Methods in applied mechanics and engineering*, 10.
- OPENSOURCE.COM. 2015. *What is open source?* [Online]. Available: <http://opensource.com/resources/what-open-source> [Accessed 30 April 2015].
- PELOSI, G. 2007. The Finite Element Method, Part 1: R.L. Courant. *IEEE Antennas and Propagation*. Florence, Italy: IEEE Antennas and Propagation Magazine.

- PRINJA, N. K. & CLEGG, R. A. 1993. *A Review of Benchmark Problems for Geometric Non-Linear Behaviour for 3-D Beams and shells*, NAFEMS.
- QUORA.COM. 2014. *What is the best open source FEA package?* [Online]. [Accessed 10 March 2015].
- REBBA, R., MAHADEVAN, S. & HUANG, S. 2006. Validation and error estimation of computational models. *Reliability engineering and system safety*, 91, 8.
- RESEARCHGATE. 2014. *In finite element analysis verification and validation with field tests, universally what is the expected percentage FEA should meet?* [Online]. Available: www.researchgate.net/post/In_finite_element_analysis_verification_and_validation_with_field_tests_universally_what_is_the_expected_percentage_FEA_should_meet [Accessed 8 June 2016].
- RESEARCHGATE.NET. 2014. *What is the best open source finite element software for mechanical problems?* [Online]. [Accessed 12 March 2015].
- RIEG, F. 2014a. *Z88 Aurora Theory Manual*, Bayreuth, Germany, Chair for Engineering Design and CAD, University of Bayreuth.
- RIEG, F. 2014b. *Z88 Aurora User Manual*, Bayreuth, Germany, Chair for Engineering Design and CAD, University of Bayreuth.
- ROBERTS, D. 2016. Interview for assistance with small sample size data handling *In*: RUGDEO, S. (ed.). Durban, KwaZulu-Natal.
- SHAH, C. 2002. Mesh Discretization Error and Criteria for Accuracy of Finite Element Solutions. International ANSYS Users Conference, 2002 Pittsburg, PA. Cummins, Inc., 1-12.
- SHINGLEY, J. & MITCHEL, L. 1983. *Mechanical Engineering Design*, New York, McGraw-Hill.
- SIEMENS PLM SOFTWARE. n.d. NX Advanced FEM. Available: www.siemens.com/plm [Accessed 9 April 2015].
- SIMSCALE GMBH. 2015. *SimScale- Engineering Simulation in your Browser* [Online]. SimScale GmbH. Available: www.simscale.com/docs/contents.html [Accessed 4 May 2015].
- SOCIÉTÉ FRANÇAISE DES MÉCANICIENS 1990. *Guide de validation des logiciels de calcul des structures*, AFNOR.
- SOUTH AFRICAN BUREAU OF STANDARDS 2010. Metallic Materials - Tensile Testing. *Method of Test at room temperature*. Pretoria, South Africa: SABS Standards Division.
- SZABÓ, B. & BABUŠK, I. 2011. *Introduction to Finite Element Analysis: Formulation, Verification and Validation*, John Wiley & Sons.

THAKORE, D. A. 2014. *Finite Element Analysis Using Open Source Software*, Brisbane, Australia, Moonish Enterprises Pty. Ltd.

THE LINUX INFORMATION PROJECT. 2005. *Proprietary Software Definition* [Online]. LINFO.org. Available: <http://www.lininfo.org/proprietary.html> [Accessed 11 November 2015].

UGS CORP. 2007. NX Nastran Verification Manual.

Z88-SUPPORT. 2016. *RE: Assistance with material non-linear analysis*. Type to RUGDEO, S.

APPENDIX A

Market Research of Low-Cost/No-Cost FEA packages

The tabulated market research of the eighteen no-cost/low-cost FEA software packages considered is not presented in this printed document. The volume of the tabulated data cannot be appropriately represented here and can instead be found on the CD supplied with this document under the file name: **Appendix_A.xls**

APPENDIX B

Images from Model Generation Procedure

There are an excessive number of images contained in this appendix and it would be impractical to present them in this printed document. The images can instead be found on the CD supplied with this printed document under the filename: **Appendix_B.docx**

APPENDIX C

Command files for Code_Aster

C.1. Command file for Test Case 1: Grid Point Load on an Articulated Truss

```

DEBUT();
MA=DEFI_MATERIAU(ELAS=_F(E=1.962E11,                               //Define materials
                  NU=0.03,));
MESH=LIRE_MALLAGE(FORMAT='MED',);                                //Load Mesh
MESH=DEFI_GROUP(reuse =MESH,
               MAILLAGE=MESH,
               CREA_GROUP_MA=_F(NOM='TOUT',
                                TOUT='OUI',),
               CREA_GROUP_NO=_F(TOUT_GROUP_MA='OUI',),);        //Create groups
                                                                //from mesh
MODEL=AFFE_MODELE(MAILLAGE=MESH,
                  AFFE=_F(TOUT='OUI',
                          PHENOMENE='MECANIQUE',                //Set           to
                                                                //mechanical
                                                                //Truss elements
                                                                //chosen
                  MODELISATION='POU_D_T',),);
MATERIAL=AFFE_MATERIAU(MAILLAGE=MESH,
                       AFFE=_F(TOUT='OUI',
                                MATER=MA,),);                  //Apply mesh to
                                                                //material
                                                                //Apply element
                                                                //characteristics
TRUSS=AFFE_CARA_ELEM(MODELE=MODEL,
                     POUTRE=_F(GROUP_MA='TOUT',
                                SECTION='RECTANGLE',
                                CARA=('HY','HZ',),
                                VALE=(0.01,0.01,),),);
CHAR=AFFE_CHAR_MECA(MODELE=MODEL,
                    DDL_IMPO=_F(GROUP_NO=('A','C',),            //Nodes           of
                                                                //interest
                                                                //Fixtures
                    DX=0,
                    DY=0,
                    DZ=0,
                    DRX=0,
                    DRY=0,
                    DRZ=0,),
                    FORCE_NODALE=_F(GROUP_NO='D',                //Node           of
                                                                //interest
                                                                //Force on node
                                                                //set analysis
                                                                //type
                                                                //to static
                                                                //mechanical
                    FY=-9810,),);
RESULT=MECA_STATIQUE(MODELE=MODEL,
                     CHAM_MATER=MATERIAL,
                     CARA_ELEM=TRUSS,
                     EXCIT=_F(CHARGE=CHAR,),);
RESULT=CALC_ELEM(reuse =RESULT,                                //specify
                 MODELE=MODEL,                                //desired
                 CHAM_MATER=MATERIAL,                          //result values
                 CARA_ELEM=TRUSS,
                 RESULTAT=RESULT,
                 OPTION=('SIEF_ELNO','SIEQ_ELNO',),
                 EXCIT=_F(CHARGE=CHAR,),);
RESULT=CALC_NO(reuse =RESULT,
               RESULTAT=RESULT,
               OPTION=('FORC_NODA','REAC_NODA',),);            //desired nodal
force                                                                 //and displacement
IMPR_RESU(FORMAT='MED',
          RESU=_F(MAILLAGE=MESH,
                  RESULTAT=RESULT,
                  NOM_CHAM=('DEPL','FORC_NODA','REAC_NODA',),),);
FIN();

```

C.2 Command file for Test Case 2: Thin Shell Wall in Pure Bending

```

DEBUT(); //begin code
material=DEFI_MATERIAU(ELAS=_F(E=2.068e11,
                                NU=0.03,)),); //define material
mesh=LIRE_MALLAGE(FORMAT='MED',); //load mesh
mesh=DEFI_GROUP(reuse =mesh,
                MAILLAGE=mesh,
                CREA_GROUP_MA=_F(NOM='TOUT',
                                TOUT='OUI',)),
                CREA_GROUP_NO=_F(TOUT_GROUP_MA='OUI',)),); //create groups
                                                                from mesh
model=AFFE_MODELE(MAILLAGE=mesh,
                 AFFE=_F(TOUT='OUI',
                         PHENOMENE='MECANIQUE',
                         MODELISATION='DKT',)),); //shell
                                                                modelisation
MAT=AFFE_MATERIAU(MAILLAGE=mesh,
                 AFFE=_F(TOUT='OUI',
                         MATER=material,)),); //apply material
                                                                to mesh
wall=AFFE_CARA_ELEM(MODELE=model,
                   COQUE=_F(GROUP_MA='TOUT',
                             EPAIS=0.00254,)),); //define shell
                                                                thickness
fix=AFFE_CHAR_MECA(MODELE=model,
                  DDL_IMPO=_F(GROUP_NO='fix',
                              //edge of
interest
                              DX=0,
                              DY=0, //fixtures
                              DZ=0,
                              DRX=0,
                              DRY=0,
                              DRZ=0,)),);
load=AFFE_CHAR_MECA(MODELE=model,
                   FORCE_ARETE=_F(GROUP_MA='load',
                                   //edge of
interest
                                   FZ=210.15,)),); //force in N
result=MECA_STATIQUE(MODELE=model,
                    //define
                    //mechanical
                    //static analysis
                    CHAM_MATER=MAT,
                    CARA_ELEM=wall,
                    EXCIT=( _F(CHARGE=fix,)),
                          _F(CHARGE=load,)),);
result=CALC_ELEM(reuse =result,
                MODELE=model, //specify required
                CHAM_MATER=MAT, //result fields
                RESULTAT=result,
                OPTION=('SIEF_ELNO','SIEQ_ELNO','SIPO_ELNO','SIGM_ELNO',)),
                EXCIT=(
                _F(CHARGE=load,)),
                _F(CHARGE=fix,)),);
result=CALC_NO(reuse =result,
              RESULTAT=result,
              OPTION=('SIPO_NOEU','SIEQ_NOEU','SIEF_NOEU','SIGM_NOEU',)),);
IMPR_RESU(FORMAT='MED',
          RESU=_F(MAILLAGE=mesh,
                 RESULTAT=result,
                 NOM_CHAM='DEPL','SIPO_NOEU','SIEQ_ELNO','SIEQ_NOEU','SIPO_ELNO','SIEF_ELNO',
                 'SIEF_NOEU','SIGM_ELNO','SIGM_NOEU',)),);
FIN(); //end code

```

C.3. Command file for Test Case 3: Axisymmetric Pressure Vessel

```
DEBUT( ); //start code
MA=DEFI_MATERIAU(ELAS=_F(E=2100000000.0, //define material
                 NU=0.3, ), );
MAIL=LIRE_MAILLAGE(FORMAT='MED', ); //load mesh
MAIL=MODI_MAILLAGE(reuse=MAIL,
                 MAILLAGE=MAIL,
                 ORIE_PEAU_2D=_F(GROUP_MA=('Pressure', ), ), //2D mesh
                 ); //transformation
MODE=AFPE_MODELE(MAILLAGE=MAIL,
                 AFPE=_F(TOUT='OUI',
                        PHENOMENE='MECANIQUE',
                        MODELISATION='AXIS', ), ), //axisymmetric
//modélisation
MATE=AFPE_MATERIAU(MAILLAGE=MAIL, //apply
                 AFPE=_F(TOUT='OUI', //material to
                        MATER=MA, ), ); //mesh
CHAR=AFPE_CHAR_MECA(MODELE=MODE,
                   DDL_IMPO=( //fixtures
                        _F(GROUP_MA='Bottom',
                           DY=0.0, ),
                        _F(GROUP_MA='Top',
                           DX=0.0, ),
                        ),
                   PRES_REP=( //pressure load
                        _F(GROUP_MA='Pressure',
                           PRES=1000000.0, ),
                        ), );
RESU=MECA_STATIQUE(MODELE=MODE, //define mechanical
                   CHAM_MATER=MATE, //static analysis
                   EXCIT=_F(CHARGE=CHAR, ), );
RESU=CALC_ELEM(reuse=RESU,
               MODELE=MODE,
               CHAM_MATER=MATE,
               RESULTAT=RESU,
               OPTION=('SIGM_ELNO', 'SIEQ_ELNO', ),
               EXCIT=_F(
                   CHARGE=CHAR, ), ); //specify results of
//interest
RESU=CALC_NO(reuse=RESU,
             RESULTAT=RESU,
             OPTION=('SIGM_NOEU', 'SIEQ_NOEU', ), );
IMPR_RESU(FORMAT='MED',
          UNITE=80,
          RESU=_F(MAILLAGE=MAIL,
                 RESULTAT=RESU,
                 NOM_CHAM=('SIGM_NOEU', 'SIEQ_NOEU', 'DEPL', ), ), );
FIN( ); //end code
```


C.5 Command file for Test Case 5: Flat Bar with Stress Concentration

```
DEBUT( );
MA=DEFI_MATERIAU(ELAS=_F(E=210000000000.0,           //define material
                 NU=0.3, ), );
MAIL=LIRE_MAILLAGE(FORMAT='MED', );                //load mesh
MAIL=MODI_MAILLAGE(reuse =MAIL,                    //orientate mesh
                  MAILLAGE=MAIL,
                  ORIE_PEAU_3D=_F(GROUP_MA='LOADED', ), );
MODE=AFFE_MODELE(MAILLAGE=MAIL,                    //orientate mesh
                 AFFE=_F(TOUT='OUI',
                         PHENOMENE='MECANIQUE',
                         MODELISATION='3D', ), );
MATE=AFFE_MATERIAU(MAILLAGE=MAIL,                  //apply material
                  AFFE=_F(TOUT='OUI',
                          MATER=MA, ), );
CHAR=AFFE_CHAR_MECA(MODELE=MODE,                  //define fixture
                   DDL_IMPO=_F(GROUP_MA='FIXED',
                               DX=0.0,
                               DY=0.0,
                               DZ=0.0, ),
                   //define load
                   FORCE_FACE=_F(GROUP_MA='LOADED',
                                 FX=1.33e+6, ), );
RESU=MECA_STATIQUE(MODELE=MODE, //specify mechanical behavior
                  CHAM_MATER=MATE,
                  EXCIT=_F(CHARGE=CHAR, ), );
RESU=CALC_ELEM(reuse =RESU, //specify required results (elemental)
              MODELE=MODE,
              CHAM_MATER=MATE,
              RESULTAT=RESU,
              OPTION=('SIGM_ELNO', 'SIEQ_ELNO', ),
              EXCIT=_F(CHARGE=CHAR, ), );
RESU=CALC_NO(reuse =RESU, //specify required results (nodal)
            RESULTAT=RESU,
            OPTION=('SIGM_NOEU', 'SIEQ_NOEU', ), );
IMPR_RESU(FORMAT='MED',
          UNITE=80,
          RESU=_F(MAILLAGE=MAIL,
                 RESULTAT=RESU,
                 NOM_CHAM=('SIGM_NOEU', 'SIEQ_NOEU', 'DEPL', ), ), );
FIN( );
```

C.6 Command file for Test Case 6: Large deflection of a Z-Shaped Cantilever Beam under End Load

```

DEBUT(); //start code

MAT=DEFI_MATERIAU(ELAS=_F(E=2e11,
                        NU=0.3),);
MESH=LIRE_MAILLAGE(FORMAT='MED',); //Load mesh
MESH=DEFI_GROUP(reuse =MESH,
                MAILLAGE=MESH,
                CREA_GROUP_MA=_F(NOM='TOUT',
                                TOUT='OUI',),
                CREA_GROUP_NO=_F(TOUT_GROUP_MA='OUI',),);
CANTI=AFFE_MODELE(MAILLAGE=MESH, //specify 3D
                  behaviour
                  AFFE=_F(TOUT='OUI',
                          PHENOMENE='MECANIQUE',
                          MODELISATION='3D',),);
MATER=AFFE_MATERIAU(MAILLAGE=MESH, //apply material to model
                    AFFE=_F(TOUT='OUI',
                            MATER=MAT,),);
F1=DEFI_FONCTION( //Define a linearly
                  interpolated ramp function
                  NOM_PARA='INST',
                  VALE=(0,0,
                        1,1,
                        ),);
Fix=AFFE_CHAR_MECA(MODELE=CANTI, //Define fixtures
                  DDL_IMPO=_F(GROUP_MA='Fix',
                              DX=0,
                              DY=0,
                              DZ=0,),);
Load=AFFE_CHAR_MECA(MODELE=CANTI, //Define load IN pA
                   FORCE_FACE=_F(GROUP_MA='Load',
                                 FZ=117647058.8,),);
timelist=DEFI_LIST_REEL(DEBUT=0, //Define list for time-
                       stepping
                       INTERVALLE=_F(JUSQU_A=1,
                                       NOMBRE=36,),

```

```

nonlin=STAT_NON_LINE(MODELE=CANTI,           //specify      nonlinear
behaviour

                    CHAM_MATER=MATER,       //specify material
                    EXCIT=( _F(CHARGE=Fix, ) , //activate fixture
                            _F(CHARGE=Load,  //activate load
                                FONC_MULT=F1, ), ), //impose ramp
                                                            Function on
                                                            load

COMP_INCR=_F(RELATION='ELAS',               //elastic behavior
DEFORMATION='GROT_GDEP' , ),

                                                    //large displacement

INCREMENT=_F(LIST_INST=timelist, ) ,        //specify increments
METHODE='NEWTON' ,

                                                    //solution method

NEWTON=_F(MATRICE='TANGENTE' ,
REAC_ITER=1, ),

CONVERGENCE=_F(RESI_GLOB_RELA=10e-6, //convergence criteria
ITER_GLOB_MAXI=30, ),
SOLVEUR=_F(METHODE='MULT_FRONT' ,
SYME='OUI' , ), );
nonlin=CALC_ELEM(reuse =nonlin,
RESULTAT=nonlin,
OPTION='SIEQ_ELNO' , );

nonlin=CALC_NO(reuse =nonlin,
RESULTAT=nonlin,
OPTION=('SIGM_NOEU' , 'SIEQ_NOEU' , ), );

IMPR_RESU(FORMAT='MED' ,
RESU=_F(MAILLAGE=MESH,
RESULTAT=nonlin,
NOM_CHAM=('DEPL' , 'SIGM_NOEU' , 'SIEQ_NOEU' , ), ), );

FIN();

```

C.7 Command file for Test Case 7: Plastic Deformation of Tensile Test Specimen

```
DEBUT( ); //start code

Mesh=LIRE_MALLAGE(UNITE=20, //load mesh
                  FORMAT='MED', );
Mesh=DEFI_GROUP(reuse =Mesh, //create groups of nodes
                and elements
                MAILLAGE=Mesh,
                CREA_GROUP_MA=_F(NOM='TOUT',
                                  TOUT='OUI', ),
                CREA_GROUP_NO=_F(TOUT_GROUP_MA='OUI', ), );

SPECIMEN=AFFE_MODELE(MAILLAGE=Mesh, //3-D modelisation
                     AFFE=_F(TOUT='OUI',
                               PHENOMENE='MECANIQUE',
                               MODELISATION='3D', ), );

TRACT=DEFI_FONCTION( //define stress-strain curve
                    NOM_PARA='EPSI',
                    NOM_RESU='SIGM',
                    VALE=(0.00105148,66478790,
                          0.001405875,71836430,
                          0.001607605,76065610,
                          0.002015892,81996640,
                          0.002408615,85719050,
                          0.003361565,91442935,
                          0.004038241,93755504,
                          0.005017943,96008589,
                          0.00660453,98376389,
                          0.008080919,99754268,
                          0.010061285,100786457,
                          0.019984268,103030553,
                          0.029647352,103920649,
                          0.03942725,104730805,
                          0.048868133,104899157,
                          0.058314426,105178115,
                          0.067721703,105239445,
                          ),
                    INTERPOL='LIN', //linear interpolation
                    PROL_DROITE='LINEAIRE',
                    PROL_GAUCHE='CONSTANT', );
ALUMI=DEFI_MATERIAU(ELAS=_F(E=66224017575, //define material
                             NU=0.33, ),
                    TRACTION=_F(SIGM=TRACT, ), ); //invoke
                    stress-strain data

FE_MATERIAU(MAILLAGE=Mesh,
            AFFE=_F(TOUT='OUI',
                    MATER=ALUMI, ), );
RAMP=DEFI_FONCTION( //define ramp function
                  NOM_PARA='INST',
                  VALE=(0,0,
                        1,1,
                        ), );
```

```

TIMELIST=DEFI_LIST_REEL(DEBUT=0,           //define time intervals
                        INTERVALLE=_F(JUSQU_A=1,
                                       NOMBRE=100,)),);
FIX=AFFE_CHAR_MECA(MODELE=SPECIMEN,       //define fixtures
                  DDL_IMPO=_F(GROUP_MA='Fix',
                              DX=0,
                              DY=0,
                              DZ=0,)),);
DISPLACE=AFFE_CHAR_MECA(MODELE=SPECIMEN, //define loads
                        DDL_IMPO=_F(GROUP_MA='Load',
                                      DY=0.004,)),);
NONLIN=STAT_NON_LINE(MODELE=SPECIMEN, //invoke nonlinear solver
                    CHAM_MATER=MATERIAL,
                    EXCIT=( _F(CHARGE=DISPLACE, //activate load
                                FONC_MULT=RAMP, ),
                            _F(CHARGE=FIX, ), ), //activate load
                    COMP_INCR=_F(RELATION='VMIS_ISOT_TRAC',
                                  //von Mises isotropic material with plasticity
                                  DEFORMATION='SIMO_MIEHE' ), ),
                    INCREMENT=_F(LIST_INST=TIMELIST, ),
                    NEWTON=_F(PREDICTION='TANGENTE',
                               REAC_ITER=1, ),

                                CONVERGENCE=_F(RESI_GLOB_RELA=1E-4,
                                                //convergence criteria
                                                ITER_GLOB_MAXI=100, ),
                    SOLVEUR=_F(METHODE='MULT_FRONT' ), );

NONLIN=CALC_ELEM(reuse =NONLIN,
                RESULTAT=NONLIN,
                OPTION=('SIEF_ELNO', 'SIEQ_ELGA', 'SIEQ_ELNO' ), );

NONLIN=CALC_NO(reuse =NONLIN,
               RESULTAT=NONLIN,
               OPTION=('FORC_NODA', 'SIEQ_NOEU' ), );

IMPR_RESU(FORMAT='MED',
          RESU=_F(MAILLAGE=Mesh,
                 RESULTAT=NONLIN,

NOM_CHAM=('SIEF_NOEU', 'SIEQ_ELNO', 'SIEQ_NOEU', 'FORC_NODA', 'DEPL',
          ), ), );

FIN();

```

APPENDIX D

Images of FEA results

The images presented are the graphical plots generated by the post-processor of the investigated package. In the event that mesh refinement was done to obtain more accurate solutions, only one instance of the result sets will be presented. This is done to mitigate repetition.

D.1.1 Test Case 1 results: Mecway

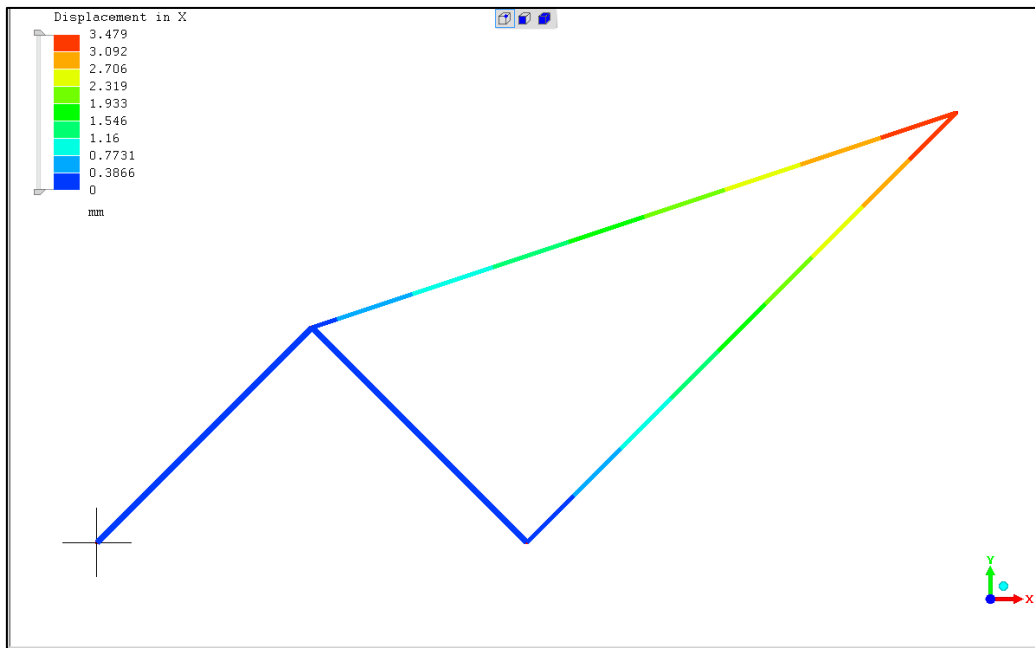


Figure D.1. Displacement in X-direction.

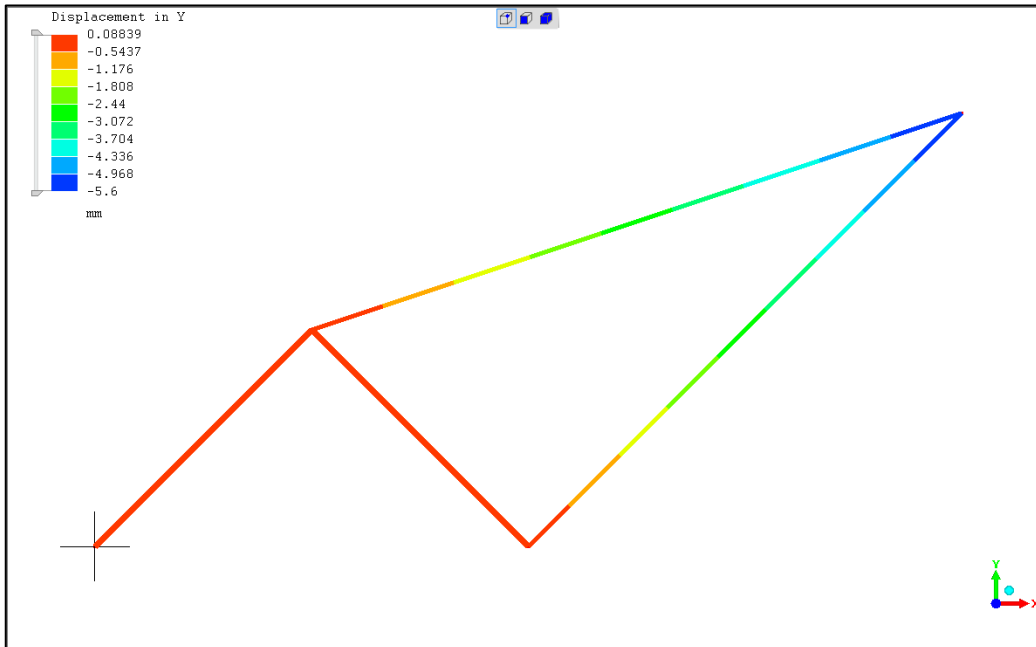


Figure D.2. Displacement in Y-direction.

D.1.2 Test case 1 results: Z88 Aurora

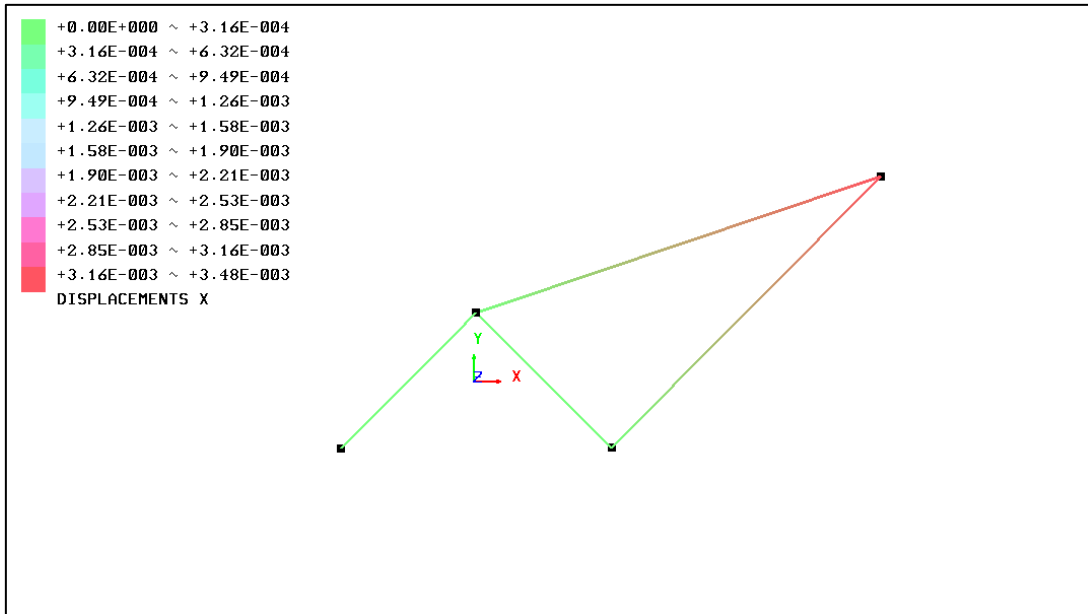


Figure D. 3. Displacement in X-direction.

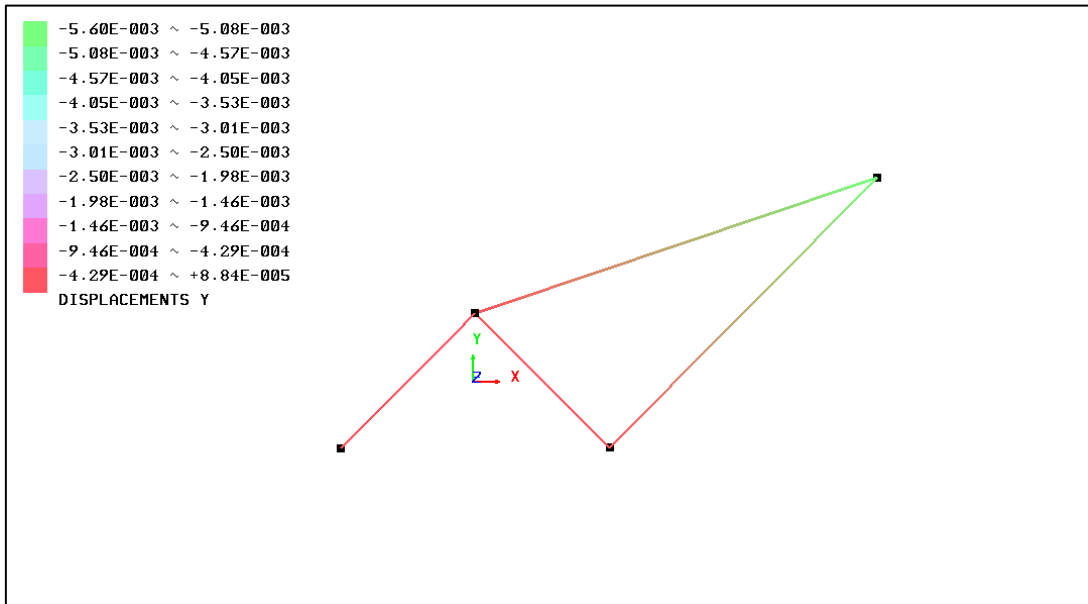


Figure D. 4. Displacement in Y-direction.

D.1.3 Test case 1 results: Code_Aster

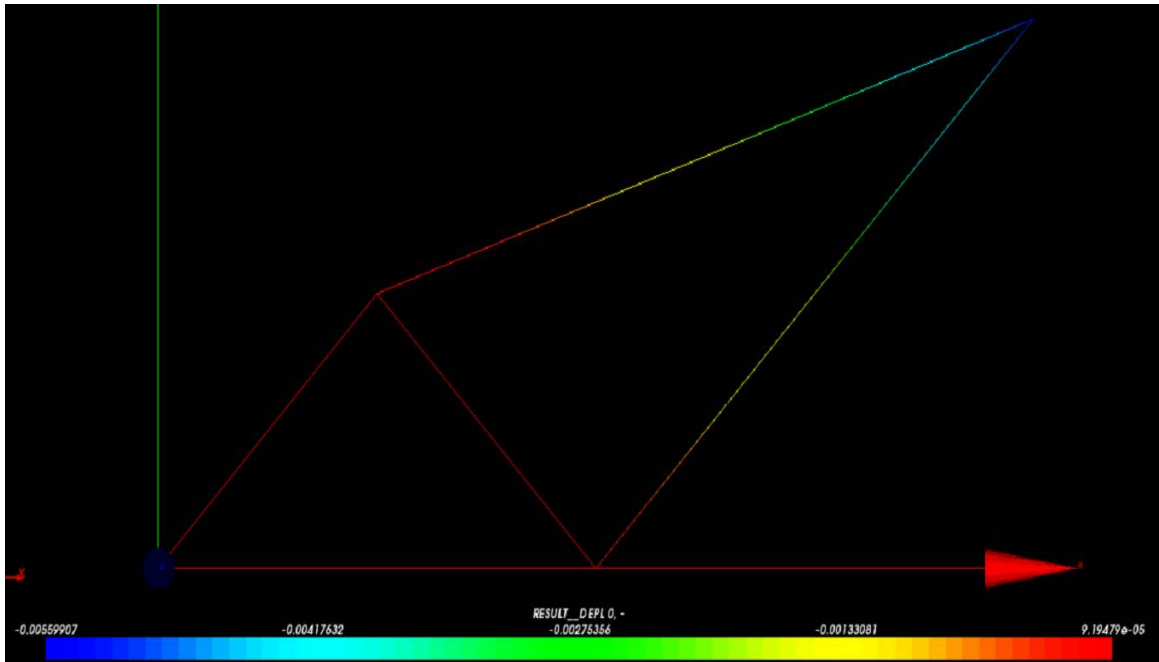


Figure D. 5. Displacement in X-direction.

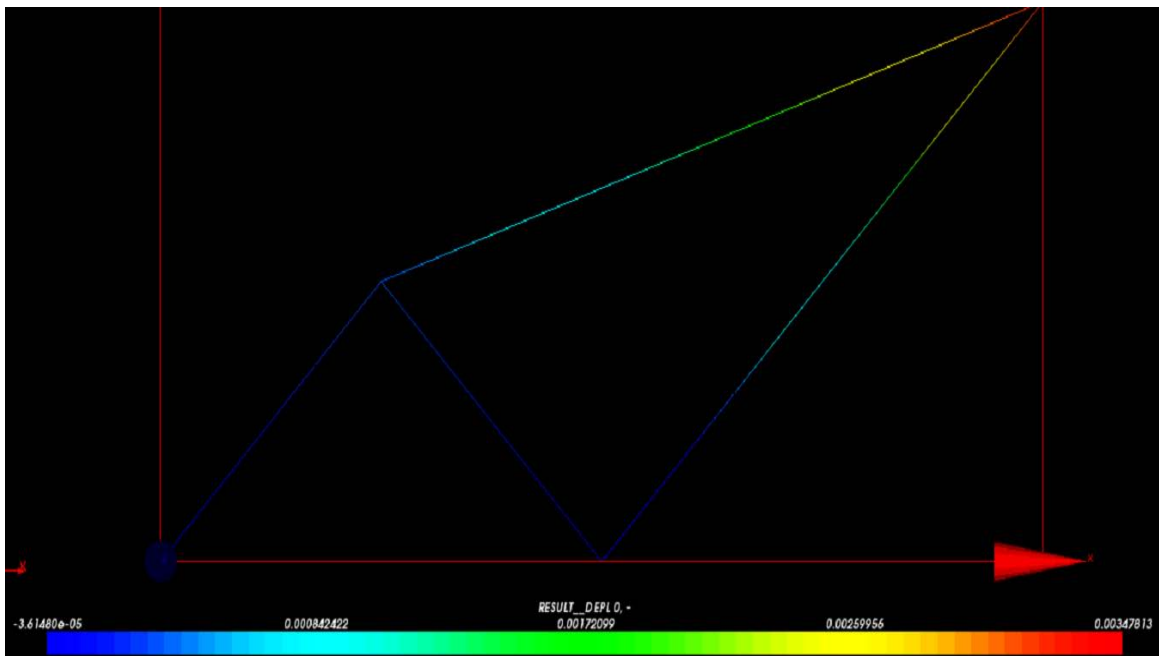


Figure D. 6. Displacement in Y-direction.

D.1.4 Test case 1 results: ANSYS

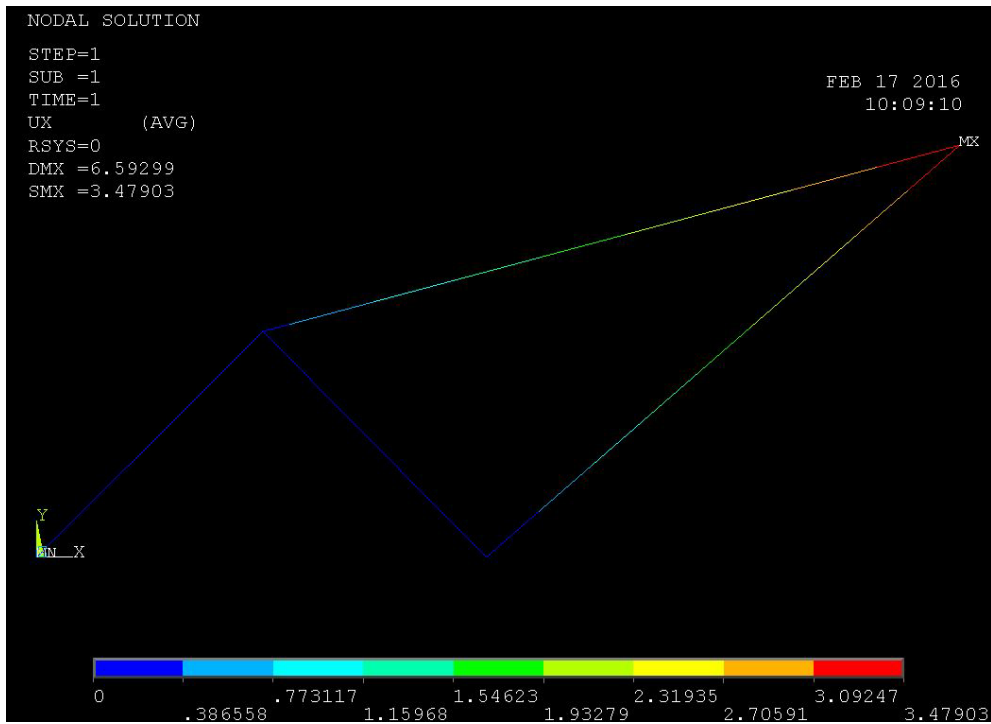


Figure D. 7. Displacement in X-direction.

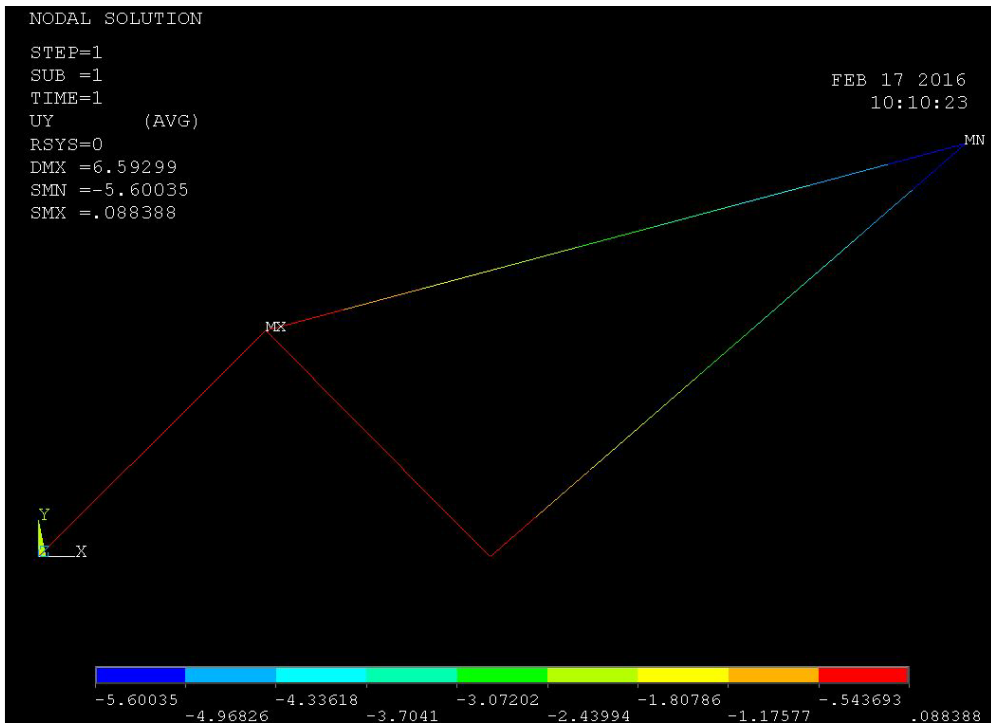


Figure D. 8. Displacement in Y-direction.

D.1.5 Test case 1 results: Siemens NX

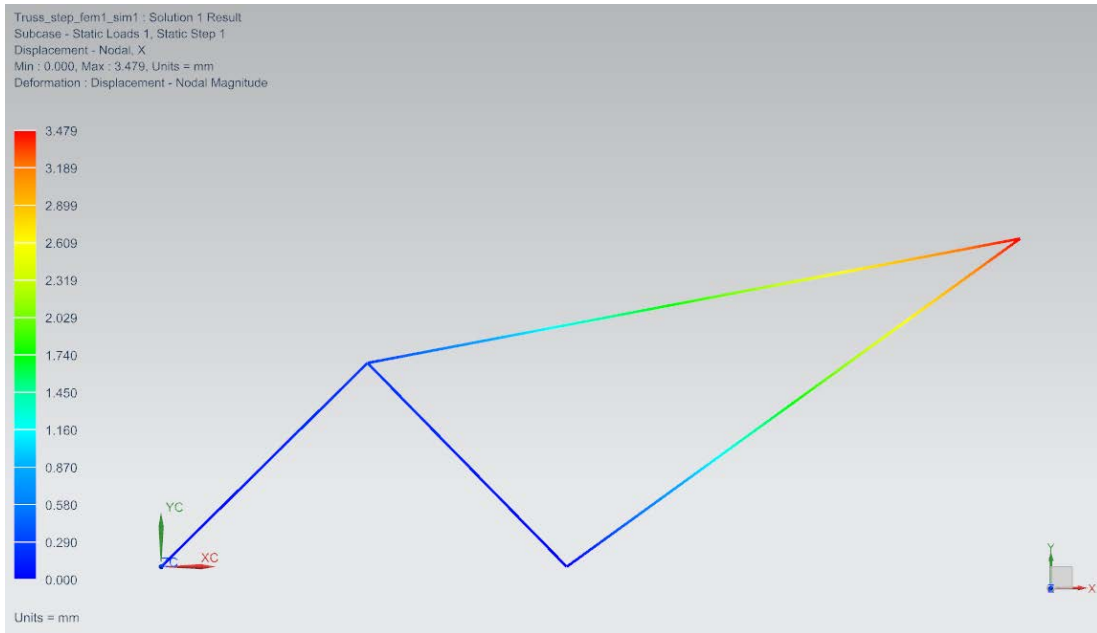


Figure D. 9. Displacement in X-direction.

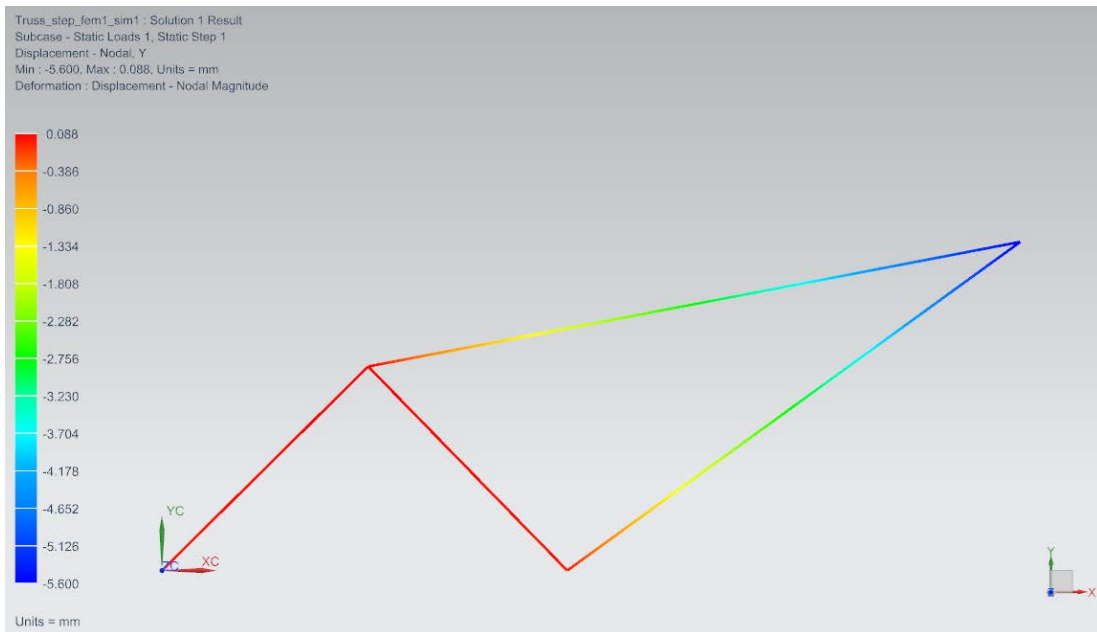


Figure D. 10. Displacement in Y-direction.

D.2.1 Test case 2 results: Mecway

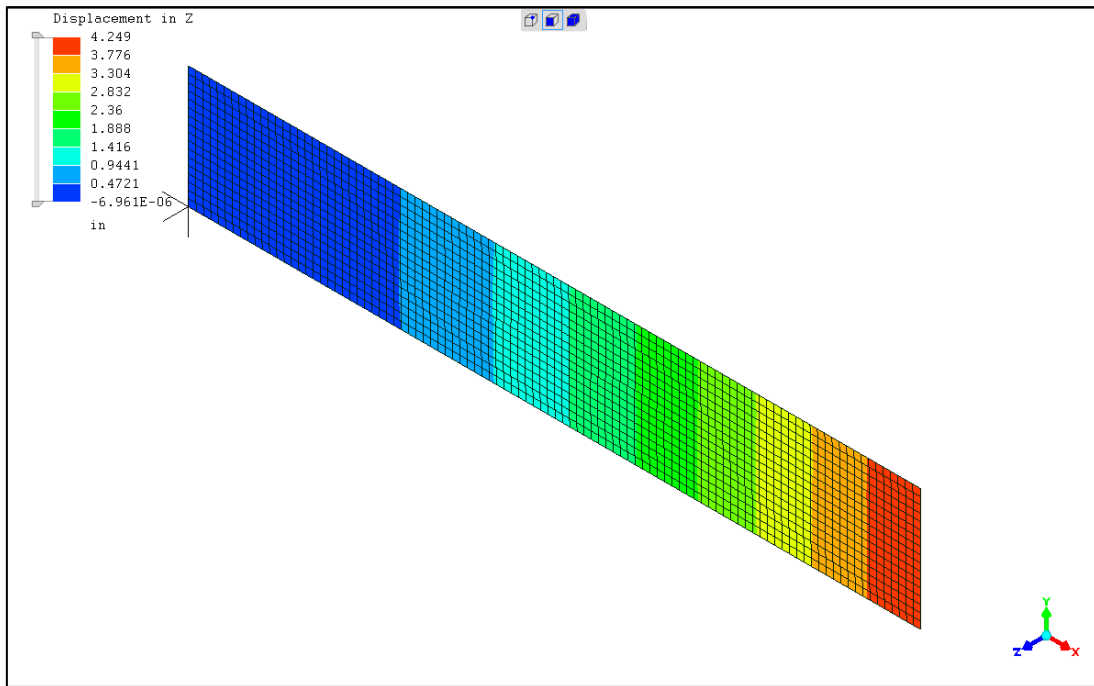


Figure D. 11. Displacement in Z-direction.

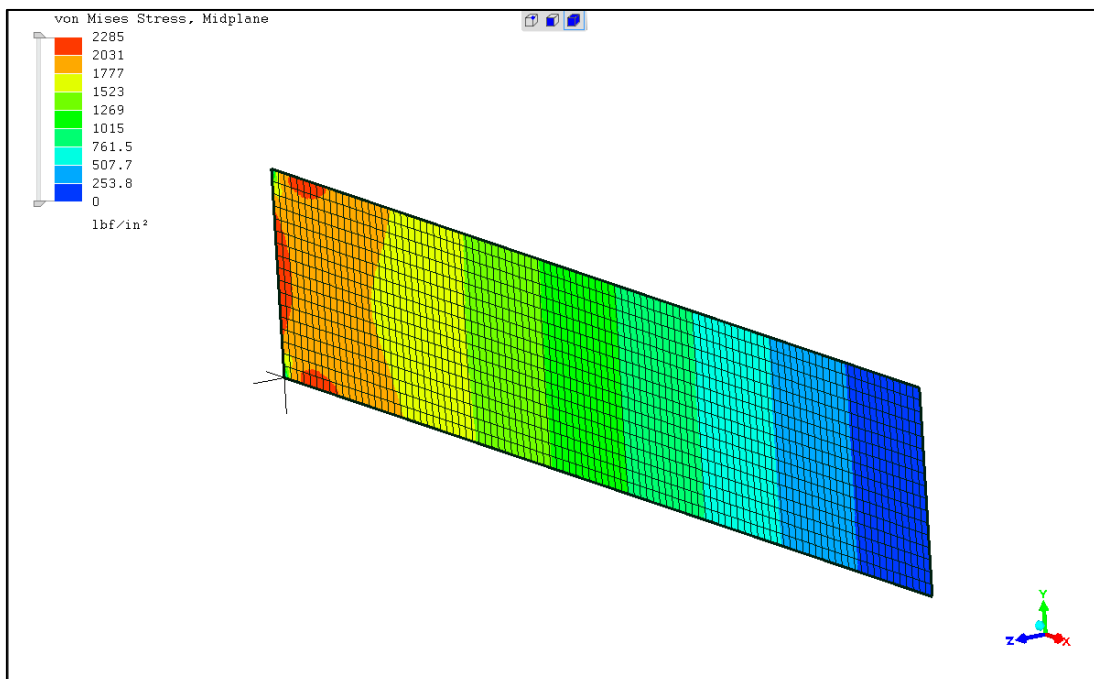


Figure D. 12. Stress in Z-direction.

D.2.2 Test case 2 results: Code_Aster

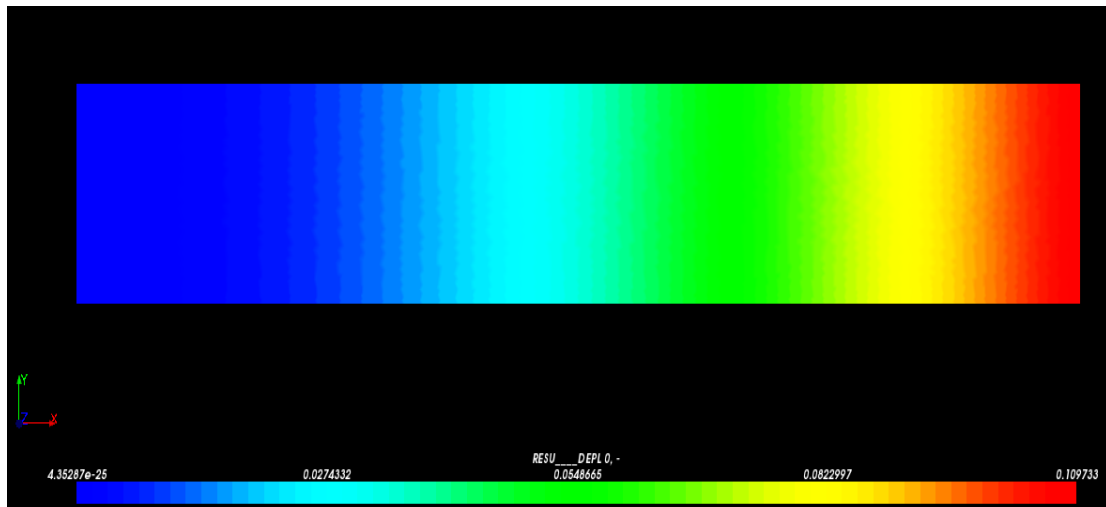


Figure D. 13. Displacement in Z-Direction (SI units).

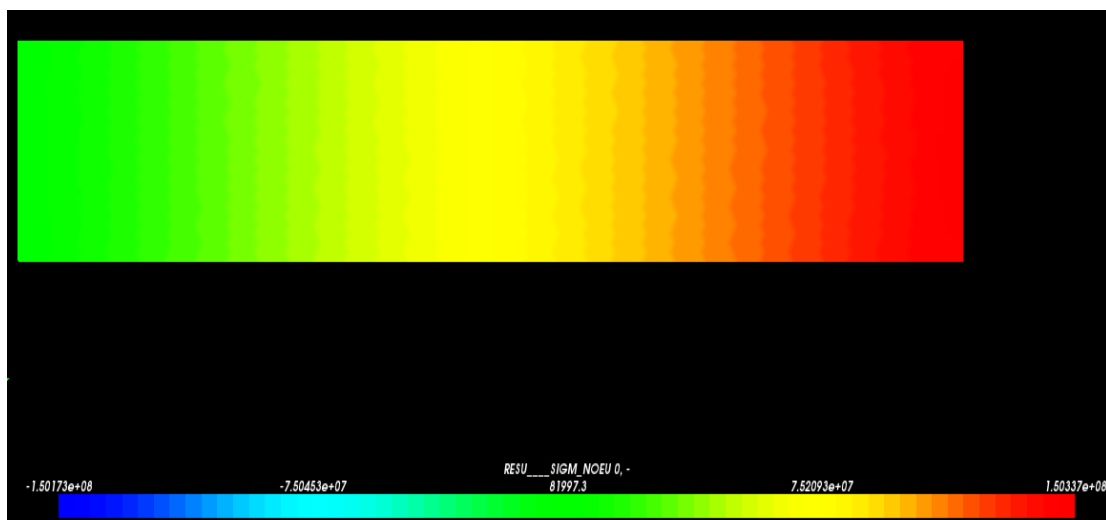


Figure D. 14. Stress in Z-direction (SI units).

D.2.3 Test case 2 results: ANSYS

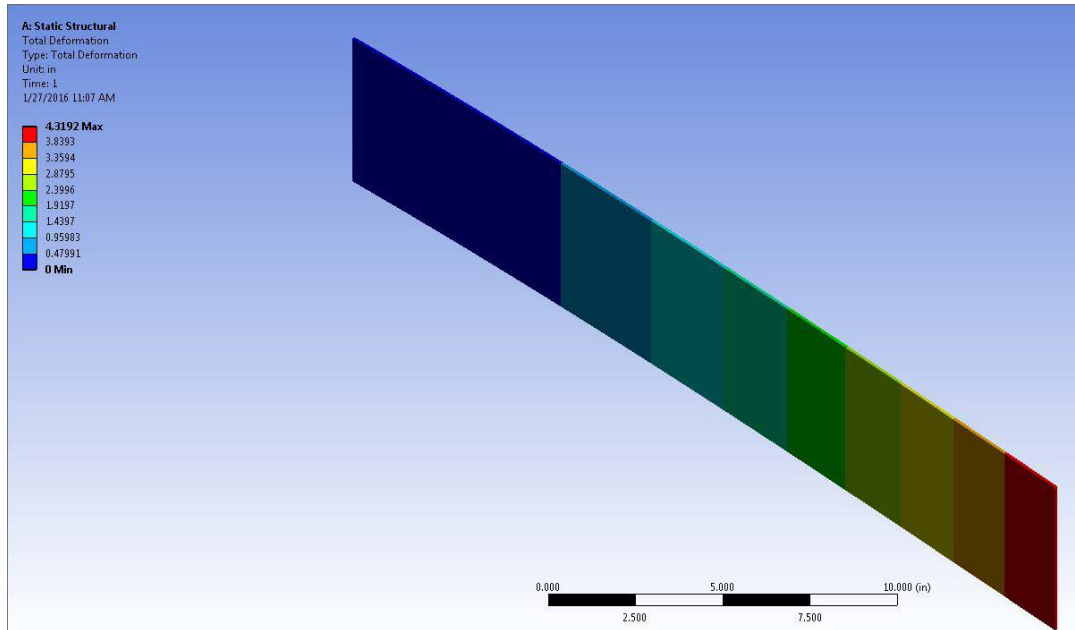


Figure D. 15. Displacement in Z-direction.

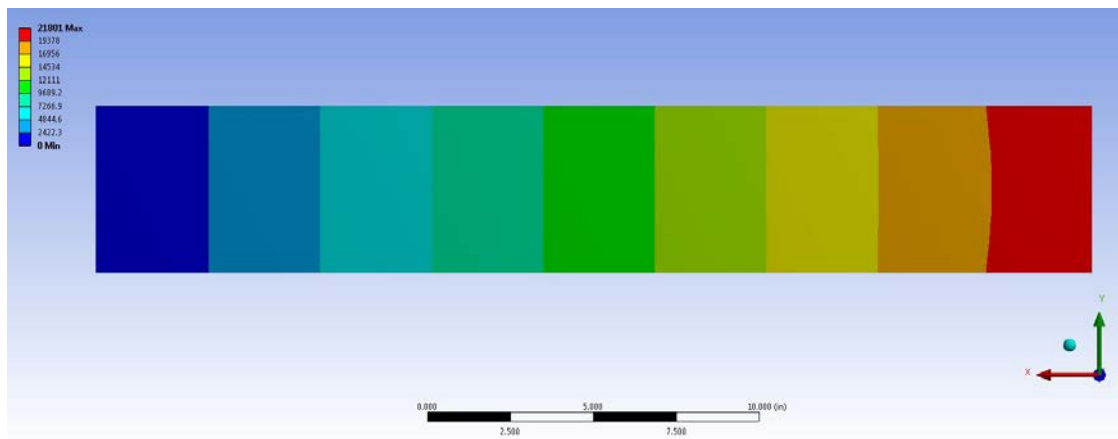


Figure D. 16. Stress in Z-direction.

D.2.4 Test case 2 results: Code_Aster

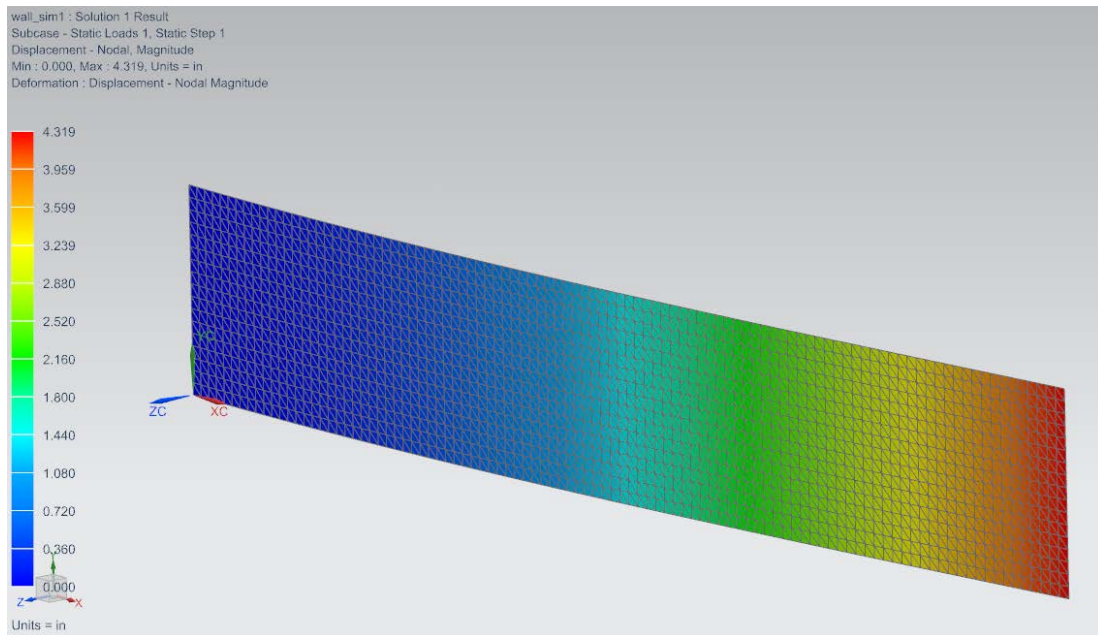


Figure D. 17. Displacement in Z-direction.

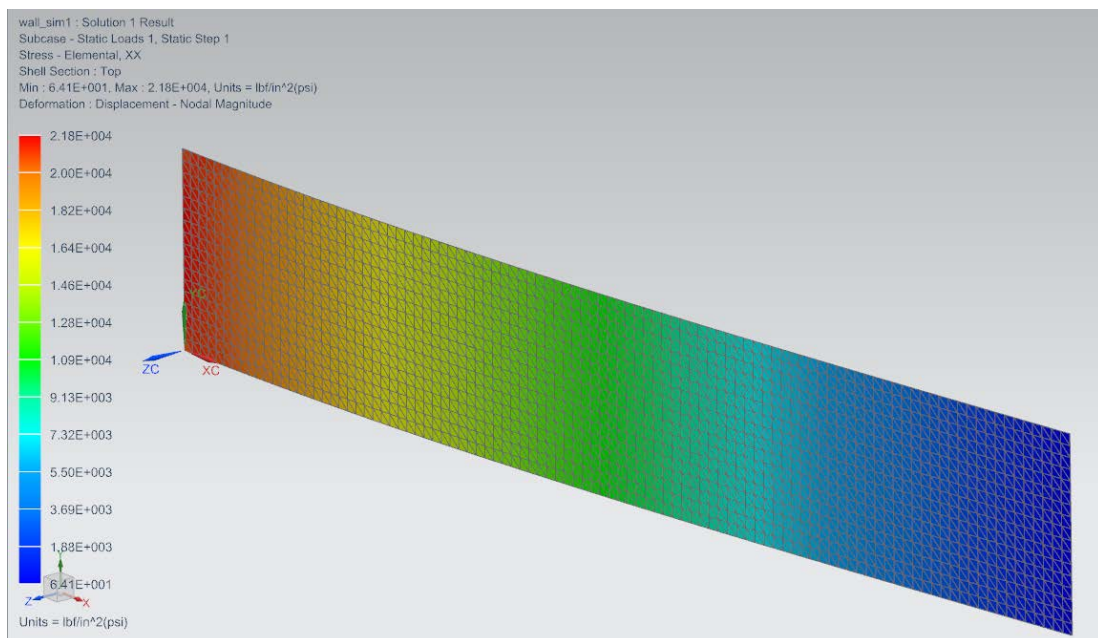


Figure D. 18. Stress in Z-direction.

D.3.1 Test case 3 results: Mecway

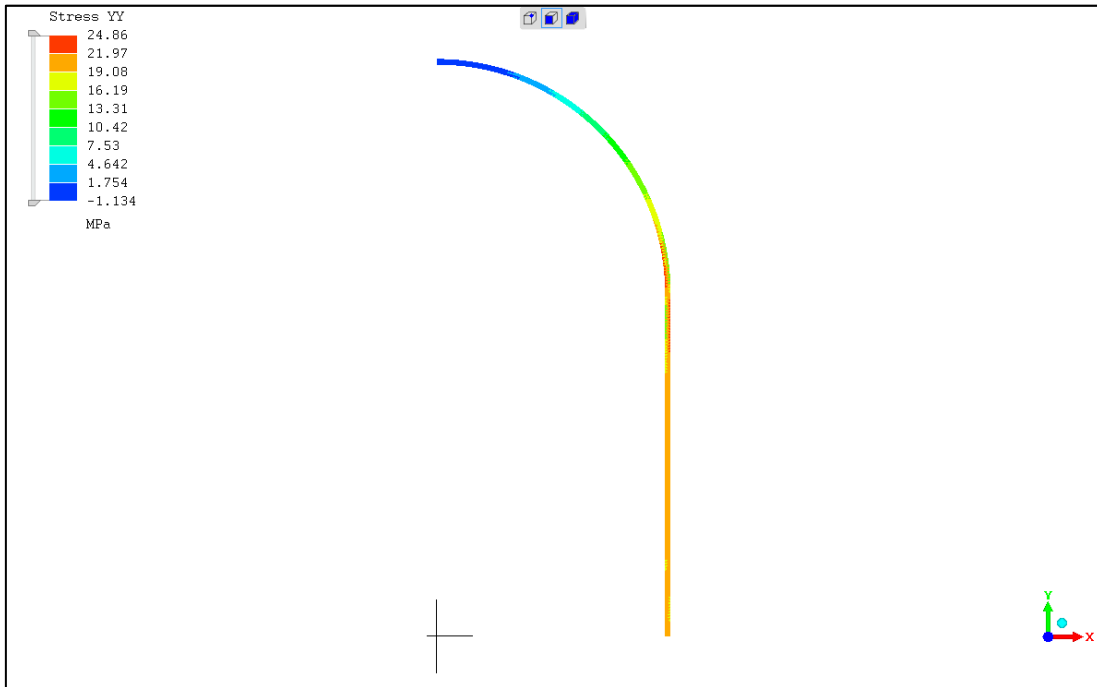


Figure D. 19. Stress (YY).

D.3.2 Test case 3 results: Z88 Aurora

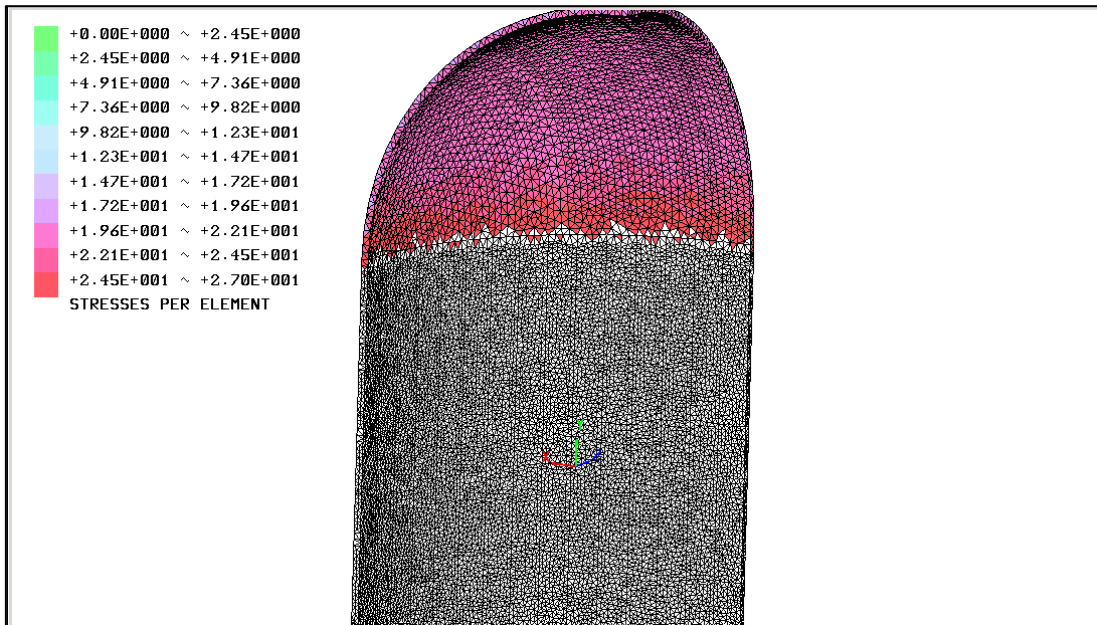


Figure D. 20. Stress (YY).

D.3.3 Test case 3 results: SimScale

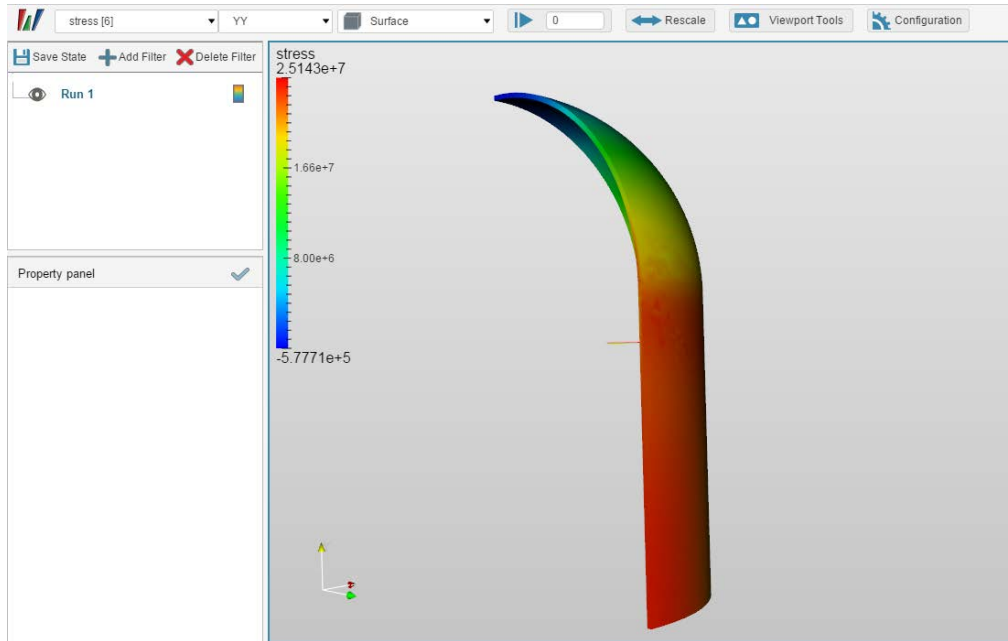


Figure D. 21. Stress (YY).

D.3.4 Test case 3 results: Code Aster

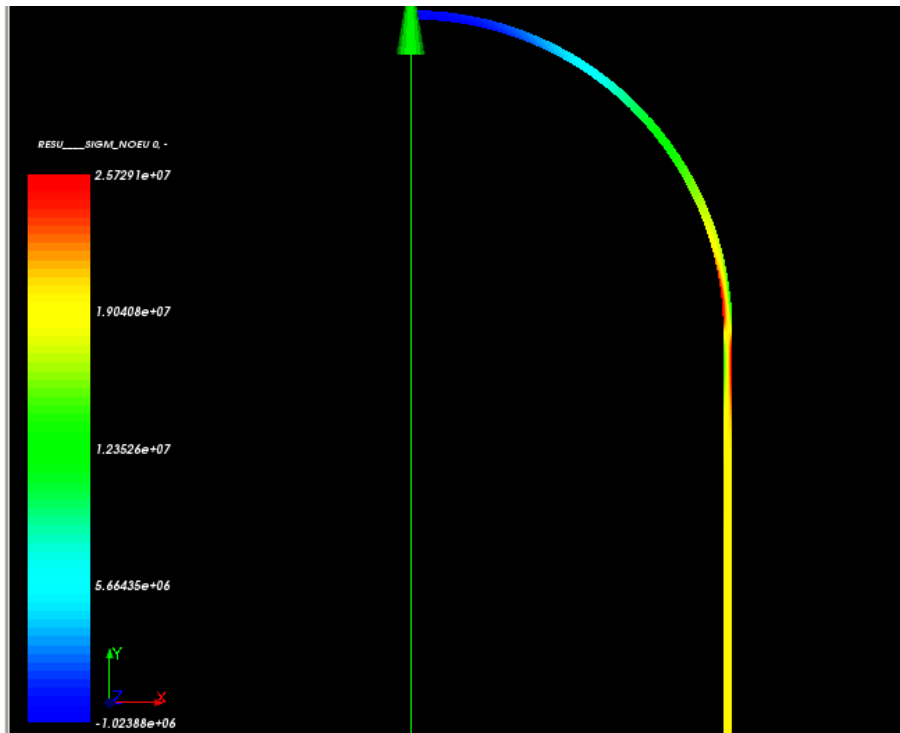


Figure D. 22. Stress (YY).

D.3.5 Test case 3 results: ANSYS Mechanical

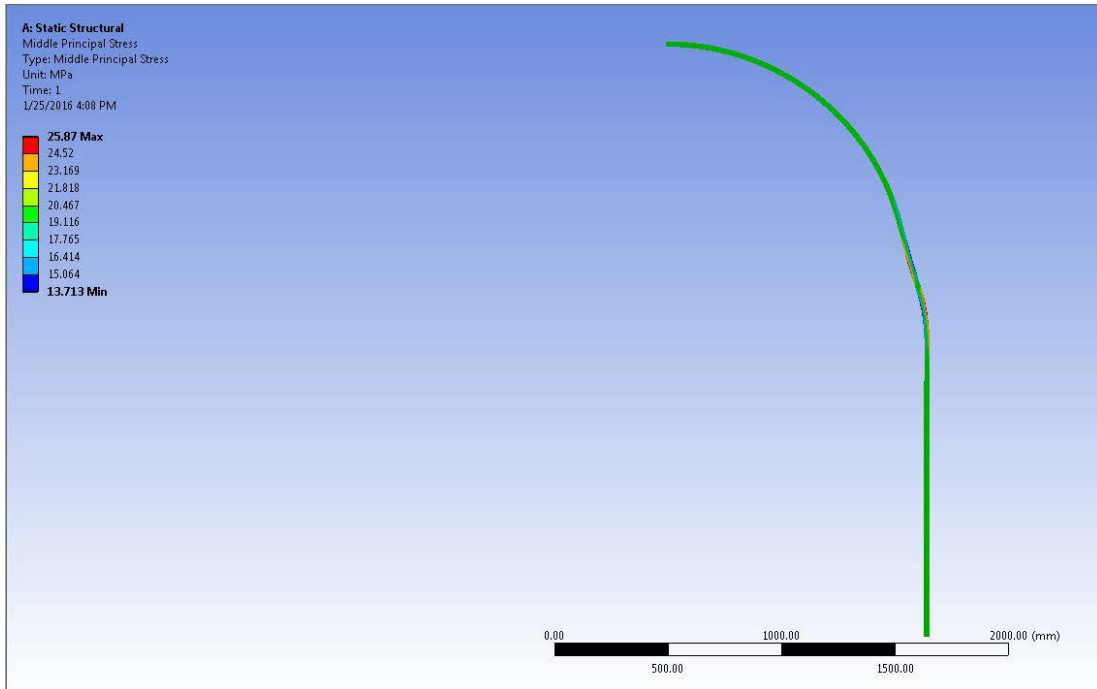


Figure D. 23. Stress (YY)..

D.3.6 Test case 3 results: Siemens NX

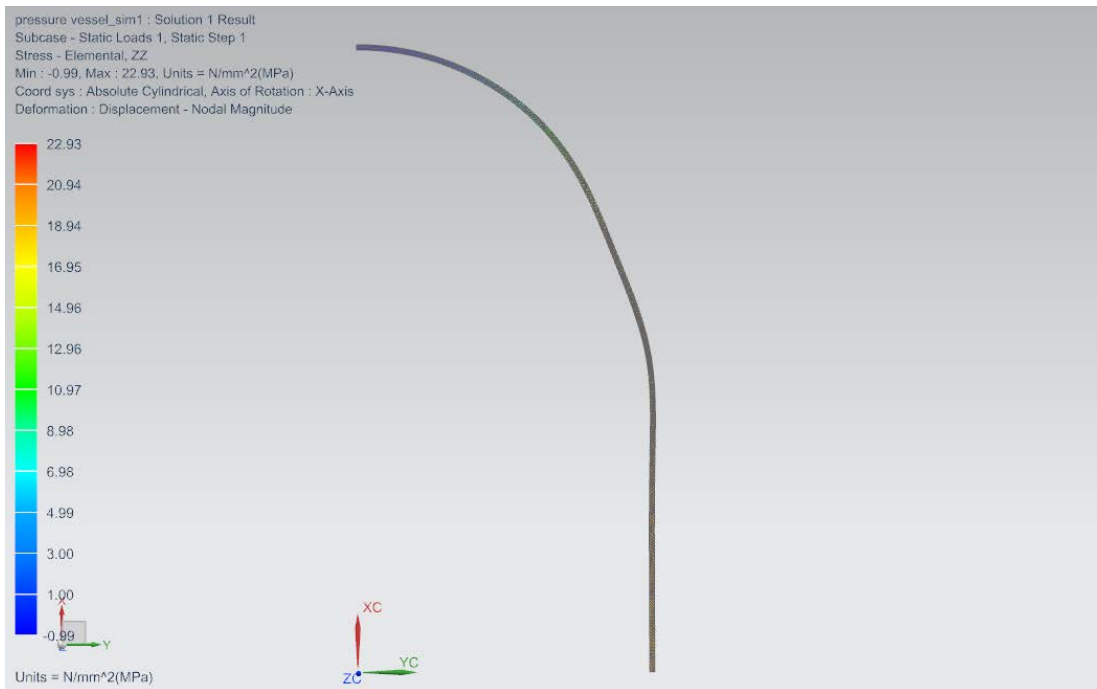


Figure D. 24. Stress (YY).

D.4.1 Test case 4 results: Mecway

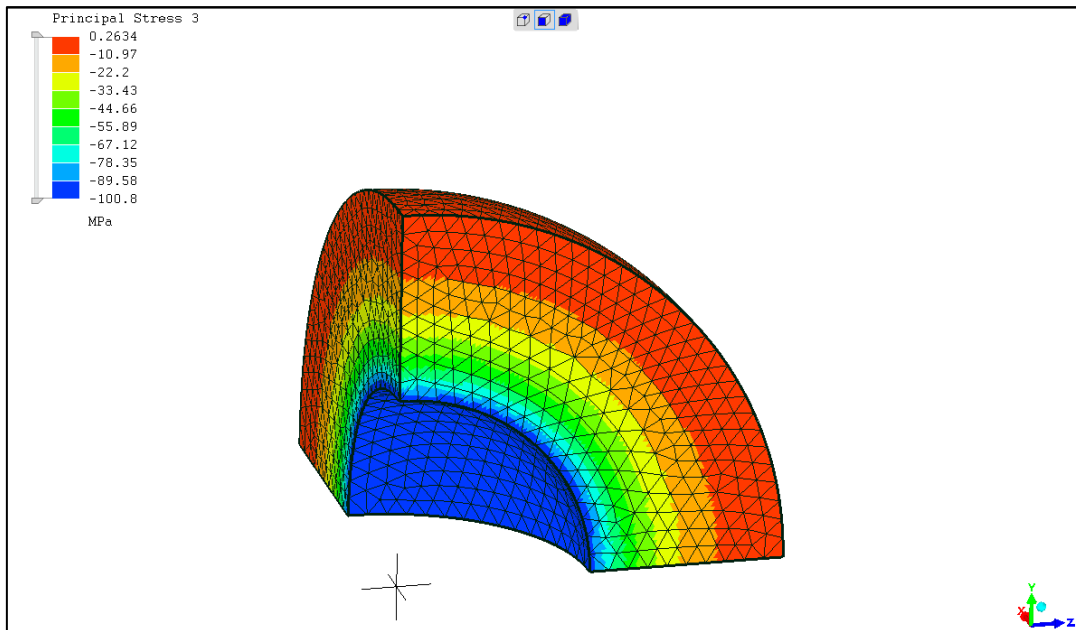


Figure D. 25. Stress σ (rr).

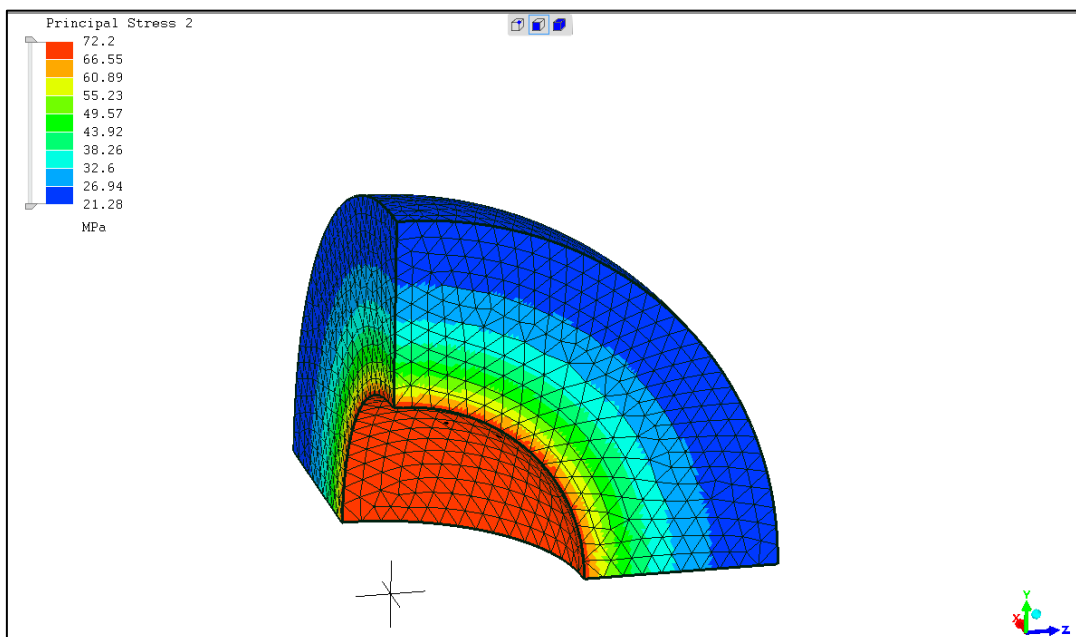


Figure D. 26. Stress σ (Θ).

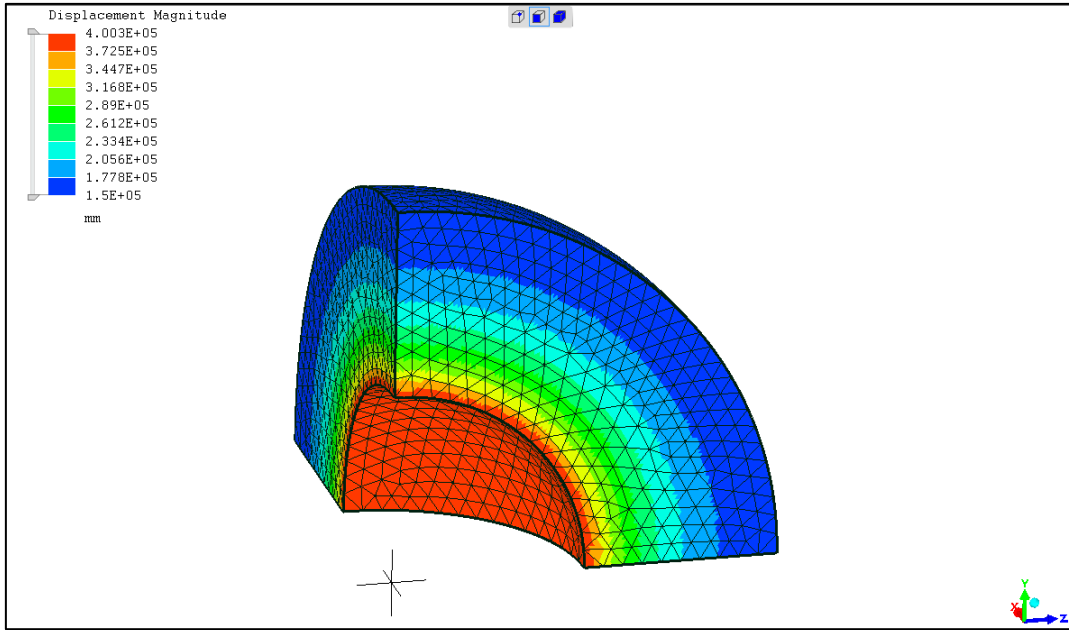


Figure D. 27. Displacement magnitude.

D.4.2 Test case 4 results: Z88 Aurora

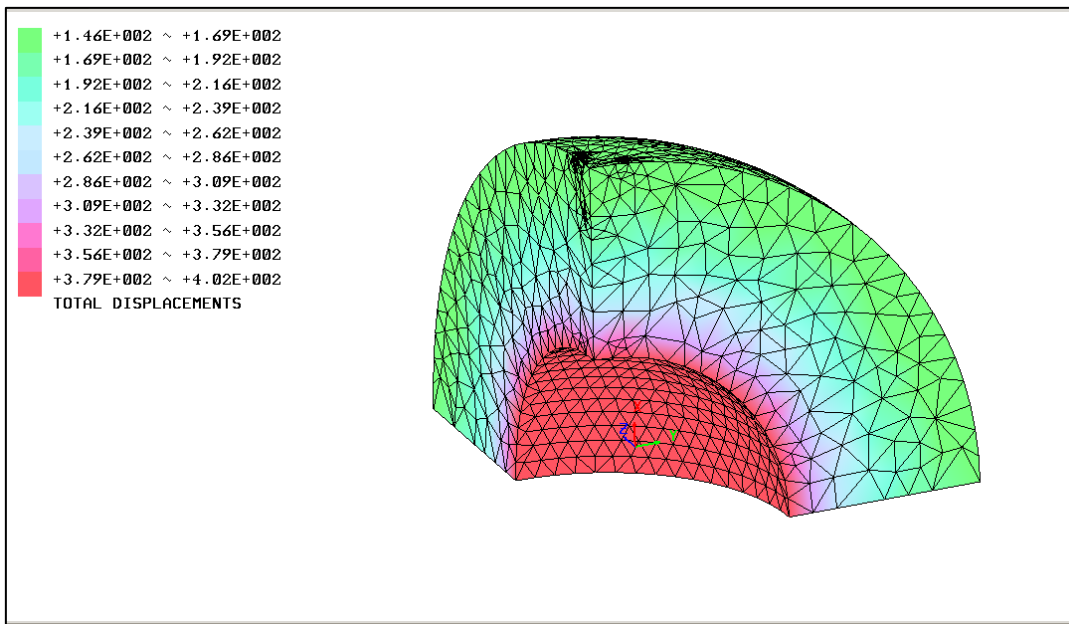


Figure D. 28. Displacement magnitude.

D.4.3 Test case 4 results: SimScale

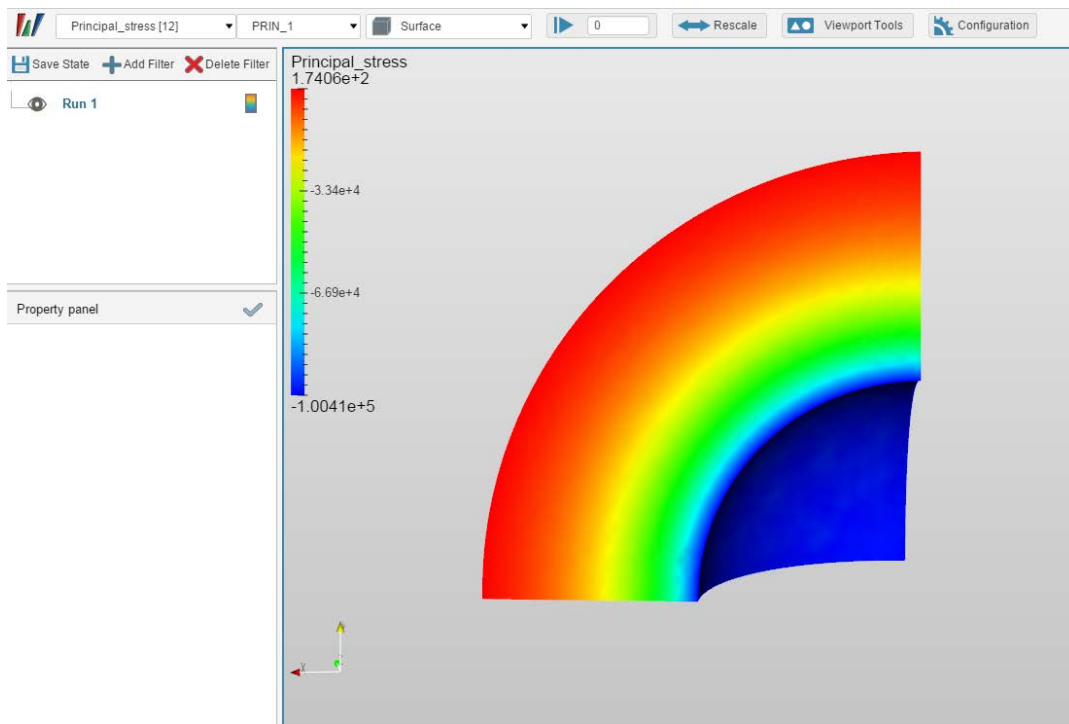


Figure D. 29. Stress σ (rr).

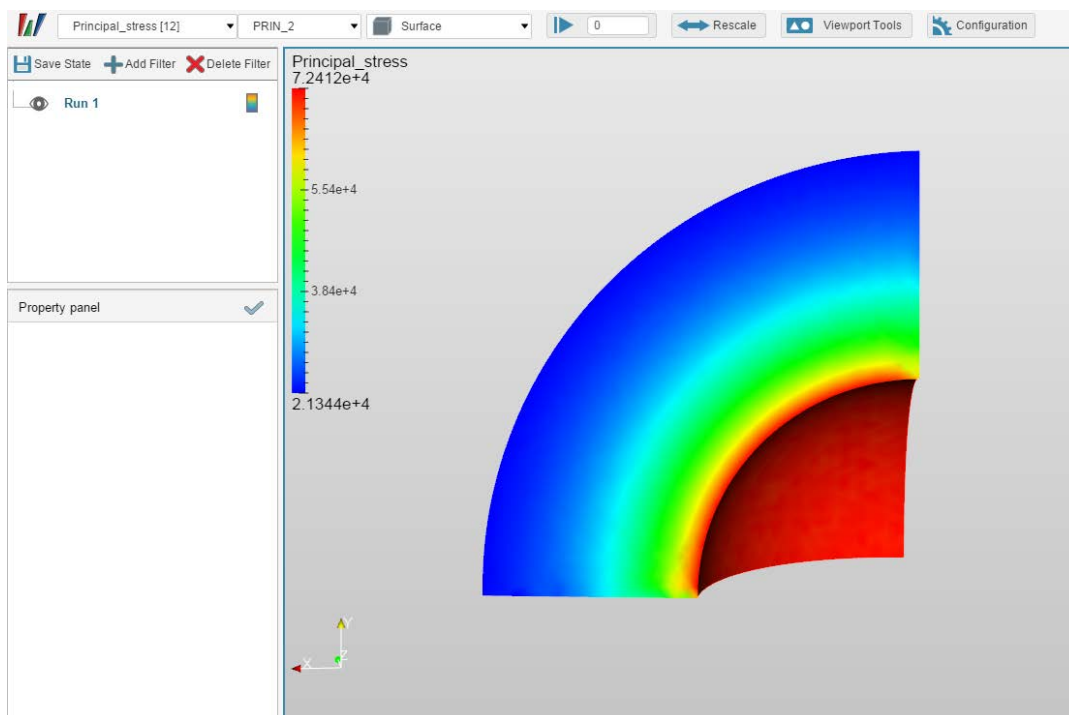


Figure D. 30 Stress σ (Θ).

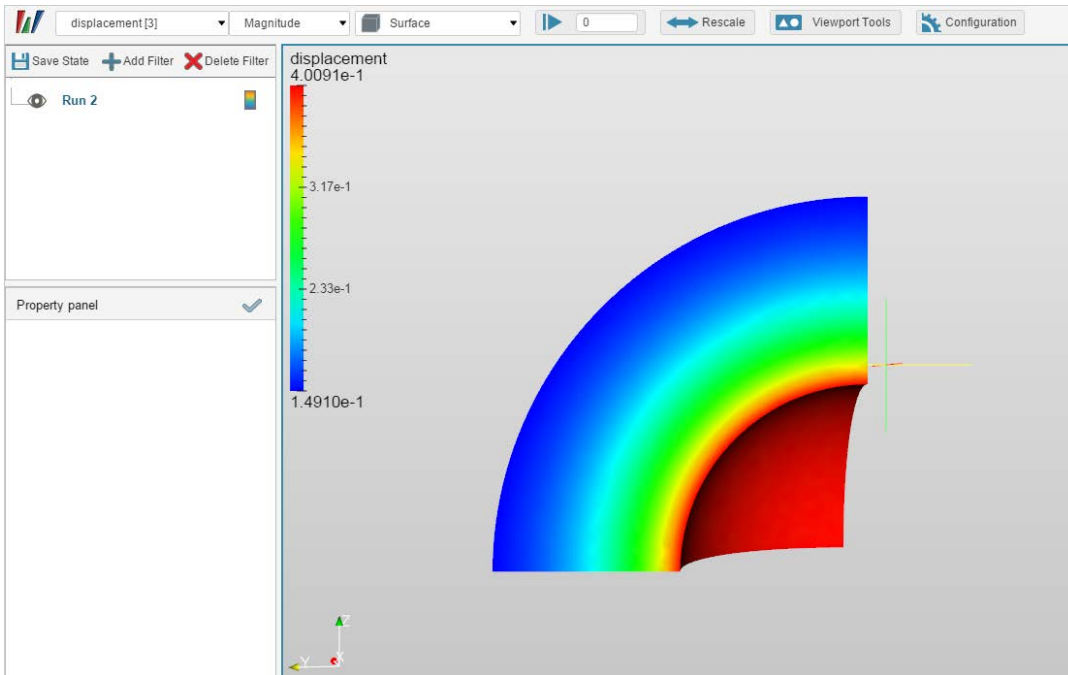


Figure D. 31. Displacement magnitude.

D.4.3 Test case 4 results: SimScale

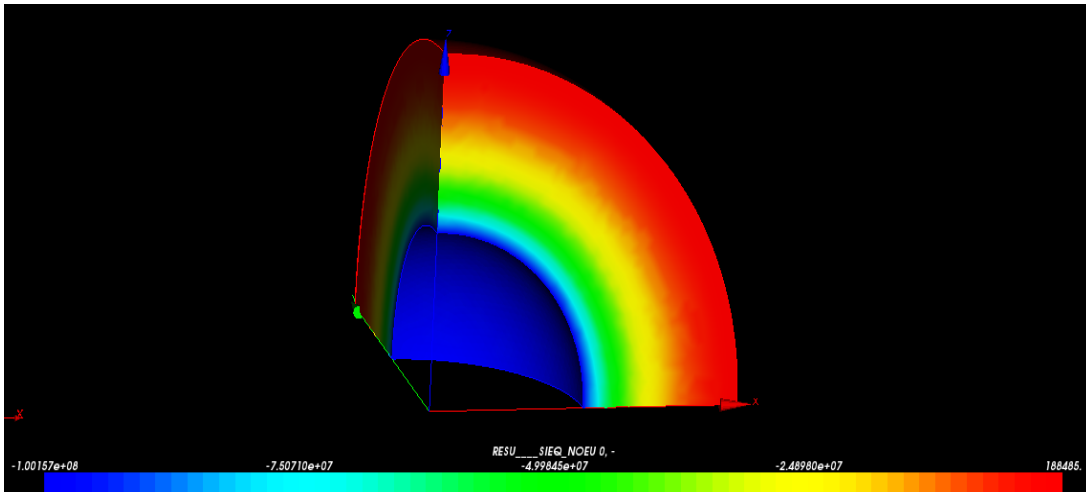


Figure D. 32. Stress σ (rr).

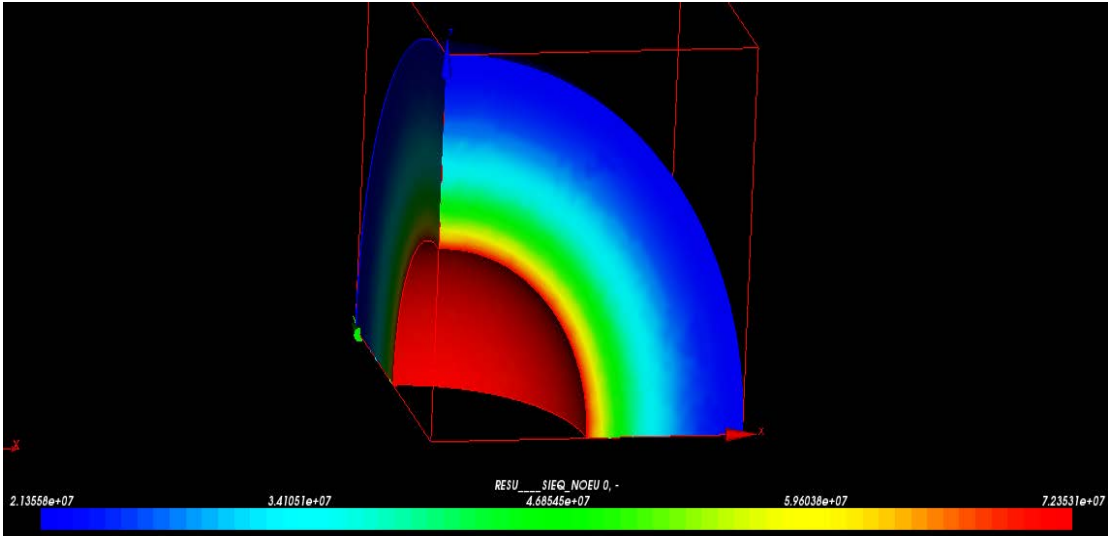


Figure D. 33. Stress σ (Θ).

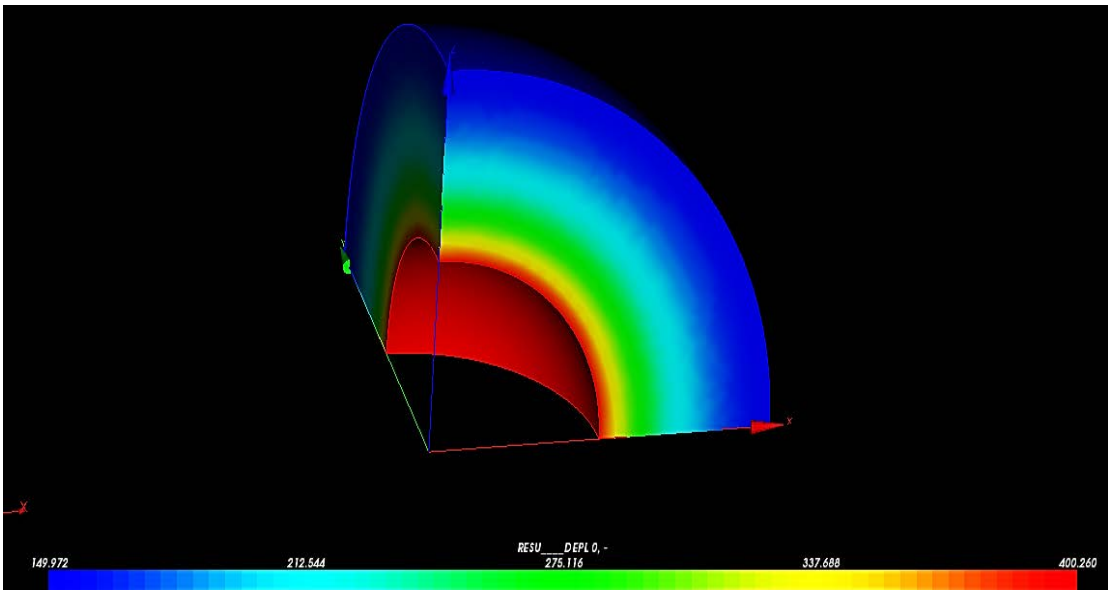


Figure D. 34. Displacement magnitude.

D.4.5 Test case 4 results: ANSYS Mechanical

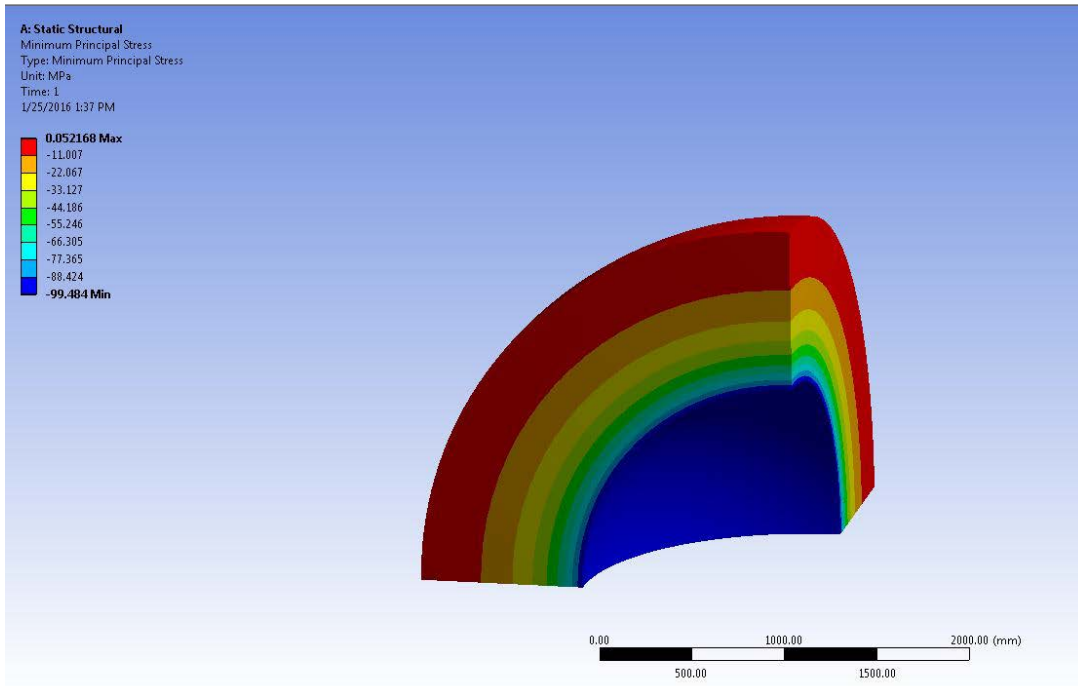


Figure D. 35. Stress σ_{rr} .

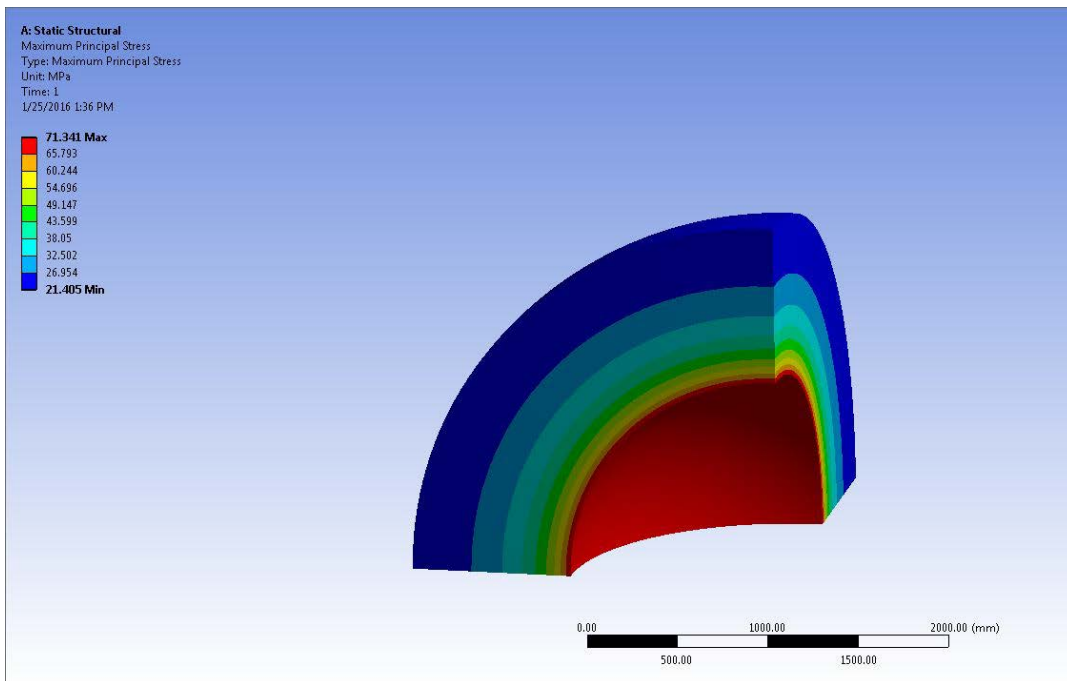


Figure D. 36. Stress σ_{θ} .

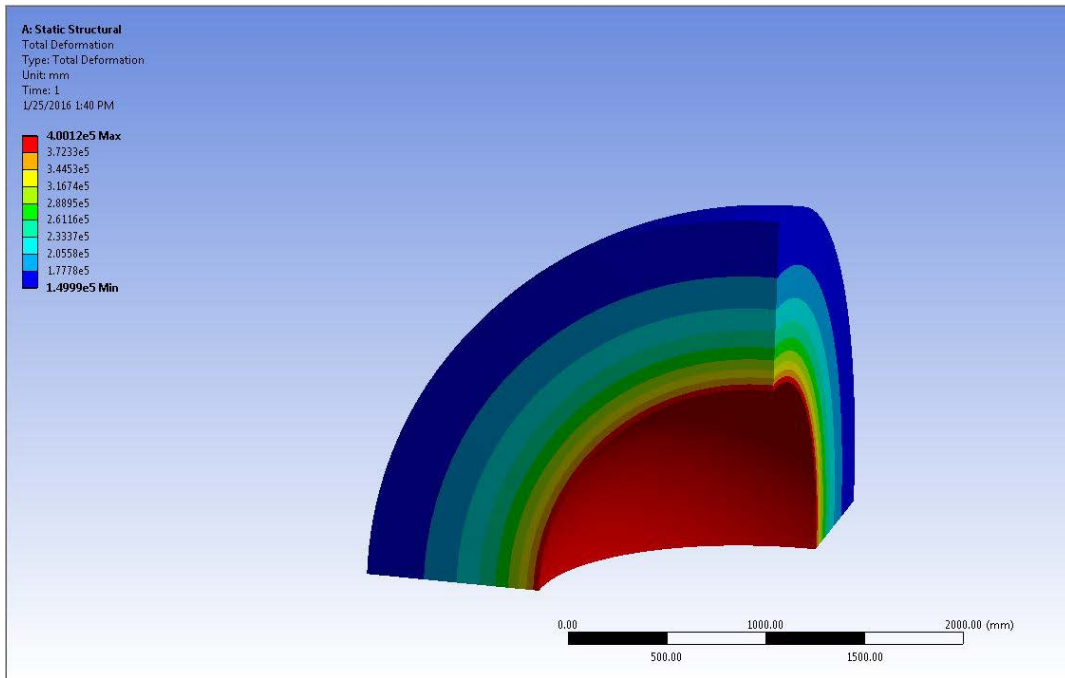


Figure D. 37. Displacement magnitude.

D.4.6 Test case 4 results: Siemens NX

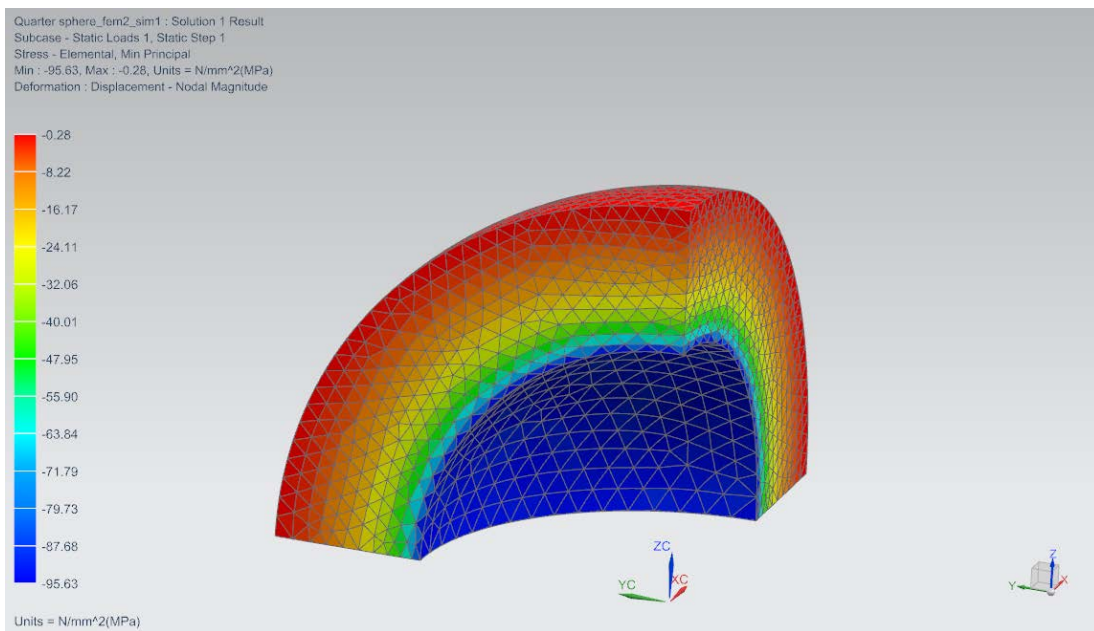


Figure D. 38. Stress σ (rr).

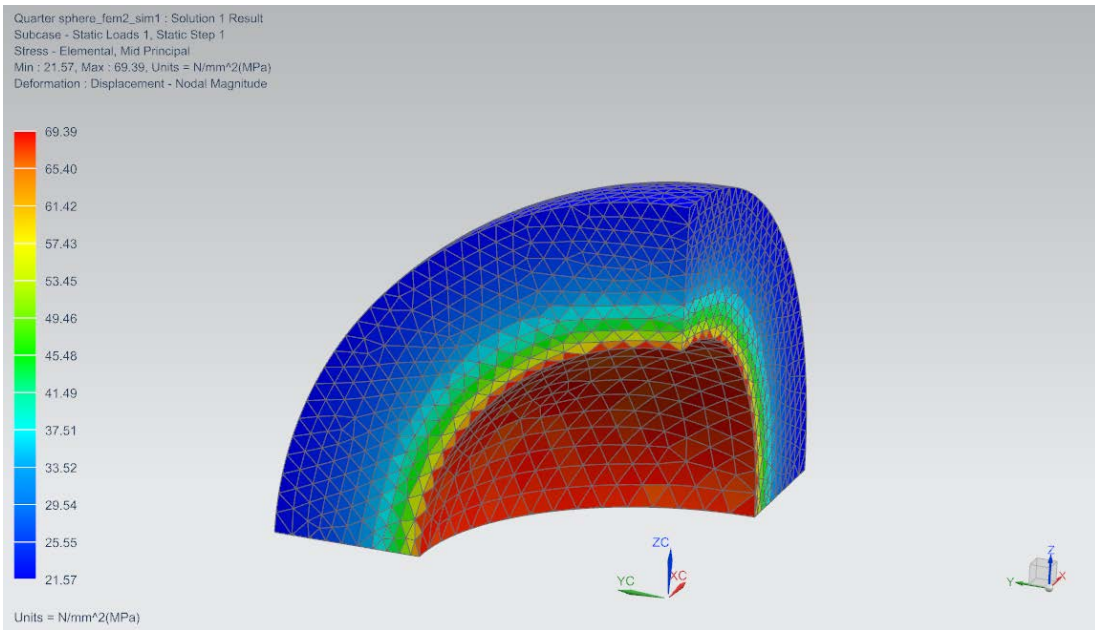


Figure D. 39. Stress σ (Θ).

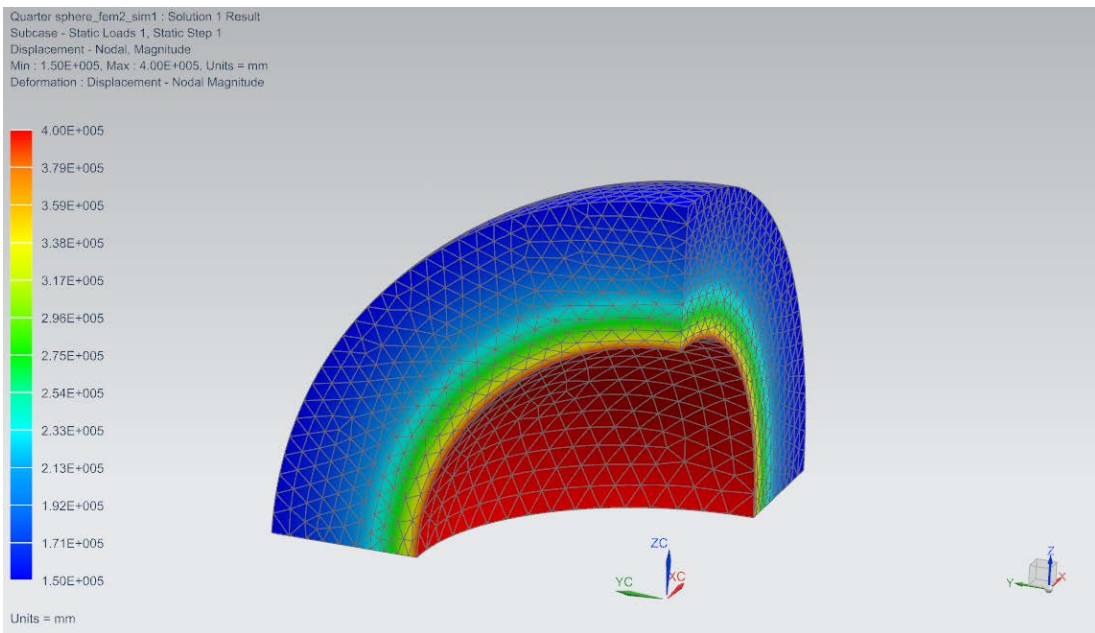


Figure D. 40. Displacement magnitude.

D.5.1 Test case 5 results: Mecway

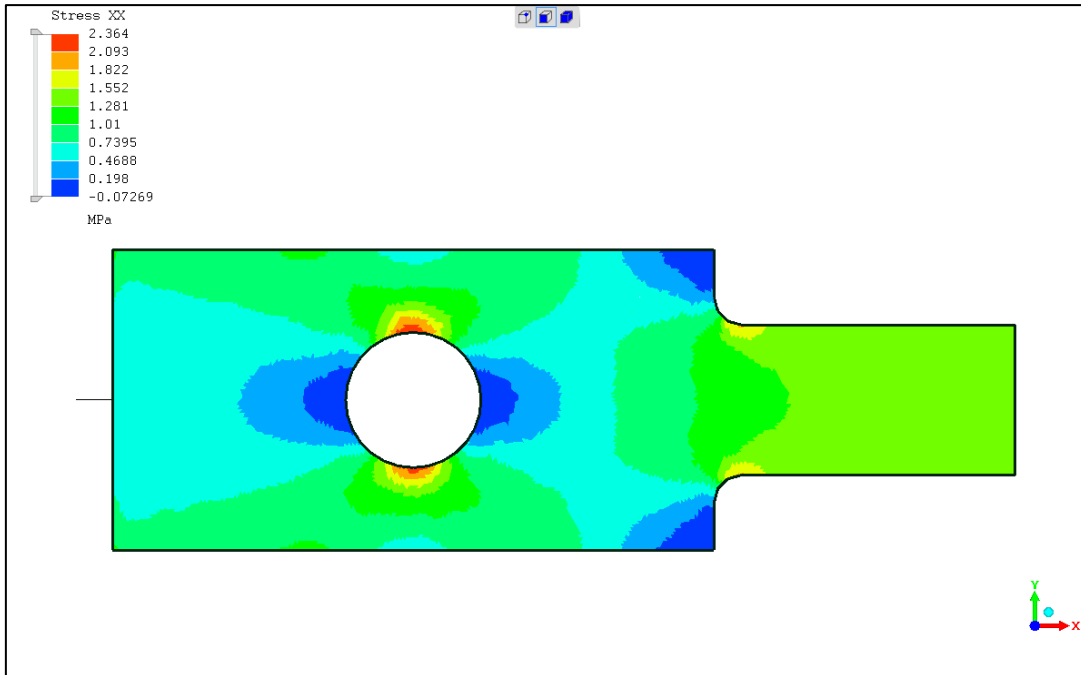


Figure D. 41. Stress along X-axis.

D.5.8 Test case 5 results: Z88 Aurora

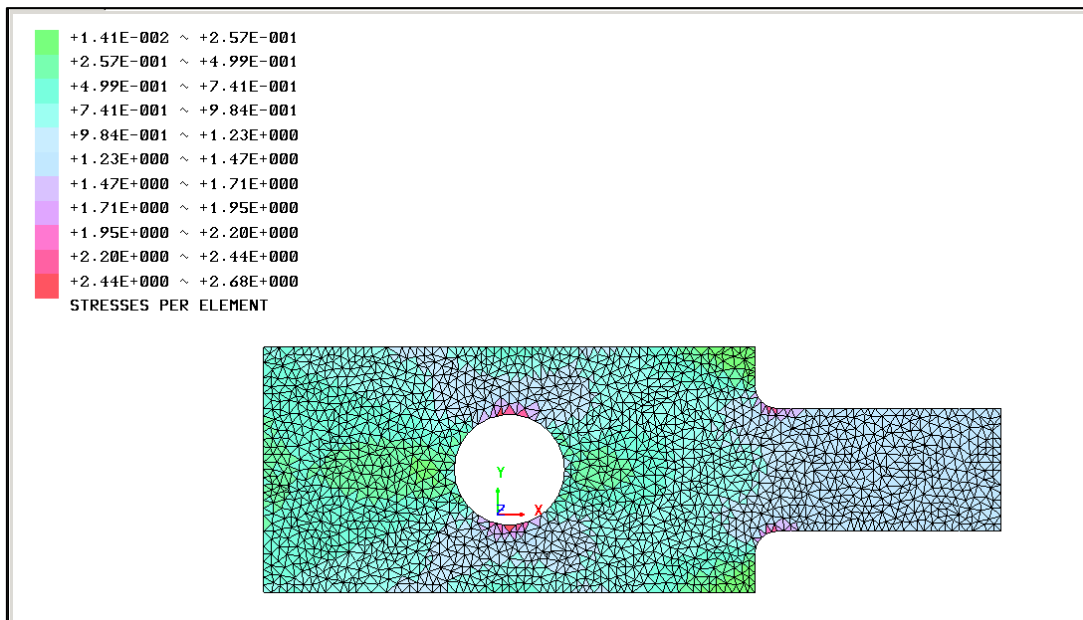


Figure D. 42. Stress along X-axis.

D.5.3 Test case 5 results: SimScale

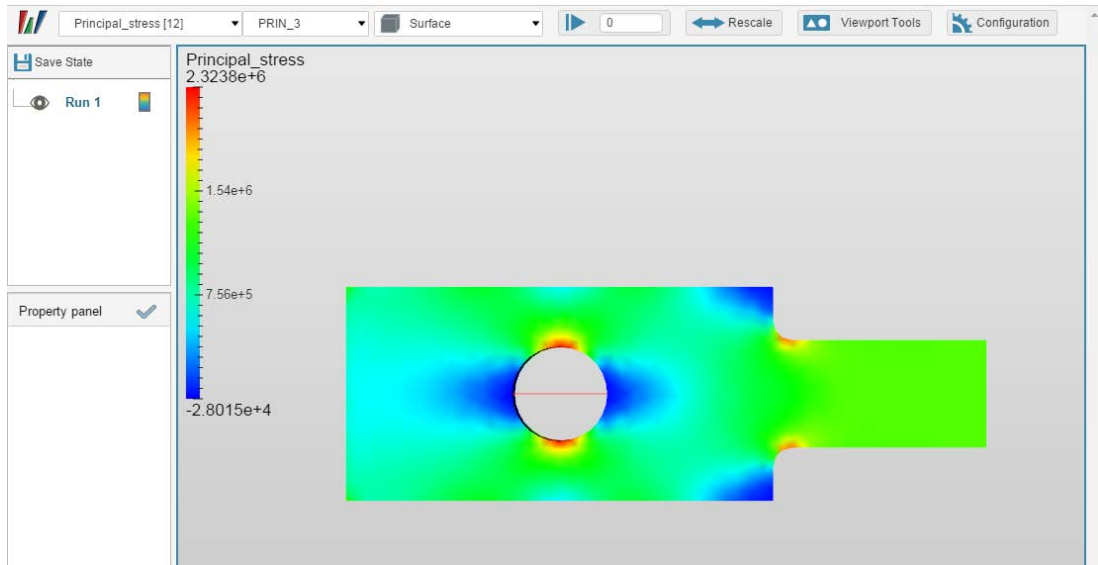


Figure D. 43. Stress along X-axis.

D.5.4 Test case 5 results: Code_Aster

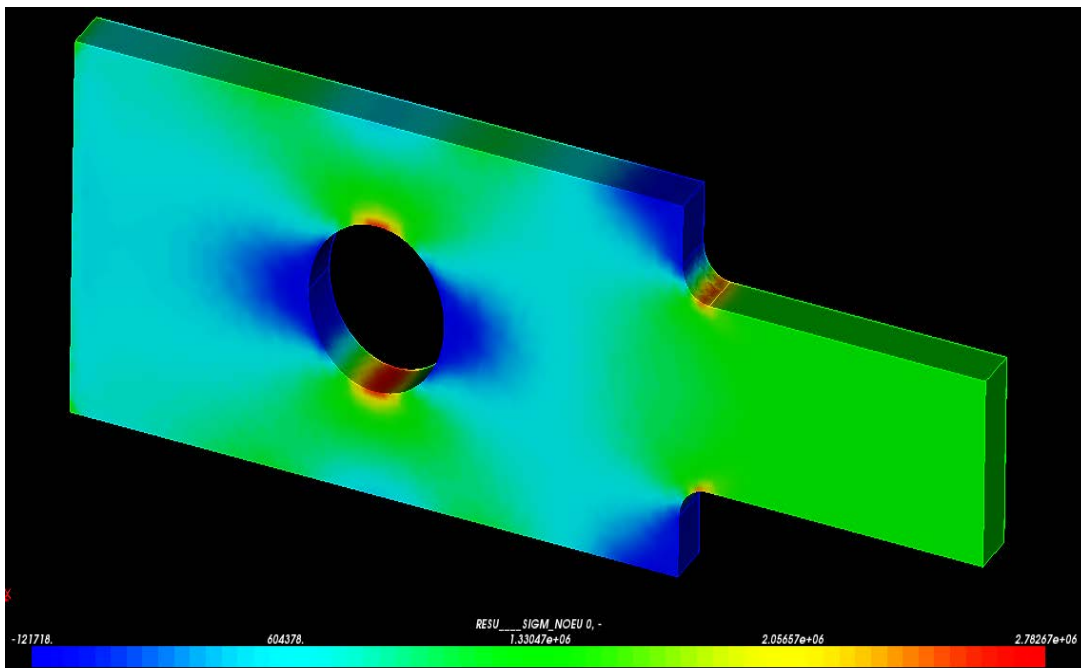


Figure D. 44. Stress along X-axis.

D.5.5 Test case 5 results: ANSYS Mechanical

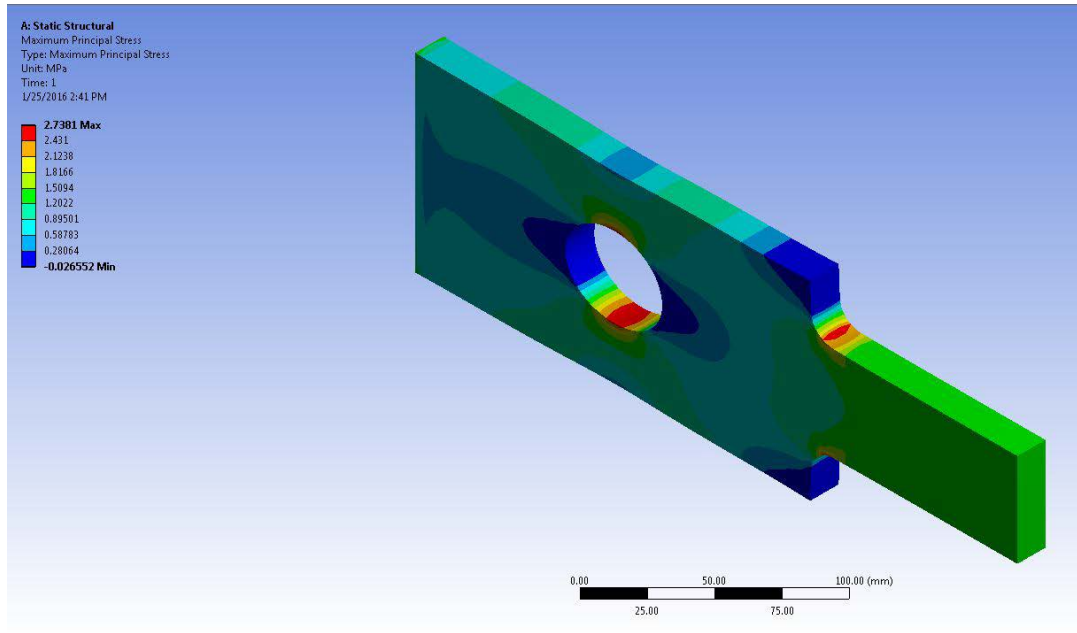


Figure D. 45. Stress along X-axis.

D.5.6 Test case 5 results: Siemens NX

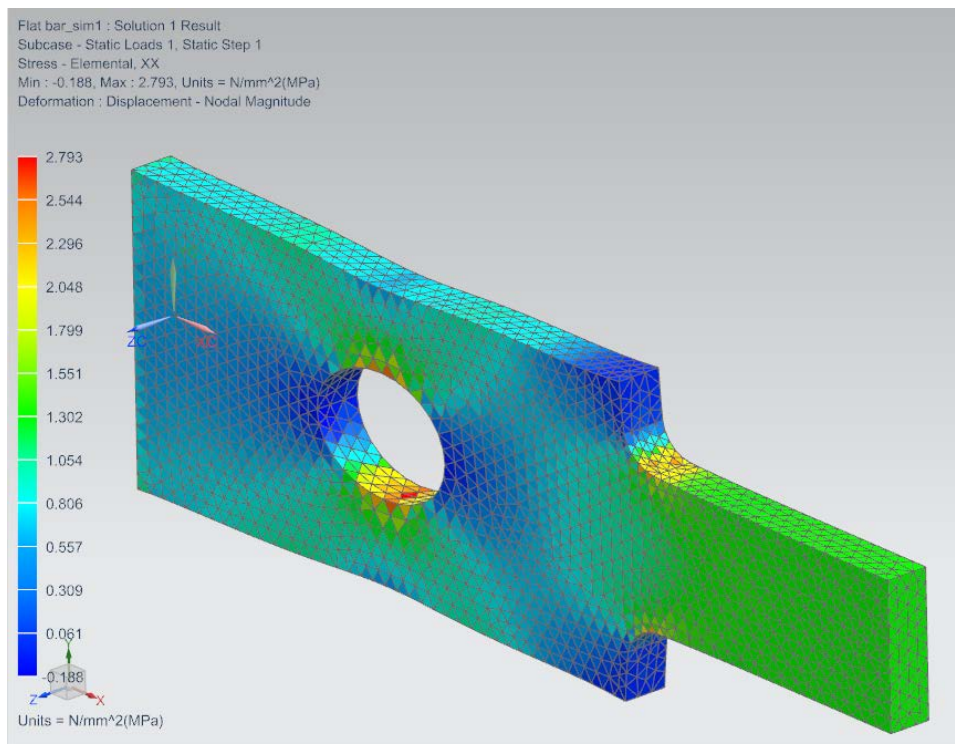


Figure D. 46. Stress along X-axis.

D.6.1 Test case 6 results: Mecway

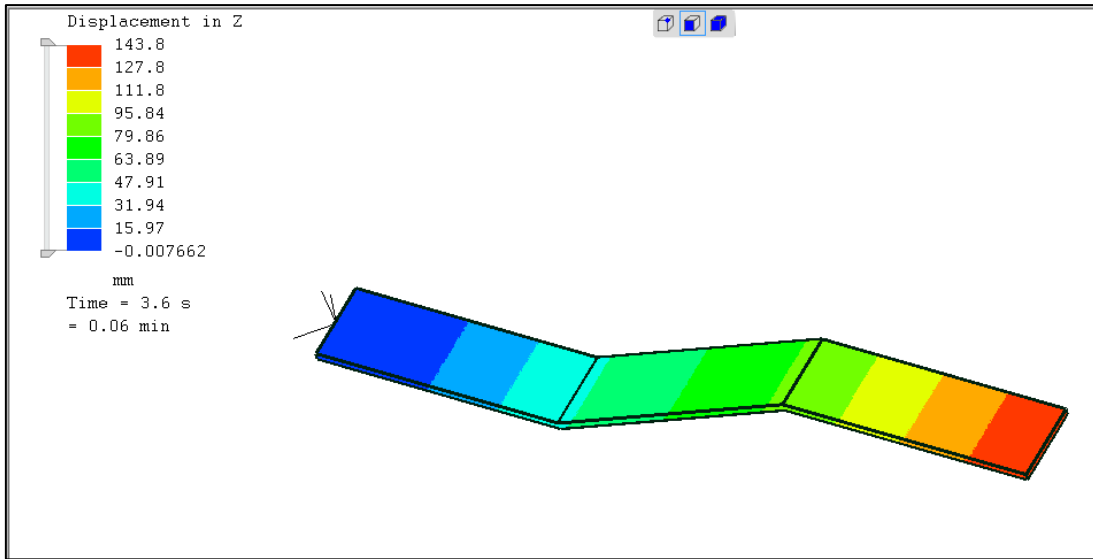


Figure D. 47. Displacement in Z-direction.

D.6.2 Test case 6 results: Z88 Aurora

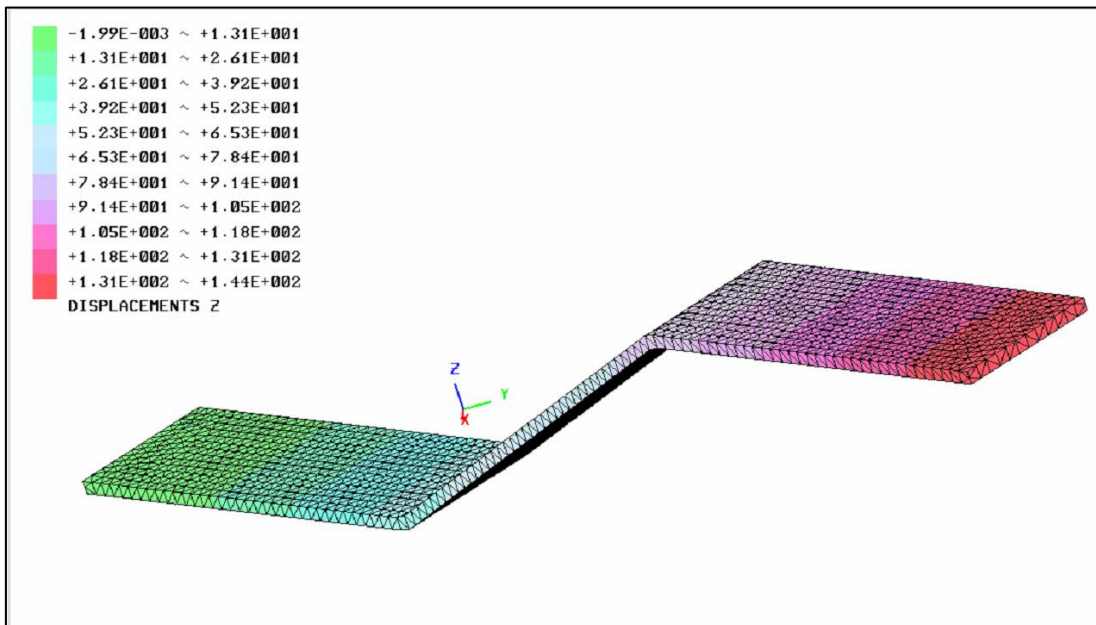


Figure D. 48. Displacement in Z-direction.

D.6.3 Test case 6 results: SimScale output through ParaView 5.0

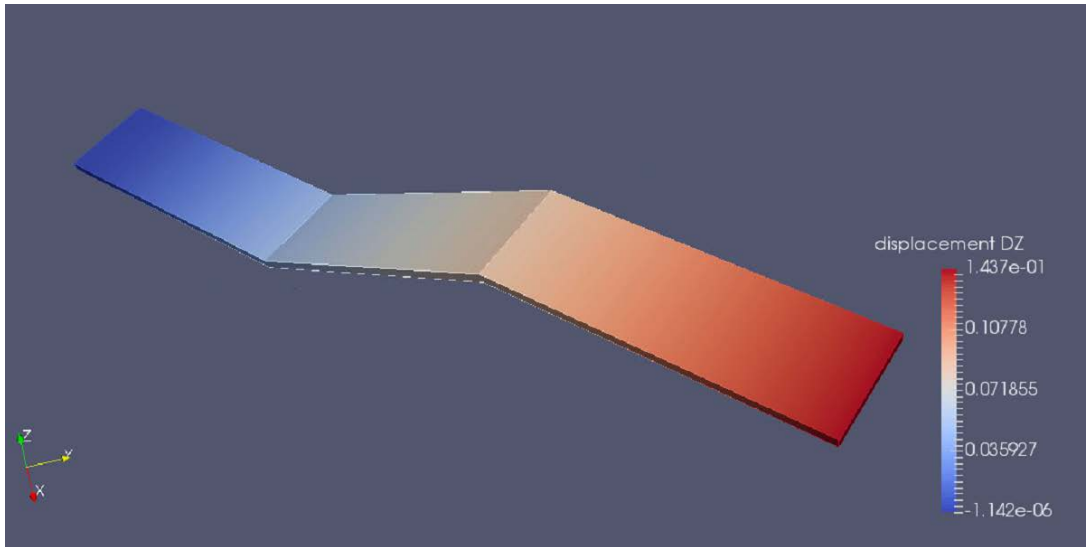


Figure D. 49. Displacement in Z-direction.

D.6.4 Test case 6 results: Code_Aster

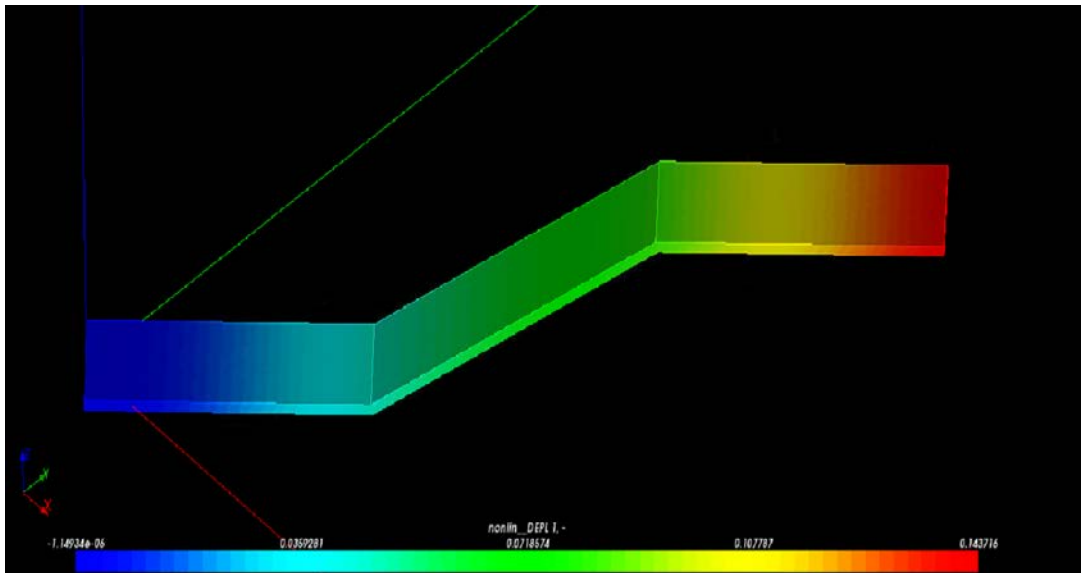


Figure D. 50. Displacement in Z-direction.

D.6.4 Test case 6 results: ANSYS

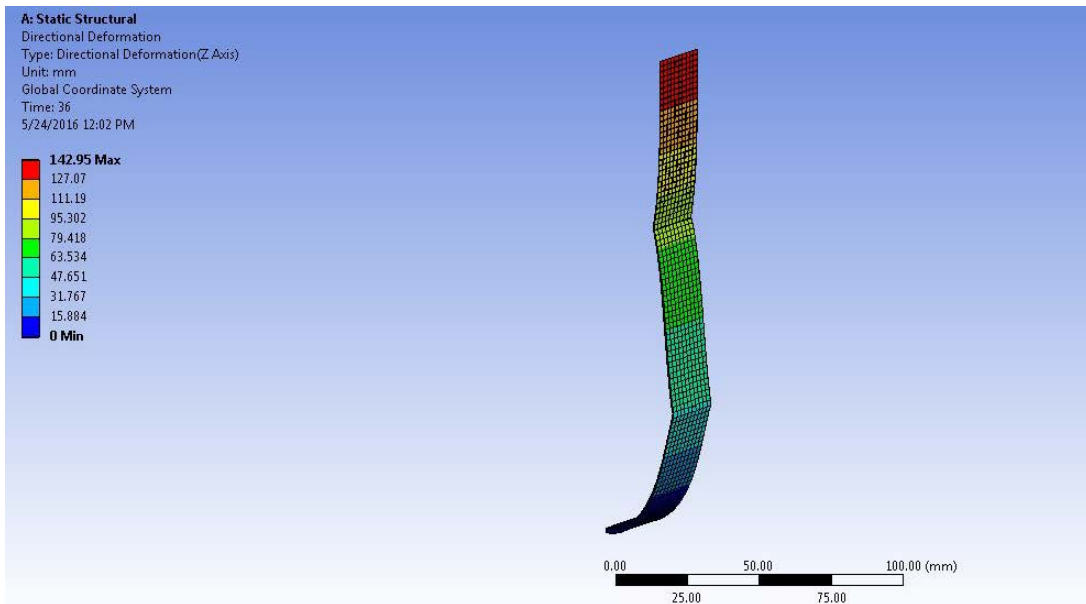


Figure D. 51. Displacement in Z-direction.

D.6.4 Test case 6 results: Siemens NX

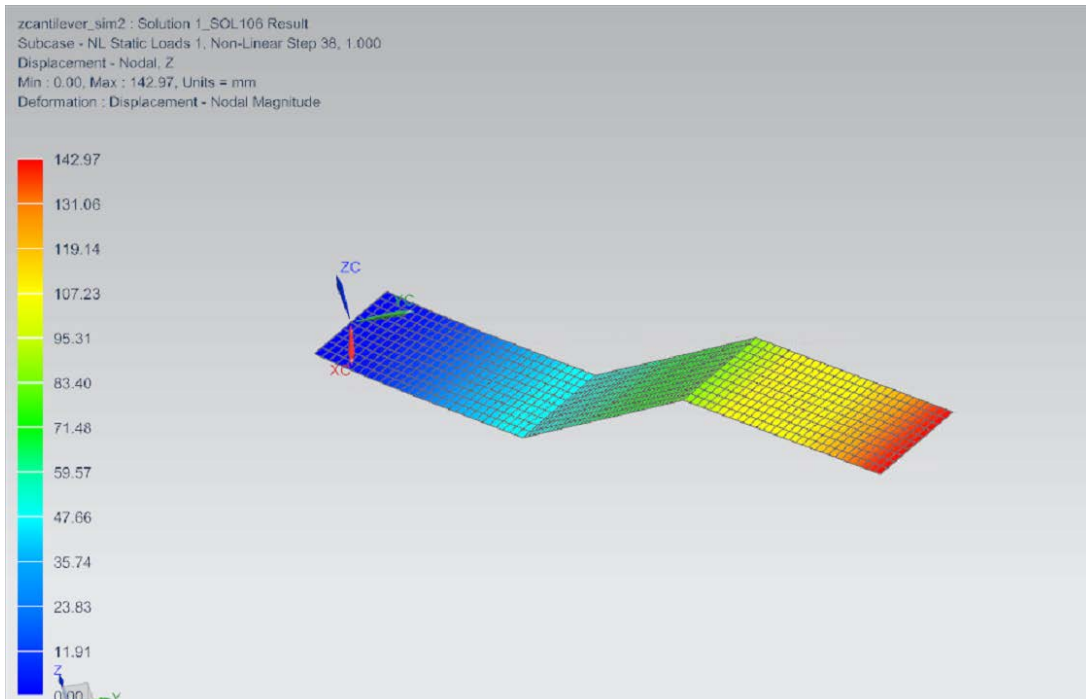


Figure D. 52. Displacement in Z-direction.

D.7.1 Test case 7 results: Mecway

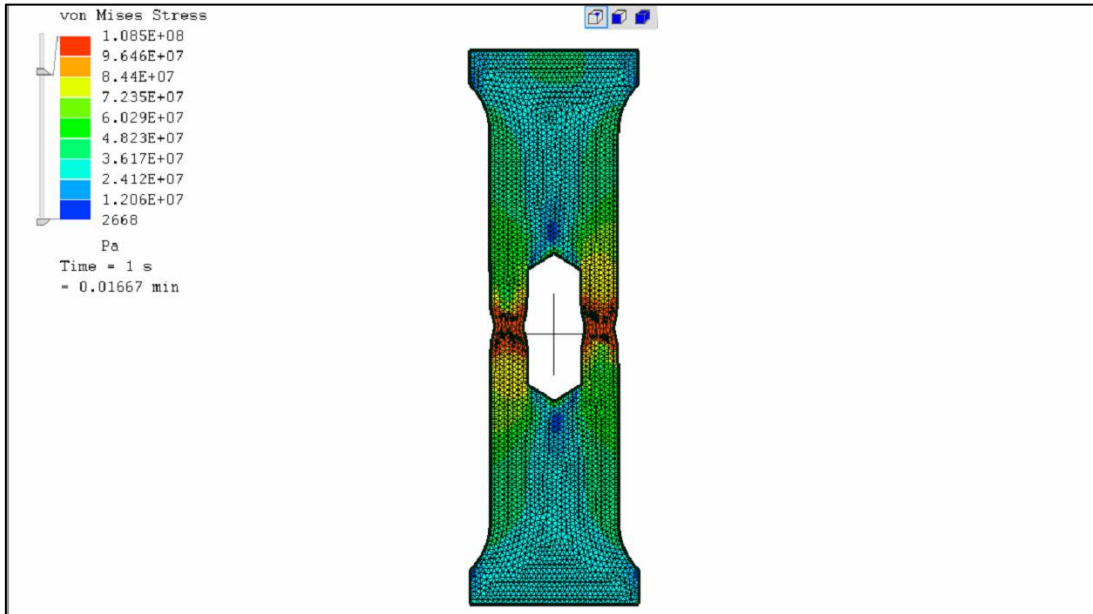


Figure D. 53. Stress observed after extension causes plastic deformation.

D.7.2 Test case 7 results: SimScale output through ParaView 5.0

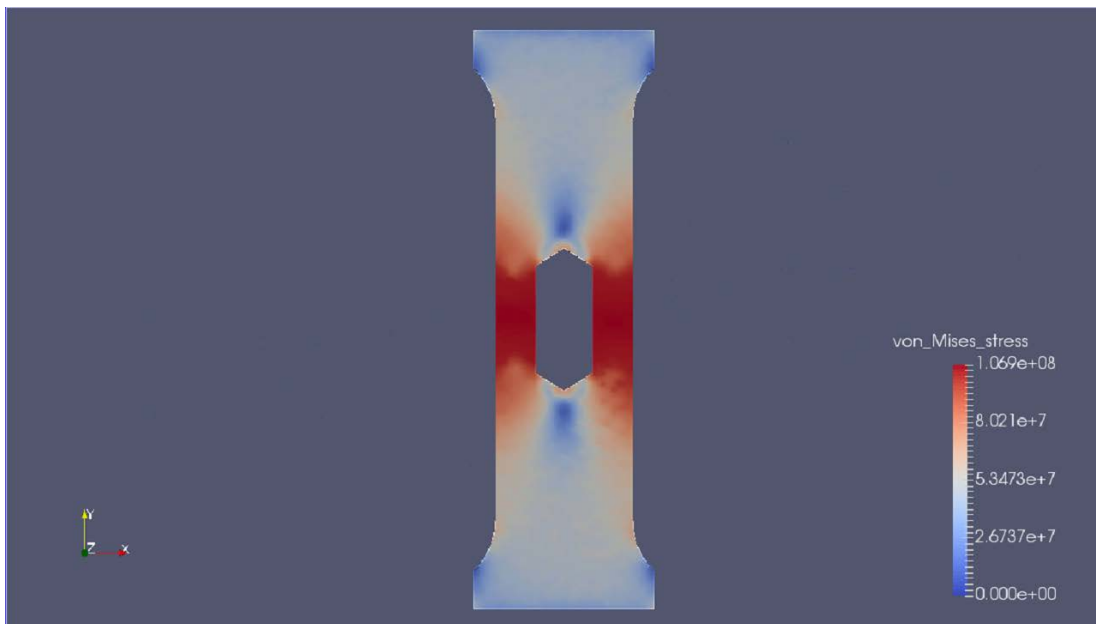


Figure D. 54. Stress observed after extension causes plastic deformation.

D.7.3 Test case 7 results: Code_Aster

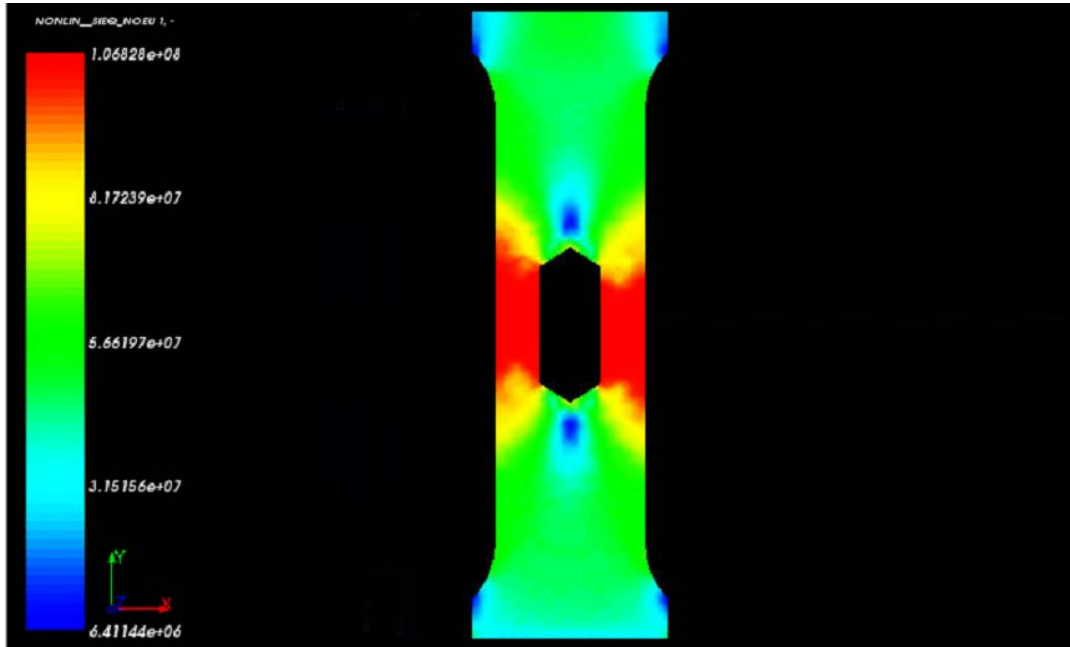


Figure D. 55. Stress observed after extension causes plastic deformation.

D.7.4 Test case 7 results: ANSYS

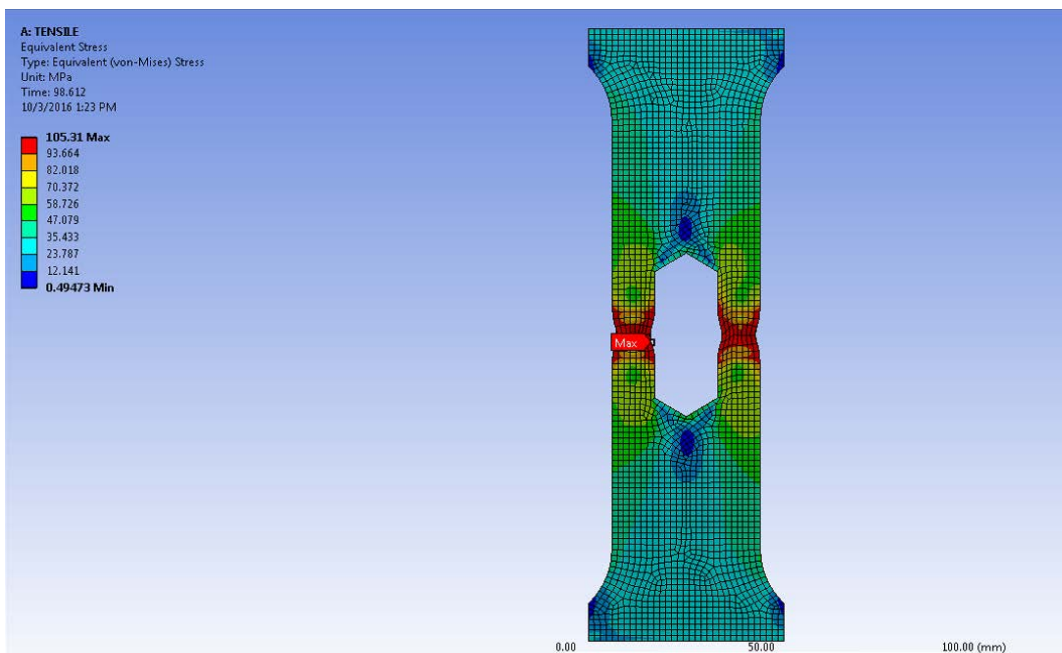


Figure D. 56. Stress observed after extension causes plastic deformation.

D.7.4 Test case 7 results: Siemens NX

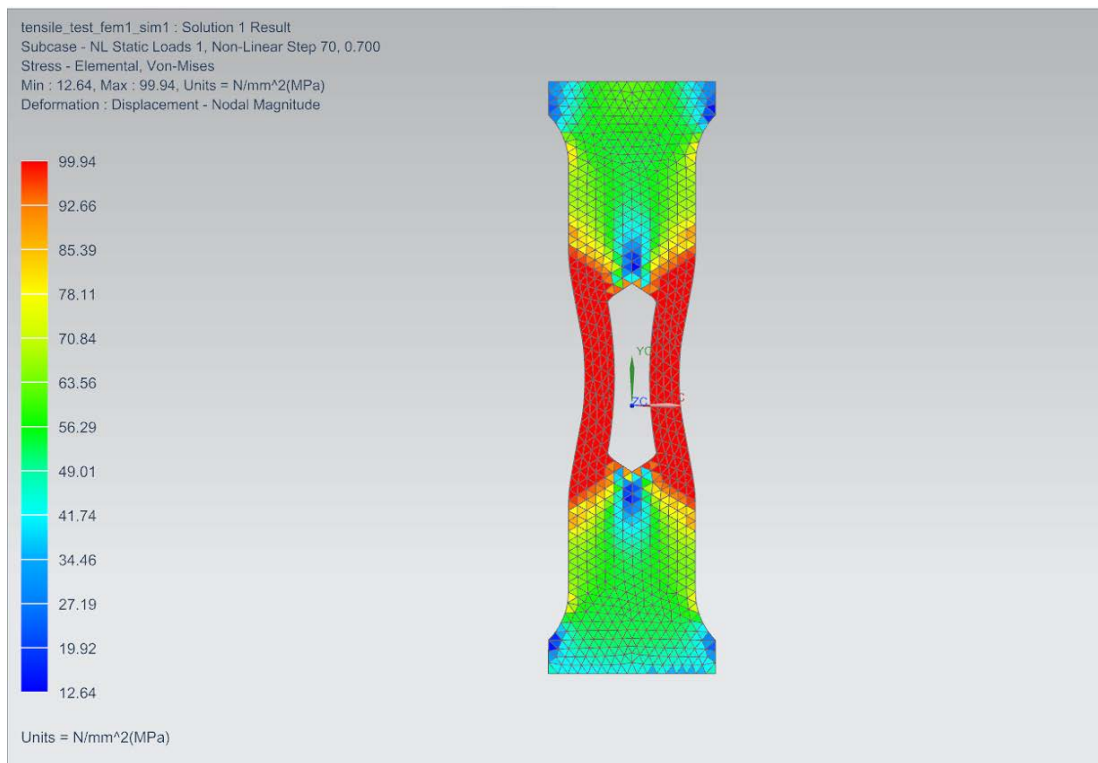


Figure D. 57. Stress observed after extension causes plastic deformation.

APPENDIX E

Tabulated Results

The tables presented here contain the tabulated results that correspond to the graphical plots found in Chapter 5. The deviation of results are presented as a percentage where applicable.

Table E. 1. Test Case 1 results from Mecway

Node	Target	Benchmark Value	Mecway Result	Deviation
C	X - displacement [m]	0.26520 E-3	0.38660 E-3	50.1%
	Y - displacement [m]	0.08839 E-3	0.08839 E-3	0.00%
D	X - displacement [m]	3.47900 E-3	3.47900 E-3	0.00%
	Y - displacement [m]	-5.60100 E-3	-5.60000 E-3	0.018%

Table E. 2. Test Case 1 results from Z88 Aurora

Node	Target	Benchmark Value	Z88 Result	Deviation
C	X - displacement [m]	0.26520 E-3	0.31600 E-3	19.1%
	Y - displacement [m]	0.08839 E-3	0.08840 E-3	0.011%
D	X - displacement [m]	3.47900 E-3	3.48000 E-3	0.028%
	Y - displacement [m]	-5.60100 E-3	-5.60000 E-3	0.018%

Table E. 3. Test Case 1 results from Code_Aster.

Node	Target	Benchmark Value	Code_Aster Result	Deviation
C	X - displacement [m]	0.26520 E-3	0.36148 E-3	36.30%
	Y - displacement [m]	0.08839 E-3	0.09195 E-3	4.03%
D	X - displacement [m]	3.47900 E-3	3.47813 E-3	0.025%
	Y - displacement [m]	-5.60100 E-3	-5.59907 E-3	0.034%

Table E. 4. Test Case 1 results from ANSYS

Node	Target	Benchmark Value	ANSYS Result	Deviation
C	X - displacement [m]	0.26520 E-3	0.38656 E-3	49.15%
C	Y - displacement [m]	0.08839 E-3	0.08839 E-3	0.00%
D	X - displacement [m]	3.47900 E-3	3.47903 E-3	0.00%
D	Y - displacement [m]	-5.60100 E-3	-5.60035 E-3	0.011%

Table E. 5. Test Case 1 results from Siemens NX

Node	Target	Benchmark Value	NX Result	Deviation
C	X - displacement [m]	0.26520 E-3	0.29000 E-3	9.35%
C	Y - displacement [m]	0.08839 E-3	0.08800 E-3	0.44%
D	X - displacement [m]	3.47900 E-3	3.47009 E-3	0.00%
D	Y - displacement [m]	-5.60100 E-3	-5.60000 E-3	0.018%

Table E. 6. Test Case 2 results from Mecway.

Point	Target	Benchmark Value	Result set	Mecway Result	Deviation
Loaded Edge	Maximum Z Deflection	4.320 [in]	1	4.228	4.32 %
			2	4.249	1.64 %
			3	4.249	1.64 %
			4	4.249	1.64 %
Fixed Edge	Maximum Z Stress	2.160 E+4 [psi]	1	2.079 E+4	3.75%
			2	2.285 E+4	5.78 %
			3	2.286 E+4	5.83 %
			4	2.283 E+4	5.69 %

Table E. 7. Test Case 2 results from Code_Aster.

Point	Target	Benchmark Value	Result set	Code_Aster Result	Deviation
Loaded Edge	Maximum Z Deflection	4.320 [in]	1	4.325	0.11 %
			2	4.325	0.11 %
			3	4.323	0.06 %
			4	4.319	0.02 %
Fixed Edge	Maximum Z Stress	2.160 E+4 [psi]	1	2.188	1.29 %
			2	2.179	0.88 %
			3	2.194	1.57 %
			4	2.156	0.18 %

Table E. 8. Test Case 2 results from ANSYS.

Point	Target	Benchmark Value	Result set	ANSYS Result	Deviation
Loaded Edge	Maximum Z Deflection	4.320 [in]	1	4.319	0.02 %
			2	4.319	0.02 %
			3	4.319	0.02 %
			4	4.319	0.02 %
Fixed Edge	Maximum Z Stress	2.160 E+4 [psi]	1	2.188 E+4	1.29 %
			2	2.167 E+4	0.32 %
			3	2.170 E+4	0.46 %
			4	2.156 E+4	0.18 %

Table E. 9. Test Case 2 results from Siemens NX.

Point	Target	Benchmark Value	Result set	NX Result	Deviation
Loaded Edge	Maximum Z Deflection	4.320 [in]	1	4.319	0.02 %
			2	4.319	0.02 %
			3	4.319	0.02 %
			4	4.319	0.02 %
Fixed Edge	Maximum Z Stress	2.160 E+4 [psi]	1	2.120 E+4	1.85 %
			2	2.180 E+4	0.93 %
			3	2.170 E+4	0.46 %
			4	2.160 E+4	0.00 %

Table E. 10. Test Case 3 results from Mecway.

Point	Target	Benchmark Value	Result set	Mecway Result	Deviation
Prescribed point on outer surface	Axial Stress $\sigma(yy)$	25.86 [MPa]	1	24.86	3.87 %
			2	25.70	0.62 %
			3	25.80	0.23 %

Table E. 11. Test Case 3 results from Z88.

Point	Target	Benchmark Value	Result set	Z88 Result	Deviation
Prescribed point on outer surface	Axial Stress $\sigma(yy)$	25.86 [MPa]	1	27.00	4.41 %
			2	-	-
			3	-	-

Table E. 12. Test Case 3 results from Code_Aster

Point	Target	Benchmark Value	Result set	Code_Aster Result	Deviation
Prescribed point on outer surface	Axial Stress $\sigma(yy)$	25.86 [MPa]	1	25.70	0.50
			2	25.84	0.15
			3	25.87	0.04

Table E. 13. Test Case 3 results from SimScale.

Point	Target	Benchmark Value	Result set	SimScale Result	Deviation
Prescribed point on outer surface	Axial Stress $\sigma(yy)$	25.86 [MPa]	1	22.44	13.22 %
			2	25.24	2.39 %
			3	-	-

Table E. 14. Test Case 3 results from ANSYS.

Point	Target	Benchmark Value	Result set	ANSYS Result	Deviation
Prescribed point on outer surface	Axial Stress $\sigma(yy)$	25.86 [MPa]	1	25.73	0.50 %
			2	25.82	0.15 %
			3	25.87	0.03 %

Table E. 15. Test Case 3 results from Siemens NX.

Point	Target	Benchmark Value	Result set	NX Result	Deviation
Prescribed point on outer surface	Axial Stress $\sigma(yy)$	25.86 [MPa]	1	20.75	19.76 %
			2	22.93	11.33 %
			3	25.72	0.54 %

Table E. 16. Test Case 4 results from Mecway.

Results : Internal Surface				
Target	Benchmark Value	Result set	Mecway Result	Deviation
$\sigma(rr)$	-100.0 [MPa]	1	- 101.8	1.80 %
		2	- 100.8	0.80 %
		3	- 100.9	0.90 %
$\sigma(\theta)$	71.43 [MPa]	1	75.44	5.61 %
		2	72.20	1.10 %
		3	72.24	1.10 %
u	0.400 E-3 [m]	1	0.4046 E-3	1.15 %
		2	0.4000 E-3	0.00 %
		3	0.4004 E-3	0.10 %
Results : External Surface				
Target	Benchmark Value	Result set	Mecway Result	Deviation
$\sigma(rr)$	0.00 [MPa]	1	3.234	3.234 MPa
		2	0.263	0.263 MPa
		3	0.322	0.322 MPa
$\sigma(\theta)$	21.43 [MPa]	1	18.01	16.07 %
		2	21.28	0.84 %
		3	21.24	1.02 %
u	0.150 E-3 [m]	1	0.148 E-3	1.27 %
		2	0.150 E-3	0.00 %
		3	0.150 E-3	0.00 %

Table E. 17. Test Case 4 partial results from Z88 Aurora.

Results : Internal Surface				
Target	Benchmark Value	Result set	Z88 Result	Deviation
$\sigma(\mathbf{rr})$	-100.0 [MPa]	1	Solver did not output this particular result	
		2		
		3		
$\sigma(\theta)$	71.43 [MPa]	1	Solver did not output this particular result	
		2		
		3		
\mathbf{u}	0.400 E-3 [m]	1	0.401 E-3	0.25%
		2	0.402 E-3	0.50%
		3	0.4004 E-3	0.10%
Results : External Surface				
Target	Benchmark Value	Result set	Z88 Result	Deviation
$\sigma(\mathbf{rr})$	0.00 [MPa]	1	Solver did not output this particular result	
		2		
		3		
$\sigma(\theta)$	21.43 [MPa]	1	Solver did not output this particular result	
		2		
		3		
\mathbf{u}	0.150 e-3 [m]	1	0.148 E-3	1.27%
		2	0.150 E-3	0.00%
		3	0.150 E-3	0.00%

Table E. 18. Test Case 4 results from Code_Aster.

Results : Internal Surface				
Target	Benchmark Value	Result set	Code_Aster Result	Deviation
$\sigma(\mathbf{rr})$	-100.00 [MPa]	1	- 78.48	21.51%
		2	- 96.46	3.54%
		3	- 100.15	0.157%
$\sigma(\theta)$	71.43 [MPa]	1	76.24	6.74%
		2	75.07	5.09%
		3	72.35	1.29%
\mathbf{u}	0.400 E-3 [m]	1	0.395 E-3	1.25%
		2	0.400 E-3	0.00%
		3	0.400 E-3	0.00%
Results : External Surface				
Target	Benchmark Value	Result set	Code_Aster Result	Deviation
$\sigma(\mathbf{rr})$	0.00 [MPa]	1	- 1.225	1.225 MPa
		2	- 0.196	0.196 MPa
		3	0.188	0.188 MPa
$\sigma(\theta)$	21.43 [MPa]	1	17.85	16.69%
		2	20.81	2.91%
		3	21.36	0.35%
\mathbf{u}	0.150 E-3 [m]	1	0.138 E-3	8.00%
		2	0.149 E-3	0.66%
		3	0.149 E-3	0.66%

Table E. 19. Test Case 4 results from SimScale.

Results : Internal Surface				
Target	Benchmark Value	Result set	SimScale Result	Deviation
$\sigma(\mathbf{rr})$	-100 [MPa]	1	- 76.75	23.25%
		2	- 96.18	3.82%
		3	- 100.41	0.14%
$\sigma(\theta)$	71.43 [MPa]	1	76.96	7.74%
		2	76.01	6.41%
		3	72.41	1.37%
\mathbf{u}	0.400e-3 [m]	1	0.396	1.00%
		2	0.401	0.25%
		3	0.401	0.25%
Results : External Surface				
Target	Benchmark Value	Result set	SimScale Result	Deviation
$\sigma(\mathbf{rr})$	0 [MPa]	1	- 1.285	1.285 [MPa]
		2	- 0.221	0.221 [MPa]
		3	0.175	0.175 [MPa]
$\sigma(\theta)$	21.43 [MPa]	1	18.03	15.86%
		2	19.83	7.47%
		3	21.34	0.42%
\mathbf{u}	0.150 e-3 [m]	1	0.138	8.00%
		2	0.149	0.66%
		3	0.149	0.66%

Table E. 20. Test Case 4 results from ANSYS.

Results : Internal Surface				
Target	Benchmark Value	Result set	ANSYS Result	Deviation
$\sigma(rr)$	-100 [MPa]	1	-98.318	1.68%
		2	-99.484	0.52%
		3	-99.875	0.13%
$\sigma(\theta)$	71.43 [MPa]	1	71.071	0.50%
		2	71.341	0.12%
		3	71.474	0.05%
u	0.4e-3 [m]	1	0.400	0.00%
		2	0.400	0.00%
		3	0.400	0.00%
Results : External Surface				
Target	Benchmark Value	Result set	ANSYS Result	Deviation
$\sigma(rr)$	0 [MPa]	1	0.201	0.201 MPa
		2	0.052	0.052 MPa
		3	0.012	0.012 MPa
$\sigma(\theta)$	21.43 [MPa]	1	21.348	0.38%
		2	21.405	0.11%
		3	21.412	0.08%
u	0.15 e-3 [m]	1	0.149	0.66%
		2	0.149	0.66%
		3	0.15	0.00%

Table E. 21. Test Case 4 results from Siemens NX.

Results : Internal Surface				
Target	Benchmark Value	Result set	NX Result	Deviation
$\sigma(\mathbf{rr})$	-100 [MPa]	1	-106.75	6.75 %
		2	-105.91	5.91 %
		3	-95.63	4.37 %
$\sigma(\theta)$	71.43 [MPa]	1	80.84	13.17 %
		2	74.81	4.73 %
		3	69.39	2.86 %
\mathbf{u}	0.4e-3 [m]	1	0.401	0.25 %
		2	0.400	0.00 %
		3	0.400	0.00 %
Results : External Surface				
Target	Benchmark Value	Result set	NX Result	Deviation
$\sigma(\mathbf{rr})$	0 [MPa]	1	1.04	1.04 MPa
		2	0.63	0.63 MPa
		3	-0.28	-0.28 MPa
$\sigma(\theta)$	21.43 [MPa]	1	20.00	6.67 %
		2	20.36	3.73 %
		3	21.57	0.65 %
\mathbf{u}	0.15 e-3 [m]	1	0.15	0.00 %
		2	0.149	0.67 %
		3	0.15	0.00 %

Table E. 22. Test Case 5 results from Mecway.

Point	Target	Benchmark Value	Result set	Mecway Result	Deviation
Hole	X - Stress	2.66 [MPa]	1	2.36	11.27 %
			2	2.45	7.89 %
			3	2.77	4.14 %
			4	2.76	3.75 %
Fillet	X - Stress	2.66 [MPa]	1	2.36	11.27 %
			2	2.45	7.89 %
			3	2.77	4.14 %
			4	2.76	3.75 %

Table E. 23. Test Case 5 results from Z88 Aurora.

Point	Target	Benchmark Value	Result set	Z88 Result	Deviation
Hole	X - Stress	2.66 [MPa]	1	2.49	6.39 %
			2	2.44	8.27 %
			3	2.68	0.75 %
			4	2.72	2.25 %
Fillet	X - Stress	2.66 [MPa]	1	2.23	16.16 %
			2	2.61	1.87 %
			3	2.87	7.89 %
			4	2.72	2.25 %

Table E. 24. Test Case 5 results from Code_Aster.

Point	Target	Benchmark Value	Result set	Code_Aster Result	Deviation
Hole	X - Stress	2.66 [MPa]	1	2.60	2.255 %
			2	2.44	8.27 %
			3	2.68	0.75 %
			4	2.68	0.75 %
Fillet	X - Stress	2.66 [MPa]	1	1.92	27.82 %
			2	2.61	1.88 %
			3	2.87	7.89 %
			4	2.68	0.75 %

Table E. 25. Test Case5 results from SimScale.

Point	Target	Benchmark Value	Result set	SimScale Result	Deviation
Hole	X - Stress	2.66 [MPa]	1	1.82	31.57 %
			2	2.32	12.78 %
			3	2.32	12.78 %
			4	2.68	0.75 %
Fillet	X - Stress	2.66 [MPa]	1	1.82	31.57 %
			2	2.52	12.78 %
			3	2.52	12.78 %
			4	2.68	0.75 %

Table E. 26. Test Case5 results from ANSYS

Point	Target	Benchmark Value	Result set	ANSYS Result	Deviation
Hole	X - Stress	2.66 [MPa]	1	2.78	4.51 %
			2	2.74	3.00 %
			3	2.89	8.64 %
			4	2.71	1.88 %
Fillet	X - Stress	2.66 [MPa]	1	2.15	19.17 %
			2	2.74	3.00 %
			3	2.89	8.64 %
			4	2.71	1.88 %

Table E. 27. Test Case5 results from Siemens NX.

Point	Target	Benchmark Value	Result set	NX Result	Deviation
Hole	X - Stress	2.66 [MPa]	1	2.19	17.70 %
			2	2.79	4.89 %
			3	2.74	3.00 %
			4	2.71	1.88 %
Fillet	X - Stress	2.66 [MPa]	1	2.19	17.70 %
			2	2.79	4.89 %
			3	2.74	3.00 %
			4	2.71	1.88 %